frontiers | Research Topics

Effects and mechanisms of bariatric surgery in relieving obesity and its complications

Edited by
Yayun Wang, Lidia Castagneto Gissey and Kaixiong Tao

Published in
Frontiers in Endocrinology

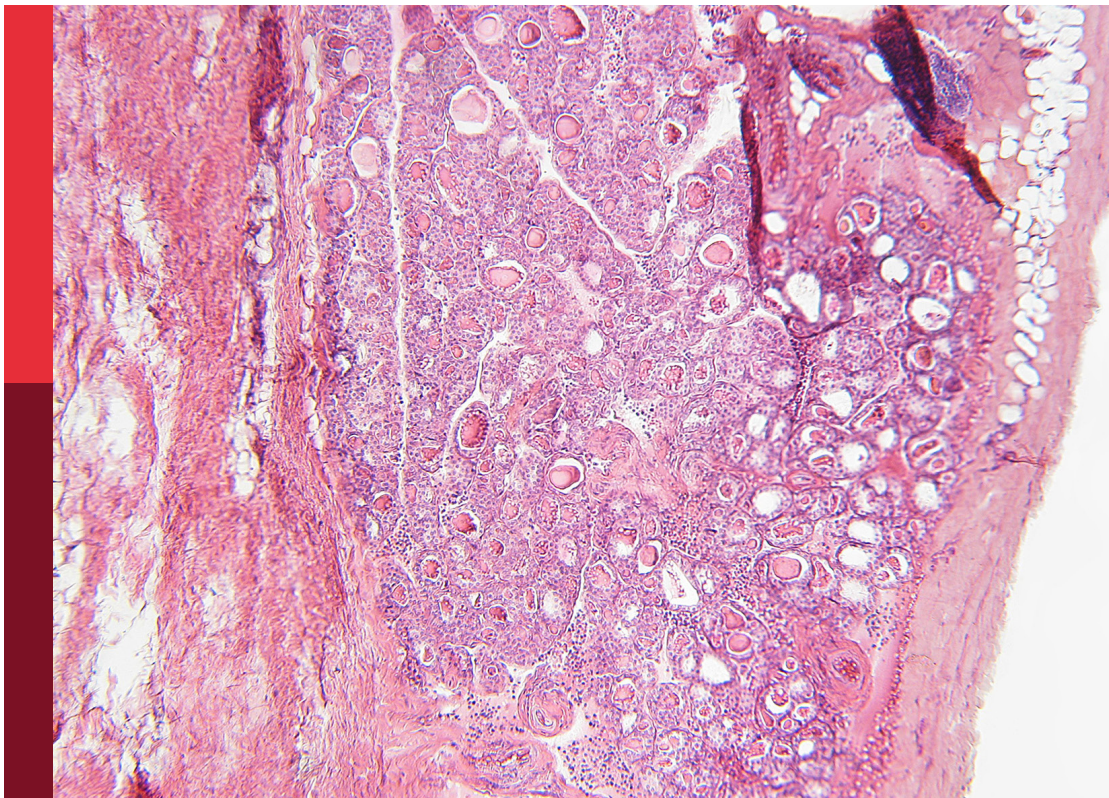

ISSN 1664-8714
ISBN 978-2-8325-6026-6
DOI 10.3389/978-2-8325-6026-6

About Frontiers

Frontiers is more than just an open access publisher of scholarly articles: it is a pioneering approach to the world of academia, radically improving the way scholarly research is managed. The grand vision of Frontiers is a world where all people have an equal opportunity to seek, share and generate knowledge. Frontiers provides immediate and permanent online open access to all its publications, but this alone is not enough to realize our grand goals.

Frontiers journal series

The Frontiers journal series is a multi-tier and interdisciplinary set of open-access, online journals, promising a paradigm shift from the current review, selection and dissemination processes in academic publishing. All Frontiers journals are driven by researchers for researchers; therefore, they constitute a service to the scholarly community. At the same time, the *Frontiers journal series* operates on a revolutionary invention, the tiered publishing system, initially addressing specific communities of scholars, and gradually climbing up to broader public understanding, thus serving the interests of the lay society, too.

Dedication to quality

Each Frontiers article is a landmark of the highest quality, thanks to genuinely collaborative interactions between authors and review editors, who include some of the world's best academicians. Research must be certified by peers before entering a stream of knowledge that may eventually reach the public - and shape society; therefore, Frontiers only applies the most rigorous and unbiased reviews. Frontiers revolutionizes research publishing by freely delivering the most outstanding research, evaluated with no bias from both the academic and social point of view. By applying the most advanced information technologies, Frontiers is catapulting scholarly publishing into a new generation.

What are Frontiers Research Topics?

Frontiers Research Topics are very popular trademarks of the *Frontiers journals series*: they are collections of at least ten articles, all centered on a particular subject. With their unique mix of varied contributions from Original Research to Review Articles, Frontiers Research Topics unify the most influential researchers, the latest key findings and historical advances in a hot research area.

Find out more on how to host your own Frontiers Research Topic or contribute to one as an author by contacting the Frontiers editorial office: frontiersin.org/about/contact

Effects and mechanisms of bariatric surgery in relieving obesity and its complications

Topic editors

Yayun Wang — Air Force Medical University, China

Lidia Castagneto Gissey — Sapienza University of Rome, Italy

Kaixiong Tao — Huazhong University of Science and Technology, China

Citation

Wang, Y., Castagneto Gissey, L., Tao, K., eds. (2025). *Effects and mechanisms of bariatric surgery in relieving obesity and its complications*.

Lausanne: Frontiers Media SA. doi: 10.3389/978-2-8325-6026-6

Table of contents

frontiers | Frontiers in Endocrinology

TYPE Editorial
PUBLISHED 07 February 2025
DOI 10.3389/fendo.2025.1563980

OPEN ACCESS

EDITED AND REVIEWED BY
Katherine Samaras,
St Vincent's Hospital Sydney, Australia

*CORRESPONDENCE
Lidia Castagneto-Gissey
lidia.castagnetogissey@uniroma1.it

RECEIVED 20 January 2025
ACCEPTED 28 January 2025
PUBLISHED 07 February 2025

CITATION
Castagneto-Gissey L, Wang Y and Tao K (2025) Editorial: Effects and mechanisms of bariatric surgery in relieving obesity and its complications.
Front. Endocrinol. 16:1563980.
doi: 10.3389/fendo.2025.1563980

Editorial: Effects and mechanisms of bariatric surgery in relieving obesity and its complications

Lidia Castagneto-Gissey [1]*, Yayun Wang [2] and Kaixiong Tao [3]

[1]Department of Surgery, Sapienza University of Rome, Rome, Italy, [2]Department of Gastroenterology, Air Force Medical University, Xi'an, China, [3]Wuhan Union Hospital, Tongji Medical College, Huazhong University of Science and Technology, Wuhan, China

KEYWORDS

obesity, bariatric surgery, gut microbiota, gerd, genetic variability, PCOS, MASH

Editorial on the Research Topic
Effects and mechanisms of bariatric surgery in relieving obesity and its complications

The global prevalence of obesity has reached alarming proportions, with its associated comorbidities imposing a significant workload on healthcare systems worldwide (1). Obesity contributes to a spectrum of metabolic, cardiovascular, and inflammatory conditions, including type 2 diabetes (T2D), metabolic dysfunction-associated steatohepatitis (MASH), and renal dysfunction, while also exacerbating issues such as periodontitis and irregular menstruation (2). Bariatric surgery has emerged as a transformative intervention for managing morbid obesity, offering not only sustained weight loss but also profound metabolic benefits (3–5). The studies featured in this Research Topic illuminate the multifaceted effects and mechanisms of bariatric surgery, particularly focusing on Roux-en-Y gastric bypass (RYGB) and sleeve gastrectomy (SG), in addressing obesity and its complications. This Research Topic spans through the key findings from these research papers, highlighting the evolving understanding of bariatric surgery's therapeutic potential.

Weight loss remains a cornerstone of bariatric surgery's benefits, with studies underscoring its pivotal role in mediating metabolic and hormonal improvements. For instance, Tian et al. demonstrated that total weight loss (TWL%) following bariatric surgery is closely correlated with reductions in thyroid-stimulating hormone (TSH) levels, suggesting enhanced thyroid function in euthyroid patients with obesity. Interestingly, this relationship was independent of baseline factors such as age, sex, or comorbidities, emphasizing the universal metabolic benefits of significant weight loss.

Similarly, Zhao et al. investigated the effects of SG on women with polycystic ovary syndrome (PCOS) and found that weight loss—rather than preoperative body mass index (BMI)—was a critical determinant of menstrual regularity. With 79.03% of participants achieving remission of irregular menstruation within a year, this study highlights the potential of bariatric surgery to address reproductive dysfunctions associated with obesity.

These findings underscore the importance of targeting substantial weight loss to maximize health outcomes, regardless of baseline BMI.

Gender-specific differences in predictors of weight loss after SG were highlighted in the study by Shu et al. Both men and women achieved comparable weight loss outcomes when baseline characteristics were matched. However, distinct predictors emerged: in men, baseline BMI and insulin dynamics were significant, while in women, age, thyroid function, and mental health measures played a more substantial role. These insights advocate for personalized preoperative evaluations to optimize weight-loss outcomes across genders.

The role of gut microbiota in mediating the metabolic benefits of bariatric surgery has garnered significant attention. Liu C. et al. employed a multi-omics approach to investigate changes in gut microbiota and metabolism following SG. They reported increased microbial diversity and enrichment of beneficial bacteria such as Alistipes and Parabacteroides. These microbial changes were correlated with enhanced lipid metabolism, as evidenced by elevated levels of free fatty acids and bile acids. Similarly, the study by Li et al. on duodenojejunal bypass (DJB) in obese T2D mice demonstrated that proximal gut microbiota play a dominant role in improving glucose metabolism and reducing inflammation. Both studies underscore the essential role of intestinal remodeling in achieving metabolic improvements post-surgery.

Bariatric surgery is not without complications, and gastroesophageal reflux disease (GERD) is a prominent concern, particularly after SG (6, 7). Liu G. et al. provided a comprehensive review of strategies to manage GERD in these patients, emphasizing the efficacy of RYGB as the gold standard for refractory cases. Innovative approaches such as magnetic sphincter augmentation and antireflux mucosectomy were also explored, offering minimally invasive alternatives for GERD management.

Periodontal health, often overlooked in obese populations, was addressed by Bi et al. Their study found significant improvements in periodontal parameters such as plaque index (PLI) and bleeding index (BI) following SG, particularly in patients with T2D. Reduced systemic inflammation, as evidenced by declines in hs-CRP and IL-6 levels, was likely a key contributor to these improvements. However, persistent disparities in pocket depth between diabetic and non-diabetic groups highlight the need for continued oral health monitoring in this population.

Chen et al. explored the molecular mechanisms underlying MASH improvement post-bariatric surgery, identifying key genes such as FASN, SCD1, and HMGCS1 that regulate lipid metabolism and inflammation. Downregulation of these genes was associated with reduced liver steatosis and enhanced metabolic health, offering potential therapeutic targets for non-surgical interventions.

Another metabolic dimension, glycine deficiency, was investigated by Tan et al. Obesity-induced glycine deficiency impairs the glycine conjugation pathway, which is crucial for detoxification and metabolite clearance. Their findings demonstrated that bariatric surgery restores glycine synthesis and improves detoxification, highlighting an additional mechanism through which weight loss enhances systemic health.

Obesity-related renal dysfunction, a growing concern, was examined by Popa et al., who emphasized gender-specific influences of visceral adiposity on renal filtration. In females, visceral adipose tissue (VAT) mass and its associated metabolic effects played a dominant role in renal dysfunction and recovery. By contrast, in males, weight loss and lean mass changes were more influential. Postoperatively, significant improvements in estimated glomerular filtration rate (eGFR) were observed across all renal function categories, reinforcing the reno-protective effects of bariatric surgery.

The interplay between genetics and weight loss outcomes was highlighted by Wang et al., who identified the CAMKK2 variant as a novel monogenic obesity variant (MOV). Using whole-exome sequencing and postoperative data, they demonstrated that carriers of the CAMKK2 mutation experienced less pronounced weight loss and metabolic improvements compared to non-carriers. This study underscores the importance of integrating genetic insights into personalized obesity treatment strategies.

The studies in this Research Topic collectively highlight the multifactorial mechanisms underlying bariatric surgery's success in addressing obesity and its complications. From gut microbiota remodeling and molecular pathway modulation to gender-specific influences and genetic predispositions, these findings emphasize the importance of a multidisciplinary approach in understanding and optimizing surgical outcomes.

While the benefits of bariatric surgery are well-documented, challenges remain in ensuring equitable access, managing complications, and refining surgical techniques. Further research is needed to develop standardized guidelines for managing postoperative complications such as GERD and nutritional deficiencies; explore long-term outcomes in diverse populations, with particular attention to sex and genetic variability; leverage multi-omics approaches to identify novel biomarkers and therapeutic targets for obesity-related diseases; enhance interdisciplinary care, integrating endocrinology, gastroenterology, and behavioral health to address the holistic needs of patients.

The insights presented in this Research Topic advance our understanding of the underlying mechanisms, paving the way for personalized and effective treatment strategies. By continuing to integrate clinical research with molecular and genetic insights, we can further harness the potential of bariatric surgery to improve the lives of individuals living with obesity.

Author contributions

LC-G: Conceptualization, Formal analysis, Funding acquisition, Investigation, Methodology, Project administration, Resources, Supervision, Validation, Visualization, Writing – original draft, Writing – review & editing. YW: Conceptualization, Writing – review & editing. KT: Conceptualization, Writing – review & editing.

Conflict of interest

The authors declare that the research was conducted in the absence of any commercial or financial relationships that could be construed as a potential conflict of interest.

The author(s) declared that they were an editorial board member of Frontiers, at the time of submission. This had no impact on the peer review process and the final decision.

Publisher's note

References

1. Ng M, Fleming T, Robinson M, Thomson B, Graetz N, Margono C, et al. Global, regional, and national prevalence of overweight and obesity in children and adults during 1980-2013: a systematic analysis for the Global Burden of Disease Study 2013. *Lancet*. (2014) 384:766–81. doi: 10.1016/S0140-6736(14)60460-8

2. Mingrone G, Castagneto-Gissey L. Type 2 diabetes mellitus in 2013: A central role of the gut in glucose homeostasis. *Nat Rev Endocrinol*. (2014) 10:73–4. doi: 10.1038/nrendo.2013.241

3. Miras AD, Kamocka A, Pérez-Pevida B, Purkayastha S, Moorthy K, Patel A, et al. The effect of standard versus longer intestinal bypass on GLP-1 regulation and glucose metabolism in patients with type 2 diabetes undergoing roux-en-Y gastric bypass: the long-limb study. *Diabetes Care*. (2021) 44:1082–90. doi: 10.2337/dc20-0762

4. Castagneto-Gissey L, Mingrone G. Insulin sensitivity and secretion modifications after bariatric surgery. *J Endocrinol Invest*. (2012) 35:692–8. doi: 10.3275/8470

5. Risi R, Rossini G, Tozzi R, Pieralice S, Monte L, Masi D, et al. Sex difference in the safety and efficacy of bariatric procedures: a systematic review and meta-analysis. *Surg Obes Relat Dis*. (2022) 18:983–96. doi: 10.1016/j.soard.2022.03.022

6. Castagneto-Gissey L, Genco A, Del Corpo G, Badiali D, Pronio AM, Casella G. Sleeve gastrectomy and gastroesophageal reflux: a comprehensive endoscopic and pH-manometric prospective study. *Surg Obes Relat Dis*. (2020) 16:1629–37. doi: 10.1016/j.soard.2020.07.013

7. Castagneto-Gissey L, Russo MF, D'Andrea V, Genco A, Casella G. Efficacy of sleeve gastrectomy with concomitant hiatal hernia repair versus sleeve-fundoplication on gastroesophageal reflux disease resolution: systematic review and meta-analysis. *J Clin Med*. (2023) 12:3323. doi: 10.3390/jcm12093323

frontiers | Frontiers in Endocrinology

TYPE Original Research
PUBLISHED 10 January 2024
DOI 10.3389/fendo.2023.1333051

OPEN ACCESS

EDITED BY
Yayun Wang,
Air Force Medical University, China

REVIEWED BY
Mohamad Mokadem,
The University of Iowa, United States
Sabrina Oussaada,
Academic Medical Center, Netherlands

*CORRESPONDENCE
Shaozhuang Liu
liushaozhuang@sdu.edu.cn
Xin Huang
huangxinsdu@163.com

RECEIVED 04 November 2023
ACCEPTED 18 December 2023
PUBLISHED 10 January 2024

CITATION
Shu J, Zhu T, Xiong S, Liu T, Zhao Y, Huang X and Liu S (2024) Sex dimorphism in the effect and predictors of weight loss after sleeve gastrectomy.
Front. Endocrinol. 14:1333051.
doi: 10.3389/fendo.2023.1333051

Sex dimorphism in the effect and predictors of weight loss after sleeve gastrectomy

Jiaxin Shu[1,2], Tao Zhu[1,2], Sisi Xiong[1,2], Teng Liu[1], Yian Zhao[1,2], Xin Huang[1*] and Shaozhuang Liu[1*]

[1]Division of Bariatric and Metabolic Surgery, Department of General Surgery, Qilu Hospital of Shandong University, Jinan, China, [2]Department of Surgery, First Clinical College, Shandong University, Jinan, China

Background: No sex-specific guidelines for surgical anti-obesity strategies have been proposed, partially due to the controversy regarding sex-related differences in weight loss after bariatric metabolic surgery.

Objectives: To explore sex dimorphism in the effect and predictors of weight loss after sleeve gastrectomy (SG), thereby providing clinical evidence for the sex-specific surgical treatment strategy.

Methods: In a prospective cohort design, participants scheduled for SG at an affiliated hospital between November 2020 and January 2022 were assessed for eligibility and allocated to the Male or Female group with a 1-year follow-up after surgery. The primary outcome was the sex difference in the weight-loss effect after SG indicated by both percentage of total weight loss (TWL%) and excess weight loss (EWL%). The secondary outcome was the analysis of sex-specific preoperative predictors of weight loss after SG based on univariate and multivariate analyses. Independent predictors were obtained to construct a nomogram model. The discrimination, calibration, and clinical utility of the nomogram were based on receiver operating characteristic curve, concordance index, calibration curve, and decision curve analysis, respectively.

Results: Ninety-five male and 226 female patients were initially included. After propensity score matching by baseline body mass index (BMI), 85 male and 143 female patients achieved comparable TWL% and EWL% for 1 year after SG. For male patients, baseline BMI, area under the curve for insulin during oral glucose tolerance test, and progesterone were independent predictors of weight loss after SG. Baseline BMI, age, thyroid stimulating hormone, and Self-Rating Anxiety Scale score were independent predictors for female patients.

Conclusion: No obvious sex difference is detected in the weight-loss effect after SG. Sex dimorphism exists in the predictors of weight loss after SG. Further research with long-term and a multicenter design is needed to confirm the predictive model.

KEYWORDS

sleeve gastrectomy, weight loss, sex dimorphism, predictor, nomogram

1 Introduction

Obesity has become a global epidemic affecting more than 988 million people worldwide by 2020 (1). Bariatric metabolic surgery has been recognized as an effective and evidence-based surgical treatment for morbid obesity (2). Sleeve gastrectomy (SG) has become the most common bariatric metabolic procedure worldwide (3). However, the weight-loss effect after SG varied among patients. Insufficient weight loss and weight regain have become challenging issues (4).

Body weight can be affected by biologic, psychosocial, and behavioral factors (5). Given sex-related differences in psychosocial status, hormonal homeostasis, and body fat distribution (6, 7), responses to weight-management strategies are likely to differ by sex. For example, males were reported to get more health benefits from moderate-intensity exercise (8). However, females are significantly more successful on pharmacotherapy for weight loss (9). Moreover, there is no consensus in clinic in terms of the sex-related differences in the weight-loss effect after SG (10, 11). As mentioned above, further research is needed to illustrate the sex differences in the weight-loss effect after SG.

Preoperative prediction of weight loss is helpful not only for defining realistic expectations and maintaining motivation for patients but also for surgeons to select good candidates and reduce failures (12). However, the factors that predict weight loss following SG cannot be conclusively determined (13). Moreover, no sex-specific guidelines for surgical anti-obesity strategies have yet been proposed. Thus, it is of great importance to identify the sex-specific preoperative predictors of weight loss after SG.

Based on a prospective cohort, the present study aims to determine the sex difference in the weight-loss effect after SG indicated by both percentage of total weight loss (TWL%) and excess weight loss (EWL%), and further construct the sex-specific nomograms based on analysis of the sex-specific preoperative predictors of weight loss after SG, providing clinical evidence for the surgical treatment strategy to help achieve better weight loss.

2 Materials and methods

2.1 Study design and patients

The protocol of this study was approved by the Ethics Committee on Scientific Research of Shandong University Qilu Hospital on February 24, 2017. All data were retrieved from a prospectively collected database (SDBMSR, https://sdbmsr.yiducloud.com.cn). The conduction of this study conformed to the principles outlined in the Declaration of Helsinki. Each participant was informed in detail about the purpose, process, potential risks and benefits of the research on the day of admission. All participants signed written informed consent forms before assessment.

2.2 Patients and follow-up

Participants were assessed for eligibility if they were scheduled for SG between November 2020 and January 2022 at University hospital. The exclusion criteria were as follows: (1) uncontrolled mental illness such as schizophrenia, bipolar affective disorder or severe organ dysfunction such as heart failure, respiratory failure; (2) treatment with weight-loss medications; (3) SG as a revision surgery; (4) pregnancy during follow-up; and (5) incomplete follow-up data. Patients were assigned into Male and Female groups according to sex.

All patients underwent follow-up at 1, 3, 6, and 12 months after surgery. The primary outcome was weight loss after surgery evaluated by the TWL% and EWL%. The secondary outcome was the analysis of predictors of weight loss after SG in male and female patients. TWL% was calculated as weight loss/baseline weight × 100%; EWL% was calculated as [preoperative weight - postoperative weight]/[preoperative weight - 23×(body length)^2)] × 100% (14, 15).

2.3 Procedure

All SG operations were performed laparoscopically by the same experienced team as reported before (16). The first step is the greater curvature was dissected free from the omentum starting 2-4 cm from the pylorus and up to the angle of His. After exposure of the left diaphragmatic crus and adequate clearance of the posterior stomach, a vertical gastrectomy was initiated from 4-6 cm proximal to the pylorus with the use of a 36-Fr bougie to create a tubular stomach. Upon discharge, the patient was given suggestions for dietary and physical activities. Dietitians recommend gradually transitioning from liquid to solid foods and achieving energy balance through higher protein, lower fat and lower carbohydrate intake. The exercise prescriber will develop an individualized exercise prescription including training frequency, intensity, time, and type.

2.4 Propensity score matching

Nearest-neighbor matching with caliper was used to balance baseline body mass index (BMI) between the Male and Female groups. Matching was performed with the use of a 1:2 protocol without replacement, with a caliper width equal to 0.2 (17).

2.5 Psychological assessment

The Chinese versions of the Self-Rating Anxiety Scale (SAS) and Self-Rating Depression Scale (SDS) were used to evaluate the psychological situation of anxiety and depression of patients the day before surgery (18, 19). A score above 50 or 53 was defined as anxiety or depression in the SAS and SDS. The levels of anxiety or depression were further classified according to the score.

2.6 Oral glucose tolerance test

Participants underwent a 2-hour oral glucose tolerance test (OGTT) (75 g of glucose in 250 ml water) on the second day of

admission after an overnight fast. Blood samples were collected at 0, 30, 60, and 120 minutes after glucose intake. The plasma levels of glucose and insulin were determined at each time point.

2.7 Body composition by dual-energy X-ray absorptiometry

Visceral fat area, and body fat percentage were determined with dual-energy X-ray absorptiometry using the HOLOGIC DELPHI system with QDR software, v.11.1 (Hologic Bedford, MA, USA). The exams were whole-body scans, all of which were performed in a temperature-controlled laboratory. All operations were carried out by trained researchers according to the manufacturer's instructional protocols. The very few cases with missing data were excluded from the analyses.

2.8 Biochemical analysis

Blood lipid analysis, index of thyroid function, sex hormone, liver and renal function, and the levels of plasma glucose were measured using a Roche Cobas 8000 modular analyzer system (Roche Diagnostics, IN, USA). Plasma insulin was determined by a two-site enzymatic assay using a Tosoh 2000 autoanalyzer (Tosoh Corp., Tokyo, Japan). The homeostasis model assessment of insulin resistance (HOMA-IR) index was calculated as fasting insulin (mU/mL) ×fasting plasma glucose (mmol/L)/22.5.

2.9 Nomogram-based prediction

Candidate clinical predictors included age, BMI, low-density lipoprotein (LDL), high-density lipoprotein (HDL), triglycerides (TG), alanine aminotransferase (ALT), thyroid stimulating hormone (TSH), area under the curve for glucose ($AUC_{glucose}$), area under the curve for insulin ($AUC_{insulin}$), HOMA-IR, estrogen, progesterone, androgen, prolactin, visceral fat area, body fat percentage, SAS score, and SDS score.

There is currently no clear standard for judging postoperative weight loss with respect to TWL%. In order to make more convincing predictions, patients in the Male and Female groups were ranked in descending order separately and further divided into three equal parts according to the 1-year TWL%. Univariate regression analysis was conducted between the one-third of patients with the highest TWL% and the one-third with the lowest TWL% for potential predictive factors. Those with $P < 0.1$ were further analyzed by multivariate regression. The results are shown as odds ratios (ORs) with 95% confidence intervals (CIs). Significant factors ($P < 0.05$) according to the results of the multivariate regression were considered independent predictors and used to establish the nomogram.

The area under the receiver operating characteristic (ROC) curve (AUC) and concordance index (C-index) were used to evaluate the predictive accuracy of the nomogram model. A calibration curve was used to evaluate the accuracy of the prediction. A decision curve analysis (DCA) was performed to assess the clinical usefulness of the nomogram. The nomogram was internally validated for discrimination and calibration by bootstrapping (1000 resamples).

2.10 Statistical analysis

Statistical analysis was performed using SPSS Statistics version 25.0 (SPSS Inc., Chicago, Illinois, US) and R version 4.2.2 (R Foundation for Statistical Computing, Vienna, Austria). Continuous variables that conformed to normal distribution were presented as the means ± SDs and compared using the independent t test; variables without normal distribution were given as median with interquartile range and compared by the Mann–Whitney U test. Categorical variables were shown as numbers with percentages and compared with the chi-squared test or Fisher's exact test. Two-way ANOVA followed by Bonferroni's multiple comparisons was performed to analyze weight loss over time after surgery, and the results were reported as the ^{A}P by group, ^{B}P over time, and ^{C}P due to the interaction of the two factors. The AUC of glucose and insulin during OGTT was calculated by the trapezoidal method. A P value <0.05 was considered to indicate significance.

3 Results

3.1 Baseline characteristics of participants

From the 353 patients assessed for eligibility, 321 patients (95 male and 226 female) were included (Figure 1). The male patients had a significantly higher BMI (45.43 ± 8.59 vs. 40.32 ± 6.95 kg/m^2; P<0.001; Table 1). After propensity score matching (PSM), 85 patients in the Male group and 143 patients in the Female group were preserved with balanced baseline BMI (42.48 ± 6.31 vs. 43.65 ± 6.72 kg/m^2; P=0.152; Table 2). The obesity comorbidities were paired between the two groups. The Male group had higher levels of ALT, TG, $AUC_{glucose}$, and androgen, while having lower levels of HDL, estrogen, progesterone, body fat percentage, SAS score and SDS score (Table 2).

3.2 Weight loss after SG

Along with the decrease in BMI, the TWL% and EWL% continued to increase for up to 1 year after SG in both the Male and Female groups (Figures 2A–C). For the original 321 patients before PSM, although no significant between-group difference was found in TWL% after SG (^{A}P =0.097), the Female group showed a higher EWL% at 6 and 12 months after SG than the Male group (Figure 2C). However, this difference disappeared after PSM by baseline BMI. The Male and Female groups showed comparable BMI, TWL% and EWL% after SG (Figures 2D–F). These results suggest that for selective patients with comparable BMI, sex was not an influencing factor of weight loss for up to 1 year after SG.

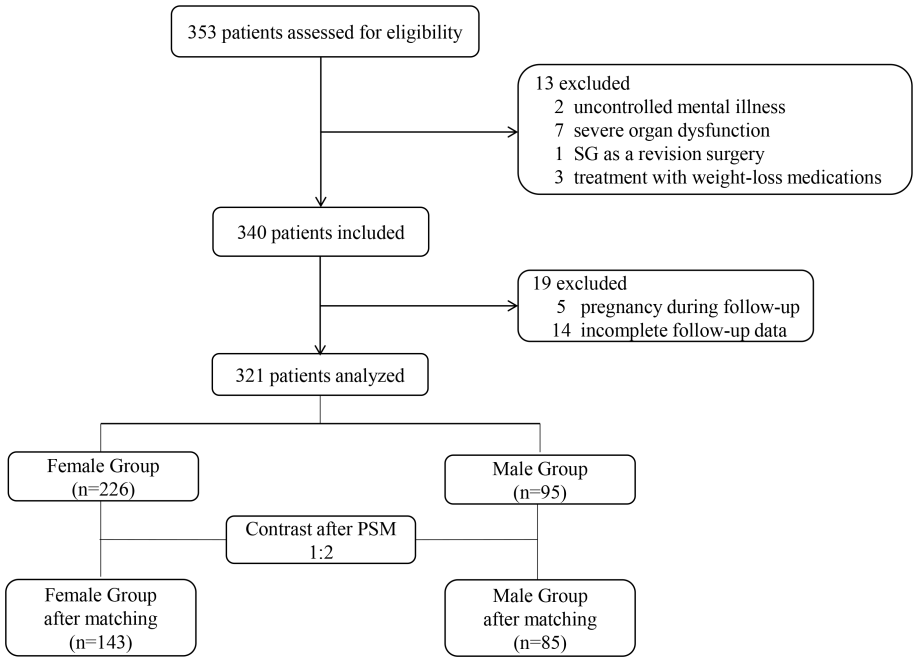

FIGURE 1
Flowchart of participants. SG, sleeve gastrectomy; PSM, propensity score matching.

3.3 Predictor selection and development of the nomogram

Patients with TWL% <27.65% and >35.29% in the Male group as well as those with TWL% <29.26% and >35.49% in the Female group were included in the analysis of predictors. In the multivariate analysis, factors significantly and independently associated with the weight-loss effect in the Male group were baseline BMI [odds ratio (OR) 1.106, 95% confidence interval (CI) 1.019-1.201, *P*=0.016], $AUC_{insulin}$ [OR 1.009, 95% CI 1.002-1.017, *P*=0.010], and progesterone [OR 3.088, 95% CI 1.031-9.256, *P*=0.044]. In the Female group, age [OR 0.929, 95% CI 0.882-0.979, *P*=0.006], baseline BMI [OR 1.076, 95% CI 1.018-1.147, *P*=0.009], TSH [OR 1.473, 95% CI 1.009-1.975, *P*=0.010], and SAS score [OR 1.053, 95% CI 1.003-1.106, *P*=0.038] were associated with the weight-loss effect after SG (Tables 3, 4). These predictor factors were incorporated into the nomogram (Figures 3, 4). Also, the visualization of sex-specific nomogram model of weight loss effect was illustrated in Figure 5.

3.4 Validation and clinical utility of the nomogram for predicting

The AUC of the predicted nomogram was 0.844 (95% CI 0.745-0.943) in the Male group and 0.761 (95% CI 0.685-0.837) in the Female group (Figures 6A, D). The corrected C-index after bootstrapping was 0.818 and 0.738 in the Male and Female groups, respectively. The calibration curves of the nomogram for the predicted weight-loss effect in both groups showed good agreement between prediction and observation (Figures 6B, E). The DCA curve shows the obvious net benefits of the nomogram in both the Male and Female groups (Figures 6C, F).

4 Discussion

The principal findings of the current study were that although there was no sex difference in the weight-loss effect after SG, sex dimorphism exists in predictors of weight loss after SG. For male patients, baseline BMI, $AUC_{insulin}$, and progesterone were independent predictors of weight loss after surgery. For female patients, baseline BMI, age, TSH, and SAS were independent predictors of weight loss after SG.

A marked sex disproportion exists in patients undergoing bariatric metabolic procedures. According to the Fourth IFSO Global Registry Report 2018, female patients was 73.7% among those who underwent the primary procedure (20). Controversy existed for a long time regarding whether male patients could achieve better weight-loss outcomes after bariatric surgery. A recent systematic review collected evidence on this issue and suggested that sex did not have a clear effect on the weight loss efficiency of SG (6). However, that conclusion was weakened by the high heterogeneity and low comparability of the study design, subject characteristics, and follow-up time in the 5 included studies. More specifically, 2 studies favored females, 1 favored males, and 2 showed similar weight loss between sex groups. Moreover, most of the 5 included studies did not have a baseline BMI that was balanced between the Male and Female

10.3389/fendo.2023.1333051

TABLE 1 Baseline characteristics of total participants.

Index	Female (n=226)	Male (n=95)	*P* value
Age, years	32.08 ± 7.28	30.63 ± 7.74	0.112
BMI, kg/m^2	40.32 ± 6.95	45.43 ± 8.59	<0.001
Obesity comorbidities			
T2D, n (%)	67 (29.65%)	43 (45.26%)	0.007
Hypertension, n (%)	99 (43.81%)	62 (65.26%)	<0.001
OSAHS, n (%)	131 (57.57%)	65 (68.42%)	0.079
PCOS, n (%)	81 (35.84%)	N/A	N/A
LDL, mmol/l	3.02 ± 0.70	3.01 ± 0.83	0.980
HDL, mmol/l	1.11 ± 0.21	0.99 ± 0.19	<0.001
ALT, u/l	26 (18, 53)	42 (22, 60)	0.001
TG, mmol/l	1.53 (1.08, 1.98)	1.86 (1.18, 3.20)	0.001
TSH, uIU/ml	2.00 (1.41, 2.97)	1.91 (1.40, 2.72)	0.392
$AUC_{glucose}$	15.83 (13.48, 19.33)	16.48 (14.04, 28.56)	0.137
$AUC_{insulin}$	144.51 (99.90, 219.74)	133.97 (67.06, 238.83)	0.202
HOMA-IR	2.50 (1.80, 3.53)	2.80 (2.00, 3.80)	0.273
Estrogens, pmol/l	176.31 (123.70, 257.61)	137.60 (107.30, 167.50)	<0.001
Progesterone, nmol/l	0.56 (0.31, 1.45)	0.48 (0.32, 0.66)	0.011
Androgen, nmol/l	1.12 (0.73, 1.68)	7.14 (5.17, 10.02)	<0.001
Prolactin, uIU/ml	257.60 (157.92, 342.48)	244.70 (170.40, 314.60)	0.453
Visceral fat area, cm^2	189 (150, 221)	193 (163, 231)	0.080
Body fat percentage, n (%)	43.32 ± 3.91	38.65 ± 5.40	<0.001
SAS	46.68 ± 8.14	45.83 ± 7.98	0.004
Normal, n (%)	130 (57.52%)	68 (71.59%)	
Mild, n (%)	75 (33.19%)	23 (24.21%)	
Moderate, n (%)	21 (9.29%)	4 (4.2%)	
SDS	51.53 ± 9.94	48.20 ± 9.97	0.005
Normal, n (%)	130 (57.52%)	67 (70.53%)	
Mild, n (%)	61 (26.99%)	18 (18.95%)	
Moderate, n (%)	29 (12.83%)	9 (9.47%)	
Severe, n (%)	6 (2.66%)	1 (1.05%)	

Data are presented as n (%), mean ± SD, or median (25th percentile, 75th percentile).
BMI, body mass index; T2D, Type 2 Diabetes; OSAHS, obstructive sleep apnea-hypopnea syndrome; PCOS, polycystic ovary syndrome; N/A, Not Applicable; LDL, low-density lipoprotein; HDL, high-density lipoprotein; ALT, alanine aminotransferase; TG, triglycerides; TSH, thyroid stimulating hormone; $AUC_{glucose}$, area under the curve for glucose; $AUC_{insulin}$, area under the curve for insulin; HOMA-IR, homeostasis model assessment of insulin resistance; SAS, Self-Rating Anxiety Scale; SDS, Self-Rating Depression Scale.

TABLE 2 Basic characteristic data in the Female and Male group after PSM.

Index	Female (n=143)	Male (n=85)	*P* value
Age, years	31.45 ± 7.26	30.86 ± 7.97	0.564
BMI, kg/m^2	42.48 ± 6.31	43.65 ± 6.72	0.152
Obesity comorbidities			
T2D, n (%)	45 (31.47%)	35 (41.18%)	0.137
Hypertension, n (%)	75 (52.45%)	54 (63.53%)	0.103
OSAHS, n (%)	86 (60.14%)	57 (67.06%)	0.296
PCOS, n (%)	51 (35.66%)	N/A	N/A
LDL, mmol/l	3.00 ± 0.70	3.04 ± 0.83	0.707
HDL, mmol/l	1.10 ± 0.19	0.99 ± 0.18	<0.001
ALT, u/l	29 (18, 56)	44 (23, 59)	0.009
TG, mmol/l	1.51 (1.08, 1.94)	2.00 (1.18, 3.36)	<0.001
TSH, uIU/ml	2.14 (1.48, 3.17)	1.86 (1.36, 2.67)	0.094
$AUC_{glucose}$	15.88 (13.27, 19.57)	17.42 (14.23, 23.57)	0.049
$AUC_{insulin}$	147.38 (103.73, 241.96)	126.26 (61.77, 240.10)	0.055
HOMA-IR	2.80 (1.90, 3.60)	2.80 (1.95, 3.75)	0.906
Estrogens, pmol/l	168.70 (121.33, 229.60)	130.60 (130.45, 163.00)	<0.001
Progesterone, nmol/l	0.56 (0.32, 0.97)	0.50 (0.35, 0.66)	0.044
Androgen, nmol/l	1.12 (0.73, 1.69)	7.62 (5.54, 10.49)	<0.001
Prolactin, uIU/ml	260.20 (158.20, 350.20)	240.00 (151.38, 330.15)	0.186
Visceral fat area, cm^2	199.00 (159.00, 228.00)	193.00 (162.00, 228.50)	0.972
Body fat percentage, n (%)	44.22 ± 3.76	37.83 ± 4.89	<0.001
SAS	48.87 ± 7.89	46.09 ± 8.11	0.012
Normal, n (%)	81 (56.64%)	59 (69.41%)	
Mild, n (%)	46 (32.17%)	19 (22.35%)	
Moderate, n (%)	16 (11.19%)	7 (8.24%)	
SDS	51.57 ± 9.96	48.62 ± 9.98	0.032
Normal, n (%)	77 (53.85%)	56 (65.88%)	
Mild, n (%)	43 (30.07%)	19 (22.35%)	
Moderate, n (%)	20 (13.99%)	9 (10.59%)	
Severe, n (%)	3 (2.09%)	1 (1.18%)	

Data are presented as n (%), mean ± SD, or median (25th percentile, 75th percentile).
PSM, propensity score matching; BMI, body mass index; T2D, Type 2 Diabetes; OSAHS, obstructive sleep apnea-hypopnea syndrome; PCOS, polycystic ovary syndrome; N/A, Not Applicable; LDL, low-density lipoprotein; HDL, high-density lipoprotein; ALT, alanine aminotransferase; TG, triglycerides; TSH, thyroid stimulating hormone; $AUC_{glucose}$, area under the curve for glucose; $AUC_{insulin}$, area under the curve for insulin; HOMA-IR, homeostasis model assessment of insulin resistance; SAS, Self-Rating Anxiety Scale; SDS, Self-Rating Depression Scale.

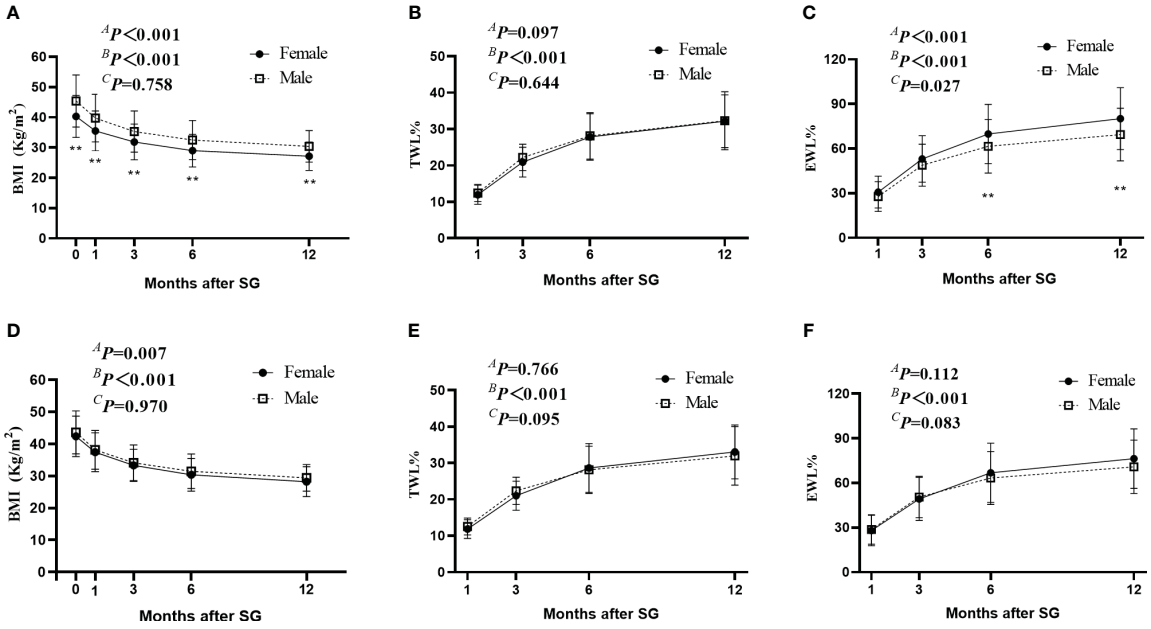

FIGURE 2
Weight-loss effect after SG. **(A–C)** indicated the change of BMI **(A)**, TWL% **(B)**, and EWL% **(C)** after SG in the original cohort before PSM. D-F indicated the change of BMI **(D)**, TWL% **(E)**, and EWL% **(F)** after SG in the Male group and Female group after PSM. ^{A}P by group, ^{B}P over time, and ^{C}P due to the interaction of the two factors. ** P <0.05 SG, sleeve gastrectomy; PSM, propensity score matching; BMI, body mass index; TWL%, percentage of total weight loss; EWL%, percentage of excess weight loss.

groups. In the present study, male patients accounted for 29.56% of the entire cohort with higher BMI before surgery. Our results confirmed that for patients with comparable BMI, no sex difference was detected in the weight-loss effect after SG.

While SG is a well-established and widely performed procedure, there are still concerns that the weight-loss effect of SG cannot catch up with that of Roux-en-Y gastric bypass. The weight-loss effect of SG varied among patients and was affected by a series of factors.

TABLE 3 Factors associated with TWL% at 1 year after sleeve gastrectomy (male).

Factor	Univariate analysis				Multivariate analysis			
	OR	95%CI		*P* value	OR	95%CI		*P* value
Age, years	0.955	0.897	1.017	0.149				
BMI, kg/m^2	1.131	1.046	1.222	0.002	1.106	1.019	1.201	0.016
LDL, mmol/l	1.119	0.580	2.159	0.738				
HDL, mmol/l	0.804	0.051	12.677	0.877				
ALT, u/l	1.010	0.995	1.026	0.196				
TG, mmol/l	0.617	0.407	0.935	0.023				
TSH, uIU/ml	0.848	0.539	1.335	0.477				
$AUC_{glucose}$	0.852	0.774	0.939	0.001				
$AUC_{insulin}$	1.012	1.005	1.019	0.001	1.009	1.002	1.017	0.010
HOMA-IR	1.512	1.039	2.199	0.031				
Estrogens, pmol/l	0.999	0.988	1.010	0.820				
Progesterone, nmol/l	2.465	1.024	5.935	0.044	3.088	1.031	9.256	0.044
Androgen, nmol/l	0.913	0.802	1.038	0.165				
Prolactin, uIU/ml	1.002	0.998	1.007	0.323				

(Continued)

TABLE 3 Continued

Factor	Univariate analysis				Multivariate analysis			
	OR	95%CI		*P* value	OR	95%CI		*P* value
Visceral fat area, cm^2	1.001	0.992	1.010	0.877				
Body fat percentage, n (%)	1.215	1.075	1.374	0.002				
SAS	0.990	0.931	1.053	0.752				
SDS	0.972	0.926	1.021	0.252				

BMI, body mass index; LDL, low-density lipoprotein; HDL, high-density lipoprotein; ALT, alanine aminotransferase; TG, triglycerides; TSH, thyroid stimulating hormone; $AUC_{glucose}$, area under the curve for glucose; $AUC_{insulin}$, area under the curve for insulin; HOMA-IR, homeostasis model assessment of insulin resistance; SAS, Self-Rating Anxiety Scale; SDS, Self-Rating Depression Scale.

Identifying such factors can help surgeons make better care plans for the specific patient and decrease the numbers of revisional patients and nonresponders. Although studies are currently exploring predictors of weight loss after SG, there is no consensus among investigators (21). More importantly, there is a particular lack of sex-specific prediction models. The present study aimed to address this issue based on a prospective cohort.

The present study showed that higher baseline BMI predicted better postoperative weight loss in both sex groups. However, some studies have suggested that patients with a lower BMI tended to have more weight loss after SG (22, 23). This inconsistency could be explained by the discrepancy in the weight-loss metric used. Specifically, those other studies used EWL% or percentage of excess BMI loss (EBMIL%), whereas TWL% was used in the present study. Researchers have referred to the issue as the "Double Booby-Trap" of EWL%/EBMIL% to indicate that the conclusion would be overturned when EWL%/EBMIL% was used instead of TWL% (24). The "Double Booby-Trap" effect worsens with lower baseline BMI due to the algebraic construction of the EWL%/EBMIL%. In fact, many official academic organizations have

TABLE 4 Factors associated with TWL% at 1 year after sleeve gastrectomy (female).

Factor	Univariate analysis				Multivariate analysis			
	OR	95%CI		*P* value	OR	95%CI		*P* value
Age, years	0.925	0.881	0.972	0.002	0.929	0.882	0.979	0.006
BMI, kg/m^2	1.081	1.026	1.139	0.003	1.076	1.018	1.137	0.009
LDL, mmol/l	1.093	0.702	1.702	0.695				
HDL, mmol/l	0.225	0.040	1.246	0.088				
ALT, u/l	0.995	0.986	1.004	0.265				
TG, mmol/l	0.942	0.605	1.465	0.790				
TSH, uIU/ml	1.450	1.089	1.931	0.011	1.473	1.099	1.975	0.010
$AUC_{glucose}$	0.956	0.905	1.010	0.107				
$AUC_{insulin}$	1.002	0.999	1.006	0.133				
HOMA-IR	1.095	0.869	1.380	0.441				
Estrogens, pmol/l	0.999	0.997	1.002	0.554				
Progesterone, nmol/l	0.997	0.920	1.080	0.939				
Androgen, nmol/l	1.506	0.956	2.370	0.077				
Prolactin, uIU/ml	1.001	0.998	1.003	0.597				
Visceral fat area, cm^2	1.003	0.997	1.010	0.284				
Body fat percentage, n (%)	1.117	1.023	1.221	0.014				
SAS	1.049	1.003	1.097	0.036	1.053	1.003	1.106	0.038
SDS	1.023	0.990	1.058	0.175				

BMI, body mass index; LDL, low-density lipoprotein; HDL, high-density lipoprotein; ALT, alanine aminotransferase; TG, triglycerides; TSH, thyroid stimulating hormone; $AUC_{glucose}$, area under the curve for glucose; $AUC_{insulin}$, area under the curve for insulin; HOMA-IR, homeostasis model assessment of insulin resistance; SAS, Self-Rating Anxiety Scale; SDS, Self-Rating Depression Scale.

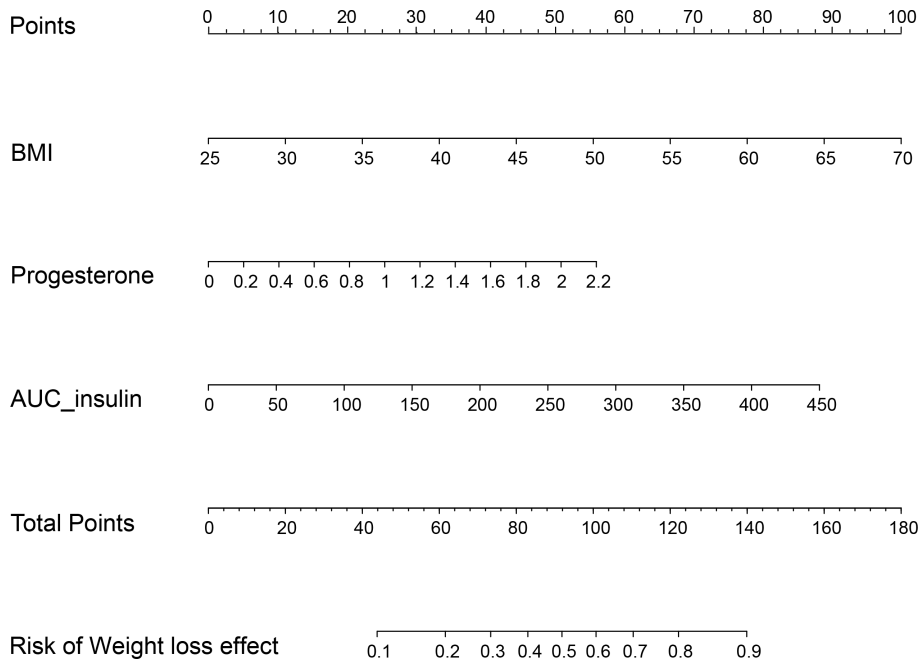

FIGURE 3
Nomogram for prediction of weight loss effect in the Male group. BMI, body mass index; $AUC_{insulin}$, area under the curve for insulin.

recommended using TWL% as an alternative to EWL% (or EBMIL %) as the primary measure of weight loss (25). Studies are needed to provide more evidence on the correlation between baseline BMI and TWL% after SG. Furthermore, the necessity of PSM for baseline BMI was further demonstrated given that baseline BMI was an important predictor of weight loss in both sex groups.

In female patients, age is negatively associated with weight-loss outcomes, as has been demonstrated in a large number of studies

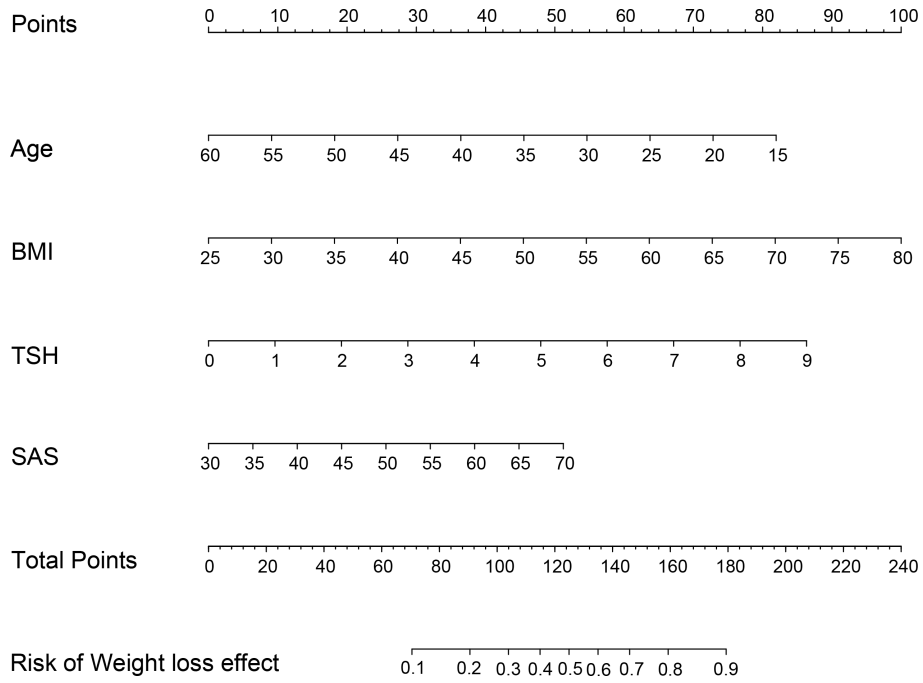

FIGURE 4
Nomogram for prediction of weight loss effect in Female group. BMI, body mass index; TSH, thyroid stimulating hormone; SAS, Self-Rating Anxiety Scale.

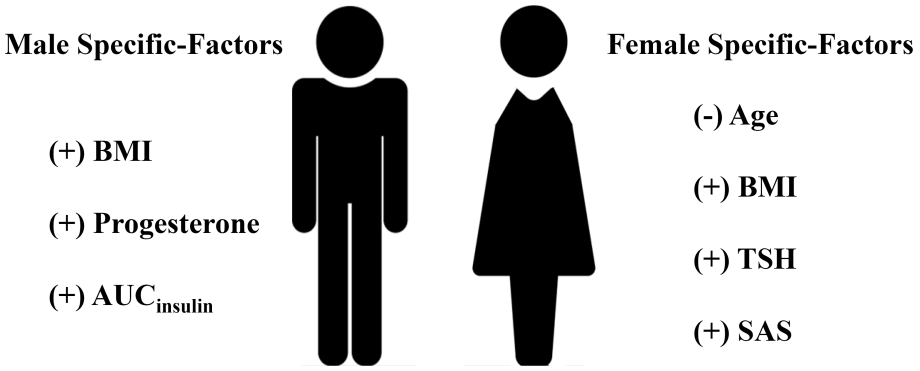

FIGURE 5
Visualization of sex-specific nomogram model of weight loss effect. (+) indicates positive correlation with weight loss effect; (-) indicates negative correlation with weight loss effect. BMI, body mass index; $AUC_{insulin}$, area under the curve for insulin; TSH, thyroid stimulating hormone; SAS, Self-Rating Anxiety Scale.

(26–29). The basal energy expenditure has a tendency to decrease tremendously with age, switching from 60 to 70% of total metabolism around the age of 20–30 to 40% at the age of 50 (30). In addition, younger female obese patients usually have higher motivation for weight loss, probably because of their expectation of regaining self-confidence (31). Our study suggests the necessity for female patients to undergo surgery without delay because older patients need to make more efforts to achieve better weight-loss results.

Female patients with higher preoperative TSH levels achieved better weight-loss outcomes. Clinical studies have demonstrated a positive correlation between obesity and plasma TSH levels (32, 33). A previous study initially reported that the TSH level decreased significantly after SG in euthyroid patients. However, the TSH decrease was not associated with EWL% (34). The exact mechanism leading to a decrease in TSH following SG is not clear. The main explanation, suggested by several studies, is related to a decrease in leptin levels following surgery, which was produced by adipocytes and was shown to have a stimulatory effect on thyroid activity. Muraca et al. reported that baseline TSH levels had no association with weight loss after SG (35). However, as most studies assessing the efficiency of SG failed to report results by sex,

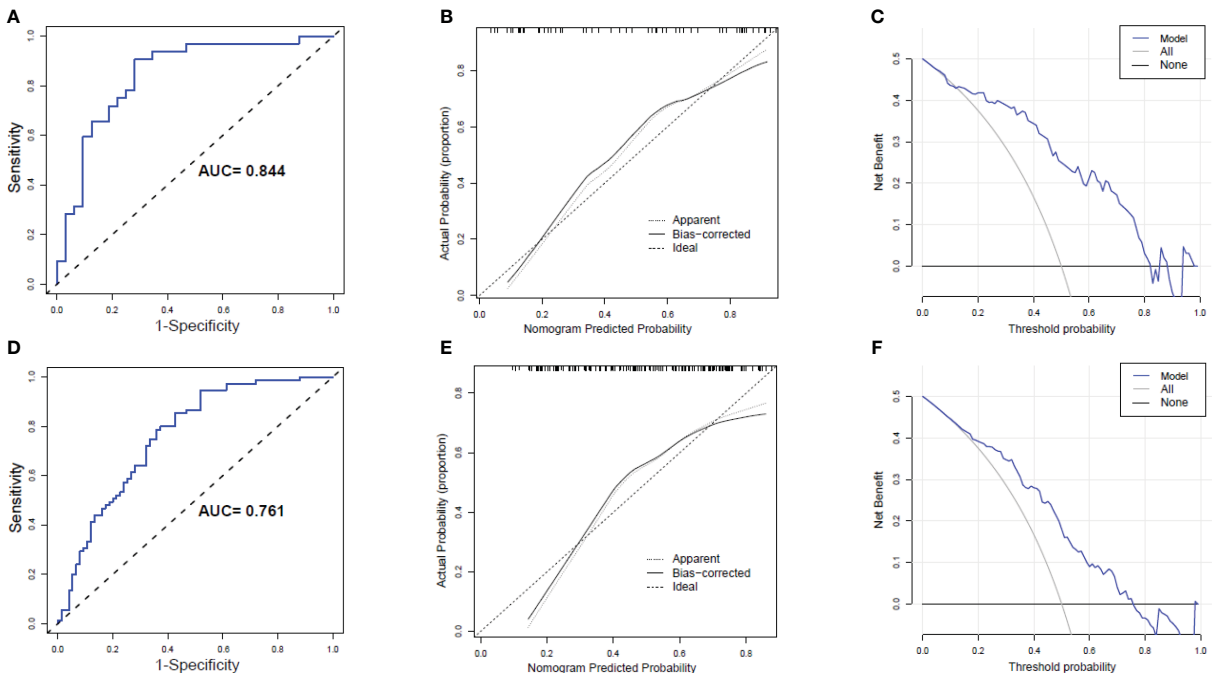

FIGURE 6
Receiver operating characteristic (ROC) curves, Calibration curves and Decision curve analysis (DCA) of the nomogram prediction in the Male group and Female group. **(A)** ROC curves in the Male group; **(B)** Calibration curves of in the Male group. **(C)** DCA in the Male group. **(D)** ROC curves in the Female group; **(E)** Calibration curves of in the Female group. **(F)** DCA in the Female group.

there is still a lack of direct evidence in terms of the correlation between baseline TSH level and the weight-loss effect after SG in female patients. The predictive value of baseline TSH needs to be confirmed by further studies.

The rate of psychological behavior abnormalities among obese people who are willing to undergo bariatric surgery is as high as 70% (36). In the present study, preoperative anxiety was another positive predictor of weight loss in female patients. These results are believed to be related to the increased adherence to the postoperative instructions and were consistent with those of previous studies (37, 38). A study published in 2022 revealed an interesting trajectory in which patients with higher levels of anxiety lost the most weight 12 months after bariatric surgery but tended to regain more weight 30 months after surgery (39). The mechanisms by which anxiety contributes to this trajectory should be examined in future research. Our study suggested that female patients are more susceptible to the impact of anxiety. For female patients, the identification and intervention of psychological disorders, especially those associated with anxiety, is of vital importance.

In the present study, higher levels of progesterone predicted better weight-loss outcomes in male patients. Although little is known about the physiology, endocrinology, and pharmacology of progesterone in male, it has been found that progesterone can bind to certain receptors in adipose tissue and regulate lipoprotein lipase, thereby increasing fat accumulation (40). In addition, progesterone can synergize with estrogen to reduce lipolysis and promote fat accumulation (41). Unfortunately, there is limited evidence on the alteration of progesterone after SG in male patients, let alone its effect on or correlation with weight loss. A meta-analysis published in 2019 reported the impact of bariatric surgery on male sex hormones (42). However, no progesterone data were included. Based on our prediction model, progesterone may play specific physiological and pathophysiological roles in the weight-loss effect after SG in male. Further studies are needed.

Insulin resistance is the fundamental pathophysiological change in obesity. An increase in body weight induces insulin resistance and compensates for hyperinsulinemia, resulting in fat accumulation and metabolic disorders (43). $AUC_{insulin}$ represents the total amount of insulin secretion after oral glucose load and can indicate insulin resistance to some extent (44). Our previous study confirmed the great effect of SG on the remission of insulin resistance (16), and the decrease in $AUC_{insulin}$ after SG was related to weight loss after surgery. Therefore, patients with higher levels of $AUC_{insulin}$ are likely to benefit more from surgery to achieve better weight loss. The present study confirmed that $AUC_{insulin}$ was another positive predictor of weight loss after SG in male patients.

The major strength of the present study is that the sex-specific preoperative predictors of weight loss after SG were explored from a comprehensive set of clinical variables based on a prospective cohort. Our study has several limitations. First, the 1-year follow-up time was not long enough. However, the period of weight loss after SG is approximately 1 year, and the longer-term outcome may be affected by more factors in addition to surgery. Second, due to the single-center design and limited sample size, the predictive model was validated internally by bootstrapping and needs to be further confirmed by external validation.

5 Conclusion

The sex was not an influencing factor of weight loss for up to 1 year after SG. However, sex dimorphism still exists in terms of the preoperative predictors of weight loss after SG. For different sex groups, there could be differences in the focus of preoperative evaluation in regard to the weight-loss effect. Research with multi-centered design and long-term follow-up as well as the mechanism of TSH affecting the weight loss effect are of great significance in the future.

Data availability statement

The raw data supporting the conclusions of this article will be made available by the authors, without undue reservation.

Ethics statement

The studies involving humans were approved by Ethics Committee on Scientific Research of Shandong University Qilu Hospital. The patients/participants provided their written informed consent to participate in this study.

Author contributions

JS: Data curation, Formal Analysis, Writing – original draft. TZ: Data curation, Formal Analysis, Writing – original draft. SX: Data curation, Formal Analysis, Writing – original draft. TL: Supervision, Validation, Writing – original draft. YZ: Supervision, Validation, Writing – original draft. XH: Funding acquisition, Writing – review & editing, Writing – original draft. SL: Funding acquisition, Writing – review & editing, Writing – original draft.

Funding

The author(s) declare financial support was received for the research, authorship, and/or publication of this article. This study was funded by grants from the National Natural Science Foundation of China (82100853), the Natural Science Foundation of Shandong Province of China (ZR2021QH028), and the Clinical Research Project of Shandong University (2020SDUCRCC024).

Acknowledgments

The authors thank the nursing staff of the Department of General Surgery, Qilu Hospital of Shandong University, for their

expert assistance in performing the studies, and all the patients included and their families for their cooperation.

Conflict of interest

The authors declare that the research was conducted in the absence of any commercial or financial relationships that could be construed as a potential conflict of interest.

Publisher's note

References

1. World Health Organization. *World Obesity Atlas* (2023). Available at: https://www.worldobesity.org/resources/resource-library/world-obesity-atlas-2023.

2. Testa G, Granero R, Siragusa C, Belligoli A, Sanna M, Rusconi ML, et al. Psychological predictors of poor weight loss following LSG: relevance of general psychopathology and impulsivity. *Eat Weight Disord* (2020) 25(6):1621–9. doi: 10.1007/s40519-019-00800-x

3. Chung AY, Thompson R, Overby DW, Duke MC, Farrell TM. Sleeve gastrectomy: surgical tips. *J Laparoendosc Adv Surg Tech A.* (2018) 28(8):930–7. doi: 10.1089/lap.2018.0392

4. Franken RJ, Sluiter NR, Franken J, de Vries R, Souverein D, Gerdes VEA, et al. Treatment options for weight regain or insufficient weight loss after sleeve gastrectomy: a systematic review and meta-analysis. *Obes Surg* (2022) 32(6):2035–46. doi: 10.1007/s11695-022-06020-0

5. Apovian CM. Obesity: definition, comorbidities, causes, and burden. *Am J Manag Care* (2016) 22(7 Suppl):s176–85.

6. Risi R, Rossini G, Tozzi R, Pieralice S, Monte L, Masi D, et al. Sex difference in the safety and efficacy of bariatric procedures: a systematic review and meta-analysis. *Surg Obes Relat Dis* (2022) 18(7):983–96. doi: 10.1016/j.soard.2022.03.022

7. Palmer BF, Clegg DJ. The sexual dimorphism of obesity. *Mol Cell Endocrinol* (2015) 402:113–9. doi: 10.1016/j.mce.2014.11.029

8. Bhogal MS, Langford R. Gender differences in weight loss; evidence from a NHS weight management service. *Public Health* (2014) 128(9):811–3. doi: 10.1016/j.puhe.2014.06.019

9. Cooper AJ, Gupta SR, Moustafa AF, Chao AM. Sex/Gender Differences in Obesity Prevalence, Comorbidities, and Treatment. *Curr Obes Rep*. (2001) 10(4):458–66. doi: 10.1007/s13679-021-00453-x

10. Groth D, Woźniewska P, Olszewska M, Zabielski P, Ładny JR, Dadan J, et al. Gender-related metabolic outcomes of laparoscopic sleeve gastrectomy in 6-month follow-up. *Wideochir Inne Tech Maloinwazyjne.* (2020) 15(1):148–56. doi: 10.5114/wiitm.2019.86800

11. Perrone F, Bianciardi E, Benavoli D, Tognoni V, Niolu C, Siracusano A, et al. Gender influence on long-term weight loss and comorbidities after laparoscopic sleeve gastrectomy and roux-en-Y gastric bypass: a prospective study with a 5-year follow-up. *Obes Surg* (2016) 26(2):276–81. doi: 10.1007/s11695-015-1746-z

12. Seyssel K, Suter M, Pattou F, Caiazzo R, Verkindt H, Raverdy V, et al. A predictive model of weight loss after roux-en-Y gastric bypass up to 5 years after surgery: a useful tool to select and manage candidates to bariatric surgery. *Obes Surg* (2018) 28(11):3393–9. doi: 10.1007/s11695-018-3355-0

13. Andersen JR, Aadland E, Nilsen RM, Våge V. Predictors of weight loss are different in men and women after sleeve gastrectomy. *Obes Surg* (2014) 24(4):594–8. doi: 10.1007/s11695-013-1124-7

14. Snehalatha C, Viswanathan V, Ramachandran A. Cutoff values for normal anthropometric variables in asian Indian adults. *Diabetes Care* (2003) 26(5):1380–4. doi: 10.2337/diacare.26.5.1380

15. van de Laar AW, van Rijswijk AS, Kakar H, Bruin SC. Sensitivity and specificity of 50% Excess weight loss (50%EWL) and twelve other bariatric criteria for weight loss success. *Obes Surg* (2018) 28(8):2297–304. doi: 10.1007/s11695-018-3173-4

16. Huang X, Zhao Y, Liu T, Wu D, Shu J, Yue W, et al. β-cell function and insulin dynamics in obese patients with and without diabetes after sleeve gastrectomy. *Diabetes*. doi: 10.2337/db22-1048

17. Witzel S, Maier A, Steinbach R, Grosskreutz J, Koch JC, Sarikidi A, et al. Safety and Effectiveness of Long-term Intravenous Administration of Edaravone for Treatment of Patients With Amyotrophic Lateral Sclerosis [published correction appears in JAMA Neurol. *JAMA Neurol* (2022) 79(2):121–30. doi: 10.1001/jamaneurol.2021.4893

18. Zung WW. A rating instrument for anxiety disorders. *Psychosomatics.* (1971) 12 (6):371–9. doi: 10.1016/S0033-3182(71)71479-0

19. ZUNG WW. A SELF-RATING DEPRESSION SCALE. *Arch Gen Psychiatry* (1965) 12:63–70. doi: 10.1001/archpsyc.1965.01720310065008

20. Welbourn R, Hollyman M, Kinsman R, Dixon J, Liem R, Ottosson J, et al. Bariatric surgery worldwide: baseline demographic description and one-year outcomes from the fourth IFSO global registry report 2018. *Obes Surg* (2019) 29(3):782–95. doi: 10.1007/s11695-018-3593-1

21. Cottam S, Cottam D, Cottam A. Sleeve gastrectomy weight loss and the preoperative and postoperative predictors: a systematic review. *Obes Surg* (2019) 29 (4):1388–96. doi: 10.1007/s11695-018-03666-7

22. Martin DJ, Lee CM, Rigas G, Tam CS. Predictors of weight loss 2 years after laparoscopic sleeve gastrectomy. *Asian J Endosc Surg* (2015) 8(3):328–32. doi: 10.1111/ases.12193

23. Binda A, Jaworski P, Kudlicka E, Ciesielski A, Cabaj H, Tarnowski W. The impact of selected factors on parameters of weight loss after sleeve gastrectomy. *Wideochir Inne Tech Maloinwazyjne.* (2016) 11(4):288–94. doi: 10.5114/wiitm.2016.64999

24. van de Laar AW. The %EBMIL/%EWL double booby-trap. A comment on studies that compare the effect of bariatric surgery between heavier and lighter patients. *Obes Surg* (2016) 26(3):612–3. doi: 10.1007/s11695-015-1967-1

25. van de Laar AW, Emous M, Hazebroek EJ, Boerma EJ, Faneyte IF, Nienhuijs SW. Reporting weight loss 2021: position statement of the dutch society for metabolic and bariatric surgery (DSMBS). *Obes Surg* (2021) 31(10):4607–11. doi: 10.1007/s11695-021-05580-x

26. Akhtar SJ, Helmer SD, Quinn KR, Lancaster BA, Howes JL, Brown NM. The effect of insurance status on bariatric surgery outcomes: A retrospective chart review study. *Am Surg* (2023) 89(5):1887–92. doi: 10.1177/00031348221074245

27. El Ansari W, Elhag W. Preoperative prediction of body mass index of patients with type 2 diabetes at 1 year after laparoscopic sleeve gastrectomy: cross-sectional study. *Metab Syndr Relat Disord* (2022) 20(6):360–6. doi: 10.1089/met.2021.0153

28. Janik MR, Rogula TG, Mustafa RR, Saleh AA, Abbas M, Khaitan L. Setting realistic expectations for weight loss after laparoscopic sleeve gastrectomy. *Wideochir Inne Tech Maloinwazyjne.* (2019) 14(3):415–9. doi: 10.5114/wiitm.2019.81661

29. Nagao Y, Diana M, Vix M, D'Urso A, Mutter D, Marescaux J. Age impact on weight loss and glycolipid profile after laparoscopic sleeve gastrectomy: experience with 308 consecutive patients. *Surg Endosc.* (2014) 28(3):803–10. doi: 10.1007/s00464-013-3261-4

30. Ferrucci L, Schrack JA, Knuth ND, Simonsick EM. Aging and the energetic cost of life. *J Am Geriatr Soc* (2012) 60(9):1768–9. doi: 10.1111/j.1532-5415.2012.04102.x

31. Theunissen CMJ, van Vlijmen A, Tak DJAM, Nykliček I, de Jongh MAC, Langenhoff BS. Motivation and weight loss expectations in bariatric surgery candidates: association with 1- and 2-year results after bariatric surgery. *Obes Surg* (2020) 30 (11):4411–21. doi: 10.1007/s11695-020-04811-x

32. Aykota MR, Atabey M. Effect of sleeve gastrectomy on thyroid-stimulating hormone levels in morbidly obese patients with normal thyroid function. *Eur Rev Med Pharmacol Sci* (2021) 25(1):233–40. doi: 10.26355/eurrev_202101_24389

33. Salman MA, Rabiee A, Salman A, Qassem MG, Ameen MA, Hassan AM, et al. Laparoscopic sleeve gastrectomy has A positive impact on subclinical hypothyroidism among obese patients: A prospective study. *World J Surg* (2021) 45(10):3130–7. doi: 10.1007/s00268-021-06201-5

34. Abu-Ghanem Y, Inbar R, Tyomkin V, Kent I, Berkovich L, Ghinea R, et al. Effect of sleeve gastrectomy on thyroid hormone levels. *Obes Surg* (2015) 25(3):452–6. doi: 10.1007/s11695-014-1415-7

35. Muraca E, Oltolini A, Pizzi M, Villa M, Manzoni G, Perra S, et al. Baseline TSH levels and short-term weight loss after different procedures of bariatric surgery. *Int J Obes (Lond).* (2021) 45(2):326–30. doi: 10.1038/s41366-020-00665-6

36. Fuchs HF, Laughter V, Harnsberger CR, Broderick RC, Berducci M, DuCoin C, et al. Patients with psychiatric comorbidity can safely undergo bariatric surgery with equivalent success. *Surg Endosc.* (2016) 30(1):251–8. doi: 10.1007/s00464-015-4196-8

37. Agüera Z, García-Ruiz-de-Gordejuela A, Vilarrasa N, Sanchez I, Baño M, Camacho L, et al. Psychological and personality predictors of weight loss and comorbid metabolic changes after bariatric surgery. *Eur Eat Disord Rev* (2015) 23 (6):509–16. doi: 10.1002/erv.2404

38. Kinzl JF, Schrattenecker M, Traweger C, Mattesich M, Fiala M, Biebl W. Psychosocial predictors of weight loss after bariatric surgery. *Obes Surg* (2006) 16 (12):1609–14. doi: 10.1381/096089206779319301

39. Aylward L, Lilly C, Tabone L, Szoka N, Abunnaja S, Cox S. Anxiety predicts reduced weight loss 30 months after bariatric surgery. *Surg Obes Relat Dis* (2022) 18 (7):919–27. doi: 10.1016/j.soard.2022.04.007

40. Hatta H, Atomi Y, Shinohara S, Yamamoto Y, Yamada S. The effects of ovarian hormones on glucose and fatty acid oxidation during exercise in female ovariectomized rats. *Horm Metab Res* (1988) 20(10):609–11. doi: 10.1055/s-2007-1010897

41. Campbell SE, Febbraio MA. Effects of ovarian hormones on exercise metabolism. *Curr Opin Clin Nutr Metab Care* (2001) 4(6):515–20. doi: 10.1097/00075197-200111000-00009

42. Lee Y, Dang JT, Switzer N, Yu J, Tian C, Birch DW, et al. Impact of bariatric surgery on male sex hormones and sperm quality: a systematic review and meta-analysis. *Obes Surg* (2019) 29(1):334–46. doi: 10.1007/s11695-018-3557-5

43. Barazzoni R, Gortan Cappellari G, Ragni M, Nisoli E. Insulin resistance in obesity: an overview of fundamental alterations. *Eat Weight Disord* (2018) 23(2):149–57. doi: 10.1007/s40519-018-0481-6

44. Liu PY, Lawrence-Sidebottom D, Piotrowska K, Zhang W, Iranmanesh A, Auchus RJ, et al. Clamping cortisol and testosterone mitigates the development of insulin resistance during sleep restriction in men. *J Clin Endocrinol Metab* (2021) 106 (9):e3436–48. doi: 10.1210/clinem/dgab375

frontiers | Frontiers in Endocrinology

TYPE Original Research
PUBLISHED 30 January 2024
DOI 10.3389/fendo.2024.1333033

OPEN ACCESS

EDITED BY
Lidia Castagneto Gissey,
Sapienza University of Rome, Italy

REVIEWED BY
Pedro Iglesias,
Puerta de Hierro University Hospital Majadahonda, Spain
Sandra Incerpi,
Roma Tre University, Italy

*CORRESPONDENCE
Yuntao Nie
nytnyt1231@163.com
Hua Meng
menghuade@hotmail.com

†These authors have contributed equally to this work

RECEIVED 04 November 2023
ACCEPTED 11 January 2024
PUBLISHED 30 January 2024

CITATION
Tian Z, Nie Y, Li Z, Wang P, Zhang N, Hei X, Ping A, Liu B and Meng H (2024) Total weight loss induces the alteration in thyroid function after bariatric surgery.
Front. Endocrinol. 15:1333033.
doi: 10.3389/fendo.2024.1333033

Total weight loss induces the alteration in thyroid function after bariatric surgery

Ziru Tian[1,2†], Yuntao Nie[1*†], Zhengqi Li[1], Pengpeng Wang[1], Nianrong Zhang[1], Xiaofan Hei[3], An Ping[2], Baoyin Liu[1] and Hua Meng[1*]

[1]Department of General Surgery & Obesity and Metabolic Disease Center, China-Japan Friendship Hospital, Beijing, China, [2]School of Basic Medical Sciences, Capital Medical University, Beijing, China, [3]Department of Emergency, China-Japan Friendship Hospital, Beijing, China

Background: Bariatric surgery is an effective approach to weight loss, which may also affect thyroid function. However, alteration in thyroid-stimulating hormone (ΔTSH) and thyroid hormones after bariatric surgery and the relationship between thyroid function and postoperative weight loss still remains controversial.

Methods: Data were collected from euthyroid patients with obesity who underwent sleeve gastrectomy and Roux-en-Y gastric bypass from 2017 to 2022. The alterations of free thyroxine (FT4), free triiodothyronine (FT3), total thyroxine (TT4), total triiodothyronine (TT3), and TSH were calculated 1 year after surgery. Pearson correlation analysis was used to assess the correlation between the percentage of total weight loss (%TWL) and ΔTSH. Multivariable linear regression was utilized to determine the association between %TWL and ΔTSH.

Results: A total of 256 patients were included in our study. The mean %TWL was 28.29% after 1 year. TSH decreased from 2.33 (1.67, 3.04) uIU/mL to 1.82 (1.21, 2.50) uIU/mL ($P < 0.001$), FT3 decreased from 3.23 ± 0.42 pg/mL to 2.89 ± 0.41 pg/mL ($P < 0.001$), FT4 decreased from 1.11 ± 0.25 ng/dL to 1.02 ± 0.25 ng/dL ($P < 0.001$), TT3 decreased from 1.13 (1.00, 1.25) ng/mL to 0.89 (0.78, 1.00) ng/mL ($P < 0.001$), and TT4 decreased from 8.28 ± 1.69 ug/mL to 7.82 ± 1.68 ug/mL 1 year postoperatively ($P < 0.001$). %TWL was found to be significantly correlated to ΔTSH by Pearson correlation analysis (Pearson correlation coefficient = 0.184, $P = 0.003$), indicating that the more weight loss, the more TSH declined. After adjusting for covariates in multivariable linear regression, %TWL was found to be independently associated with ΔTSH (β = 0.180 [95% confidence interval (CI), 0.048 – 0.312], $P = 0.008$). Moreover, %TWL was divided into 3 categorical groups (%TWL ≤ 25%, 25% < %TWL ≤ 35%, and %TWL > 35%) for further exploration, and was also found to be an independent predictor for ΔTSH after adjusting for covariates in multivariable linear regression (β = 0.153 [95% CI, 0.019 – 0.287], $P = 0.025$).

10.3389/fendo.2024.1333033

Conclusion: TSH, FT4, FT3, TT4, and TT3 decrease significantly 1 year after bariatric surgery. The decline in TSH is independently mediated by postoperative weight loss; the more the weight loss, the more the TSH decrease.

KEYWORDS

bariatric surgery, sleeve gastrectomy, Roux-en-Y gastric bypass, thyroid function, weight loss

1 Introduction

Obesity has emerged as a global health concern, accompanied by a variety of endocrine comorbidities, including thyroid dysfunction (1). Evidence has shown that body weight is associated with thyroid function, in which obesity can lead to a higher risk of overt or subclinical hypothyroidism (2). In contrast, weight loss may have the potential to ameliorate abnormalities in blood glucose and lipids, reduce the inflammatory state of the body, and protect the thyroid gland (3).

Bariatric surgery has been demonstrated to be an effective and permanent approach to weight loss, with sleeve gastrectomy (SG) and Roux-en-Y gastric bypass (RYGB) being the most commonly performed procedures (4, 5). Based on previous literature, bariatric surgery was associated with the relief of thyroid dysfunction, alleviating overt or subclinical hypothyroidism, and reducing the need for thyroid hormone-lowering therapy (6, 7). These effects may be attributed to the declines in serum levels of leptin, adipokines, and ghrelin levels after surgery (8, 9). However, changes in thyroid-stimulating hormone (TSH) after bariatric surgery reported by different studies varied dramatically. TSH levels were found to decline significantly following bariatric surgery in the majority of studies involving patients with subclinical or overt hypothyroidism (10–12). Similar results have been noted in a number of researches involving patients with normal thyroid function (13–15). Nonetheless, a retrospective study by MacCuish et al. (16) including 55 euthyroid patients undergoing RYGB found that TSH levels remained steady after 2 years. Dall'Asta et al. (17) conducted a retrospective study in 258 euthyroid patients who had received gastric banding also failed to find a significant change in TSH postoperatively. The effect of bariatric surgery on the serum levels of free triiodothyronine (FT3) and free thyroxine (FT4) is not yet fully understood. Patients from different countries who underwent various surgical procedures were reported to exhibit elevated, unchanged, or decreased FT3 and FT4 levels following surgery in prior studies (15, 18, 19). A recent meta-analysis in 2017 revealed that FT3 decreased in euthyroid individuals after bariatric surgery, while FT4 remained unchanged (20). Therefore, the impact of weight loss following bariatric surgery on thyroid function in euthyroid patients with obesity remains controversial.

The aim of our study was to investigate the alterations in TSH and thyroid hormones 1 year after bariatric surgery in euthyroid patients with obesity, and explore the relationship between the percentage of total weight loss (%TWL) and alterations of TSH (ΔTSH).

2 Materials and methods

2.1 Study design and participants

This is a retrospective observational analysis of prospectively collected data of patients with obesity who underwent SG or RYGB at China-Japan Friendship Hospital from September 2017 to May 2022. All the patients were selected for bariatric surgery according to the Chinese Surgical Guideline for Obesity and Type 2 Diabetes by the Chinese Society for Metabolic and Bariatric Surgery (CSMBS) (21). The inclusion criteria were (1) patients with obesity (BMI ≥ 27.5 kg/m^2 according to Chinese guidelines (21), and guidelines from the American Society for Metabolic and Bariatric Surgery and International Federation for the Surgery of Obesity and Metabolic Disorders (5)), (2) age between 16 and 65 years, (3) complete preoperative and postoperative thyroid function tests, and (4) normal preoperative TSH (< 0.50 uIU/mL or > 4.80 uIU/mL) and FT4 (< 0.58 ng/dL or > 1.75 ng/dL) levels. Patients with a history of pituitary and/or thyroid disease, abnormal thyroid hormone levels, a history of drug application that might affect thyroid function (e.g. amiodarone, lithium, anticonvulsants, and glucocorticoids), and those who had undergone a second bariatric surgery were excluded from the study. Patients with a metformin usage history were not excluded because it is commonly used in patients with obesity and type 2 diabetes mellitus (T2DM), despite it might affect thyroid function.

This study was performed in accordance with the Helsinki Declaration and was approved by the Institutional Review Board (IRB) of China-Japan Friendship Hospital (2021-112-K70). Informed consent was waived by the IRB because the study was observational and noninvasive.

2.2 Variables collection

All sociodemographic variables were extracted from the electronic medical record system, including sex, age, height,

weight, waist circumstance, hip circumstance, type of surgery, T2DM, hypertension, systolic blood pressure, diastolic blood pressure, smoking history, and alcohol consumption. The T2DM was diagnosed according to the American Diabetes Association guidelines (22), including fasting plasma glucose (FPG) ≥ 7.0 mmol/L and/or 2-h plasma glucose ≥ 11.1 mmol/L during oral glucose tolerance test and/or glycated hemoglobin (HbA1c) ≥ 6.5% and/or patients with classic symptoms of hyperglycemia or hyperglycemic crisis, a random plasma glucose ≥ 11.1 mmol/L and/or a diagnosis of T2DM in the past. Diagnosis of hypertension was based on systolic blood pressure ≥ 140 mmHg and/or diastolic blood pressure ≥ 90 mmHg and/or a history of hypertension (23).

The biochemical variables of blood samples were collected and examined within a week preoperatively, including TSH, thyroid hormones, lipid profiles, and glycemic profiles, et al. The serum levels of TSH, FT4, FT3, total thyroxine (TT4), and total triiodothyronine (TT3) were measured by electrochemiluminescence immunoassay. The enzymatic colorimetric method was utilized to measure the serum levels of FPG, while HbA1c was measured by high-performance liquid chromatography. Total cholesterol (TC) and total triglyceride (TG) were measured by standard enzymatic methods. The serum levels of high-density lipoprotein cholesterol (HDL-C) and low-density lipoprotein cholesterol (LDL-C) were measured by the direct method. The normal ranges for all biochemical variables are listed in Supplementary Table 1.

In addition, the alterations of clinical parameters were calculated by subtracting the levels at baseline from the levels at 1 year, and the %TWL was calculated from the follow-up data.

2.3 Surgical procedures

Symmetric three-port laparoscopic SG and RYGB were performed as described in our previous studies (24, 25). The patients were positioned supine, with their arms extended laterally and their legs joined. Laparoscopic SG was performed over a 36-Fr bougie, with the sleeve beginning 4-6 cm from the pylorus. Laparoscopic RYGB was performed using a standard 30 mL pouch, a biliopancreatic limb measuring 100 cm, and a Roux limb measuring 100 cm. Gastrojejunostomy was made with a linear stapler with hand-sewn defect closure. Patients with a long duration of T2DM, weakened islet function, or severe gastroesophageal reflux disease symptoms were recommended RYGB as a priority, but patient preference was also considered.

2.4 Postoperative management

All patients were instructed to take a daily oral micronutrient/multivitamin supplement (Centrum®), which contained the following nutrients: vitamin A (4000 IU), vitamin D (400 IU), vitamin E (30 IU), vitamin B1 (1.5 mg), vitamin B2 (1.7 mg), vitamin B6 (2 mg), vitamin C (60 mg), vitamin B12 (6 μg), folate (400 μg), calcium (162 mg), iron (18 mg), zinc (15 mg), and magnesium (100 mg). This supplementation regimen was advised to be continued for at least 1 year for patients undergoing SG, and a lifelong duration for patients undergoing RYGB.

Follow-up were scheduled at 3 months, 6 months, 1 year postoperatively, and subsequently on an annual basis. Various parameters including weight, blood pressure, and biochemical tests were regularly monitored during these follow-ups.

2.5 Statistical analysis

Continuous variables were presented as means ± standard deviation (SD) for normal data and medians with interquartile range for non-normal data, and the categorical variables were shown as frequency (percentage). The changes between clinical variables at baseline and 1 year postoperatively were tested by paired sample t-test or the Mann-Whitney U test. Differences between groups were evaluated by analysis of variance (ANOVA) tests for continuous data. Correlation between ΔTSH and %TWL was determined using the Pearson correlation analysis, in which a $P < 0.05$ indicated the presence of a significant correlation. The %TWL was utilized as both continuous and categorical variables (%TWL group) to explore their relationship with ΔTSH. The %TWL group was divided as follows: %TWL ≤ 25%, 25% < %TWL ≤ 35%, and %TWL > 35%. The univariable and multivariable stepwise linear regression was conducted to examine the association between ΔTSH and %TWL. Three linear regression models were performed. The Model 1 was unadjusted; Model 2 adjusted for sex, age, and body mass index (BMI); The Model 3 further adjusted for waist-to-hip ratio, type of surgery, T2DM, metformin use, hypertension, smoking history, and alcohol consumption. In addition, the subgroup analysis was conducted to assess whether the potential covariates (sex, age, BMI, T2DM, metformin use, and hypertension) modified the relationship between ΔTSH and %TWL using multivariable linear regression models with full adjustment in Model 3. The significance level was a $P < 0.05$ in all tests. Data analysis was carried out with SPSS version 24 and R 4.1.3 software (https://r-project.org/).

3 Results

3.1 Patient characteristics

The clinical characteristics of patients are summarized in Table 1. A total of 256 patients were included in the study, 64.8% of patients were female, and their median age was 35.00 (29.00, 43.75) years. The baseline average BMI was 38.37 ± 7.24 kg/m^2, and the mean waist-to-hip ratio was 0.96 ± 0.08. Two hundred and two (78.9%) patients underwent SG, and 54 (21.1%) underwent RYGB. Among these patients, 148 (57.8%) were diagnosed as T2DM, and 75 (29.30%) had a history of metformin use. One-hundred and nine (46.4%) patients were diagnosed as hypertension, and the mean

10.3389/fendo.2024.1333033

TABLE 1 Patient characteristics.

Variables	Total (N = 256)
Female (%)	166 (64.84)
Age (years)	35.00 (29.00 43.75)
Height (cm)	168.00 (162.25, 175.00)
Weight (kg)	107.00 (91.00, 123.75)
BMI (kg/m^2)	38.37 ± 7.24
Waist (cm)	117.62 ± 16.06
Hip (cm)	121.89 ± 14.46
Waist-to-hip ratio	0.96 ± 0.08
T2DM (%)	148 (57.8)
Metformin use (%)	75 (29.30)
Hypertension (%)	119 (46.4)
SBP (mmHg)	138.08 ± 19.57
DBP (mmHg)	87.16 ± 15.28
Smoking history (%)	47 (18.36)
Alcohol consumption (%)	37 (14.45)
Type of surgery	
SG (%)	202 (78.91)
RYGB (%)	54 (21.09)

Abbreviations: BMI, body mass index; DBP, diastolic blood pressure; RYGB, Roux-en-Y gastric bypass; SBP, systolic blood pressure; SG, sleeve gastrectomy; T2DM, type 2 diabetes mellitus.

systolic blood pressure was 138.08 ± 19.57 mmHg, and the diastolic blood pressure was 87.16 ± 15.28 mmHg.

3.2 Postoperative weight loss

The body weight of all the patients decreased from 110.57 ± 27.42 kg at baseline to 88.37 ± 21.76 at 3 months, 81.45 ± 19.11 at 6 months, and 77.86 ± 17.08 kg at 1 year. The %TWL was 20.08 ± 6.39% at 3 months, 25.57 ± 7.59% at 6 months, and 28.62 ± 9.12% at 1 year, respectively (Figure 1).

3.3 Alterations in thyroid function and other biochemical markers

Table 2 and Figure 2 present the serum levels of TSH and thyroid hormones at baseline and 1 year after bariatric surgery. The serum level of TSH decreased from 2.33 (1.67, 3.04) uIU/mL to 1.82 (1.21, 2.50) uIU/mL ($P < 0.001$). The serum level of FT3 decreased from 3.23 ± 0.42 pg/mL to 2.89 ± 0.41 pg/mL ($P < 0.001$). The serum level of FT4 decreased from 1.11 ± 0.25 ng/dL to 1.02 ± 0.25 ng/dL ($P < 0.001$). The serum level of TT3 decreased from 1.13 (1.00, 1.25) ng/mL to 0.89 (0.78, 1.00) ng/mL ($P < 0.001$). The serum level of TT4 decreased from 8.28 ± 1.69 ug/dL to 7.82 ± 1.68 ug/dL ($P < 0.001$).

The decline was also observed in serum levels of FPG, HbA1c, TC, TG, LDL-C, and HDL-C with statistical significance ($P < 0.001$ for all, Table 2).

3.4 The association between ΔTSH and %TWL

According to the Pearson correlation analysis (Figure 3A), ΔTSH exhibited a significant positive correlation with %TWL

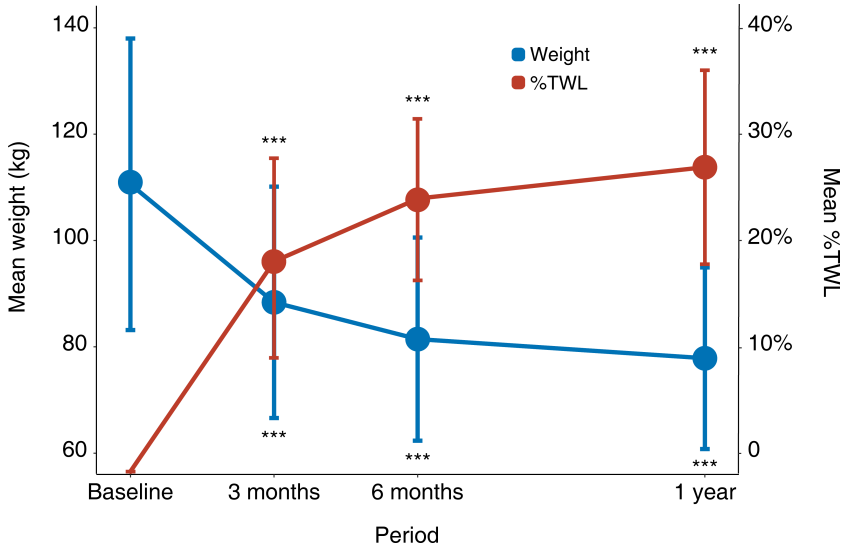

FIGURE 1
Weight loss after surgery. Error bars represent standard deviations. *: $P < 0.05$, **: $P < 0.01$, ***: $P < 0.001$ for each visit time compared with baseline. %TWL, percentage of total weight loss.

10.3389/fendo.2024.1333033

TABLE 2 Alterations in TSH, thyroid hormones, and other biochemical variables.

Variables	Baseline	1 year	*P*
TSH (uIU/mL)	2.33 (1.67, 3.04)	1.82 (1.21, 2.50)	<0.001
FT3 (pg/mL)	3.23 ± 0.42	2.89 ± 0.41	<0.001
FT4 (ng/dL)	1.11 ± 0.25	1.02 ± 0.25	<0.001
TT3 (ng/mL)	1.13 (1.00, 1.25)	0.89 (0.78, 1.00)	<0.001
TT4 (ug/dL)	8.28 ± 1.69	7.82 ± 1.68	<0.001
Other biochemical variables			
FPG (mmol/L)	6.26 (5.36, 9.15)	4.82 (4.38, 5.24)	<0.001
HbA1c (%)	6.30 (5.53, 8.38)	5.33 (5.10, 5.70)	<0.001
TC (mmol/L)	4.89 ± 1.00	4.48 ± 0.96	<0.001
TG (mmol/L)	1.79 (1.33, 2.35)	0.89 (0.69, 1.21)	<0.001
HDL-C (mmol/L)	1.03 (0.88, 1.20)	1.24 (1.08, 1.44)	<0.001
LDL-C (mmol/L)	3.06 ± 0.80	2.58 ± 0.76	<0.001

FPG, fasting plasma glucose; FT3, free triiodothyronine; FT4, free thyroxine; HbA1c, glycated hemoglobin; HDL-C, high-density lipoprotein cholesterol; LDL-C, low-density lipoprotein cholesterol; TC, total cholesterol; TG, total triglyceride; TSH, thyroid-stimulating hormone; TT3, total triiodothyronine; TT4, total thyroxine.

(Pearson correlation coefficient = 0.184, $P = 0.003$), indicating that the more the weight loss, the more the TSH decrease. After further dividing the %TWL into 3 groups, ΔTSH levels differed significantly between groups ($P = 0.018$) and increased as the %TWL increased (Figure 3B).

Table 3 presents the association between ΔTSH and %TWL/%TWL group. The %TWL revealed a significant linear relationship with the ΔTSH (β = 0.184 [95% confidence interval (CI), 0.063 – 0.306], $P = 0.003$) according to the univariable linear regression (Model 1). After accounting for age, sex, and BMI, the similar correlation was observed (β = 0.144 [95% CI, 0.017 – 0.271], $P = 0.026$) (Model 2). After making further adjustment for baseline sociodemographic variables, the %TWL still remained correlated with ΔTSH (β = 0.180 [95% CI, 0.048 – 0.312], $P = 0.008$) (Model 3).

The %TWL group had a significant linear relationship with ΔTSH (β = 0.176 [95% CI, 0.054 – 0.298], $P = 0.005$) according to univariable linear regression (Model 1). After adjusting for age, sex, and BMI, the %TWL group still presented a significant relationship with ΔTSH (β = 0.136 [95% CI, 0.009 – 0.263], $P = 0.035$) (Model 2). In the fully adjusted model, the %TWL group was also found to be an independent predictor for ΔTSH (β = 0.153 [95% CI, 0.019 – 0.287], $P = 0.025$) (Model 3).

In addition, patients in subgroup analyses were categorized based on sex (male or female), age (≤ 40 years or >40 years), BMI (≤ 37.5 kg/m^2 or >37.5 kg/m^2), T2DM (yes or no), metformin use (yes or no), and hypertension (yes or no). No significant

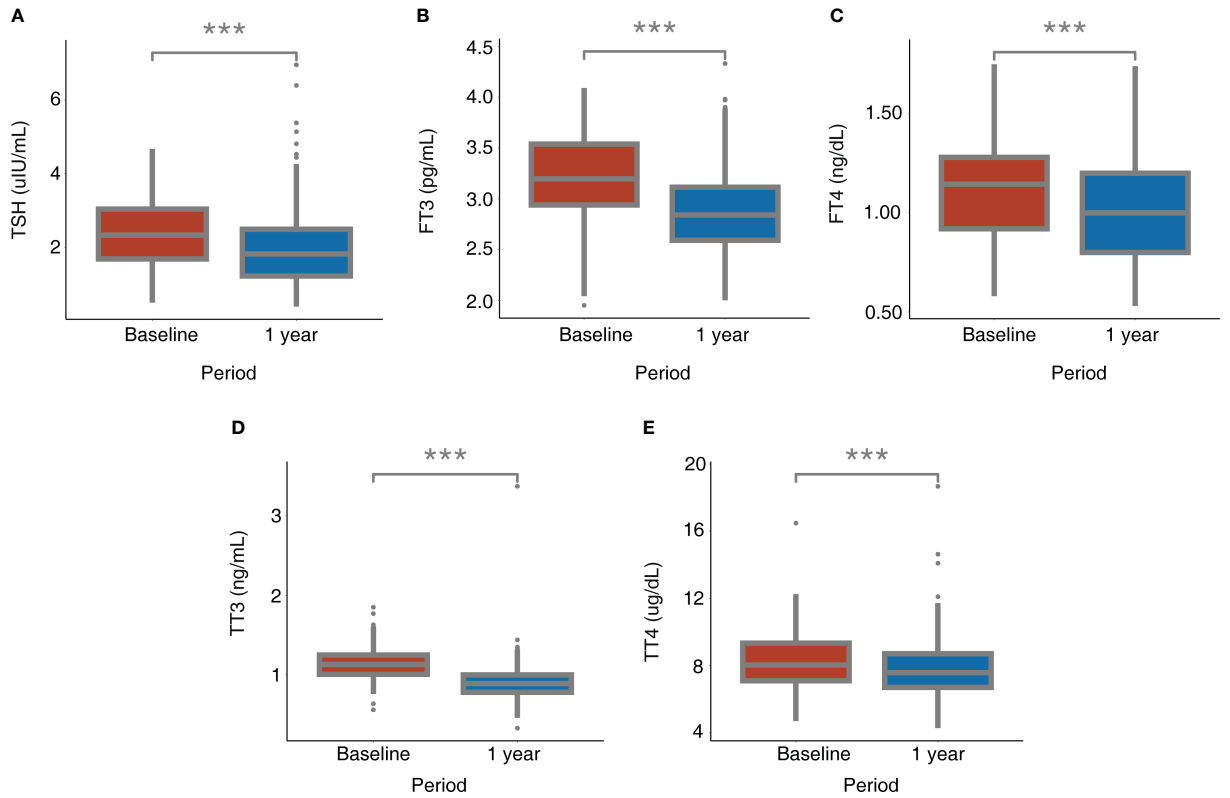

FIGURE 2
Alterations of TSH and thyroid hormones after bariatric surgery. **(A)** TSH; **(B)** FT3; **(C)** FT4; **(D)** TT3; **(E)** TT4. *: $P < 0.05$, **: $P < 0.01$, ***: $P < 0.001$ for 1 year after surgery compared with baseline. FT3, free triiodothyronine; FT4, free thyroxine; TSH, thyroid-stimulating hormone; TT3, total triiodothyronine; TT4, total thyroxine.

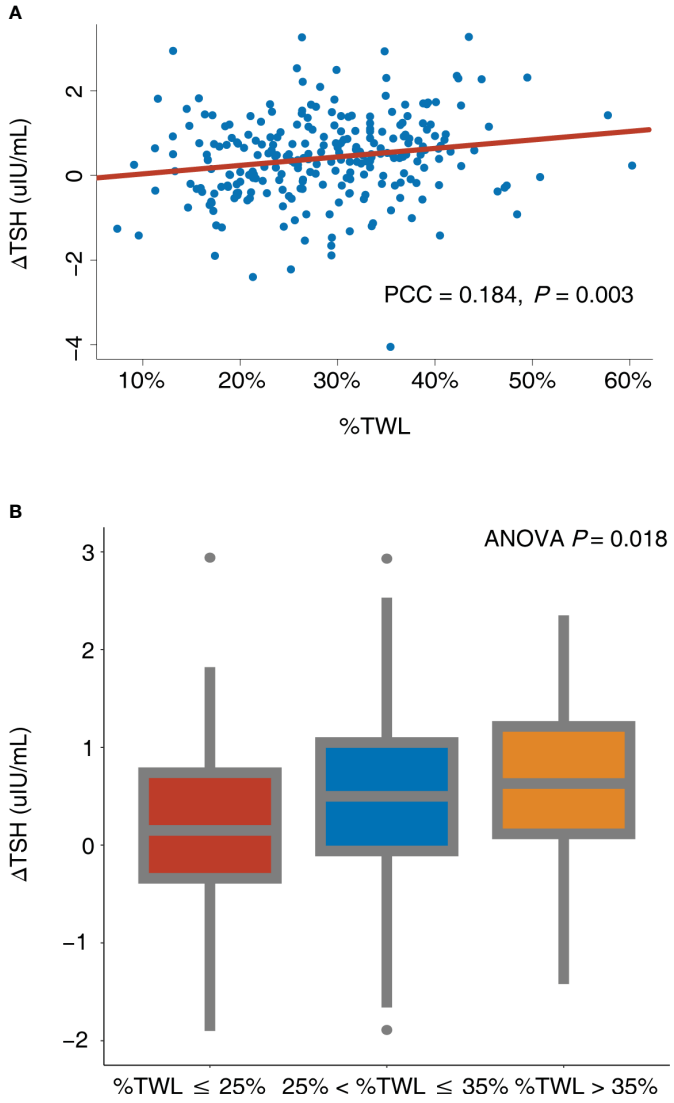

FIGURE 3
Correlation between ΔTSH and %TWL. **(A)** %TWL was used as continuous variable; **(B)** %TWL was used as categorical variable. ANOVA, analysis of variance; PCC, Pearson correlation coefficient; TSH, thyroid-stimulating hormone; %TWL, percentage of total weight loss.

interactions between %TWL and these potential covariates were observed (all *P* values for interaction > 0.05) (Figure 4).

4 Discussion

Thyroid hormones play an essential role in regulating dietary intake and energy expenditure and therefore interact with body weight (26). Patients with obesity frequently suffer from thyroid dysfunction, which has the potential to exacerbate the obese state. However, the effect of bariatric surgery, a powerful method of weight loss, on thyroid function is not known with certainty. The main results of this study showed that TSH, FT3, FT4, TT3, and TT4 decreased significantly 1 year after bariatric surgery in euthyroid patients. TSH reduction was independently correlated with %TWL, with greater weight loss correlating to greater TSH reduction.

Individuals with obesity have been found to have elevated TSH when compared to normal-weight controls, as well as thyroid hormones (27–30). According to a bidirectional Mendelian randomization study by Wang et al. (31), it is more likely that obesity causes elevated TSH than that elevated TSH causes weight gain. Obesity was found to reduce the expression of TSH receptors on adipocytes, which may induce the downregulation of thyroid hormone receptors and action and further increase TSH (32). Moreover, the elevation of TSH can be mediated by compensatory activation of the hypothalamus-pituitary-thyroid (HPT) axis in response to an increase in leptin in adipose tissue (33, 34). Thus, the combined effect of peripheral thyroid hormone resistance and central leptin regulation increases TSH in plasma and has detrimental impacts on organs beyond the thyroid.

Changes in TSH and thyroid hormones after bariatric surgery remain controversial. We analyzed the data of 256 Chinese patients and revealed a significant decrease in TSH and other thyroid

10.3389/fendo.2024.1333033

TABLE 3 Standardized β and 95% CIs of ΔTSH according to %TWL.

	Model 1		Model 2		Model 3	
Variables	β (95% CI)	*P*	β (95% CI)	*P*	β (95% CI)	*P*
%TWL	0.184 (0.063 - 0.306)	0.003	0.144 (0.017 - 0.271)	0.026	0.180 (0.048 - 0.312)	0.008
%TWL group	0.176 (0.054 - 0.298)	0.005	0.136 (0.009 - 0.263)	0.035	0.153 (0.019 - 0.287)	0.025

Model 1: unadjusted. Model 2: adjusted for sex, age, and BMI. Model 3: adjusted for sex, age, BMI, waist-to-hip ratio, type of surgery, T2DM, metformin use, hypertension, smoking history, and alcohol consumption.
CI, confidence interval; TSH, thyroid-stimulating hormone; %TWL, percentage of total weight loss.

hormones (FT3, FT4, TT3, and TT4) 1 year after SG and RYGB. The majority of studies on patients with normal thyroid function or subclinical hypothyroidism have yielded similar outcomes (13, 18). In contrast, Dall'Asta et al. (17) examined the effect of gastric banding on thyroid hormones and found no postoperative change in TSH. Zhang et al. (35) and MacCuish et al. (16) investigated the variations in thyroid function following RYGB and discovered that TSH remained steady. FT3 and FT4 have also been reported to be elevated, unchanged, or decreased after bariatric surgery in previous studies, with the varying results primarily attributable to differences in ethnic groups, surgical procedures, and sample sizes (9, 14, 19, 36, 37). However, the present study included, to the best of our knowledge, the largest number of Chinese euthyroid patients with obesity and comprehensively analyzed the two most common bariatric surgical procedures (SG and RYGB), so it may be able to provide more reliable data for Chinese patients.

Although a few studies failed to identify a relationship between TSH decline and weight loss after bariatric surgery (19, 37–40), most studies initially explored a positive correlation using correlation analysis (14, 17, 19, 41). Neves et al. (42) analyzed preoperative and 1-year postoperative thyroid function in 949 euthyroid patients who underwent SG, RYGB, or gastric banding and revealed that a decrease in TSH was significantly associated with excessive body weight loss. Juiz-Valiña et al. (27) conducted a study comparing the TSH levels of 129 euthyroid patients before and after SG and RYGB and observed that TSH reduction was associated with excessive BMI loss. Moreover, a recent prospective study by Kamal et al. (43), involving 106 euthyroid patients undergoing SG has indicated a positive linear relationship between %TWL and ΔTSH. Using Pearson correlation analysis, we also discovered a significant correlation between ΔTSH and % TWL (PCC = 0.184, $P = 0.003$), which is consistent with previous findings. Similar results were observed after dividing %TWL into 3

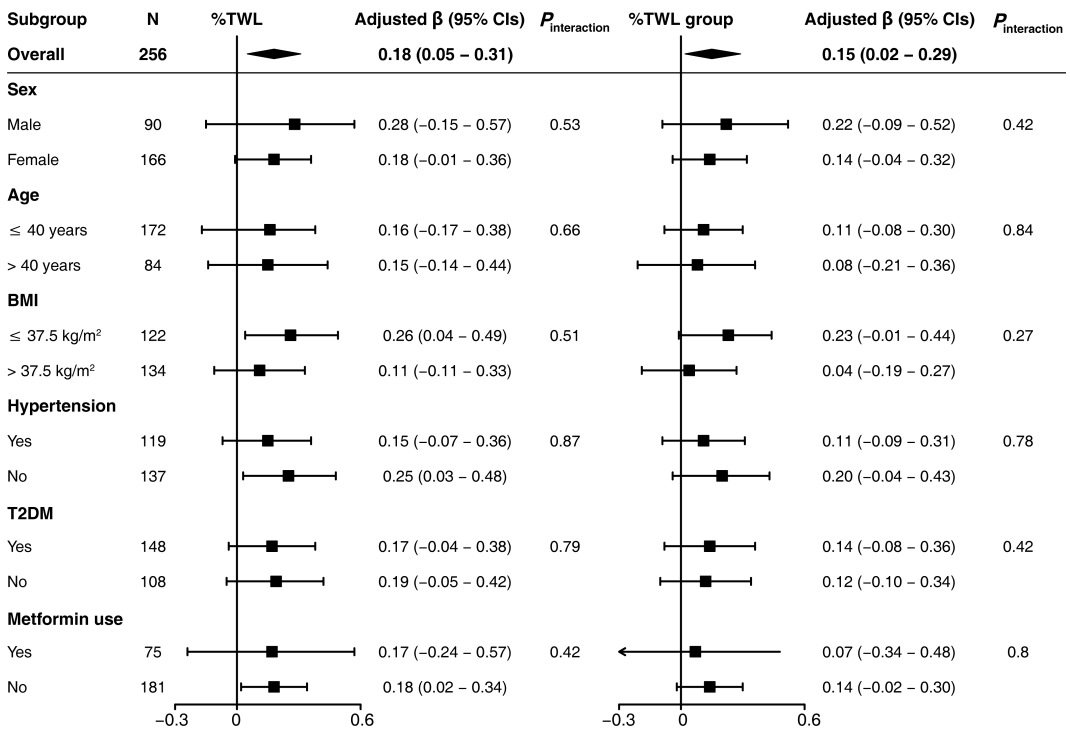

FIGURE 4
Subgroup analysis for the association between ΔTSH and %TWL. The %TWL was used as continuous variable (%TWL) and categorical variable (%TWL group). Each subgroup analysis adjusted for sex, age, BMI, waist-to-hip ratio, type of surgery, hypertension, T2DM, metformin use, smoking history, and alcohol consumption. BMI, body mass index; T2DM, type 2 diabetes mellitus; %TWL, percentage of total weight loss.

groups, with greater TSH variations as %TWL increased. To confirm the relationship between ΔTSH and %TWL, we performed multivariable stepwise linear regression. After adjusting for several covariates, both %TWL and %TWL groups were found to be independent predictors of TSH decline, suggesting that changes in thyroid function after bariatric surgery are mediated by surgically induced weight loss, with more weight loss resulting in better thyroid function improvement.

How weight loss after bariatric surgery affects TSH and thyroid hormones is not yet fully understood. One viewpoint proposed that the improvement of thyroid function is mediated by weight loss independently, rather than being exclusively attributed to the effects of bariatric surgery (44). This was supported by the fact that weight loss induced by lifestyle changes can also reduce TSH levels (45). Although there are no studies directly comparing the effects of bariatric surgery and lifestyle interventions on thyroid function, we concluded by comparing differing degrees of weight loss after surgery that %TWL > 35% was associated with greater TSH changes than 25 ≤ %TWL < 35% and greater than %TWL < 25%. Given that bariatric surgery is the most effective method of weight loss currently available, its effect on thyroid function should be the most significant.

Various potential factors may cause the alteration in thyroid function after bariatric surgery. First, the tremendous decrease in fat mass and leptin released from adipocytes after bariatric surgery not only reduces the stimulation of the HPT axis but also inhibits the peripheral conversion of T4 to T3, resulting in a decrease in TSH and thyroid hormones, which may be the main mechanism for the alteration of thyroid function after bariatric surgery (46–48). Second, decreased expression of the TSH receptor due to obesity can be reversed by weight loss, thereby reducing peripheral thyroid hormone resistance (32). Third, the growth hormone is considered as an important factor that could regulate the HPT axis and decreased significantly in patients with obesity. After bariatric surgery, the growth hormone rises and lowers TSH through the HPT axis (44, 49). Fourth, the body inflammation state declined after bariatric surgery, which has been reported to be associated with the reduction of TSH, resulting in the improvement of thyroid hormone resistance after surgery (50). Fifth, bariatric surgery can inhibit the activity of B and T lymphocytes and reduce the circulating levels of thyroid autoimmune antibodies and various inflammatory cytokines, which may protect the thyroid gland from inflammatory injuries and the forced release of stored thyroid hormones (51). Finally, improvements in glycemic and lipid profiles after bariatric surgery have also been reported to play a role in promoting a decrease in TSH (19, 41, 52), which aligns with our findings as the FPG, HbA1c, TC, TG, LDL-C, and HDL-C all declined significantly after surgery.

From a clinical perspective, the present study identified a positive correlation between bariatric surgery-induced weight loss and TSH reduction in patients with normal thyroid function, providing physiological encouragement for the clinical therapeutic strategy of surgical treatment for obesity-related thyroid dysfunction. TSH will decrease following weight loss after bariatric surgery in patients with TSH levels approaching the upper normal limit, without the need for additional thyroid hormone-lowering medication. For patients with hypothyroidism, the current study was in accordance with the previous study that TSH would decline after bariatric surgery, supporting the view that the thyroid replacement medication dosage might be reduced (53). If enhanced efficacy is needed, weight management, such as dietary control and exercise interventions, can be strengthened postoperatively to increase %TWL, which leads to a further decrease in TSH.

Some limitations to our study should be noted. Firstly, since this was a retrospective, single-center study, there was a selection bias. Secondly, the study population comprised only Chinese patients with obesity, so it is unknown whether these results can be generalized to Western populations. Thirdly, antithyroid antibodies and cytokines such as leptin were not routinely measured in the present study, so we may not be able to further explore the specific mechanism underlying the impact of weight loss on TSH levels. Fourthly, due to a significant portion of patients lacking thyroid function-related data at 3 months and 6 months after surgery, we have not included that for analysis. Finally, the follow-up period of this study was only 1 year; hence, the alterations in thyroid function after 1 year and the influence of weight regain on thyroid function cannot be studied. Future research should establish multicenter, prospective, and long-term follow-up cohorts to obtain more reliable data.

In conclusion, our study revealed a significant reduction in TSH, FT3, FT4, TT3, and TT4 in Chinese euthyroid patients with obesity 1 year after bariatric surgery. Weight loss following SG and RYGB will improve thyroid function. The more weight loss occurs, the more TSH decreases.

Data availability statement

The original contributions presented in the study are included in the article/Supplementary Materials, further inquiries can be directed to the corresponding author/s.

Ethics statement

The studies involving humans were approved by Institutional Review Board of China-Japan Friendship Hospital. The studies were conducted in accordance with the local legislation and institutional requirements. The human samples used in this study were acquired from primarily isolated as part of your previous study for which ethical approval was obtained. Written informed consent for participation was not required from the participants or the participants' legal guardians/next of kin in accordance with the national legislation and institutional requirements.

Author contributions

ZT: Data curation, Formal analysis, Software, Visualization, Writing – original draft, Writing – review & editing. YN: Conceptualization, Methodology, Writing – review & editing,

Funding acquisition, Writing – original draft. ZL: Writing – review & editing, Data curation, Funding acquisition. PW: Data curation, Investigation, Writing – review & editing. NZ: Data curation, Writing – review & editing. XH: Data curation, Writing – review & editing. AP: Software, Writing – review & editing. BL: Methodology, Writing – review & editing. HM: Conceptualization, Supervision, Writing – review & editing, Funding acquisition.

Funding

The author(s) declare financial support was received for the research, authorship, and/or publication of this article. This study was supported by the China-Japan Friendship Hospital National High Level Hospital Clinical Research Funding (grant ID: 2023-NHLHCRF-YYPP-TS-02 to HM, and 2023-NHLHCRF-YS-0103 to Hua Meng), National High Level Hospital Clinical Research Funding (grant ID: NO.ZRJY2023-QM15 to YN, and NO.ZRJY2023-QM09 to ZL), and Elite Medical Professionals Project of China-Japan Friendship Hospital (grant ID: NO.ZRJY2023-QM15 to YN, and NO.ZRJY2023-QM09 to ZL).

Conflict of interest

The authors declare that the research was conducted in the absence of any commercial or financial relationships that could be construed as a potential conflict of interest.

Publisher's note

Supplementary material

The Supplementary Material for this article can be found online at: https://www.frontiersin.org/articles/10.3389/fendo.2024.1333033/full#supplementary-material

References

1. Laclaustra M, Moreno-Franco B, Lou-Bonafonte JM, Mateo-Gallego R, Casasnovas JA, Guallar-Castillon P, et al. Impaired sensitivity to thyroid hormones is associated with diabetes and metabolic syndrome. *Diabetes Care* (2019) 42(2):303–10. doi: 10.2337/dc18-1410

2. Babić Leko M, Gunjača I, Pleić N, Zemunik T. Environmental factors affecting thyroid-stimulating hormone and thyroid hormone levels. *Int J Mol Sci* (2021) 22 (12):6521. doi: 10.3390/ijms22126521

3. Gajda SN, Kuryłowicz A, Żach M, Bednarczuk T, Wyleżoł M. Diagnosis and treatment of thyroid disorders in obese patients - what do we know? *Endokrynol Pol* (2019) 70(3):271–6. doi: 10.5603/EP.a2018.0089

4. Wiggins T, Guidozzi N, Welbourn R, Ahmed AR, Markar SR. Association of bariatric surgery with all-cause mortality and incidence of obesity-related disease at a population level: A systematic review and meta-analysis. *PloS Med* (2020) 17(7): e1003206. doi: 10.1371/journal.pmed.1003206

5. Eisenberg D, Shikora SA, Aarts E, Aminian A, Angrisani L, Cohen RV, et al. 2022 American society for metabolic and bariatric surgery (Asmbs) and international federation for the surgery of obesity and metabolic disorders (Ifso): indications for metabolic and bariatric surgery. *Surg Obes Relat Dis* (2022) 18(12):1345–56. doi: 10.1016/j.soard.2022.08.013

6. Abdelbaki TN, Elkeleny MR, Sharaan MA, Talha A, Bondok M. Impact of laparoscopic sleeve gastrectomy on obese patients with subclinical hypothyroidism. *J Laparoendosc Adv Surg Tech A* (2020) 30(3):236–40. doi: 10.1089/lap.2019.0642

7. Richou M, Gilly O, Taillard V, Paul De Brauwere D, Donici I, Guedj AM. Levothyroxine dose adjustment in hypothyroid patients following gastric sleeve surgery. *Ann Endocrinol (Paris)* (2020) 81(5):500–6. doi: 10.1016/j.ando.2020.04.011

8. Azran C, Hanhan-Shamshoum N, Irshied T, Ben-Shushan T, Dicker D, Dahan A, et al. Hypothyroidism and levothyroxine therapy following bariatric surgery: a systematic review, meta-analysis, network meta-analysis, and meta-regression. *Surg Obes Relat Dis* (2021) 17(6):1206–17. doi: 10.1016/j.soard.2021.02.028

9. Aykota MR, Atabey M. Effect of sleeve gastrectomy on thyroid-stimulating hormone levels in morbidly obese patients with normal thyroid function. *Eur Rev Med Pharmacol Sci* (2021) 25(1):233–40. doi: 10.26355/eurrev_202101_24389

10. Salman MA, Rabiee A, Salman A, Qassem MG, Ameen MA, Hassan AM, et al. Laparoscopic sleeve gastrectomy has a positive impact on subclinical hypothyroidism among obese patients: A prospective study. *World J Surg* (2021) 45(10):3130–7. doi: 10.1007/s00268-021-06201-5

11. Zendel A, Abu-Ghanem Y, Dux J, Mor E, Zippel D, Goitein D. The impact of bariatric surgery on thyroid function and medication use in patients with hypothyroidism. *Obes Surg* (2017) 27(8):2000–4. doi: 10.1007/s11695-017-2616-7

12. Garcia-Moreno RM, Cos-Blanco AI, Calvo-Vinuela I, Zapatero-Larrauri M, Herranz L. Change in levothyroxine requirements after bariatric surgery in patients with hypothyroidism. *Endocr Regul* (2022) 3056(2):81–6. doi: 10.2478/enr-2022-0009

13. Liu F, Di J, Yu H, Han J, Bao Y, Jia W. Effect of roux-en-Y gastric bypass on thyroid function in euthyroid patients with obesity and type 2 diabetes. *Surg Obes Relat Dis* (2017) 13(10):1701–7. doi: 10.1016/j.soard.2017.06.001

14. Yang J, Gao Z, Yang W, Zhou X, Lee S, Wang C. Effect of sleeve gastrectomy on thyroid function in Chinese euthyroid obese patients. *Surg Laparosc Endosc Percutan Tech* (2017) 27(4):e66–e8. doi: 10.1097/sle.0000000000000432

15. Gokosmanoglu F, Aksoy E, Onmez A, Ergenç H, Topkaya S. Thyroid homeostasis after bariatric surgery in obese cases. *Obes Surg* (2020) 30(1):274–8. doi: 10.1007/s11695-019-04151-5

16. MacCuish A, Razvi S, Syed AA. Effect of weight loss after gastric bypass surgery on thyroid function in euthyroid people with morbid obesity. *Clin Obes* (2012) 2(1-2):25–8. doi: 10.1111/j.1758-8111.2012.00036.x

17. Dall'Asta C, Paganelli M, Morabito A, Vedani P, Barbieri M, Paolisso G, et al. Weight loss through gastric banding: effects on tsh and thyroid hormones in obese subjects with normal thyroid function. *Obes (Silver Spring)* (2010) 18(4):854–7. doi: 10.1038/oby.2009.320

18. Yu H, Li Q, Zhang M, Liu F, Pan J, Tu Y, et al. Decreased leptin is associated with alterations in thyroid-stimulating hormone levels after roux-en-Y gastric bypass surgery in obese euthyroid patients with type 2 diabetes. *Obes Facts* (2019) 12 (3):272–80. doi: 10.1159/000499385

19. Chen Y, Zhang W, Pan Y, Chen W, Wang C, Yang W. Thyroid Function before and after Laparoscopic Sleeve Gastrectomy in Patients with Obesity. *Obes Surg* (2022) 32(6):1954–61. doi: 10.1007/s11695-022-06035-7

20. Guan B, Chen Y, Yang J, Yang W, Wang C. Effect of bariatric surgery on thyroid function in obese patients: A systematic review and meta-analysis. *Obes Surg* (2017) 27 (12):3292–305. doi: 10.1007/s11695-017-2965-2

21. Wang Y, Wang C, Zhu S, Zhang P, Liang H. Chinese surgical guidelines for obesity and type 2 diabetes (2019). *Chin J Pract Surg* (2019) 39(04):301–6. doi: 10.19538/j.cjps.issn1005-2208.2019.04.01

22. American Diabetes Association. 2. Classification and diagnosis of diabetes: standards of medical care in diabetes-2021. *Diabetes Care* (2021) 44(Suppl 1):S15–S33. doi: 10.2337/dc21-S002

23. Williams B, Mancia G, Spiering W, Enrico AR, Michel A, Michel B, et al. 2018 Practice Guidelines for the management of arterial hypertension of the European Society of Hypertension and the European Society of Cardiology: ESH/ESC Task Force

for the Management of Arterial Hypertension. *J Hypertens* (2018) 36(12):2284–309. doi: 10.1097/HJH.0000000000001961

24. Zhou B, Cao X, Wang Z, Zhang N, Liu B, Meng H. Symmetric three-port laparoscopic roux-en-Y gastric bypass: A novel technique that is safe, effective, and feasible. *Surg Today* (2023) 53(6):702–8. doi: 10.1007/s00595-022-02629-x

25. Zhou B, Ji H, Liu Y, Chen Z, Zhang N, Cao X, et al. Eras reduces postoperative hospital stay and complications after bariatric surgery: A retrospective cohort study. *Med (Baltimore)* (2021) 100(47):e27831. doi: 10.1097/md.0000000000027831

26. Biondi B, Kahaly GJ, Robertson RP. Thyroid dysfunction and diabetes mellitus: two closely associated disorders. *Endocr Rev* (2019) 40(3):789–824. doi: 10.1210/er.2018-00163

27. Juiz-Valiña P, Outeiriño-Blanco E, Pértega S, Varela-Rodriguez BM, García-Brao MJ, Mena E, et al. Effect of weight loss after bariatric surgery on thyroid-stimulating hormone levels in euthyroid patients with morbid obesity. *Nutrients* (2019) 11(5):1121. doi: 10.3390/nu11051121

28. Rotondi M, Leporati P, La Manna A, Pirali B, Mondello T, Fonte R, et al. Raised serum tsh levels in patients with morbid obesity: is it enough to diagnose subclinical hypothyroidism? *Eur J Endocrinol* (2009) 160(3):403–8. doi: 10.1530/eje-08-0734

29. Reinehr T, Andler W. Thyroid Hormones before and after Weight Loss in Obesity. *Arch Dis Child* (2002) 87(4):320–3. doi: 10.1136/adc.87.4.320

30. Valdés S, Maldonado-Araque C, Lago-Sampedro A, Lillo-Muñoz JA, Garcia-Fuentes E, Perez-Valero V, et al. Reference values for tsh may be inadequate to define hypothyroidism in persons with morbid obesity: di@Bet.Es study. *Obes (Silver Spring)* (2017) 25(4):788–93. doi: 10.1002/oby.21796

31. Wang X, Gao X, Han Y, Zhang F, Lin Z, Wang H, et al. Causal association between serum thyrotropin and obesity: A bidirectional, mendelian randomization study. *J Clin Endocrinol Metab* (2021) 106(10):e4251–e9. doi: 10.1210/clinem/dgab183

32. Nannipieri M, Cecchetti F, Anselmino M, Camastra S, Niccolini P, Lamacchia M, et al. Expression of thyrotropin and thyroid hormone receptors in adipose tissue of patients with morbid obesity and/or type 2 diabetes: effects of weight loss. *Int J Obes (Lond)* (2009) 33(9):1001–6. doi: 10.1038/ijo.2009.140

33. Lloyd RV, Jin L, Tsumanuma I, Vidal S, Kovacs K, Horvath E, et al. Leptin and leptin receptor in anterior pituitary function. *Pituitary* (2001) 4(1-2):33–47. doi: 10.1023/a:1012982626401

34. Mantzoros CS, Ozata M, Negrao AB, Suchard MA, Ziotopoulou M, Caglayan S, et al. Synchronicity of frequently sampled thyrotropin (Tsh) and leptin concentrations in healthy adults and leptin-deficient subjects: evidence for possible partial tsh regulation by leptin in humans. *J Clin Endocrinol Metab* (2001) 86(7):3284–91. doi: 10.1210/jcem.86.7.7644

35. Zhang H, Liu W, Han X, Yu H, Zhang P, Jia W. Effect of laparoscopic roux-en-Y gastric bypass surgery on thyroid hormone levels in Chinese patients, could it be a risk for thyroid nodules? *Obes Surg* (2017) 27(10):2619–27. doi: 10.1007/s11695-017-2684-8

36. Karaman K, Mansıroglu K, Subasi O, Biricik A, Yirgin H, Kose E, et al. Thyroid Hormone Changes after Sleeve Gastrectomy with and without Antral Preservation. *Obes Surg* (2021) 31(1):224–31. doi: 10.1007/s11695-020-04896-4

37. Abu-Ghanem Y, Inbar R, Tyomkin V, Kent I, Berkovich L, Ghinea R, et al. Effect of sleeve gastrectomy on thyroid hormone levels. *Obes Surg* (2015) 25(3):452–6. doi: 10.1007/s11695-014-1415-7

38. Fazylov R, Soto E, Cohen S, Merola S. Laparoscopic roux-en-Y gastric bypass surgery on morbidly obese patients with hypothyroidism. *Obes Surg* (2008) 18(6):644–7. doi: 10.1007/s11695-007-9279-8

39. Moulin de Moraes CM, Mancini MC, de Melo ME, Figueiredo DA, Villares SM, Rascovski A, et al. Prevalence of subclinical hypothyroidism in a morbidly obese population and improvement after weight loss induced by roux-en-Y gastric bypass. *Obes Surg* (2005) 15(9):1287–91. doi: 10.1381/096089205774512537

40. Granzotto PCD, Mesa Junior CO, Strobel R, Radominski R, Graf H, de Carvalho GA. Thyroid Function before and after Roux-En-Y Gastric Bypass: An Observational Study. *Surg Obes Relat Dis* (2020) 16(2):261–9. doi: 10.1016/j.soard.2019.11.011

41. Ruiz-Tovar J, Boix E, Galindo I, Zubiaga L, Diez M, Arroyo A, et al. Evolution of subclinical hypothyroidism and its relation with glucose and triglycerides levels in morbidly obese patients after undergoing sleeve gastrectomy as bariatric procedure. *Obes Surg* (2014) 24(5):791–5. doi: 10.1007/s11695-013-1150-5

42. Neves JS, Castro Oliveira S, Souteiro P, Pedro J, Magalhães D, Guerreiro V, et al. Effect of weight loss after bariatric surgery on thyroid-stimulating hormone levels in patients with morbid obesity and normal thyroid function. *Obes Surg* (2018) 28(1):97–103. doi: 10.1007/s11695-017-2792-5

43. Kamal M, Aisha HAA, Fahmy MH, Abosayed AK. The impact of laparoscopic sleeve gastrectomy on thyroid functions in Egyptian patients with obesity. *J Gastrointest Surg* (2023) 27(7):1345–52. doi: 10.1007/s11605-023-05662-4

44. Cordido M, Juiz-Valiña P, Urones P, Sangiao-Alvarellos S, Cordido F. Thyroid function alteration in obesity and the effect of bariatric surgery. *J Clin Med* (2022) 11(5):1340. doi: 10.3390/jcm11051340

45. Reinehr T, de Sousa G, Andler W. Hyperthyrotropinemia in obese children is reversible after weight loss and is not related to lipids. *J Clin Endocrinol Metab* (2006) 91(8):3088–91. doi: 10.1210/jc.2006-0095

46. Guo F, Bakal K, Minokoshi Y, Hollenberg AN. Leptin signaling targets the thyrotropin-releasing hormone gene promoter in vivo. *Endocrinology* (2004) 145(5):2221–7. doi: 10.1210/en.2003-1312

47. Ortega FJ, Jílková ZM, Moreno-Navarrete JM, Pavelka S, Rodriguez-Hermosa JI, Kopeck Ygrave J, et al. Type I iodothyronine 5'-deiodinase mrna and activity is increased in adipose tissue of obese subjects. *Int J Obes (Lond)* (2012) 36(2):320–4. doi: 10.1038/ijo.2011.101

48. Duntas LH, Biondi B. The interconnections between obesity, thyroid function, and autoimmunity: the multifold role of leptin. *Thyroid* (2013) 23(6):646–53. doi: 10.1089/thy.2011.0499

49. Glad CAM, Svensson PA, Nystrom FH, Jacobson P, Carlsson LMS, Johannsson G, et al. Expression of ghr and downstream signaling genes in human adipose tissue-relation to obesity and weight change. *J Clin Endocrinol Metab* (2019) 104(5):1459–70. doi: 10.1210/jc.2018-01036

50. Zhu C, Gao J, Mei F, Lu L, Zhou D, Qu S. Reduction in thyroid-stimulating hormone correlated with improved inflammation markers in chinese patients with morbid obesity undergoing laparoscopic sleeve gastrectomy. *Obes Surg* (2019) 29(12):3954–65. doi: 10.1007/s11695-019-04063-4

51. Xia MF, Chang XX, Zhu XP, Yan HM, Shi CY, Wu W, et al. Preoperative thyroid autoimmune status and changes in thyroid function and body weight after bariatric surgery. *Obes Surg* (2019) 29(9):2904–11. doi: 10.1007/s11695-019-03910-8

52. Chen X, Zhang C, Liu W, Zhang J, Zhou Z. Laparoscopic sleeve gastrectomy-induced decreases in ft3 and tsh are related to fasting C-peptide in euthyroid patients with obesity. *Diabetes Metab Syndr Obes* (2020) 13:4077–84. doi: 10.2147/dmso.S277486

53. Khan WF, Singla V, Aggarwal S, Gupta Y. Outcome of bariatric surgery on hypothyroidism: experience from a tertiary care center in India. *Surg Obes Relat Dis* (2020) 16(9):1297–301. doi: 10.1016/j.soard.2020.03.035

frontiers | Frontiers in Endocrinology

TYPE Original Research
PUBLISHED 02 February 2024
DOI 10.3389/fendo.2024.1338147

OPEN ACCESS

EDITED BY
Yayun Wang,
Air Force Medical University, China

REVIEWED BY
Li Li,
University of Texas Southwestern Medical Center, United States
Francesco Pizza,
ASL Napoli 2 Nord, Italy

*CORRESPONDENCE
Guangyong Zhang
guangyongzhang@hotmail.com

†These authors have contributed equally to this work

RECEIVED 14 November 2023
ACCEPTED 09 January 2024
PUBLISHED 02 February 2024

CITATION
Liu C, Xu Q, Dong S, Ding H, Li B, Zhang D, Liang Y, Li L, Liu Q, Cheng Y, Wu J, Zhu J, Zhong M, Cao Y and Zhang G (2024) New mechanistic insights of anti-obesity by sleeve gastrectomy-altered gut microbiota and lipid metabolism. *Front. Endocrinol.* 15:1338147. doi: 10.3389/fendo.2024.1338147

New mechanistic insights of anti-obesity by sleeve gastrectomy-altered gut microbiota and lipid metabolism

Chuxuan Liu[1†], Qian Xu[1†], Shuohui Dong[2], Huanxin Ding[1], Bingjun Li[1], Dexu Zhang[1], Yongjuan Liang[1], Linchuan Li[1], Qiaoran Liu[1], Yugang Cheng[1], Jing Wu[3], Jiankang Zhu[1], Mingwei Zhong[1], Yihai Cao[4] and Guangyong Zhang[1*]

[1]Department of General Surgery, The First Affiliated Hospital of Shandong First Medical University, Jinan, Shandong, China, [2]Department of General Surgery, Qilu Hospital, Shandong University, Jinan, Shandong, China, [3]Department of Clinical Pharmacy, The First Affiliated Hospital of Shandong First Medical University, Jinan, Shandong, China, [4]Department of Microbiology, Tumor and Cell Biology, Karolinska Institute, Stockholm, Sweden

Background: The obesity epidemic has been on the rise due to changes in living standards and lifestyles. To combat this issue, sleeve gastrectomy (SG) has emerged as a prominent bariatric surgery technique, offering substantial weight reduction. Nevertheless, the mechanisms that underlie SG-related bodyweight loss are not fully understood.

Methods: In this study, we conducted a collection of preoperative and 3-month postoperative serum and fecal samples from patients who underwent laparoscopic SG at the First Affiliated Hospital of Shandong First Medical University (Jinan, China). Here, we took an unbiased approach of multi-omics to investigate the role of SG-altered gut microbiota in anti-obesity of these patients. Non-target metabolome sequencing was performed using the fecal and serum samples.

Results: Our data show that SG markedly increased microbiota diversity and Rikenellaceae, *Alistipes*, *Parabacteroides*, Bactreoidales, and Enterobacteraies robustly increased. These compositional changes were positively correlated with lipid metabolites, including sphingolipids, glycerophospholipids, and unsaturated fatty acids. Increases of Rikenellaceae, *Alistipes*, and *Parabacteroide* were reversely correlated with body mass index (BMI).

Conclusion: In conclusion, our findings provide evidence that SG induces significant alterations in the abundances of Rikenellaceae, *Alistipes*, *Parabacteroides*, and Bacteroidales, as well as changes in lipid metabolism-related metabolites. Importantly, these changes were found to be closely linked to the alleviation of obesity. On the basis of these findings, we have identified a number of microbiotas that could be potential targets for treatment of obesity.

KEYWORDS

sleeve gastrectomy, obesity, microbiota, metagenome, metabolome

1 Introduction

The prevalence of obesity has been steadily increasing over the past half century (1). Notably, the number of people with obesity in China grew threefold between 2004 and 2018; the mean body mass index (BMI) increased from 22.7 to 24.4 kg/m^2 (2). Obesity contributes to numerous metabolic diseases, such as nonalcoholic fatty liver disease (NAFLD), type 2 diabetes mellitus (T2DM), cardiovascular disease, hypertension, coronary heart disease, depression, and cancer (3). A sedentary lifestyle, minimal exercise, and excessive energy intake are the main causes of obesity; obesity-related genes also constitute important genetic factors (4). Effective alleviation and reversal of obesity, as well as prevention of its complications and potential damaging effects, have received considerable public health interest.

The gut microbiota is the largest microbial community in the human body (5). At the genetic level, it contains approximately 30-fold more genes than the human genome (6), and it is closely associated with normal physiological functions of the human body (7). Recent studies have shown that changes in gut microbiota are strongly associated with the onset of obesity and obesity-related complications (e.g., reduced intestinal microbiota richness; reductions in Clostridiales, Deltaproteobacteria, and Pasteurellales; and an associated increase in Burkholderiales) in patients with obesity (8). The use of oral antibiotics may increase obesity risk (9), whereas fecal microbiota transplantation from lean donors can improve the metabolic status of obese patients and attenuate obesity-related metabolic diseases such as insulin resistance (10); these findings indicate that the gut microbiota plays an important role in obesity onset and progression. *Dysosmobacter welbionis*, a newly discovered gut probiotic, can effectively alleviate obesity, insulin resistance, and inflammation in adipose tissue, thereby improving host metabolic status (11). The specific mechanism of its effects may be closely associated with the small molecule metabolites it produces during fermentation, which can influence the local gut environment and systemic metabolic status (12). Short-chain fatty acids in the gut environment can regulate the progression of obesity through various effects on appetite and the systemic metabolic profile (13). The gut microbiota also has important effects on the production, transportation, and enterohepatic circulation of bile acids, which are important small molecule metabolites (14). Thus, targeted therapy against gut microbiota is gradually becoming an important intervention for obesity and obesity-related diseases.

Bariatric surgery, one of the most effective treatments for obesity and hyperglycemia, has substantial effects on metabolic status; it can alleviate and prevent obesity-related diseases such as T2DM and NAFLD (15, 16). Sleeve gastrectomy (SG), a common bariatric surgery approach, is widely used as treatment for obesity because of its simplicity, robust weight reduction effect, and low malnutrition risk (17, 18). The substantial weight-loss benefits of SG do not solely depend on gastric volume reduction; this surgical treatment can reorganize systemic endocrine functioning to improve glucose–lipid metabolism by regulating hormone levels, appetite, and other factors (19, 20). However, the details of the mechanism require further investigation. There is evidence that SG also influences gut microbiota composition and function, in a manner closely associated with its apparent therapeutic benefits (21). However, only a few studies have investigated the effects of SG on gut microbiota, mainly via 16S ribosomal RNA gene amplicon sequencing; additional research is needed concerning the precision and depth of its effects on microbial communities (22). Whole metagenome shotgun sequencing, a new technique that allows all microbial genomes in a sample to be sequenced, can localize bacteria to the species level and facilitate functional annotation; these results cannot be achieved using conventional 16S rDNA amplicon sequencing (23). Because of dietary and lifestyle differences among countries and regions, the gut microbiota displays substantial geographical variation. Although China has a large population, there have been few studies regarding the effects of SG on the gut microbiota and metabolites of Chinese obese patients. Here, we used whole metagenome shotgun sequencing, in combination with non-targeted metabolomic profiling, to elucidate the therapeutic mechanisms of SG from a gut microbiota perspective, identify biomarkers of SG, and provide new insights for obesity treatment.

Abbreviations: SG, sleeve gastrectomy; OB, obesity; FMT, fecal microbiota transplantation; BMI, body mass index; NAFLD, nonalcoholic fatty liver disease; T2DM, type 2 diabetes mellitus; HFD, high-fat diet; PBS, phosphate-buffered saline; CCS, circular consensus sequence; TG, triglyceride; IPGTT, intraperitoneal glucose tolerance test; AUC, area under the curve; LDA, linear discriminant analysis; NIM, negative ion mode; PIM, positive ion mode; MS, mass spectrometry; PCA, principal component analysis; PLSDA, partial least squares-discriminant analysis; PUFAs, polyunsaturated fatty acids; Ile-Glu, isoleucine- glutamate; COVID-19, coronavirus disease 2019; NASH, nonalcoholic steatohepatitis; FXR, farnesoid X receptor; FAHFA, fatty acid esters of hydroxy fatty acid.

2 Methods

2.1 Participants and sample collection

From September 2021 to May 2022, this study recruited obese patients who underwent laparoscopic SG at the First Affiliated Hospital of Shandong First Medical University (Jinan, China). None of the obese patients participating in this research had a drug history or medication withdrawal. Inclusion criteria were (1) a diagnosis of morbid obesity, (2) unsatisfactory results despite lifestyle and medical therapies, and (3) age 18–65 years. Exclusion criteria were (1) serious complications (e.g., poor cardiopulmonary function or any vital organ dysfunction), (2) cognitive impairment or intellectual disability, and/or (3) contraindications to laparoscopic SG or general anesthesia. Participants' anthropometric data, serum samples, and fecal samples were collected (after an overnight fast) before surgery and 3 months after laparoscopic SG. After collection, serum and fecal samples were frozen at -80°C until analysis.

2.2 Operative procedure

After the induction of general anesthesia, each patient was placed in the supine position and a pneumoperitoneum was created at 12 mmHg with a Veress needle. A 10-mm trocar

was placed for insertion of the 30° laparoscope, and four 5-mm trocars were inserted. The gastrocolic and gastrosplenic ligaments were dissected along the greater curvature of the stomach; dissection was continued proximally to the angle of His. Subsequently, excess gastric body and fundus were removed along the greater curvature of the stomach at 4 cm from the pylorus. Barbed sutures were used for continuous suturing to reinforce the cutting line. Next, a drainage tube was placed in the abdominal cavity. Finally, all trocars were removed, and the abdomen was deflated.

2.3 Whole metagenome shotgun sequencing

2.3.1 Extraction of microbial DNA

Microbial DNA was extracted from fecal samples using the E.Z.N.A.® Stool DNA Kit (D4015-02, Omega, Inc., USA), in accordance with the manufacturer's instructions. This reagent, specifically formulated for the extraction of DNA from minimal sample sizes, has proven to be highly efficient in extracting DNA from a wide range of bacterial species. Sample blanks consisted of unused swabs that were subjected to DNA extraction and confirmed to be DNA amplicon-free. In accordance with the manufacturer's protocol (QIAGEN), total DNA was eluted in 50 µl of elution buffer, then frozen at -80°C. Finally, total DNA was quantified by Lc-bio Technologies (Hangzhou) Co., Ltd. (Hangzhou, China).

2.3.2 Construction of microbial DNA libraries

Microbial DNA libraries were constructed using the TruSeq Nano DNA LT Library Preparation Kit (FC-121-4001). DNA was fragmented by incubation with dsDNA Fragmentase (NEB, M0348S) at 37°C for 30 min. Library construction begins with fragmented cDNA. Blunt-end DNA fragments were generated using a combination of fill-in reactions and exonuclease activity, then ligated to indexed adapters. Each adapter is designed with a T-base overhang, enabling the seamless ligation of the adapter to the A-tailed fragmented DNA. Next, polymerase chain reaction amplification of the ligated products was conducted under the following conditions: initial denaturation at 95°C for 3 min; 8 cycles of denaturation at 98°C for 15 sec, annealing at 60°C for 15 sec, and extension at 72°C for 30 sec; and a final extension at 72°C for 5 min.

2.3.3 Data processing

The raw sequencing reads underwent processing to extract valid reads for subsequent analysis. Initially, sequencing adapters were eliminated from the reads using cutadapt v1.9. Subsequently, fqtrim v0.94 was employed to trim low-quality reads using a sliding-window algorithm. Finally, the reads were aligned to the host genome using bowtie2 v2.2.0 to eliminate any host contamination. Quality-filtered data were subjected to *de novo* assembly by IDBA-UD v1.1.1 to construct the metagenome for each sample. MetaGeneMark v3.26 was used to predict all coding regions of metagenomic contigs. CD-HIT v4.6.1 was used to remove redundant genes to obtain unigenes. To generate functional information, the unigenes were used as queries for functional database (Kyoto Encyclopedia of Genes and Genomes [KEGG]) analysis by DIAMOND v0.9.14. Based on the above data, as well as the unigene abundance profile, the Mann–Whitney U test, Kruskal–Wallis test (replicated groups), Unweighted Pair Group Method with Arithmetic Mean (UPGMA), and Linear discriminant analysis Effect Size (LEfSe) methods were used to identify features with significant differential abundances across groups. Subsequently, differentially enriched KEGG pathways were identified. Alpha diversity was quantified using the Chao1, good coverage, observed species, and Shannon indices. Beta diversity was calculated using Bray–Curtis distance or Jensen–Shannon Divergence distance.

2.4 Metabolomics analysis

2.4.1 Metabolite extraction

Serum and fecal samples (20 µl each) were extracted with 120 µl or 1 ml of precooled 50% methanol, respectively, then incubated at room temperature for 10 min. Subsequently, extraction mixtures were stored at -20°C overnight. After centrifugation (4000 × g for 20 min), supernatants were transferred into 96-well plates and stored at -80°C for liquid chromatography–mass spectrometry (LC-MS) analysis.

2.4.2 LC-MS data acquisition

Samples were analyzed by LC-MS in accordance with the system manufacturer's instructions. The Vanquish Flex UHPLC system (Thermo Fisher Scientific, Bremen, Germany) was used for chromatographic separation. Reversed phase separation was performed using an ACQUITY UPLC TC column (35°C, 0.4 ml/min, 100 mm × 2.1 mm, 1.8 µm, Waters, Milford, USA); the mobile phase consisted of solvent A (water, 0.1% formic acid) and solvent B (acetonitrile, 0.1% formic acid). The gradient elution conditions were as follows: 0–0.5 min, 5% B; 0.5–7 min, 5% to 100% B; 7–8 min, 100% B; 8–8.1 min, 100% to 5% B; and 8.1–10 min, 5%B. Eluted metabolites were detected using a Q-Exactive high-resolution tandem mass spectrometer (Thermo Fisher Scientific, Bremen, Germany). Precursor spectra (70–1050 m/z) were gathered at 70000 resolutions; the first three configurations for data acquisition used DDA mode. Finally, fragment spectra were collected at 17500 resolutions.

2.4.3 Data processing

The above MS data preprocessing steps (including peak picking, peak grouping, retention time correction, second peak grouping, and annotation of isotopes and adducts) were performed with XCMS software. LC–MS raw data files were converted into mzXML format and then processed by the XCMS, CAMERA and metaX toolbox implemented with the R software. Each peak intensity was recorded; a three-dimensional matrix was generated containing arbitrarily assigned peak indices, sample names, and ion intensity information. The KEGG database and the human metabolome database (HMDB) were used to annotate

metabolites. If the mass difference between the observed and the database value was less than 10 ppm, the metabolite was annotated, and the molecular formula of the metabolites was further identified and validated through isotopic distribution measurements. An in-house fragment spectrum library of metabolites was also used to annotate metabolites.

Meta X was used for additional preprocessing of peak intensity data. Features detected in fewer than 50% of quality control samples or 80% of biological samples were removed to improve data quality, the remaining peaks with missing values were imputed using the k-nearest neighbor algorithm, enhancing the overall data quality. Moreover, standard deviations were calculated across quality control samples; samples with standard deviations > 30% were removed. Finally, Student's t-test was conducted to identify differences in metabolite concentrations. Meta X software was used to distinguish variables across groups. Furthermore, variable importance in projection (VIP) values were calculated; a VIP cut-off value of 1.0 was used to select important features.

2.5 Integration of metagenomic with metabolomics data and clinical data

SPSS v26.0 was used to analyze the correlations of highly variable microbiota with blood metabolomics data, fecal metabolomics data, and clinical data. It was also used to evaluate the relationships among metagenomic, metabolomic, and clinical data. *P* values for hypothesis testing were considered statistically significant when $P<0.05$.

3 Results

3.1 Whole metagenome shotgun sequencing analysis of community structure changes in gut microbiota diversity after SG

We collected preoperative and postoperative fecal samples from obese patients who underwent SG; the patients' clinical characteristics are shown in Tables 1 and 2. We defined the preoperative obese patients as the OB group and the post-SG patients as the SG group, the samples and clinical data between these two groups were then analyzed. We first constructed and plotted dilution curves for core and pan genes (Supplementary Figures 1A, B). For our sample size, the number of genes was generally stable, indicating that the data were ready for subsequent analysis. Alpha diversity analysis at the species level revealed that the Chao1, observed species, and Shannon indices were statistically significantly higher in the SG group than in the OB group, suggesting that SG caused significantly higher gut microbiota richness, evenness, and diversity (Figures 1A-D). We then investigated the effects of SG on gut microbiota composition in obese patients via principal coordinates analysis based on Bray–Curtis distance (Figure 1E) and sample clustering using UPGMA (Figure 1F). We observed significant differences in microbial composition between the two groups. These results were validated by ANOSIM and Adonis analyses (Supplementary Figures 1C, D).

TABLE 1 Demographic characteristics and operation status of study subjects.

Variables	Mean ± SD/n (%)
Participants	5
Age (years)	28.4 ± 3.2
Height (m)	1.7 ± 0.1
Body weight (kg)	127.2 ± 17.1
BMI (kg/m^2)	43.9 ± 3.8
Gender	
Male	2 (40%)
Female	3 (60%)
Waistline (cm)	133.4 ± 4.7
Hipline (cm)	137.0 ± 7.2
Hospital stays (days)	7.4 ± 1.1
Comorbidities	
Metabolic syndrome	1 (20%)
Hypertension	1 (20%)
Hyperlipemia	1 (20%)
T2DM	1 (20%)
PCOS	1 (20%)
SAHS	5 (100%)
OGTT (mmol/L)	
1 h	10.1 ± 3.8
2 h	8.1 ± 4.1
3 h	5.9 ± 3.4
Operative time (min)	141.0 ± 9.6

Data are expressed as mean ± SD or as numbers and percentages. T2DM, type 2 diabetes mellitus; PCOS, polycystic ovary syndrome; SAHS, sleep apnoea/hypopnoea syndrome; OGTT, oral glucose tolerance tests.

3.2 Changes in gut microbial composition after SG

Comparative metagenomics analysis via stacked bar charts and heat maps at the phylum and order level revealed that taxonomic distributions significantly differed between groups (Figures 2A, B, Supplementary Figures 2A–D). At the phylum level, Verrucomicrobia richness was significantly increased in the SG group, compared with the OB group. Additionally, at the order level, Enterobacterales, Desulfovibrionales, Acidaminococcales, Verrucomicrobiales, and Bacteroidetes were significantly increased after SG, whereas Veillonellales was decreased. To more comprehensively investigate the remodeling effect of SG on gut microbiota, we focused on changes at the species level, which is an

TABLE 2 Clinical parameters before and after laparoscopic sleeve gastrectomy.

Variables	Before LSG	1 month	2 months	3 months
Body weight (kg)	127.2 ± 17.1	108.6 ± 17.1	102.6 ± 16.2*	98.8 ± 16.0*
BMI (kg/m^2)	43.9 ± 3.8	37.4 ± 3.9*	35.4 ± 3.9*	34.0 ± 3.8*
Alanine aminotransferase (U/L)	52.2 ± 30.3	53.1 ± 29.5	40.5 ± 20.0	22.7 ± 10.8
Aspartate aminotransferase (U/L)	28.8 ± 13.0	28.6 ± 12.8	23.8 ± 7.7	16.6 ± 3.8
Uric acid (μmol/L)	469.0 ± 143.1	538.6 ± 132.0	516.6 ± 132.7	489.2 ± 149.6
Triglyceride (mmol/L)	3.7 ± 5.3	2.4 ± 2.3	1.8 ± 1.4	1.8 ± 0.7
Total cholesterol (mmol/L)	4.7 ± 1.3	4.2 ± 1.4	4.3 ± 1.3	4.9 ± 1.4
High-density lipoprotein (mmol/L)	1.1 ± 0.1	1.2 ± 0.3	1.1 ± 0.3	1.0 ± 0.2
Low-density lipoprotein (mmol/L)	2.3 ± 1.0	2.4 ± 1.0	2.4 ± 1.1	2.4 ± 1.0
Haemoglobin A1c (%)	6.0 ± 1.2	6.1 ± 1.1	5.7 ± 0.5	5.3 ± 0.4
Fasting blood glucose (mmol/L)	5.7 ± 2.8	5.3 ± 1.0	5.1 ± 1.1	5.2 ± 0.9

Data are expressed as mean ± SD. *P < 0.05 versus before LSG. LSG, laparoscopic sleeve gastrectomy; BMI, body mass index.

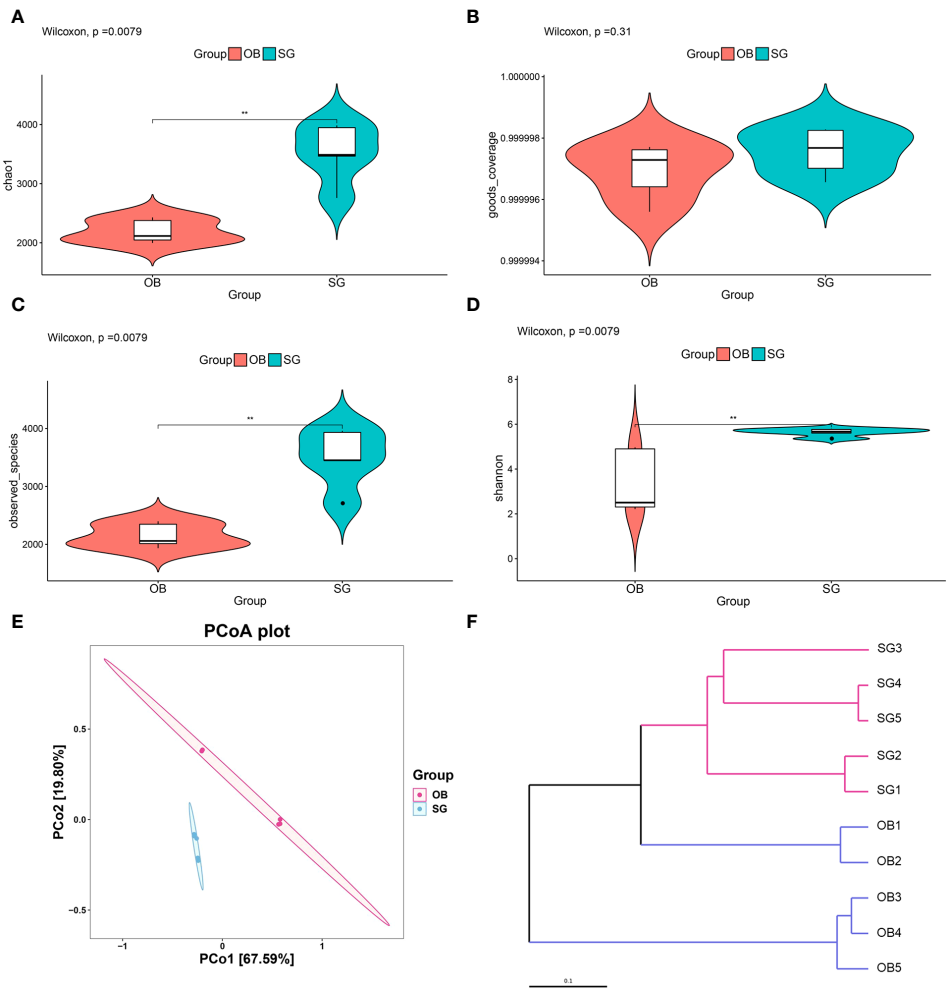

FIGURE 1
Analysis of community structural changes in the diversity of gut microbiota after sleeve gastrectomy by the whole metageome shotgun sequencing. **(A)** chao1, **(B)** goods coverage, **(C)** observed species and **(D)** Shannon estimators to indicate changes of α-diversity after SG; **(E)** Principal-coordinate analysis (PCoA) of samples derived from two groups based on the Bray-Curtis distance; **(F)** The Unweighted Pair Group Method with Arithmetic Mean (UPGMA) method was used to cluster the samples depending on Bray-Curtis distance. ** means P<0.01.

10.3389/fendo.2024.1338147

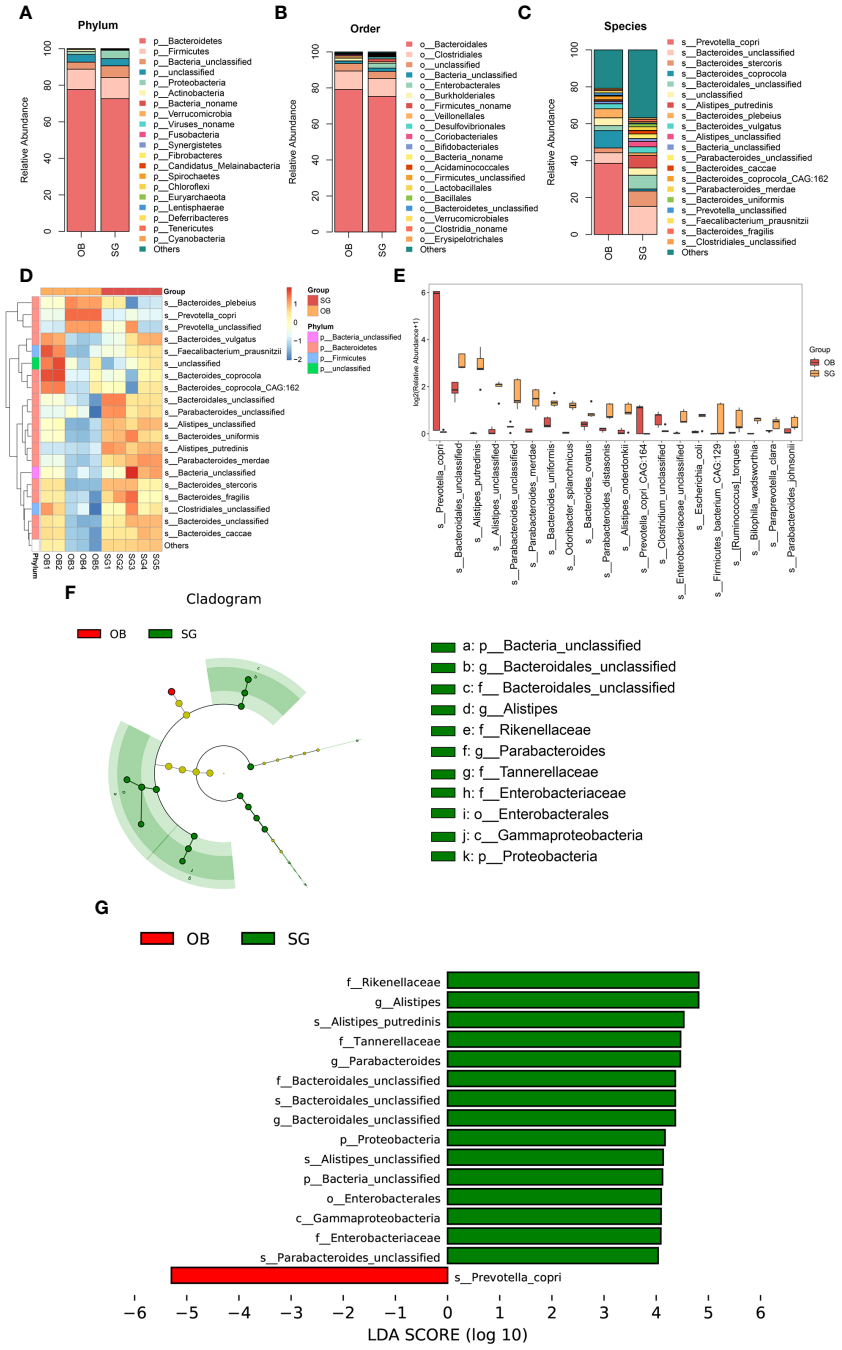

FIGURE 2
Changes in the gut microbial composition after SG. **(A)** Difference between two groups in the composition of the gut microbiota at the phylum level presented as stacked plot; **(B)** Difference between two groups in the composition of the gut microbiota at the order level presented as stacked plot; **(C)** Difference between two groups in the composition of the gut microbiota at the species presented as stacked plot; **(D)** Changes of post-SG bacterial population at the species level presented as the heat map; **(E)** The TOP 20 differential bacteria species caused by SG, according to the P value; **(F)** Cladogram of LDA Effect Size (LEfSe) for identifying species with significant differences in abundance of the SG group (LDA>4.0); **(G)** LDA score of LDA Effect Size (LEfSe) for identifying species with significant differences in abundance of the SG group (LDA>4.0).

advantage of shotgun sequencing and metagenome-wide association studies compared with conventional 16S rDNA sequencing. The resulting data were categorized and presented as stacked bar charts, heat maps, and bar charts (Figures 2C-E). At the species level, we found significant increases in Bacteroidales, *Alistipes*, and *Parabacteroides*, along with substantial decreases in *Prevotella* and *Clostridium*, after SG treatment compared with samples collected prior to SG. To identify species with significantly different abundances, we established a linear discriminant analysis (LDA) threshold value of > 3.0 and performed analysis using the LEfSe tool. Numerous taxa were significantly different between the two groups (Supplementary Figures 2E, F). To identify biomarkers with greater potential for biological relevance, we established an LDA threshold value of 4.0;

using this value, we detected biomarker species for SG, including Rikenellaceae, *Alistipes*, *Parabacteroides*, Bacteroidales, and Enterobacterales; we also detected a biomarker for OB (*Prevotella*) (Figures 2F, G).

3.3 SG significantly alters the genetic characteristics and functions of gut microbiota

Comparative analysis revealed that the number of genes in the gut microbiota was significantly higher in the SG group than in the OB group (Figure 3A). Furthermore, compared with the OB group, the SG group displayed 113,420 upregulated genes and 9,305 downregulated genes (Figure 3B). Analysis using the KEGG database revealed that the differential genes were mainly enriched in metabolism-related pathways, suggesting that the changes in gut microbiota after SG are associated with improvements in host metabolic status (Figure 3C, Supplementary Figure 3A). Next, we analyzed differences in microbial function between the two groups based on KEGG database findings. We found no statistically significant differences between the two groups at KEGG level1 (Supplementary Figure 3B). However, a significant difference between the two groups was present at KEGG level2 (Figure 3D, Supplementary Figures 3C–E). Among the differential pathways, the lipid metabolism pathway was statistically significantly enhanced in the SG group (Figure 3E). Further analysis according to KEGG pathway definitions revealed additional differences in metabolic pathways (Figure 3F, Supplementary Figures 3F–H). We identified the top 30 functional pathways with the greatest differences in KEGG PathwayDefinition (Figure 3G), then ranked the top 20 and depicted them in a box plot (Figure 3H). The results showed that the levels of amino acid metabolism (e.g., lysine and tryptophan) and lipid metabolism (e.g., fatty acids, ether lipids, and α-linolenic acid) pathway components were significantly increased after SG.

3.4 Altered gut metabolite profiles after SG

Non-target metabolome sequencing of fecal samples yielded 10955 features in negative ion mode (NIM) and 18498 features in positive ion mode (PIM), with 1194 and 986 ions of all secondary metabolites identified, respectively. And there were 5576 and 9053 annotated primary metabolites in NIM and PIM, respectively (Table 3). In single-stage mass spectrometry (MS1) analysis, the data identified were applied as a bulk query to the human metabolome database (HMDB) and annotated with 4333 and 7296 individual samples of the identifying features identified in the PIM and NIM, respectively, and the highest abundant metabolites were lipids or lipid analogues (Table 3; Supplementary Figure 4A). It was found that they were mainly enriched in metabolic functional pathways, including lipid metabolism, amino acid metabolism, cofactors, and vitamins, and were also closely associated with endocrine disorders, in addition to digestive disease, as shown by MS1 analysis based on the KEGG (Figure 4A). Afterwads, we performed secondary-mass spectrometry analysis (MS2) and found that the metabolites were mainly related to lipid metabolism such as sphingolipids, glycerophospholipids, and unsaturated fatty acids (Figure 4B and Supplementary Figure 4B). Subsequently, PCA and PLSDA showed significant group differences between the SG and OB groups (Figure 4C and Supplementary Figure 4C). There were 2899 metabolic ions upregulated and 2827 metabolic ions downregulated in the SG group compared to the OB group (Figure 4D). The difference in metabolites between the two groups was visualized by the volcano and heat maps (Supplementary Figure 4D and 4E). We then listed the 20 metabolites identified by MS2 as differential features with the highest differences according to P values by annotating them into the database (Figure 4E), and demonstrated a significant increase in small molecular lipid molecules including free fatty acids, triglycerides, ceramides, etc., and an increase in esterified bile acids after SG, predominantly esterified deoxycholic acid and esterified glyodeoxycholic acid. In order to clarify the functions of the metabolites, we annotated them into the KEGG database according to the identified primary and secondary metabolites. The different primary metabolites between the two groups were mainly enriched in unsaturated fatty acid (PUFAs) metabolic pathways such as linolenic acid, linoleic acid, and arachidonic acid and were closely associated with metabolic pathways such as primary bile acid synthesis and steroid synthesis (Figure 4F). Secondary metabolites are likewise mainly enriched in metabolism-related pathways, including fatty acid synthesis, prolongation, degradation, glycerophospholipids, ether lipids, linoleic acid, etc. (Figure 4G). All the above results can be corresponded to metagenome-wide association studies above.

3.5 Serum metabolic profiles change after SG

Non-targeted metabolomic profiling of serum samples revealed 11451 and 15496 metabolic features according to MS1, 348 and 477 metabolic features according to MS2, and 6062 and 7812 annotated primary metabolites in NIM and PIM, respectively (Table 4). Similar to the fecal metabolomic analysis, the primary metabolites identified were mainly lipids or lipid analogs, according to the HMDB (Supplementary Figure 5A). Meanwhile, on the basis of the KEGG database, the functional pathways of the primary metabolites were amino acid metabolism, lipid metabolism, cofactor and vitamin metabolism, which was consistent with the results obtained from the fecal samples (Figure 5A). We further annotated the features obtained from secondary mass spectrometry into KEGG, showing that the functions of the metabolites in the serum samples are mainly closely related to the metabolic pathways (Figure 5B and Supplementary Figure 5B). We identified metabolites that differed between the SG and OB groups, then analyzed those metabolic features via PCA (Figure 5C) and PLSDA (Supplementary Figure 5C); we found that samples demonstrated similarity within the OB and SG groups, whereas they significantly differed between groups. After SG, 2060 features were upregulated, and 1913 features were downregulated (Figure 5D). Metabolites with changes after SG were visualized using heat and volcano plots (Supplementary Figures 5D, E). To further clarify the differential metabolites

10.3389/fendo.2024.1338147

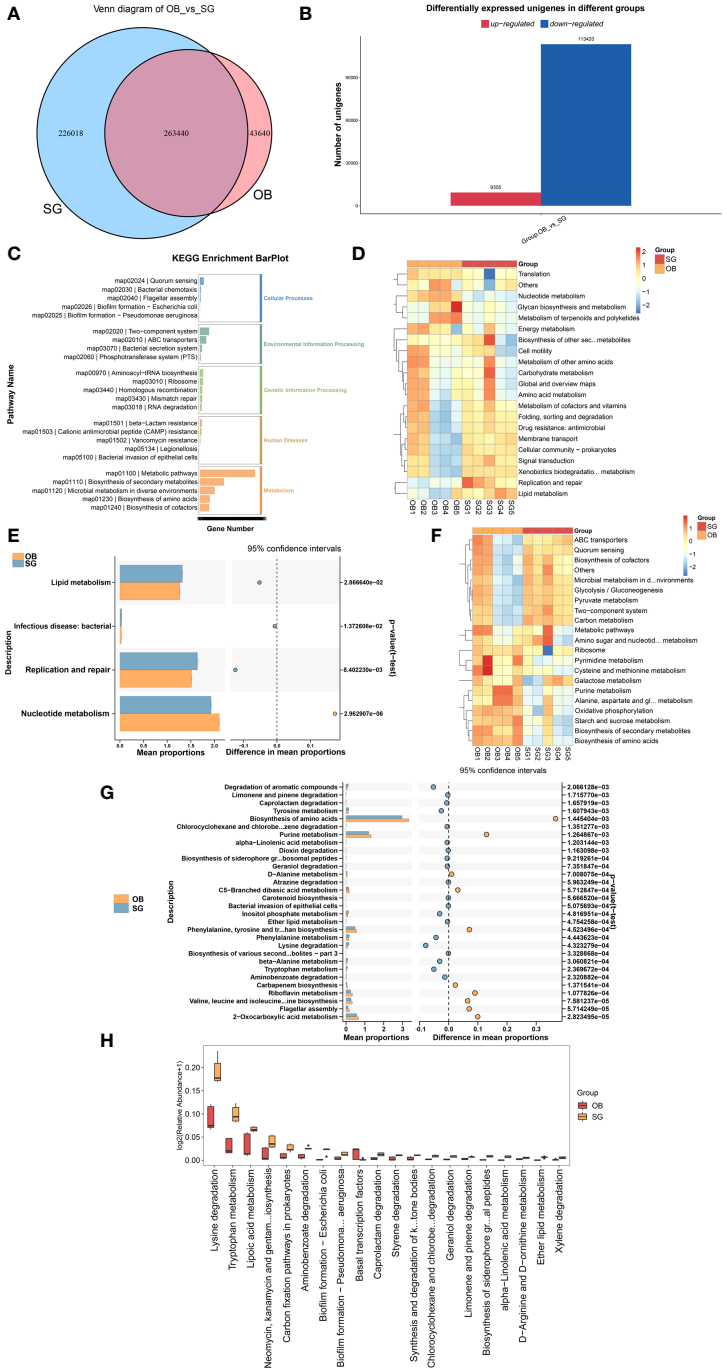

FIGURE 3
SG significantly alters gut microbiota genetic characteristics and functions **(A)** Venn diagram for differential genes between two groups; **(B)** Altered gut microbial gene counts after SG; **(C)** KEGG enrichment analysis of differential genes between groups; **(D, E)** Altered function of gut microbiota after SG based on KEGG database at the KEGG level 2; **(F, G)** Altered function of gut microbiota after SG based on KEGG database at the KEGG PathwayDefinition level; **(H)** Top 20 most significantly different functions of gut microbiota between the two groups.

TABLE 3 Identification of the fecal metabolome.

Mode	All	MS2	HMDB	KEGG	Annotated
Negative	10955	1194	4333	2371	5576
Positive	18498	986	7926	4268	9053

10.3389/fendo.2024.1338147

TABLE 4 Identification of the serum metabolome.

Mode	All	MS2	HMDB	KEGG	Annotated
Negative	11451	348	5065	4431	6062
Positive	14296	477	6815	5523	7812

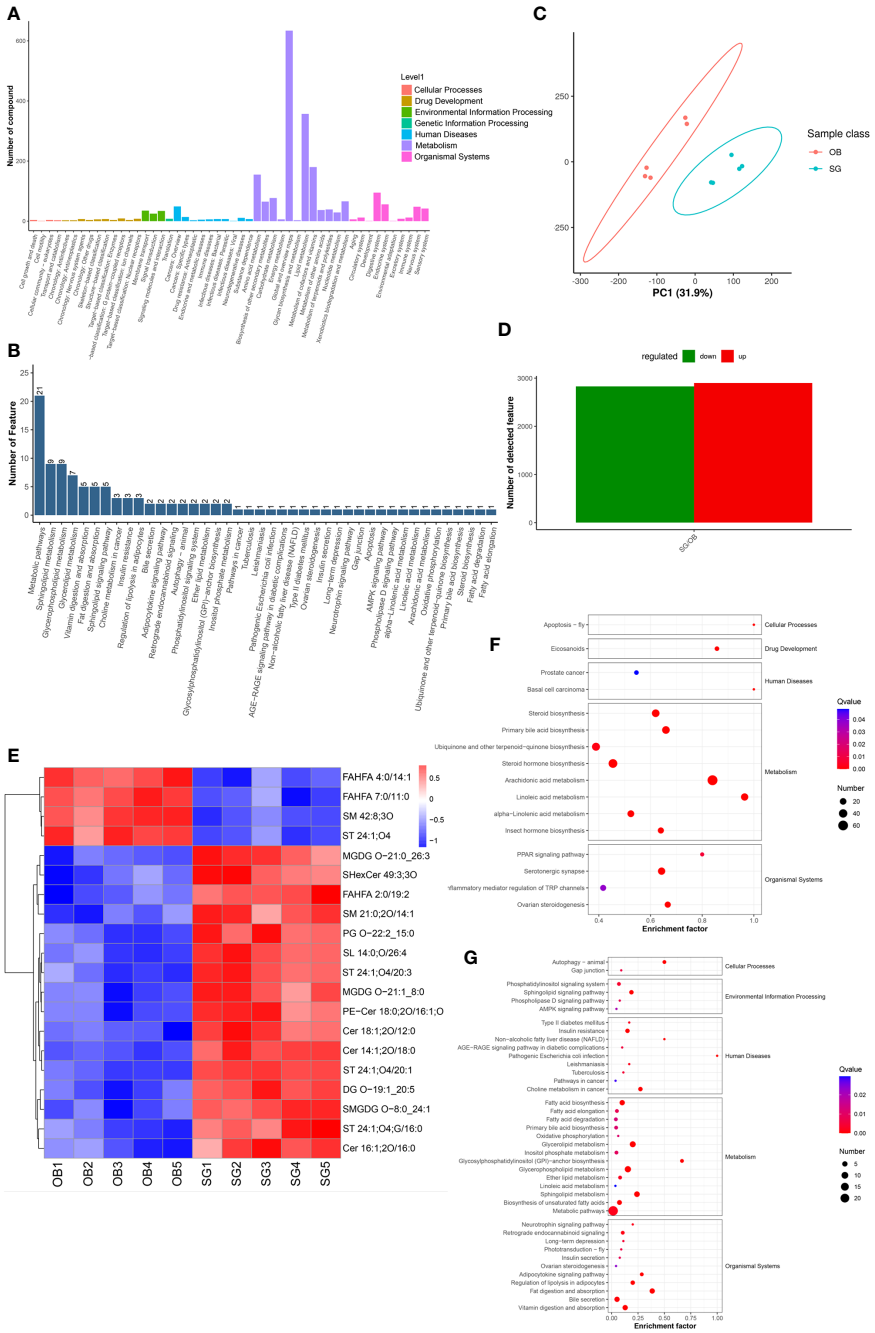

FIGURE 4
Comparative metabolomics analysis revealed the alteration in gut metabolites after SG. **(A)** Annotation of overall gut metabolic features identified by MS1 based on the KEGG database; **(B)** Annotation of overall gut metabolic features identified by MS2 based on the KEGG database; **(C)** PCA for gut metabolites from two groups; **(D)** Statistical bar graph of the change in the count of differentially metabolized ions, caused by SG; **(E)** Heat maps revealing the different intestinal metabolites between the two groups; **(F)** The KEGG Enrichment Analysis for gut metabolites identified by MS1; **(G)** The KEGG Enrichment Analysis for gut metabolites identified by MS2.

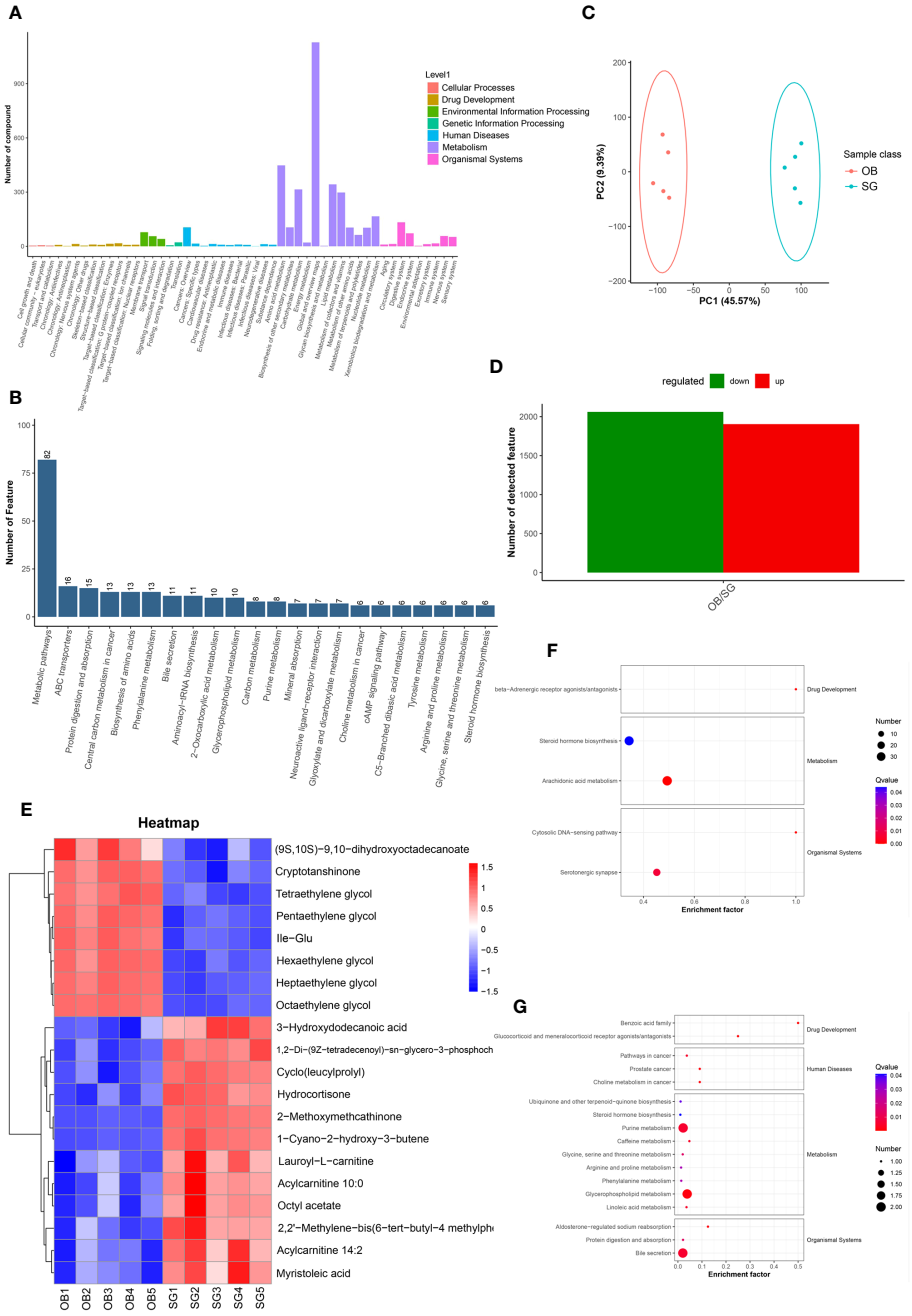

FIGURE 5
Comparative metabolomics analysis revealed the alteration in serum metabolites after SG. **(A)** Annotation of overall serum metabolic features identified by MS1 based on the KEGG database; **(B)** Annotation of overall serum metabolic features identified by MS2 based on the KEGG database; **(C)** PCA for serum metabolites from two groups; **(D)** Statistical bar graph of the change in the count of differentially metabolized ions, caused by SG; **(E)** Heat maps revealing the different serum metabolites between the two groups; **(F)** The KEGG Enrichment Analysis for serum metabolites identified by MS1; **(G)** The KEGG Enrichment Analysis for serum metabolites identified by MS2.

between groups, the identified metabolite ions were annotated into the database and a visual analysis of the TOP20 differential metabolites was performed based on *P* values (Figure 5E). The levels of dihydroxyoctadecanoate, cryptotanshinone, tetraethylene glycol, and isoleucine- glutamate (Ile-Glu) significantly decreased after SG, whereas the levels of 3-hydroxydodecanoic acid, hydrocortisone, lauroyl-L-carnitine, and acylcarnitine significantly increased. Finally, we performed separate functional analyses of primary and secondary differential metabolites via KEGG enrichment analysis and bubble mapping. Differential primary metabolites were mainly associated with linoleic acid, a type of polyunsaturated fatty acids (PUFAs), and steroid hormone biosynthetic pathways (Figure 5F). In contrast, differential secondary metabolites were mainly associated with purine metabolism, glycerophosphate metabolism, and linoleic acid metabolism (Figure 5G).

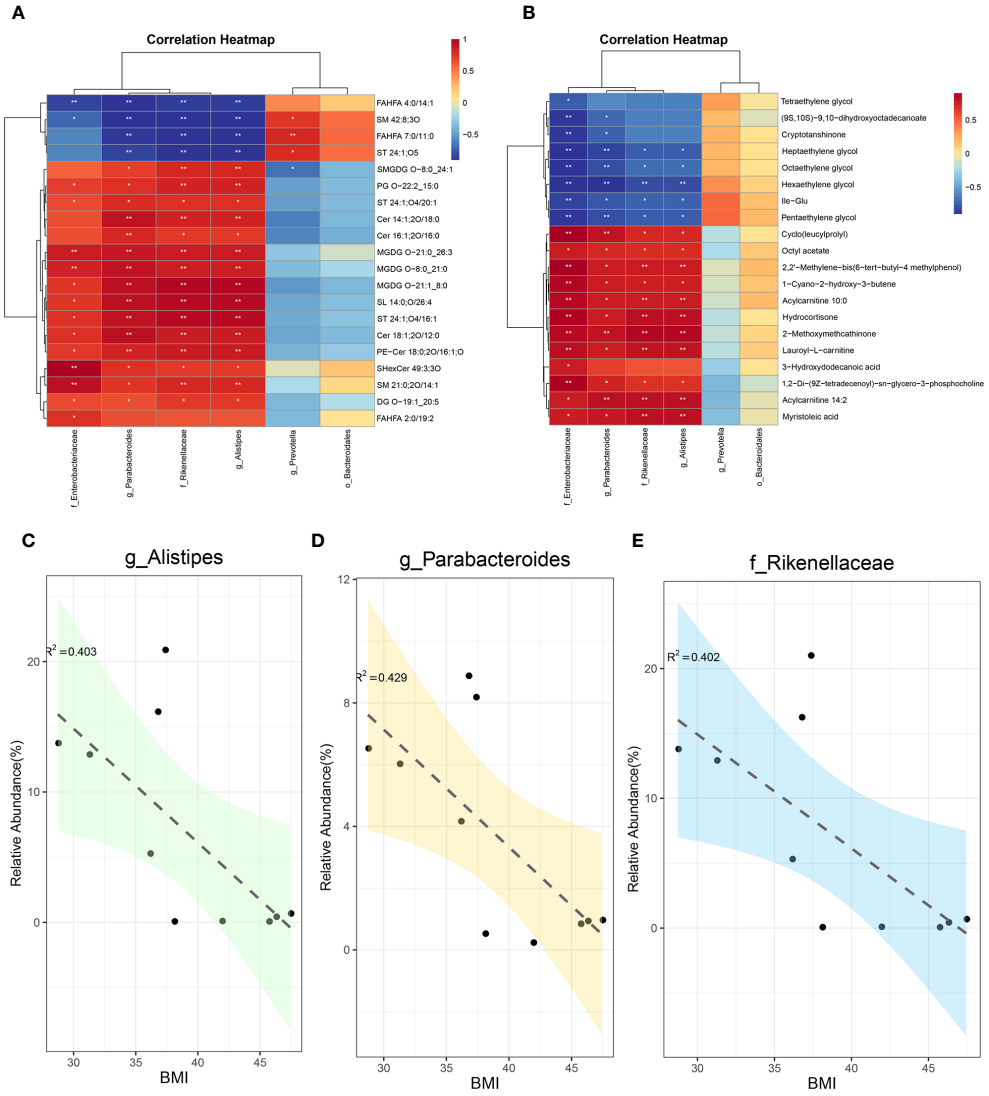

FIGURE 6
Integreted multi-omics analysis revealed the remodeling of intestinal microenvironment mediated by SG. **(A)** The correlation analysis between specific differential bacteria and TOP 20 fecal differential metabolites; **(B)** The correlation analysis between specific differential bacteria and TOP 20 serum differential metabolites; **(C)** The linear correlation analysis between abundance of Alistipes and BMI; **(D)** The linear correlation analysis between abundance of Parabacteroides and BMI; **(E)** The linear correlation analysis between abundance of Rikenellaceae and BMI.

3.6 Combined multi-omics analysis reveals SG-mediated remodeling of the gut microenvironment

For systematic assessment of the mechanism by which SG alleviates obesity through gut microenvironment remodeling, we performed integrated analysis using a multi-omics approach in combination with clinical data. During whole metagenome shotgun sequencing and LEfSe analysis, we tentatively identified several microbes with substantial changes in abundance after SG, including Rikenellaceae, *Alistipes*, *Parabacteroides*, Bacteroidales, Enterobacterales, and *Prevotella*; we compared them with differential metabolites from fecal samples (Supplementary Figure 6A) and serum samples (Supplementary Figure 6B). Because of the large amount of data, we performed correlation analysis between the above differential microbiota and the 20 most significantly different metabolites in feces (Figure 6A) and serum (Figure 6B). We found that Rikenellaceae, *Alistipes*, *Parabacteroides*, and Enterobacterales had statistically significant correlations with most of the differential metabolites, whereas *Prevotella* and Bacteroidales were poorly correlated with differential metabolites; these findings were consistent across metabolites from fecal and serum samples, suggesting that the first four bacteria contribute to the weight-loss effect of SG. Accordingly, we performed a linear analysis of BMI, an important clinical indicator of obesity, using the above six groups of bacteria. We found that Rikenellaceae, *Alistipes*, and *Parabacteroides* were correlated with BMI (Figures 6C-E), whereas the other three microbiota were not correlated with BMI (Supplementary Figures 6C–E). Taken together, these results suggest that the increased abundances of Rikenellaceae, *Alistipes*, and *Parabacteroides* in the gut microbiota after SG have important effects on the outcome of SG-mediated weight reduction therapy.

4 Discussion

Obesity and its related complications pose a serious public health threat worldwide (1, 24). In the context of the COVID-19 pandemic, the metabolic disease aspect of obesity has received increasing attention based on findings that it increases COVID-19 risk and severity (25, 26). SG as a common bariatric surgery operation, has demonstrated a substantial weight-loss effect in obese patients; it also alleviates obesity-related complications and delays their progression (27, 28). However, additional research is needed to fully elucidate the therapeutic mechanisms of SG, particularly from an gut microecological perspective. In the present study, we utilized a multi-omics approach to analyze changes in gut microbiota and metabolites after SG among obese patients from Shandong, China. Such changes had important effects on host metabolism and might offer biomarkers forgut microecology after SG.

Previous studies have shown that bariatric surgery can significantly contribute to improvement in the gut dysbacteriosis associated with obesity (29). SG alters the normal structure of the gastrointestinal tract and rearranges the gut microecology whcih may play a central role in the effect of SG. In this study, the whole metagenome shotgun sequencing revealed a significant increase in alpha diversity after SG, suggesting significant increases in microbiota richness and diversity. Subsequently, principal coordinates analysis of samples from the OB and SG groups revealed similarities within each group and differences between groups. Based on these results, we conducted further exploration of the gut microbiota composition. LEfSe analysis was performed to investigate the effect of SG on gut microbial community composition at various levels, especially the species level. Rikenellaceae, *Alistipes*, *Parabacteroides*, Bacteroidales, and Enterobacterales were identified as characteristic bacteria in the SG group; *Prevotella* was identified as the characteristic bacteria in the OB group. In a previous study, Rikenellaceae abundance was considerably decreased in the intestines of obese patients compared with lean patients; its abundance was positively correlated with the level of ClpB, a bacterial protein that was negatively correlated with BMI, waist circumference, and total fat mass (30). *Alistipes* abundance in the gut microbiota is significantly dysregulated in obese mice; modifications that restore its abundance can partially reverse lipid metabolism disorders (31). The abundance of *Alistipes* gradually decreases as NAFLD progresses to nonalcoholic steatohepatitis and cirrhosis (32). *Parabacteroides* spp. are suspected to mediate anti-obesity effects through enhancement of fat thermogenesis, maintenance of gut integrity, and reduction of the serum insulin resistance level (33). Fecal microbiota transplantation from bariatric surgery patients to experimental mice revealed a significant increase in *Parabacteroides* abundance in the mice, along with improved glucose metabolism (34). Similarly, Bacteroidales spp. are closely associated with obesity-related diseases such as NAFLD and hepatic fibrosis. Additionally, they have demonstrated significant correlations with the abundances of bile acids, such as deoxycholic acid (35) Enterobacterales spp. are generally the focus of infectious disease research, but their roles in lipid metabolism and related fields have not been extensively explored (36). Considering the increased abundance of Enterobacterales observed after SG in the present study, the roles of Enterobacterales spp. in metabolism require further investigation. Notably, the abundance of *Prevotella* in the intestinal contents of rats was significantly increased after SG compared with the control group, indicating that *Prevotella* spp. could have a therapeutic effect on the disturbance of host glucose metabolism by increasing bile acid production and activating farnesoid X receptor (FXR) (37). However, our findings suggested that *Prevotella* abundance decreased after SG and this discrepancy may be the result of species differences, sample sources, differences in dietary structure, and differences in study location. Furthermore, this difference illustrates the need for analyses of gut microbiology to be conducted via clinical trials, rather than animal models alone.

For the alteration of gut microbial function after SG, a series of related analyses at the gene level were performed and showed that a number of genes in the gut contents was substantially increased after SG. Subsequently, we elucidated the mechanism by which SG improves obesity through the gut microbiota, using an approach that involved KEGG-mediated functional annotation of the microbiota at various levels. We found that overall metabolic functions (e.g., fatty acids, amino acids such as tryptophan, and PUFAs metabolic pathways) were generally upregulated after SG. Tryptophan metabolism plays an essential role in the microbiota–gut–brain axis; it is also involved in many psychiatric and neurological disorders (38). Moreover, tryptophan-related metabolites in the gut environment can bind to aryl hydrocarbon receptor ligands and regulate metabolic functions (39). In patients with metabolic disorders, an important gut finding is a decrease in tryptophan, which leads to a decrease in aryl hydrocarbon receptor binding and the activation of both GLP-1 and interleukin-22; this pathway ultimately promotes inflammation, insulin resistance, and hepatic steatosis (40, 41). PUFAs are susceptible to oxidative degradation because of their unstable double bonds; this degradation can lead to tissue damage (42). However, the gut microbiota can allow the host to resist obesity during high-fat diet intake via regulation of PUFAs metabolism (43). The present study also revealed that SG significantly increased the levels of tryptophan and PUFAs, helping to explain the mechanism underlying the superior weight-loss effect of SG from the perspective of gut microecology.

According to the whole metagenome shotgun sequencing, SG could lead to changes in the metabolic function of gut microbiota. Therefore, we conducted non-targeted metabolomic profiling of fecal samples from obese patients undergoing SG; this approach enabled the identification of a greater number of small molecule metabolites. Metabolic ions identified in fecal samples were mainly lipid molecules, which may be associated with the production of short-chain fatty acids by the gut microbiota that were subsequently absorbed by the intestine and finally excreted into feces (44); our whole metagenome shotgun sequencing results corroborated this previous finding. Furthermore, we observed a small increase in the number of gut metabolites after SG, which may be associated with greater gut microbial diversity and richness. We focused on the top 20 different small molecule metabolites according to *P*-values. A decrease in sphingomyelin in the gut environment was observed after SG. Sphingomyelin has been significantly positively correlated with the level of serum cholesterol; a lower level of sphingomyelin was significantly associated with alleviation of hypercholesterolemia (45). We also found that fatty acid esters of hydroxy fatty acids

(FAHFAs) were significantly downregulated after SG. Notably, the effects of FAHFAs on metabolism are controversial; some studies show anti-inflammatory and anti-diabetic effects (46), whereas other studies show contrasting findings (47). Thus, the roles of FAHFAs in metabolism, particularly lipid metabolism, require further investigation. Additionally, we found that SG led to increases in gut sterol sulfate, glycodeoxycholic acid, and phosphatidylglycerol. In a previous study, sterol sulfate tended to be negatively correlated with serum cholesterol and low-density lipoprotein (48). Glycodeoxycholic acid was negatively correlated with insulin clearance, and patients with obesity generally exhibited lower insulin clearance (49). Phosphatidylglycerol remodeling can significantly improve hepatic steatosis by stabilizing mitochondrial structure (50). Although SG leads to a significant weight-loss effect and improves lipid metabolism, we observed significant increases in the levels of free fatty acids and triglycerides in fecal samples collected from patientsunderwent SG. Recent studies have shown that short-chain fatty acids, among the major products of gut microbiota, can function as signaling molecules to regulate lipid metabolism and glucose homeostasis in liver, adipose tissue, and skeletal muscle, thereby exerting anti-obesity effects (51, 52). In summary, the increased levels of various metabolites with favorable roles in the regulation of glucolipid metabolism after SG, along with decreases in the levels of some metabolically harmful substances, provide important insights concerning the weight-loss therapeutic effect of SG from an gut metabolite perspective.

Considering the altered metabolic profile observed after SG, we profiled serum small molecule metabolites. We initially analyzed the metabolic ions identified in our study which were dominated by lipid-like molecules and closely associated with metabolism-related functional pathways, such as amino acids and lipids. Analysis of differential metabolites after SG revealed a significant reduction in isoleucine, a type of branched-chain amino acid; this finding was consistent with the results of a study regarding altered serum metabolic profiles after bariatric surgery (53). Moreover, it may partially explain the mechanism of SG because an elevated serum branched-chain amino acid level was strongly associated with obesity, insulin resistance, and T2DM in humans (54). Additionally, hexaethylene glycol, heptaethylene glycol, cryptotanshinone, and tetraethylene glycol were substantially lower after SG. To our knowledge, the roles of these four metabolites in glucose–lipid metabolism and obesity have not been determined thus far; follow-up studies are needed to explore whether they can be used as therapeutic targets for obesity. Furthermore, we found increases in serum myristoleic acid, hydrocortisone, lauroyl-L-carnitine, and acylcarnitine after SG, compared with samples collected before SG. An increase in myristoleic acid, a class of long-chain fatty acids, has potential anti-obesity effects that involve activating brown adipose tissue and promoting the production of beige fat. In a previous study, the serum hydrocortisone concentration reportedly was decreased after SG (55), which is inconsistent with our findings. This discrepancy is probably related to regional differences in dietary structure, which may influence bacterial metabolites (56). An elevated level of acylcarnitine may enhance mitochondrial β-oxidation, thereby reducing lipid accumulation (57). However, lauroyl-L-carnitine had a positive association with T2DM in a clinical study (58).

The human metabolic profile involves multidimensional crosstalk, and a single omics approach cannot fully illuminate the intricate mechanisms by which SG improves metabolism. Therefore, a multi-omics approach was performed in combination with an analysis of clinical data. We initially identified several candidate bacterial groups via LEfSe analysis, then explored their relationships with differential metabolites in feces and serum samples. We identified four types of bacteria—Rikenellaceae, *Alistipes*, *Parabacteroides*, and Enterobacterales—that were negatively correlated with pro-obesity metabolites (e.g., sphingomyelin) and positively correlated with anti-obesity metabolites (e.g., myristoleic acid). Additionally, linear correlation analysis between these bacteria and BMI revealed that only Rikenellaceae, *Alistipes*, and *Parabacteroides* were both significantly associated with differential metabolites and linearly correlated with BMI. Thus, we concluded that Rikenellaceae, *Alistipes*, and *Parabacteroides* are key bacteria with important roles in the ability of SG to alleviate obesity.Among these, Alistipes was identified as a novel distinctive feature in gut microbiota after SG in this study, compared to previous studies using 16S ribosomal RNA sequencing to detect the effects of SG on gut microbiota (22). These bacteria represent potential targets for future obesity therapies, and set the stage for exploring new non-invasive modality in treating obesity and its related complications.

However, there are several limitations to our study. Due to the fact that many patients undergoing bariatric surgery come from other regions, it is challenging for them to return to our hospital for follow-up examinations due to the long distances involved. Additionally, post-surgery constipation experienced by many patients makes it difficult to collect fecal samples. Consequently, the sample size in this study is relatively small. A larger sample cohort experiment is still needed in the future to further verify the above conclusion, and provide novel targeted drugs with specific gut microbiota for obese patients. Moreover, there was only a correlation between these bacteria we identified and the altered metabolic and clinical parameters. In order to establish causation, additional animal experiments should be further performed.

5 Conclusions

In the present study, we collected fecal and serum samples from obese patients before and after SG, and then classified and functionally analyzed the samples using the whole metagenome shotgun sequencing and the non-targeted metabolomic profiling. We revealed the remodeling of gut microbiota by SG through a multi-omics approach, and identified Rikenellaceae, *Alistipes*, and *Parabacteroide* as the key strains of SG exerting weight-loss effects. This study elucidated the mechanism of SG from the perspectives of gut microbiota and metabolites.

Trial registration

This study was granted approval by the Ethics Review Committee of the First Affiliated Hospital of Shandong First Medical University (Permission number: 2023-S358). Registered 12 May 2023. Retrospectively registered.

Ethics approval and consent to participate

This study was granted approval by the Ethics Review Committee of the First Affiliated Hospital of Shandong First Medical University (Permission number: 2023-S358).

Permission to reuse and copyright

Permission must be obtained for use of copyrighted material from other sources (including the web). Please note that it is compulsory to follow figure instructions.

Data availability statement

The datasets presented in this study can be found in online repositories. The names of the repository/repositories and accession number(s) can be found in the article/https://doi.org/10.6084/m9.figshare.23659710.

Ethics statement

The studies involving humans were approved by Ethics Review Committee of the First Affiliated Hospital of Shandong First Medical University. The studies were conducted in accordance with the local legislation and institutional requirements. The participants provided their written informed consent to participate in this study.

Author contributions

CL: Formal Analysis, Investigation, Writing – original draft. QX: Formal Analysis, Investigation, Writing – original draft. SD: Conceptualization, Writing – review & editing. HD: Investigation, Validation, Writing – original draft. BL: Investigation, Writing – original draft. DZ: Writing – original draft. YL: Writing – original draft. LL: Data curation, Writing – original draft. QL: Writing – original draft. YuC: Supervision, Writing – original draft. JW: Formal Analysis, Validation, Writing – review & editing. JZ: Project administration, Validation, Writing – review & editing. MZ: Project administration, Supervision, Validation, Writing – review & editing. YiC: Methodology, Project administration, Supervision, Validation, Writing – review & editing. GZ: Conceptualization, Funding acquisition, Project administration, Validation, Writing – review & editing.

Funding

The author(s) declare financial support was received for the research, authorship, and/or publication of this article. This work was supported by the Major Basic Research Project of Natural Science Foundation of Shandong Province [Grant Number ZR2020ZD15].

Acknowledgments

We thank Ryan Chastain-Gross, Ph.D., from Liwen Bianji (Edanz) (www.liwenbianji.cn/) for editing the English text of a draft of this manuscript.

Conflict of interest

The authors declare that the research was conducted in the absence of any commercial or financial relationships that could be construed as a potential conflict of interest.

Publisher's note

All claims expressed in this article are solely those of the authors and do not necessarily represent those of their affiliated organizations, or those of the publisher, the editors and the reviewers. Any product that may be evaluated in this article, or claim that may be made by its manufacturer, is not guaranteed or endorsed by the publisher.

Supplementary material

The Supplementary Material for this article can be found online at: https://www.frontiersin.org/articles/10.3389/fendo.2024.1338147/full#supplementary-material

SUPPLEMENTARY FIGURE 1
(A) The dilution curves for Core genes; **(B)** The dilution curves for Pan genes; **(C)** The result for the Analysis of similarities (Anosim) between the two groups; **(D)** The result for the Adonis analysis between the two groups.

SUPPLEMENTARY FIGURE 2
(A) Changes of post-SG bacterial population at the phylum level presented as the heat map; **(B)** Changes of post-SG bacterial population at the order level presented as the heat map; **(C)** The TOP 20 differential microbial composition at the phylum level caused by SG, according to the P value; **(D)** The TOP 20 differential microbial composition at the order level caused by SG, according to the P value; **(F)** Cladogram of LDA Effect Size (LEfSe) for identifying species with significant differences in abundance of the SG group (LDA>3.0); **(G)** LDA score of LDA Effect Size (LEfSe) for identifying species with significant differences in abundance of the SG group (LDA>3.0).

SUPPLEMENTARY FIGURE 3
(A) The KEGG enrichment analysis of differential genes between groups presented as the scatterplot map; **(B)** Altered function of gut microbiota after SG based on KEGG database at the level1; **(C, D, E)** Altered function of gut microbiota after SG based on KEGG database at the KEGG level2; **(F, G, H)** Altered function of gut microbiota after SG based on KEGG database at the KEGG PathwayDefinition level.

SUPPLEMENTARY FIGURE 4
(A) the HMDB super class graph of the overall annotated gut metabolic features identified by MS1 based on the HMDB database; **(B)** the scatterplot graph of the overall annotated gut metabolic features identified by MS2 based

on the KEGG database; **(C)** The partial least squares discriminant analysis (PLSDA) for gut metabolites between the two groups; **(D)** The volcano plot revealing the different gut metabolites between the two groups; **(E)** The heat maps revealing the different gut metabolites between the two groups.

SUPPLEMENTARY FIGURE 5

(A) the HMDB super class graph of the overall annotated serum metabolic features identified by MS1 based on the HMDB database; **(B)** the scatterplot graph of the overall annotated serum metabolic features identified by MS2 based on the KEGG database; **(C)** The partial least squares discriminant analysis (PLSDA) for serum metabolites between the two groups; **(D)** The volcano plot revealing the different serum metabolites between the two groups; **(E)** The heat maps revealing the different serum metabolites between the two groups.

SUPPLEMENTARY FIGURE 6

(A) The correlation analysis between differential gut microbiota and gut differential metabolites; **(B)** The correlation analysis between differential gut microbiota and serum differential metabolites; **(C)** The linear correlation analysis between abundance of Bacteroidales and BMI; **(D)** The linear correlation analysis between abundance of Enterobacteriaceae and BMI; **(E)** The linear correlation analysis between abundance of Prevotella and BMI.

References

1. Blüher M. Obesity: global epidemiology and pathogenesis. *Nat Rev Endocrinol* (2019) 15(5):288–98. doi: 10.1038/s41574-019-0176-8

2. Wang L, Zhou B, Zhao Z, Yang L, Zhang M, Jiang Y, et al. Body-mass index and obesity in urban and rural China: findings from consecutive nationally representative surveys during 2004-18. *Lancet* (2021) 398(10294):53–63. doi: 10.1016/s0140-6736(21)00798-4

3. Fan Y, Pedersen O. Gut microbiota in human metabolic health and disease. *Nat Rev Microbiol* (2021) 19(1):55–71. doi: 10.1038/s41579-020-0433-9

4. McAllister EJ, Dhurandhar NV, Keith SW, Aronne LJ, Barger J, Baskin M, et al. Ten putative contributors to the obesity epidemic. *Crit Rev Food Sci Nutr* (2009) 49(10):868–913. doi: 10.1080/10408390903372599

5. Lindell AE, Zimmermann-Kogadeeva M, Patil KR. Multimodal interactions of drugs, natural compounds and pollutants with the gut microbiota. *Nat Rev Microbiol* (2022) 20(7):431–43. doi: 10.1038/s41579-022-00681-5

6. Li J, Jia H, Cai X, Zhong H, Feng Q, Sunagawa S, et al. An integrated catalog of reference genes in the human gut microbiome. *Nat Biotechnol* (2014) 32(8):834–41. doi: 10.1038/nbt.2942

7. Aron-Wisnewsky J, Warmbrunn MV, Nieuwdorp M, Clément K. Metabolism and metabolic disorders and the microbiome: the intestinal microbiota associated with obesity, lipid metabolism, and metabolic health-pathophysiology and therapeutic strategies. *Gastroenterology* (2021) 160(2):573–99. doi: 10.1053/j.gastro.2020.10.057

8. Li R, Huang X, Liang X, Su M, Lai KP, Chen J. Integrated omics analysis reveals the alteration of gut microbe-metabolites in obese adults. *Brief Bioinform* (2021) 22(3):bbaa165. doi: 10.1093/bib/bbaa165

9. Cox LM, Blaser MJ. Antibiotics in early life and obesity. *Nat Rev Endocrinol* (2015) 11(3):182–90. doi: 10.1038/nrendo.2014.210

10. de Vos WM, Tilg H, Van Hul M, Cani PD. Gut microbiome and health: mechanistic insights. *Gut* (2022) 71(5):1020–32. doi: 10.1136/gutjnl-2021-326789

11. Le Roy T, Moens de Hase E, Van Hul M, Paquot A, Pelicaen R, Régnier M, et al. Dysosmobacter welbionis is a newly isolated human commensal bacterium preventing diet-induced obesity and metabolic disorders in mice. *Gut* (2022) 71(3):534–43. doi: 10.1136/gutjnl-2020-323778

12. den Besten G, Bleeker A, Gerding A, van Eunen K, Havinga R, van Dijk TH, et al. Short-chain fatty acids protect against high-fat diet-induced obesity via a PPARγ-dependent switch from lipogenesis to fat oxidation. *Diabetes* (2015) 64(7):2398–408. doi: 10.2337/db14-1213

13. Frost G, Sleeth ML, Sahuri-Arisoylu M, Lizarbe B, Cerdan S, Brody L, et al. The short-chain fatty acid acetate reduces appetite via a central homeostatic mechanism. *Nat Commun* (2014) 5:3611. doi: 10.1038/ncomms4611

14. Jia W, Xie G, Jia W. Bile acid-microbiota crosstalk in gastrointestinal inflammation and carcinogenesis. *Nat Rev Gastroenterol Hepatol* (2018) 15(2):111–28. doi: 10.1038/nrgastro.2017.119

15. Miras AD, le Roux CW. Metabolic surgery: shifting the focus from glycaemia and weight to end-organ health. *Lancet Diabetes Endocrinol* (2014) 2(2):141–51. doi: 10.1016/s2213-8587(13)70158-x

16. Nguyen NT, Varela JE. Bariatric surgery for obesity and metabolic disorders: state of the art. *Nat Rev Gastroenterol Hepatol* (2017) 14(3):160–9. doi: 10.1038/nrgastro.2016.170

17. Brajcich BC, Hungness ES. Sleeve gastrectomy. *Jama* (2020) 324(9):908. doi: 10.1001/jama.2020.14775

18. Aminian A. Sleeve gastrectomy: metabolic surgical procedure of choice? *Trends Endocrinol Metab* (2018) 29(8):531–4. doi: 10.1016/j.tem.2018.04.011

19. Miras AD, le Roux CW. Mechanisms underlying weight loss after bariatric surgery. *Nat Rev Gastroenterol Hepatol* (2013) 10(10):575–84. doi: 10.1038/nrgastro.2013.119

20. Steenackers N, Vanuytsel T, Augustijns P, Tack J, Mertens A, Lannoo M, et al. Adaptations in gastrointestinal physiology after sleeve gastrectomy and Roux-en-Y gastric bypass. *Lancet Gastroenterol Hepatol* (2021) 6(3):225–37. doi: 10.1016/s2468-1253(20)30302-2

21. Liu R, Hong J, Xu X, Feng Q, Zhang D, Gu Y, et al. Gut microbiome and serum metabolome alterations in obesity and after weight-loss intervention. *Nat Med* (2017) 23(7):859–68. doi: 10.1038/nm.4358

22. Ikeda T, Aida M, Yoshida Y, Matsumoto S, Tanaka M, Nakayama J, et al. Alteration in faecal bile acids, gut microbial composition and diversity after laparoscopic sleeve gastrectomy. *Br J Surg* (2020) 107(12):1673–85. doi: 10.1002/bjs.11654

23. Le Chatelier E, Nielsen T, Qin J, Prifti E, Hildebrand F, Falony G, et al. Richness of human gut microbiome correlates with metabolic markers. *Nature* (2013) 500(7464):541–6. doi: 10.1038/nature12506

24. American Diabetes Association Professional Practice Committee. 8. Obesity and weight management for the prevention and treatment of type 2 diabetes: standards of medical care in diabetes-2022. *Diabetes Care* (2022) 45(Suppl 1):S113–s124. doi: 10.2337/dc22-S008

25. Stefan N, Birkenfeld AL, Schulze MB. Global pandemics interconnected - obesity, impaired metabolic health and COVID-19. *Nat Rev Endocrinol* (2021) 17(3):135–49. doi: 10.1038/s41574-020-00462-1

26. Le Brocq S, Clare K, Bryant M, Roberts K, Tahrani AA. Obesity and COVID-19: a call for action from people living with obesity. *Lancet Diabetes Endocrinol* (2020) 8(8):652–4. doi: 10.1016/s2213-8587(20)30236-9

27. Brown EM, Clardy J, Xavier RJ. Gut microbiome lipid metabolism and its impact on host physiology. *Cell Host Microbe* (2023) 31(2):173–86. doi: 10.1016/j.chom.2023.01.009

28. Seeberg KA, Borgeraas H, Hofsø D, Småstuen MC, Kvan NP, Grimnes JO, et al. Gastric bypass versus sleeve gastrectomy in type 2 diabetes: effects on hepatic steatosis and fibrosis: A randomized controlled trial. *Ann Intern Med* (2022) 175(1):74–83. doi: 10.7326/m21-1962

29. Aron-Wisnewsky J, Prifti E, Belda E, Ichou F, Kayser BD, Dao MC, et al. Major microbiota dysbiosis in severe obesity: fate after bariatric surgery. *Gut* (2019) 68(1):70–82. doi: 10.1136/gutjnl-2018-316103

30. Arnoriaga-Rodríguez M, Mayneris-Perxachs J, Burokas A, Pérez-Brocal V, Moya A, Portero-Otin M, et al. Gut bacterial ClpB-like gene function is associated with decreased body weight and a characteristic microbiota profile. *Microbiome* (2020) 8(1):59. doi: 10.1186/s40168-020-00837-6

31. Yin J, Li Y, Han H, Chen S, Gao J, Liu G, et al. Melatonin reprogramming of gut microbiota improves lipid dysmetabolism in high-fat diet-fed mice. *J Pineal Res* (2018) 65(4):e12524. doi: 10.1111/jpi.12524

32. Rau M, Rehman A, Dittrich M, Groen AK, Hermanns HM, Seyfried F, et al. Fecal SCFAs and SCFA-producing bacteria in gut microbiome of human NAFLD as a putative link to systemic T-cell activation and advanced disease. *United Eur Gastroenterol J* (2018) 6(10):1496–507. doi: 10.1177/2050640618804444

33. Wu TR, Lin CS, Chang CJ, Lin TL, Martel J, Ko YF, et al. Gut commensal Parabacteroides goldsteinii plays a predominant role in the anti-obesity effects of polysaccharides isolated from Hirsutella sinensis. *Gut* (2019) 68(2):248–62. doi: 10.1136/gutjnl-2017-315458

34. Thingholm LB, Rühlemann MC, Koch M, Fuqua B, Laucke G, Boehm R, et al. Obese individuals with and without type 2 diabetes show different gut microbial functional capacity and composition. *Cell Host Microbe* (2019) 26(2):252–264.e210. doi: 10.1016/j.chom.2019.07.004

35. Adams LA, Wang Z, Liddle C, Melton PE, Ariff A, Chandraratna H, et al. Bile acids associate with specific gut microbiota, low-level alcohol consumption and liver fibrosis in patients with non-alcoholic fatty liver disease. *Liver Int* (2020) 40(6):1356–65. doi: 10.1111/liv.14453

36. de Lastours V, Poirel L, Huttner B, Harbarth S, Denamur E, Nordmann P. Emergence of colistin-resistant Gram-negative Enterobacterales in the gut of patients receiving oral colistin and neomycin decontamination. *J Infect* (2020) 80(5):578–606. doi: 10.1016/j.jinf.2020.01.003

37. Péan N, Le Lay A, Brial F, Wasserscheid J, Rouch C, Vincent M, et al. Dominant gut Prevotella copri in gastrectomised non-obese diabetic Goto-Kakizaki rats improves glucose homeostasis through enhanced FXR signalling. *Diabetologia* (2020) 63 (6):1223–35. doi: 10.1007/s00125-020-05122-7

38. Cryan JF, O'Riordan KJ, Cowan CSM, Sandhu KV, Bastiaanssen TFS, Boehme M, et al. The microbiota-gut-brain axis. *Physiol Rev* (2019) 99(4):1877–2013. doi: 10.1152/physrev.00018.2018

39. Lavelle A, Sokol H. Gut microbiota-derived metabolites as key actors in inflammatory bowel disease. *Nat Rev Gastroenterol Hepatol* (2020) 17(4):223–37. doi: 10.1038/s41575-019-0258-z

40. Natividad JM, Agus A, Planchais J, Lamas B, Jarry AC, Martin R, et al. Impaired aryl hydrocarbon receptor ligand production by the gut microbiota is a key factor in metabolic syndrome. *Cell Metab* (2018) 28(5):737–749.e734. doi: 10.1016/j.cmet.2018.07.001

41. Taleb S. Tryptophan dietary impacts gut barrier and metabolic diseases. *Front Immunol* (2019) 10:2113. doi: 10.3389/fimmu.2019.02113

42. Ma XH, Liu JH, Liu CY, Sun WY, Duan WJ, Wang G, et al. ALOX15-launched PUFA-phospholipids peroxidation increases the susceptibility of ferroptosis in ischemia-induced myocardial damage. *Signal Transduct Target Ther* (2022) 7(1):288. doi: 10.1038/s41392-022-01090-z

43. Miyamoto J, Igarashi M, Watanabe K, Karaki SI, Mukouyama H, Kishino S, et al. Gut microbiota confers host resistance to obesity by metabolizing dietary polyunsaturated fatty acids. *Nat Commun* (2019) 10(1):4007. doi: 10.1038/s41467-019-11978-0

44. de la Cuesta-Zuluaga J, Mueller NT, Álvarez-Quintero R, Velásquez-Mejía EP, Sierra JA, Corrales-Agudelo V, et al. Higher fecal short-chain fatty acid levels are associated with gut microbiome dysbiosis, obesity, hypertension and cardiometabolic disease risk factors. *Nutrients* (2018) 11(1):51. doi: 10.3390/nu11010051

45. Wu Q, Sun L, Hu X, Wang X, Xu F, Chen B, et al. Suppressing the intestinal farnesoid X receptor/sphingomyelin phosphodiesterase 3 axis decreases atherosclerosis. *J Clin Invest* (2021) 131(9):e142865. doi: 10.1172/jci142865

46. Patel R, Santoro A, Hofer P, Tan D, Oberer M, Nelson AT, et al. ATGL is a biosynthetic enzyme for fatty acid esters of hydroxy fatty acids. *Nature* (2022) 606 (7916):968–75. doi: 10.1038/s41586-022-04787-x

47. Pflimlin E, Bielohuby M, Korn M, Breitschopf K, Löhn M, Wohlfart P, et al. Acute and repeated treatment with 5-PAHSA or 9-PAHSA isomers does not improve glucose control in mice. *Cell Metab* (2018) 28(2):217–227.e213. doi: 10.1016/j.cmet.2018.05.028

48. Marlatt KL, Redman LM, Beyl RA, Smith SR, Champagne CM, Yi F, et al. Racial differences in body composition and cardiometabolic risk during the menopause transition: a prospective, observational cohort study. *Am J Obstet Gynecol* (2020) 222 (4):365.e361–365.e318. doi: 10.1016/j.ajog.2019.09.051

49. Fu Z, Wu Q, Guo W, Gu J, Zheng X, Gong Y, et al. Impaired insulin clearance as the initial regulator of obesity-associated hyperinsulinemia: novel insight into the underlying mechanism based on serum bile acid profiles. *Diabetes Care* (2022) 45 (2):425–35. doi: 10.2337/dc21-1023

50. Zhang X, Zhang J, Sun H, Liu X, Zheng Y, Xu D, et al. Defective phosphatidylglycerol remodeling causes hepatopathy, linking mitochondrial dysfunction to hepatosteatosis.y. *Cell Mol Gastroenterol Hepatol* (2019) 7(4):763–81. doi: 10.1016/j.jcmgh.2019.02.002

51. Zhao L, Zhang F, Ding X, Wu G, Lam YY, Wang X, et al. Gut bacteria selectively promoted by dietary fibers alleviate type 2 diabetes. *Science* (2018) 359(6380):1151–6. doi: 10.1126/science.aao5774

52. Canfora EE, Jocken JW, Blaak EE. Short-chain fatty acids in control of body weight and insulin sensitivity. *Nat Rev Endocrinol* (2015) 11(10):577–91. doi: 10.1038/nrendo.2015.128

53. West KA, Kanu C, Maric T, McDonald JAK, Nicholson JK, Li JV, et al. Longitudinal metabolic and gut bacterial profiling of pregnant women with previous bariatric surgery. *Gut* (2020) 69(8):1452–9. doi: 10.1136/gutjnl-2019-319620

54. Yoneshiro T, Wang Q, Tajima K, Matsushita M, Maki H, Igarashi K, et al. BCAA catabolism in brown fat controls energy homeostasis through SLC25A44. *Nature* (2019) 572(7771):614–9. doi: 10.1038/s41586-019-1503-x

55. El-Zawawy HT, El-Aghoury AA, Katri KM, El-Sharkawy EM, Gad SMS. Cortisol/DHEA ratio in morbidly obese patients before and after bariatric surgery: Relation to metabolic parameters and cardiovascular performance. *Int J Obes (Lond)* (2022) 46(2):381–92. doi: 10.1038/s41366-021-00997-x

56. Kolodziejczyk AA, Zheng D, Elinav E. Diet-microbiota interactions and personalized nutrition. *Nat Rev Microbiol* (2019) 17(12):742–53. doi: 10.1038/s41579-019-0256-8

57. Fujiwara N, Nakagawa H, Enooku K, Kudo Y, Hayata Y, Nakatsuka T, et al. CPT2 downregulation adapts HCC to lipid-rich environment and promotes carcinogenesis via acylcarnitine accumulation in obesity. *Gut* (2018) 67(8):1493–504. doi: 10.1136/gutjnl-2017-315193

58. Zhao S, Feng XF, Huang T, Luo HH, Chen JX, Zeng J, et al. The association between acylcarnitine metabolites and cardiovascular disease in Chinese patients with type 2 diabetes mellitus. *Front Endocrinol (Lausanne)* (2020) 11:212. doi: 10.3389/fendo.2020.00212

frontiers | Frontiers in Endocrinology

TYPE Original Research
PUBLISHED 26 February 2024
DOI 10.3389/fendo.2024.1338889

OPEN ACCESS

EDITED BY
Evan P. Nadler,
Consultant, Washington DC, WA,
United States

REVIEWED BY
Yanlong Shi,
Nanjing Medical University, China
Giovanni Tarantino,
University of Naples Federico II, Italy

*CORRESPONDENCE
Yanling Yang
yangyanl@fmmu.edu.cn
Yayun Wang
wangyy@fmmu.edu.cn

RECEIVED 15 November 2023
ACCEPTED 22 January 2024
PUBLISHED 26 February 2024

CITATION
Chen X, Deng S-Z, Sun Y, Bai Y, Wang Y and Yang Y (2024) Key genes involved in nonalcoholic steatohepatitis improvement after bariatric surgery.
Front. Endocrinol. 15:1338889.
doi: 10.3389/fendo.2024.1338889

Key genes involved in nonalcoholic steatohepatitis improvement after bariatric surgery

Xiyu Chen[1], Shi-Zhou Deng[1], Yuze Sun[1], Yunhu Bai[1,2], Yayun Wang[3]* and Yanling Yang[1]*

[1]Department of Hepatobiliary Surgery, Xi-Jing Hospital, The Fourth Military Medical University, Xi'an, China, [2]Department of General Surgery, 988 Hospital of Joint Logistic Support Force, Zhengzhou, China, [3]Specific Lab for Mitochondrial Plasticity Underlying Nervous System Diseases, National Demonstration Center for Experimental Preclinical Medicine Education, The Fourth Military Medical University, Xi'an, China

Background: Nonalcoholic steatohepatitis (NASH) is the advanced stage of nonalcoholic fatty liver disease (NAFLD), one of the most prevalent chronic liver diseases. The effectiveness of bariatric surgery in treating NASH and preventing or even reversing liver fibrosis has been demonstrated in numerous clinical studies, but the underlying mechanisms and crucial variables remain unknown.

Methods: Using the GSE135251 dataset, we examined the gene expression levels of NASH and healthy livers. Then, the differentially expressed genes (DEGs) of patients with NASH, at baseline and one year after bariatric surgery, were identified in GSE83452. We overlapped the hub genes performed by protein-protein interaction (PPI) networks and DEGs with different expression trends in both datasets to obtain key genes. Genomic enrichment analysis (GSEA) and genomic variation analysis (GSVA) were performed to search for signaling pathways of key genes. Meanwhile, key molecules that regulate the key genes are found through the construction of the ceRNA network. NASH mice were induced by a high-fat diet (HFD) and underwent sleeve gastrectomy (SG). We then cross-linked the DEGs in clinical and animal samples using quantitative polymerase chain reaction (qPCR) and validated the key genes.

Results: Seven key genes (FASN, SCD, CD68, HMGCS1, SQLE, CXCL10, IGF1) with different expression trends in GSE135251 and GSE83452 were obtained with the top 30 hub genes selected by PPI. The expression of seven key genes in mice after SG was validated by qPCR. Combined with the qPCR results from NASH mice, the four genes FASN, SCD, HMGCS1, and CXCL10 are consistent with the biological analysis. The GSEA results showed that the 'cholesterol homeostasis' pathway was enriched in the FASN, SCD, HMGCS1, and SQLE high-expression groups. The high-expression groups of CD68 and CXCL10 were extremely enriched in inflammation-related pathways. The construction of the ceRNA

network obtained microRNAs and ceRNAs that can regulate seven key genes expression.

Conclusion: In summary, this study contributes to our understanding of the mechanisms by which bariatric surgery improves NASH, and to the development of potential biomarkers for the treatment of NASH.

KEYWORDS

bariatric surgery, sleeve gastrectomy, nonalcoholic fatty liver disease, nonalcoholic steatohepatitis, gene expression omnibus datasets, competitive endogenous RNA

1 Introduction

Nonalcoholic fatty liver disease (NAFLD) is the most prevalent chronic liver disease (1). It is estimated that more than one billion people worldwide suffer from NAFLD, representing approximately 25% of the global population (2). Nonalcoholic steatohepatitis (NASH), and nonalcoholic fatty liver disease (NAFL), commonly referred to as simple fatty liver, are two of the diseases that fall under the umbrella of NAFLD (3). A patient is considered to have NAFLD if the liver steatosis is more than 5%. If the steatosis is accompanied by hepatocellular balloon degeneration and lobular inflammation, the patient is considered to have NASH (4). Patients with NAFLD are often associated with metabolic syndrome comorbidities such as obesity, hyperlipidemia, hypertension, and type 2 diabetes mellitus (T2DM) (5). They share the same epidemiologic and pathophysiologic features (6). T2DM seems to be the most significant risk factor for NAFLD and NASH among these comorbidities, as well as the most significant predictor of unfavorable outcomes like advanced liver fibrosis and mortality (7).

Although NAFLD is usually clinically asymptomatic, over time NASH can progressively deteriorate and lead to cirrhosis, hepatocellular carcinoma (HCC), end-stage liver disease, or the necessity for transplantation (8). NAFLD treatment currently lacks U.S. Food and Drug Administration (FDA)-approved drugs. Moderate weight loss has demonstrated efficacy in reducing hepatic steatosis, improving the histological manifestations of steatohepatitis, and reversing biopsy-proven fibrosis (9). However, achieving and maintaining the necessary level of weight loss through dietary control and increased physical activity remains challenging for NASH improvement. Right now, bariatric surgery is the most successful therapeutic approach to achieve significant (i.e. 25 - 30%) and enduring weight reduction (10), effectively treating NAFLD (11), along with comorbidities such as Obstructive sleep apnea (OSA) (12), T2DM, and hypertension (13). Bariatric surgery encompasses gastric restriction techniques (e.g. SG), malabsorption procedures (e.g. Biliopancreatic diversion), or a combination thereof (e.g. Roux-en-Y gastric bypass) (14). At present, SG is the most widely utilized bariatric surgery technique globally (15).

The mechanism of NAFLD progression is often described by the "multiple hit" theory, which states that triglyceride accumulation, endoplasmic reticulum stress response, protein misfolding, oxidative stress, and mitochondrial damage in stressed cells lead to a persistent chronic inflammatory state. This leads to excessive activation of immunity and inflammation in liver tissue (16). Activation of the innate and adaptive immune systems triggers, and exacerbates liver inflammation and damage, contributing to NAFLD/NASH (17). Moreover, it has been noticed that an understanding of the interrelationships between gut hormones, the microbiome, obesity, and bariatric surgery may lead to the exploration of new, more specific, non-surgical therapeutic measures to cure severe obesity and its co-morbidities (18). In addition to this, there are a number of factors that have been associated with remission after NASH, including bile acid metabolism (19), gut microbiota (20), gut - brain - liver axis (21), mitochondrial function (22), lipid metabolism (23), and chronic inflammation (24). Future research is needed to explore the effects of these factors on the improvement of obesity-related co-morbidities.

Transcriptome analysis, a widely utilized bioinformatics tool, enables the identification and quantification of transcript levels in different states. It has been extensively employed in mining transcriptome data, elucidating disease pathogenesis, and identifying key targets for diagnosis and treatment (25, 26). The application of transcriptome technology facilitates a better understanding of disease pathogenesis and establishes the connections between RNAs and diseases in the field of disease research.

In this study, we aimed to explore the potential mechanism underlying the improvement of NASH induced by bariatric surgery. We conducted a comprehensive analysis of the differentially expressed genes (DEGs) in NASH patients compared to healthy individuals, as well as before and after bariatric surgery in NASH patients. This allowed us to describe the changes occurring in NASH patients and evaluate the effects of bariatric surgery on NASH. By overlapping the genes with different expression from both datasets with the top 30 genes from protein-protein interaction (PPI) analysis, we identified core genes that play crucial roles in NASH pathogenesis. Furthermore, we employed Genomic enrichment analysis (GSEA) and genomic variation analysis (GSVA) to identify signaling pathways associated with these key genes. To explore regulatory molecules targeting key genes, we constructed a competitive endogenous RNA (ceRNA) network. In

addition, we established high fat diet (HFD) induced NASH mouse models and performed Sleeve gastrectomy (SG) to verify the glycolipid metabolism and the expression of key genes following bariatric surgery. Our findings aim to uncover key factors involved in improving NASH through bariatric surgery and provide insights for non-operative treatment strategies for this condition.

2 Methods

2.1 Bioinformatics analysis

2.1.1 Data source and analysis

The RNA-seq data and corresponding clinical and pathological data used in our study were obtained from the Gene Expression Omnibus (GEO, https://www.ncbi.nlm.nih.gov/geo/) database, including GSE135251, GSE83452, GSE48452, and GSE61260. GSE135251 collected 155 NASH liver samples and 10 healthy liver samples. GSE61260 collected 24 NASH liver samples and 38 healthy liver samples. GSE48452 collected 17 NASH liver samples and 12 healthy liver samples. GSE83452 is a large dataset from liver samples of obese patients, we selected samples for 14 NASH patients, they were diagnosed with "not NASH" 1 year after bariatric surgery. The differentially expressed genes (DEGs) between NASH and normal liver samples in GSE135251 were identified by the "DESeq2" package, while the DEGs between Pre-surgery and Post-surgery in GSE83452 were identified by the "Limma" package (27, 28). The inclusion criteria of DEGs were$|\log2\ FC| \geq 0.585$ and p-adjust < 0.05. Venn diagraming was used to find the overlap DEGs between GSE135251 and GSE83452.

2.1.2 Functional enrichment analysis

To investigate the biological role of DEGs, enrichment analysis using the GO (Gene Ontology) and KEGG (Kyoto Encyclopedia of Genes and Genomes) dictionaries was carried out using the R package "clusterProfiler" (29, 30). Pathways with $p < 0.05$ were considered statistically significant. A part of the results was visualized using the "ggplot2" package.

2.1.3 Protein-protein interaction network construction

To predict the interaction of DEGs, we construct a protein-protein interaction (PPI) network by an online tool STRING (http://www.string-db.org/) with the cut-off standard as a combined score >0.4. Cytoscape software (version 3.9.0) was used to visualize the PPI network of the DEGs which are linked to each other (31). In addition, to explore the hub genes in the PPI network, we employed a plug-in of Cytoscape named Cytohubba to construct a sub-network by the Maximal Clique Centrality (MCC) algorithm (32).

2.1.4 Gene set enrichment analysis and gene set variation analysis

Depending on the median hub gene value, patients were divided into high and low subgroups. The potential biological significance of the hub genes was investigated using gene set enrichment analysis (GSEA) and gene set variation analysis (GSVA).

Two predefined gene sets including "h.all.v2023.1.Hs.symbols" and "c2.cp.kegg.v2023.1.Hs.symbol" were downloaded on Molecular Signatures Database (MSigDB, https://www.gsea-msigdb.org/gsea/msigdb/index.jsp).

The R package "clusterProfiler" was used to conduct GSEA analysis, the inclusion criteria of the pathway were normalized enrichment score (NES) > 1, adjusted p value < 0.05, and false discovery rate (FDR) < 0.25 (33).

GSVA analysis was performed to calculate the specific pathway scores (GSVA scores) of each sample. Then, the GSVA scores were compared between high and low subgroups (34).

2.1.5 ceRNA network construction

Miranda (http://www.microrna.org/microrna/home.do), miRDB (http://mirdb.org/), and TargetScan Human 7.2 (http://www.targetscan.org/vert_72/) were online databases to predict the miRNAs of mRNA (35–37). SpongeScan was an online database to predict the interaction of lncRNA and miRNA (38). By using the above online tools, we have built the ceRNA networks of hub genes respectively. The ceRNA networks were visualized by Cytoscape software.

2.2 Animal experiment

2.2.1 Mouse NASH model

8-week-old male C57BL/6J mice (The Jackson Laboratory, Bar Harbor, Maine, USA) were given a high-fat diet (HFD) with 60% of the kcal derived from fat (D12492, 60% kcal Fat Diet, biopike, China) and the control group was given normal chow diet (NCD), kept on the same diet after the surgery. Mice were housed at 24 - 26 °C with a circadian rhythm of 12 h for ad libitum food and water intake. All animal protocols followed the Guidelines for the Care and Use of Laboratory Animals (license number IACUC-20190107) and were carried out in accordance with the rules of the Animal Welfare Ethics Committee of the Air Force Military Medical University. Mice (n = 6 per group) were sacrificed by intraperitoneal injection with sodium pentobarbital (50 mg/kg) at 16 weeks after HFD or NCD, and at 12 weeks after surgery.

2.2.2 Sleeve gastrectomy

After 16 weeks of HFD, mice underwent SG or sham surgery, and the surgical approach was referred to in the previous research (39). In the sham group, only the abdomen was opened and sutured, but the same duration of anesthesia was ensured. 10% sugar water was given from 6 hours postoperatively and a liquid diet was started after 24 hours, and a normal HFD was started after 3 days. At the same time, the sugar water was replaced with normal drinking water.

2.2.3 Glucose and lipid metabolism analysis

Intraperitoneal glucose tolerance test (IPGTT): After six hours of fasting, mice in each group were intraperitoneally injected with 20 percent glucose (1 g/kg). Tail vein glucose levels were then recorded using a glucometer (Roche, Germany) before, 15, 30, 60, 90, and 120

minutes after the injection. Intraperitoneal insulin tolerance test (IPITT): The mice in every group were fasted for six hours before receiving an intraperitoneal injection of insulin (0.05 U/kg). Blood glucose levels were taken in the tail vein before the injection and 15, 30, 60, 90, and 120 minutes later. The free fatty acid (FFA) in serum samples was tested with the FFA Content Assay Kit (BC0590, Solarbio, Beijing, China).

2.2.4 Histological analysis

Liver specimens were fixed in 4% formalin buffer, paraffin-embedded, and serial 4 μm thick sections were used for HE staining to evaluate hepatocyte morphology. To assess hepatic steatosis, the frozen section oil red O staining of the fixed liver specimens was performed.

2.2.5 Quantitative PCR analysis

TRIzol reagent (DP419, Tiangen, Beijing, China) was used to extract total RNA, and then employing a PrimeScript RT reagent Kit (RR037A, Takara, Dalian, China) for reverse transcription into cDNA. The PCR-amplification products were quantified using TB Green (RR820A, Takara, Dalian, China). As directed by the manufacturer, qPCR assays were run on the CFX Connect real-time PCR detection system (1855201, Biorad, USA). The associated genes' mRNA expression levels were adjusted to match the level of the housekeeping gene β-actin. Primer information is in Supplementary Table 1.

2.2.6 Statistical analysis

All the bioinformatics studies in this research were statistically analyzed using R software (V.4.1.2), and the rest were statistically analyzed using GraphPad Prism V.8 (GraphPad Software, La Jolla, California, USA). The significant differences between the groups were analyzed with Student's t-test (parametric samples) and Wilcoxon signed-rank test (non-parametric samples). A p value of < 0.05 was considered statistically significant. Significance was represented by $^{*}p < 0.05$, $^{**}p < 0.01$ and $^{***}p < 0.001$. Error bars used the Standard error of mean (SEM).

3 Results

3.1 Identification of DEGs between NASH patients and healthy individuals

The workflow of this article was illustrated in Figure 1. To investigate the DEGs associated with NASH, we compared the

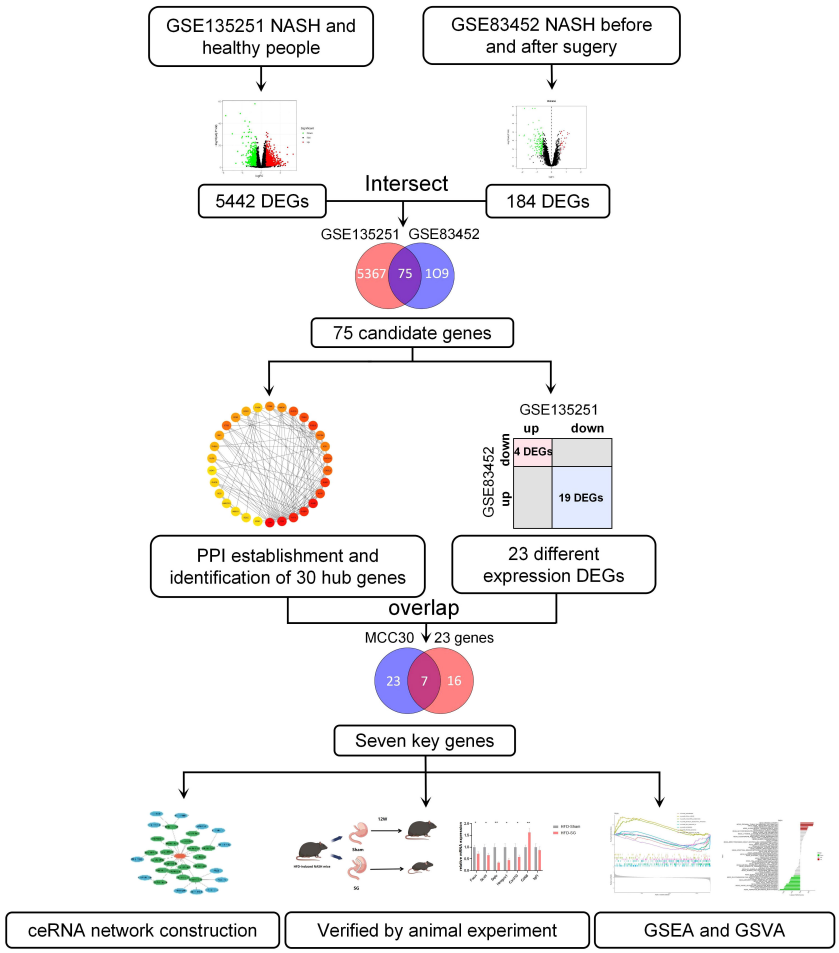

FIGURE 1
The work flowchart in this study.

transcriptome information of 155 NASH patients and 10 healthy individuals in GSE135251. A total of 5442 DEGs were obtained, 2944 DEGs were upregulated and 2498 DEGs were downregulated (Figure 2A). Gene ontology (GO) analysis and KEGG enrichment analysis were performed to elucidate the biological pathways associated with DEGs. Detailed information about the GO analysis was shown in Figure 2B. DEGs were mainly enriched in lipid localization and lipid transport in biological process (BP). They were associated with the cellular component (CC) such as the cell-substrate junction, vacuolar membrane and lysosomal membrane. Pathways related to molecular function (MF) include carbohydrate blinding, kinase regulator activity, oxidoreductase activity, and lipid transporter activity. The analysis of KEGG signaling pathways revealed that DEGs were primarily linked to the insulin, FoxO, apelin, and AMPK signaling pathways, which are involved in signaling pathways that regulate inflammation and glycolipid metabolism (Figure 2C).

3.2 Identification of DEGs before and after bariatric surgery

To investigate the key factors for remission of NSAH by bariatric surgery, we chose the GSE83452 dataset and selected 14 patients to compare baseline (NASH liver specimens obtained

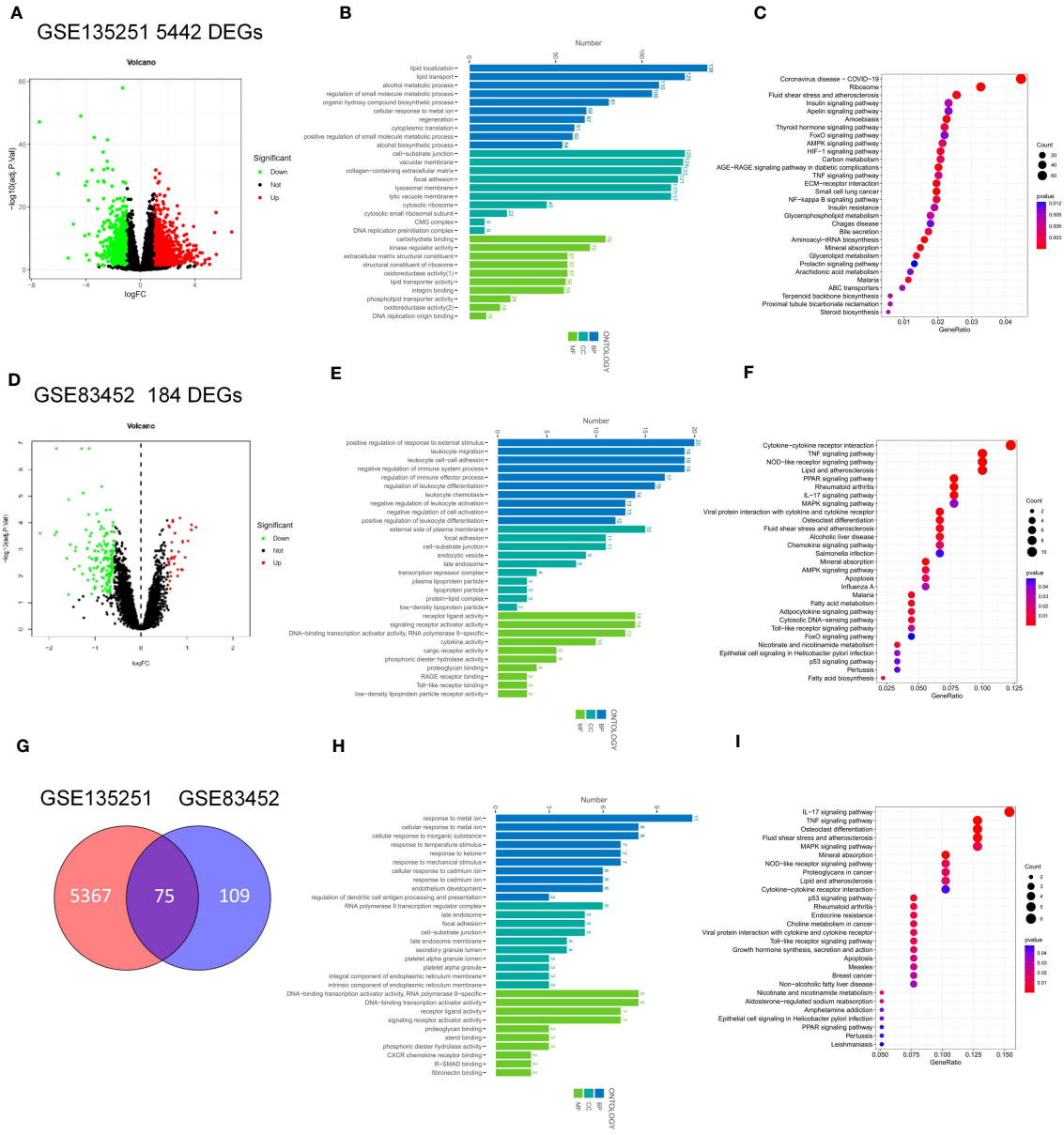

FIGURE 2
Identification and Enrichment analysis of DEGs in GSE135251 and GSE83452. **(A)** Volcano plots of gene expression in GSE135251, with the threshold of P<0.05 and |log FC| > 0.5. **(B)** GO enrichment analysis of the DEGs in GSE135251. **(C)** KEGG enrichment analysis of the DEGs in GSE135251. **(D)** Volcano plots of gene expression in GSE83452. **(E)** GO enrichment analysis of the DEGs in GSE83452. **(F)** KEGG enrichment analysis of the DEGs in GSE83452. **(E)** Venn diagram of the common DEGs in GSE135251 and GSE83452. **(F)** GO enrichment analysis of the common DEGs. **(G)** KEGG enrichment analysis of the common DEGs.

during bariatric surgery) and follow-up (NASH remission at one year after bariatric surgery) transcriptomic data. A total of 184 DEGs were identified compared to the baseline, with 32 genes upregulated and 152 genes downregulated after bariatric surgery (Figure 2D). The BP of the GO dataset was mainly enriched in leukocyte migration and leukocyte cell-cell adhesion. CC was most significantly enriched in the external side of plasma membrane, focal adhesion, and enriched in plasma lipoprotein particle, lipoprotein particle, and protein-lipid complex, which are closely related to lipid metabolism. DEGs were also enriched in MF with cytokine activity, RAGE receptor binding, and cargo receptor activity (Figure 2E). The three most frequently enriched pathways for DEGs in the KEGG database were the TNF signaling pathway, PPAR signaling pathway, and Rheumatoid arthritis (Figure 2F). The remaining signaling pathways were mainly associated with inflammation, lipid metabolism, and immunity.

3.3 Identification of common DEGs between GSE135251 and GSE83452

The DEGs in GSE135251 and GSE83452 were intersected using the Venn diagram, and a total of 75 common genes were obtained (Figure 2G). To understand the functions of these common DEGs, GO and KEGG enrichment analyses were performed. In GO analysis, it was found that BP was mainly focused on the response to metal ions, such as cellular response to cadmium ion, response to metal ion, etc. Pathways related to CC were mainly enriched in RNA polymerase II transcription regulator complex and platelet alpha granule lumen. The most significant differences in MF statistics were in proteoglycan binding, DNA-binding transcription activator activity, and RNA polymerase II-specific (Figure 2H). The remaining pathways were mainly related to inflammation and chemokines. KEGG analysis showed that the candidate genes were mainly enriched in pathways related to inflammation such as the IL-17 signaling pathway, TNF signaling pathway, and p53 signaling pathway. Other pathways Lipid and atherosclerosis, non-alcoholic fatty liver disease, and PPAR signaling pathway are related to lipid metabolism. The rest are Mineral absorption, Osteoclast differentiation, Rheumatoid arthritis, etc (Figure 2I).

3.4 PPI network construction and key genes identification

To determine the interaction of 75 common genes and screen hub genes, we constructed a PPI network of 75 common genes using the STRING online database (Figure 3A). Next, we hid separate nodes in the network, 51 genes remained in the network and were visualized by Cytoscape (Figure 3B). Subsequently, the top 30 hub genes for the MCC algorithm were identified by the CytoHubba plugin (Figure 3C). To identify the key factors of bariatric surgery to alleviate NASH, we intersected the DEGs downregulated in GSE135251 with those upregulated in GSE83452, to obtain a total of 4 candidate genes (Figure 3D). The DEGs upregulated in GSE135251 and downregulated in GSE83452 were overlapped to obtain 19 candidate genes (Figure 3E). The top 30 genes of PPI were considered to intersect with 23 candidate genes, and finally, seven key genes were obtained (FASN, HMGCS1. SQLE, SCD1, CXCL10, CD68, IGF1, Figure 3F). After bariatric surgery, the expressions of FASN, HMGCS1.SQLE, SCD1, and CXCL10 were decreased, while the expression of IGF1 was increased (Figure 1). To verify the accuracy of the selection of these seven key genes, we obtained similar results in the NASH-related datasets GSE48452 (Figure 3G) and GSE61260 (Figure 3H). Merging the results from the two datasets yielded similar results (Figure 3I). FASN, HMGCS1.SQLE, SCD1, CXCL10, and IGF1 showed the same trend and were statistically significant. Although there was no statistical difference in CD68, the trend was the same.

3.5 Functional enrichment of key genes

To further study the potential role of seven key genes in improving NASH after bariatric surgery, we performed GSEA and GSVA analysis. In the HALLMARK gene set, the GSEA results showed that the 'cholesterol homeostasis' pathway was enriched in the FASN, SCD1, HMGCS1, and SQLE high expression groups (Figures 4A, B, D, E), and the 'protein section' pathway was enriched in the SCD, HMGCS1, SQLE, and IGF1 high expression group, but in the FASN low expression group (Figures 4A, B, D, E, G). The 'myogenesis' pathway was enriched in the FASN, SCD1, HMGCS1, and SQLE low expression groups (Figures 4A, B, D, E). The 'allograft rejection', 'IL2 STAT5 signaling', 'inflammatory response', 'interferon gamma response', and 'KRAS signaling up' pathways were enriched in the CD68 and CXCL10 high expression groups (Figures 4C, F). In the KEGG gene set, the GSEA results are shown in Supplementary Figure 1.

The GSVA results of the HALLMARK gene set are shown in Figure 5, 'KRAS signaling DN' pathway was enriched in the FASN, SCD, HMGCS1, SQLE, CXCL10, and IGF1 high expression groups (Figures 5A, B, D–G) and CD68 low expression groups (Figure 5C). 'WNT β catenin signaling' pathway was enriched in the SCD, CD68, HMGCS1, SQLE, CXCL10, and IGF1 high expression groups (Figures 5B, C, D–G) and FASN low expression groups (Figure 5A). Different from GSEA, the 'cholesterol homeostasis' pathway was enriched in the FASN, SCD, HMGCS1, and SQLE low expression groups (Figures 5A, B, D, E). The results in the KEGG gene set are shown in Supplementary Figure 2.

3.6 ceRNA network construction of key genes

We created a ceRNA network construction to investigate what influences the regulation of key genes. By binding to mRNAs, microRNAs could silence genes, but ceRNAs-which include

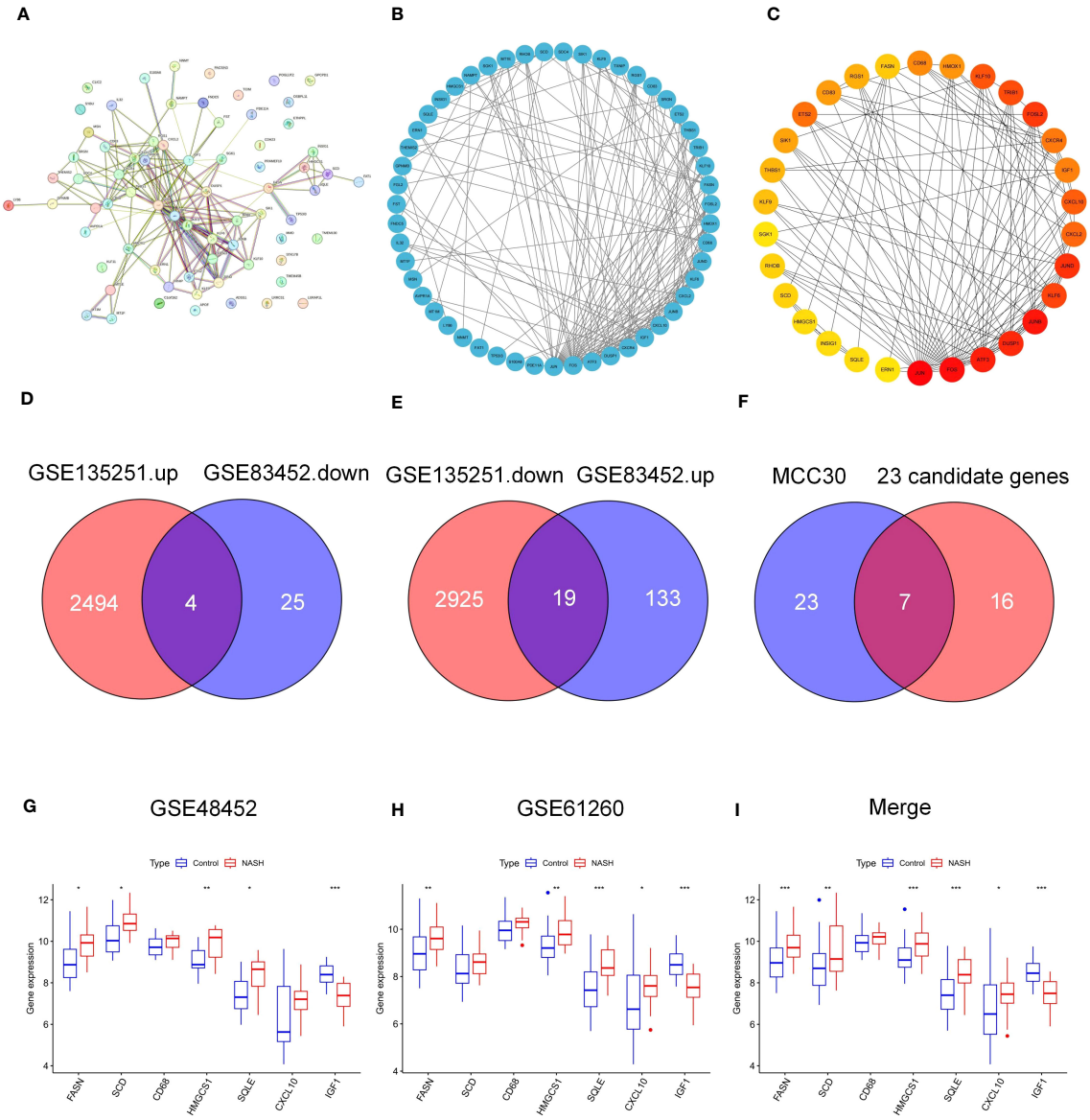

FIGURE 3
PPI network of common genes and identification of key genes. **(A–C)** PPI nrtwork of 75 common DEGs in GSE135251 and GSE83452. **(D)** Venn diagram of candidate DEGS down-regulation in GSE135251 and up-regulation in GSE83452. **(E)** Venn diagram of candidate genes up-regulation in GSE135251 and down-regulation in GSE83452. **(F)** Venn diagram of top 30 DEGs of PPI and 23 candidate genes in **(D, E)**, obtained 7 key genes (FASN, SCD, CD68, HMGCS1, SQLE, CXCL10, IGF-1). **(G)** 7 key genes expression in NASH dataset GSE48452. **(H)** 7 key genes expression in NASH dataset GSE61260. **(I)** Merge the expression of 7 key genes in two datasets **(G, H)**.

circRNAs and lncRNAs-can control gene expression by competitively binding to microRNAs (40). A ceRNA can bind multiple microRNAs, and the microRNA binding sites on ceRNAs are called microRNA recognition elements (MREs) (41). Normally there are one or more MREs on the ceRNAs, and as the expression of the ceRNAs increases, the microRNAs compete for binding, leading to an increase in the transcription level of the mRNAs and ultimately an increase in the expression level of the proteins and vice versa (41, 42). We constructed a ceRNA network of seven key genes (Figures 6A–G), indicating the miRNAs that can bind to the mRNAs of the key genes and the ceRNAs that can bind to the miRNAs. We established the role of seven key genes in NASH remission after bariatric surgery (Figure 7).

3.7 The expression level of key genes and glycolipid metabolism in NASH mouse models

To verify the expression of key genes and glycolipid metabolism in NASH, we induced a mouse NASH model with HFD (Figure 8A). After 16 weeks of HFD, the liver of the mice increased in size and yellow granules were visible to the naked eye (Figure 8B). HE staining and oil red O staining were performed on the livers (Figure 8B), which showed balloon-like hepatocytes, inflammatory cell infiltration, and a large number of lipid droplet aggregates in the livers of HFD mice. The percentage of steatosis of liver tissue is shown in the Figure 8C. Meanwhile, free fatty acids (FFA) in serum were significantly elevated

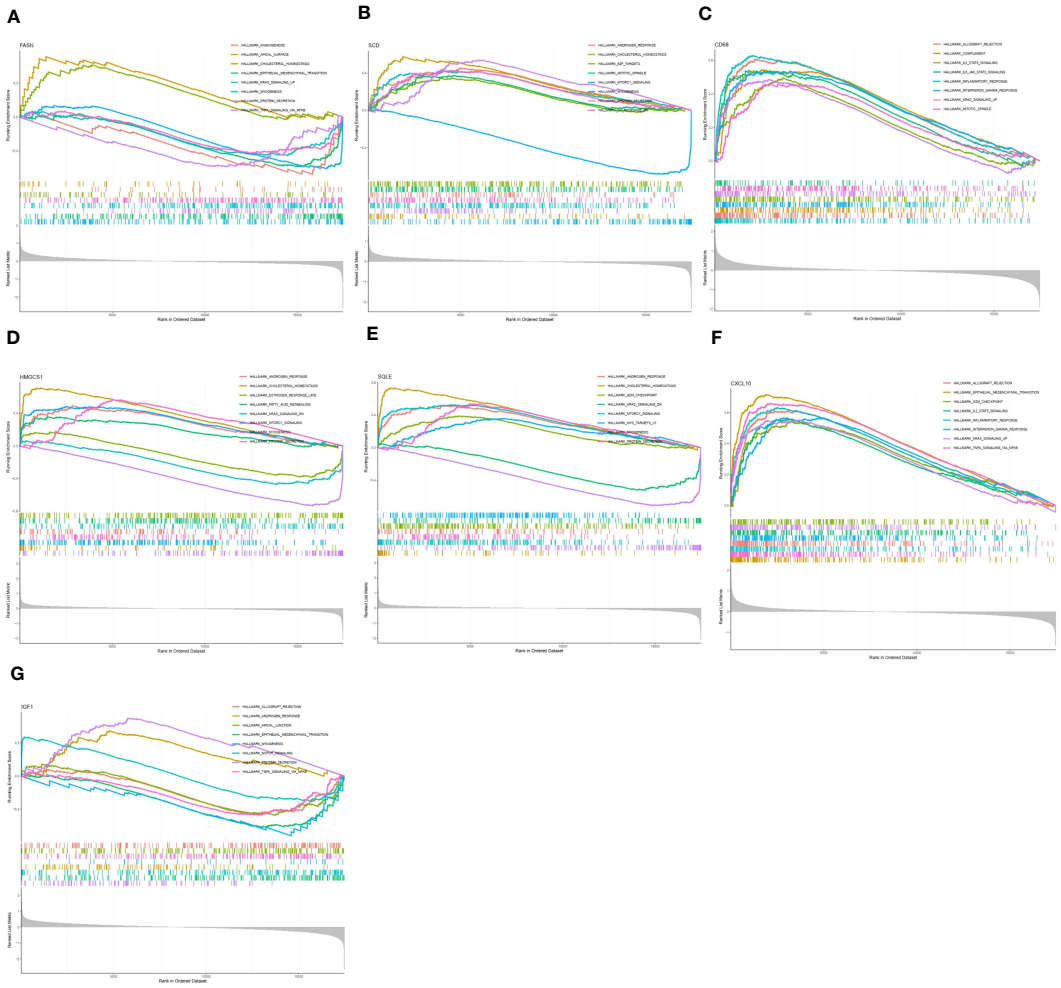

FIGURE 4
Gene set enrichment analysis (GSEA) of key genes in HALLMARK gene set. GSEA of FASN **(A)**, SCD **(B)**, CD68 **(C)**, HMGCS1 **(D)**, SQLE **(E)**, CXCL10 **(F)**, and IGF1 **(G)** in HALLMARK gene set.

(Figure 8D). IPGTT found that blood glucose in the HFD group decreased slowly after increasing blood glucose, with an increase in the area under the curve (AUC) and impaired glucose tolerance (Figure 8E). IPITT found that after insulin injection, blood glucose decreased more slowly in the mice of the HFD group than that of the NCD group, the AUC was higher than that of the NCD group, and insulin sensitivity was reduced (Figure 8F). We verified the expression of seven key genes in NASH mice by qPCR. Compared with NCD, HFD mice showed upregulated expression of FASN, SCD1, HMGCS1 and CXCL10 and reduced expression of IGF1, which was consistent with the results of bioinformatics analysis. However, no significant changes were detected in the expression of SQLE and CD68 (Figure 8G).

3.8 The expression level of key genes and glycolipid metabolism in NASH mouse models after SG

To explore the effect of bariatric surgery on the expression of key genes and metabolic changes in NASH mice, we performed SG on NASH mice. 12 weeks after SG (Figures 9A, D), the liver of mice had a regular liver arrangement, ballooning hepatocytes, inflammatory cells and fat granules were significantly reduced compared to the Sham group (Figure 9B). The percentage of steatosis of liver tissue is shown in the Figure 9C. Serum FFA was significantly decreased (Figure 9E). The IPTGG results showed that blood glucose increased slowly and decreased in magnitude in the SG group, with a lower AUC and an increase in glucose tolerance (Figure 9F). IPITT results showed that the curve decreased in the SG group, the AUC decreased, and insulin sensitivity increased (Figure 9G). The expression of seven key genes in SG mice was verified by qPCR (Figure 9H). Compared with the Sham group, the expression of FASN, SCD, HMGCS1, CXCL10, and SQLE was downregulated, and the expression of CD68 was upregulated, but the expression of IGF1 did not show any significant change. Among them, FASN, SCD1, HMGCS1, CXCL10, and SQLE expressions were consistent with the analyzed results. Combined with the qPCR results of NASH mice, all four genes of FASN, SCD1, HMGCS1, and CXCL10 were consistent with the biological analysis.

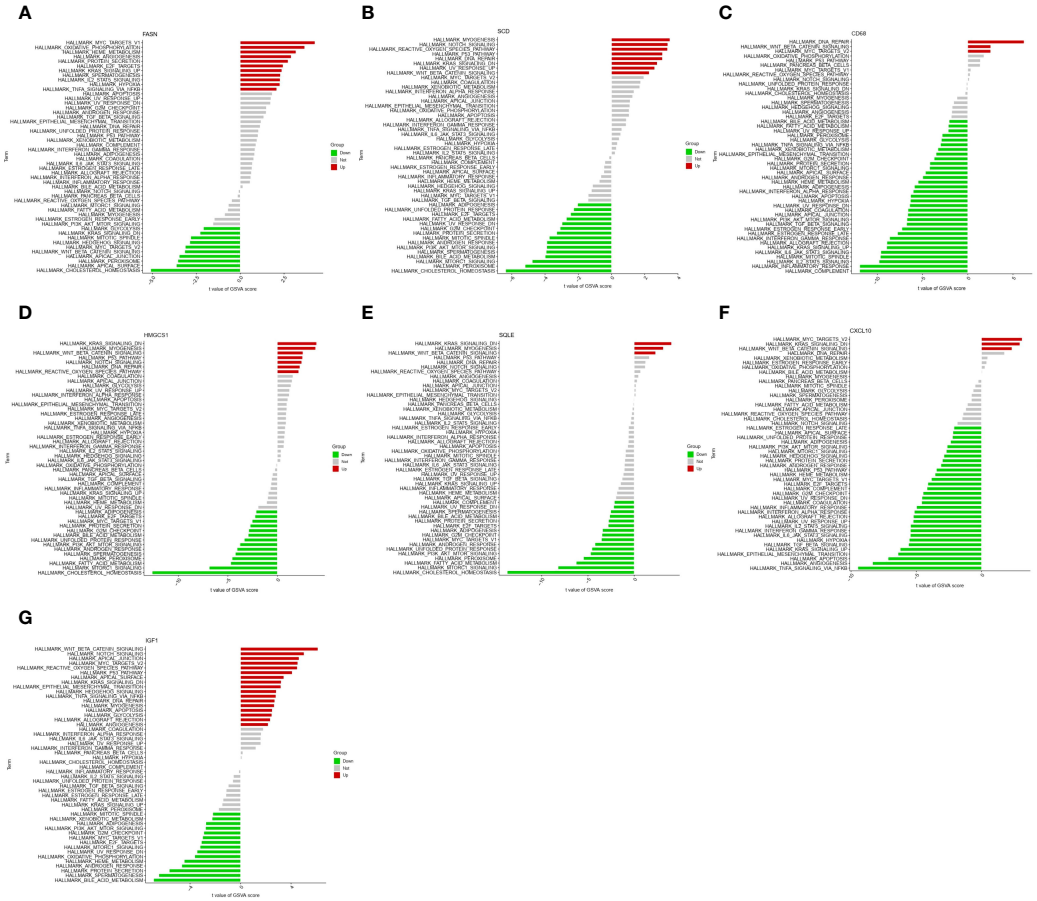

FIGURE 5
Gene set variation analysis (GSVA) of key genes in HALLMARK gene set. GSVA of FASN **(A)**, SCD **(B)**, CD68 **(C)**, HMGCS1 **(D)**, SQLE **(E)**, CXCL10 **(F)**, and IGF1 **(G)** in HALLMARK gene set.

4 Discussion

With the rising prevalence of obesity, NAFLD has become the most prevalent chronic liver disease worldwide (43). Despite many advances in disease research, there are still no FDA-approved medications for NASH (44). Current evidence suggests that weight reduction is an effective way to alleviate NAFLD (45). However, achieving sustained and significant weight loss through dietary improvements and increased exercise remains challenging. Bariatric surgery is effective in reducing weight and alleviating metabolism-related diseases such as T2DM and dyslipidemia, making it a promising long-term treatment option for NASH (46). Although it is uncontroversial that bariatric surgery relieves NASH, the underlying mechanisms remain unclear. Bioinformatic methods have been widely used to mine transcriptomic information to explore the key factors affecting disease onset and progression. Therefore, we performed a whole transcriptome analysis using bioinformatic methods to search for key genes that may mediate bariatric surgery to alleviate NASH. Additionally, we established a mouse model of NASH and performed qPCR assays to verify the expression of key genes.

In this study, we included two microarray studies comparing transcriptome information from NASH patients and healthy individuals in GSE135251. A total of 5442 DEGs were obtained, 2944 DEGs were upregulated and 2498 DEGs were downregulated (Figure 2A). Also, when comparing baseline (NASH liver samples collected during bariatric surgery) and follow-up (patients with NASH remission one year after bariatric surgery) in GSE83452, a total of 184 DEGs were obtained, with 32 genes upregulated and 152 genes downregulated in the postoperative DEGs (Figure 2D). Intersecting the two datasets yielded a total of 75 candidate genes (Figure 2G). To identify the key factors for the alleviation of NASH by bariatric surgery, we intersected the genes with different expressions in the two datasets and obtained a total of 23 candidate genes (Figures 3D, E). Using the PPI network, the top 30 DEGs were sorted by degree value and taken as candidate genes. Seven key genes (FASN, HMGCS1. SQLE, SCD1, CXCL10, CD68, IGF1, Figure 3F) were finally obtained by intersecting with 23 candidate genes. Among them, FASN, HMGCS1, SQLE, SCD1, CXCL10, and CD68 were downregulated and IGF1 was upregulated after bariatric surgery.

Fatty acid synthase (FASN) is a pivotal enzyme in the process of fatty acid synthesis. The initial step in hepatic lipogenesis involves the conversion of citrate to acetyl-coenzyme A (CoA) by ATP citrate lyase. Acetyl-CoA Carboxylases (ACC) 1 and 2 next convert CoA to malonyl-CoA, which is then transformed into fatty acids by

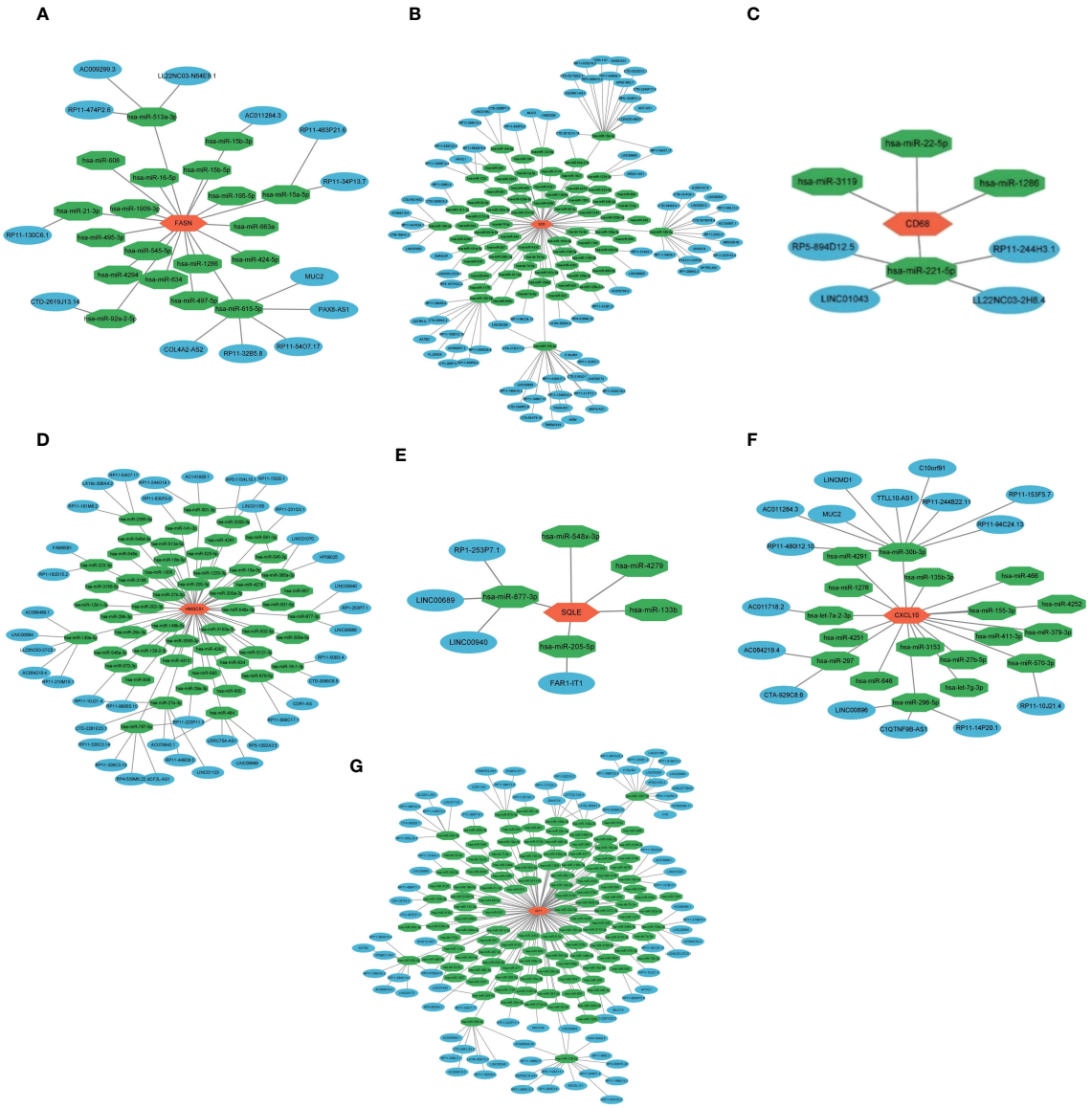

FIGURE 6
ceRNA network construction of key genes. ceRNA network construction of FASN **(A)**, SCD **(B)**, CD68 **(C)**, HMGCS1 **(D)**, SQLE **(E)**, CXCL10 **(F)**, and IGF1 **(G)**.

FASN (47). FASN expression is increased in NAFLD patients and HFD mice (48, 49), and excess fatty acids in the animals can form fats through esterification, which increases fat deposition in the animals. However, studies on FASN expression after bariatric surgery are lacking. In this experiment, we found that the expression of FASN was reduced after SG. This reduction suggests that bariatric surgery may reduce fatty acid synthesis by down-regulating FASN expression, thereby reducing the deposition of lipids in the liver and alleviating NAFLD. At the same time, the reduction in FASN expression leads to the accumulation of malonyl-CoA, which acts on the hypothalamus to suppress appetite and induce significant weight loss and fat reduction (50).

Steroidal coenzyme A desaturase (SCD) is the rate-limiting enzyme of monounsaturated fatty acids and a key enzyme in the synthesis of triglycerides (TG) (51). SCD also known as SCD1, was estimated to be higher in NASH patients than in patients with normal liver function (52), while SCD expression was increased in HFD-induced NASH mice (Figure 8G), suggesting that high SCD activity is associated with NASH. Hepatic SCD expression is required for carbohydrate-induced obesity (53). In rodents, downregulation of SCD expression reduces body fat, increases energy expenditure, and upregulates the expression of several genes for fatty acid β-oxidases in the liver. It has been observed that lowering SCD enhances insulin sensitivity and activates adenosine monophosphate-activated protein kinase (AMPK) (54). Intraperitoneal injection of SCD-targeted antisense oligonucleotide (ASO) in mice inhibits SCD in the liver and adipose, resulting in increased insulin sensitivity, decreased hepatic fatty acid synthesis, and prevention of HFD-induced obesity and hepatic steatosis (55). Lipid metabolism plays a key role in the onset of insulin resistance and diabetes, and insulin resistance is a direct result of obesity and the buildup of extra lipids in non-adipose tissues. Therefore,

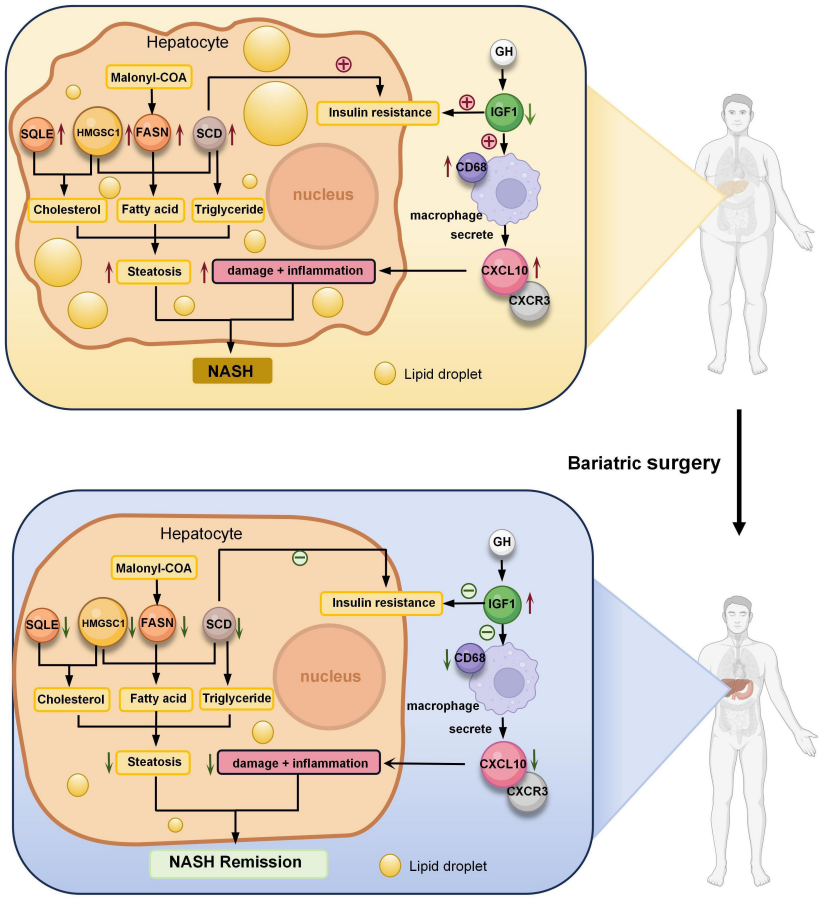

FIGURE 7
Role of seven key genes in remission of NASH after bariatric surgery. Fatty acid synthase (FASN) is a key enzyme in fatty acid synthesis. Malonyl-CoA is changed into fatty acids (FA) by FASN. Steroidal coenzyme A desaturase (SCD) is the rate-limiting enzyme of monounsaturated fatty acids and a key enzyme in the synthesis of triglycerides (TG). It has been observed that lowering SCD enhances insulin sensitivity. Hydroxy-3-methylglutaryl-CoA synthetase 1 (HMGCS1) is a protein-coding gene associated with cholesterol (TC) biosynthesis and steroid metabolism and promotes FA synthesis and disruption of lipid metabolism. The enzyme squalene epoxidase (SQLE) limits the rate at which TC is synthesized and encourages the build-up of TC and cholesteryl esters in hepatocytes. C-X-C motif chemokine 10 (CXCL10) is secreted by macrophages and causes an inflammatory cascade response when it interacts with its cognate receptor C-X-C motif receptor 3 (CXCR3), resulting in inflammation and hepatocyte damage. the expression of hepatic inflammation-related marker CD68 was elevated in NASH. Insulin-like growth factor 1 (IGF1) is primarily produced by growth hormone (GH) stimulated hepatic production in adults. IGF1-induced insulin sensitization has been in rodent models of liver disease, including models of NAFLD and NASH. And IGF1 can have an anti-inflammatory effect by acting on macrophages. Bariatric surgery alleviates NASH by altering the expression of these seven key genes, reducing liver steatosis, hepatocyte damage, inflammation.

increased insulin sensitivity in SCD-deficient mice is predicted by the reduced lipid synthesis and increased lipid oxidation seen in these animals. In hepatic stellate cells, reduced SCD expression resulted in a reversal of their fibrotic phenotype (56). Aramchol is an SCD inhibitor in a Phase II B clinical study of the effect of Aramchol on NASH. Compared to the placebo group, the Aramchol group had significantly lower liver fat content ($p = 0.045$) and a higher rate of NASH remission (16.7% vs 5%, OR = 4.74; $p = .0514$) (57). However, the effect of bariatric surgery on SCD expression is missing. In this study, SG reduced SCD expression (Figure 9H), one of the important factors in the theory of palliation of NASH by bariatric surgery.

Hydroxy-3-methylglutaryl-CoA synthetase 1 (HMGCS1) is a protein-coding gene associated with cholesterol biosynthesis and steroid metabolism (58). HMGCS1 expression is upregulated in NASH mice (Figure 8G), which promotes fatty acid synthesis and disruption of lipid metabolism (59) and facilitates intrahepatic lipid deposition, leading to excessive lipid content in the liver (60). Like regulating FASN, SCD1, SG also downregulated HMGCS1 expression. Rather than alleviating NASH by specifically reducing the expression of a particular gene, SG seems to restore insulin sensitivity (Figure 9G), inhibit fatty acid synthesis (Figure 9E), and reduce lipid deposition in the liver by attenuating the expression of FASN, SCD1, and HMGCS1 (Figure 9H).

The enzyme squalene epoxidase (SQLE) limits the rate at which cholesterol is synthesized and encourages the build-up of cholesterol and cholesteryl esters in hepatocytes (61). In both NASH mouse models and humans, SQLE is expressed at a high level. However, in this experiment, there was no significant difference in SQLE expression in NASH mice (Figure 8G). Meanwhile, in a porcine NASH model, SQLE was negatively correlated with hepatic lipid droplet area (62). The reason for this

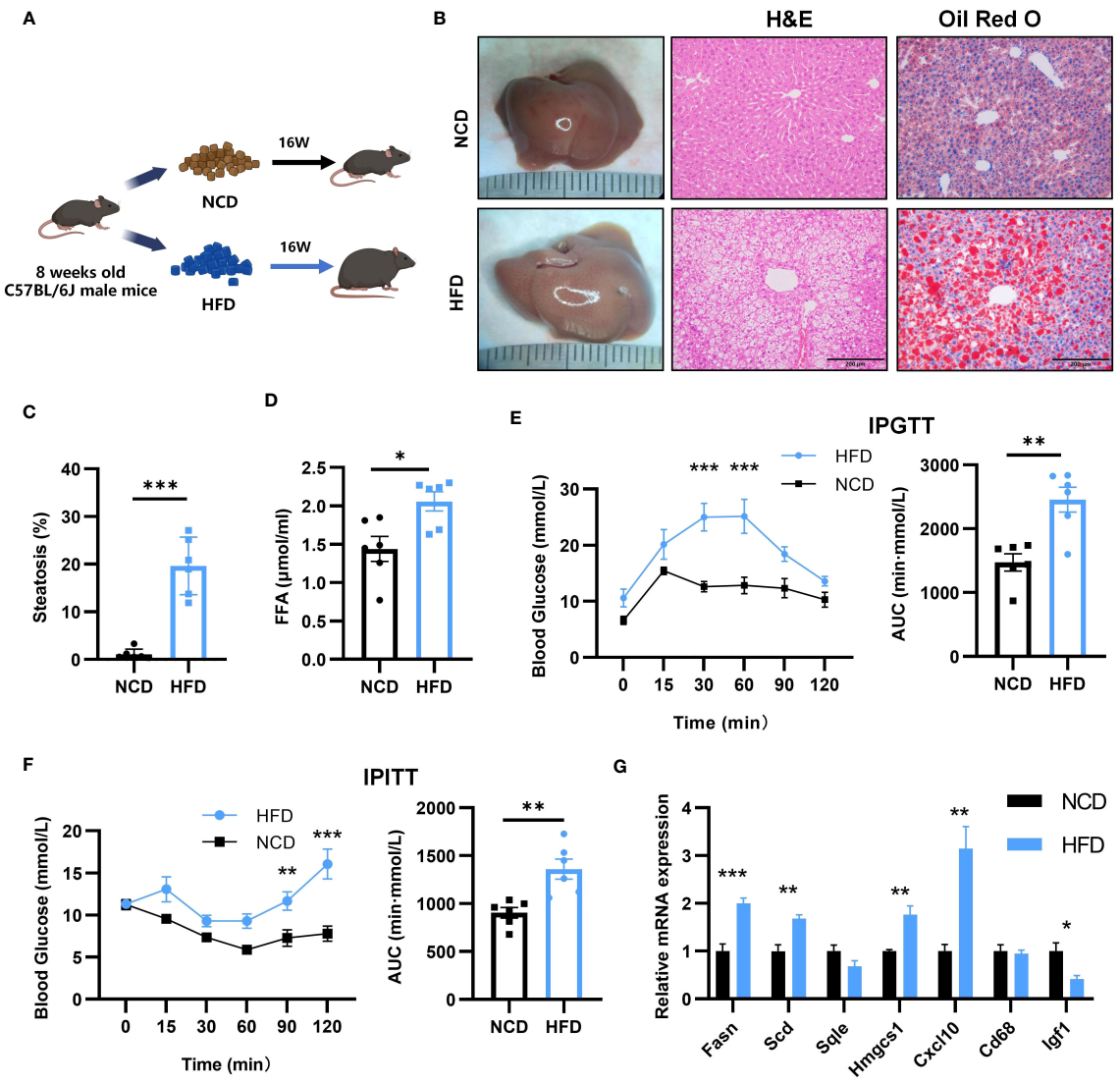

FIGURE 8
Establishment of mouse NASH model and key gene expression. **(A)** Flow chart of HFD-NASH mice (n=6/group). **(B)** Gross morphology, H&E staining and Oil Red O staining of hepatic tissue from control and HFD diet mice (16 weeks on the indicated diet, n=6/group), Scale bar: 200mm. **(C)** Percentage of liver tissue with steatosis. **(D)** Intraperitoneal glucose tolerance test (IPGTT) and the areas under the curve (AUC) at 16 weeks after the indicated diet (n=6/group). **(E)** Serum free fatty acid (FFA) content at 16 weeks after indicated diet (n=6/group). **(F)** Intraperitoneal insulin tolerance test (IPITT) and AUC at 16 weeks after indicated diet (n=6/group). **(G)** Relative mRNA expression in the liver of 7 key genes by qPCR (16 weeks after indicated diet, n=6/group). All Figures: ns, no significance; *p < 0.05, **p < 0.01, ***p < 0.001.

may be due to insufficient modeling time and species differences. SQLE overexpression in transgenic TG mice leads to hepatic cholesterol accumulation, which triggers pro-inflammatory nuclear factor-kB signaling and steatohepatitis. By directly binding to carbonic anhydrase III (CA3), SQLE triggers the activation of sterol regulatory element binding protein 1C, as well as the expression of SCD, FASN, and acetyl coenzyme A carboxylase, which in turn triggers *de novo* hepatic lipogenesis (63). Through the induction of cholesterol biosynthesis and adipogenesis, which is mediated by the SQLE/CA3 axis, SQLE drives the initiation and progression of NASH. It has been demonstrated that targeting SQLE and CA3 together is effective in treating NASH (63). Decrease in SQLE expression after SG surgery (Figure 9H), thereby reducing cholesterol synthesis. Sharing a similar function with FASN, SCD, and HMGCS1, i.e., being involved in explaining the reduction of hepatic fat deposition.

Persistent inflammation is an important factor in the progression of NASH. Chemokines, which control the movement and activity of hepatocytes, Kupffer cells, hepatic stellate cells, endothelial cells, and circulating immune cells, regulate hepatic inflammation (64). A chemotactic ligand known as C-X-C motif chemokine 10 (CXCL10), which is secreted by macrophages, causes an inflammatory cascade response when it interacts with its cognate receptor C-X-C motif receptor 3 (CXCR3). CXCL10, highly expressed in NASH mice (Figure 8G), targets CXCR3 to directly cause hepatocyte damage, resulting in inflammation and liver injury (65). This may mediate macrophage-associated inflammation in NASH mouse models. Macrophage p38α induces the secretion of

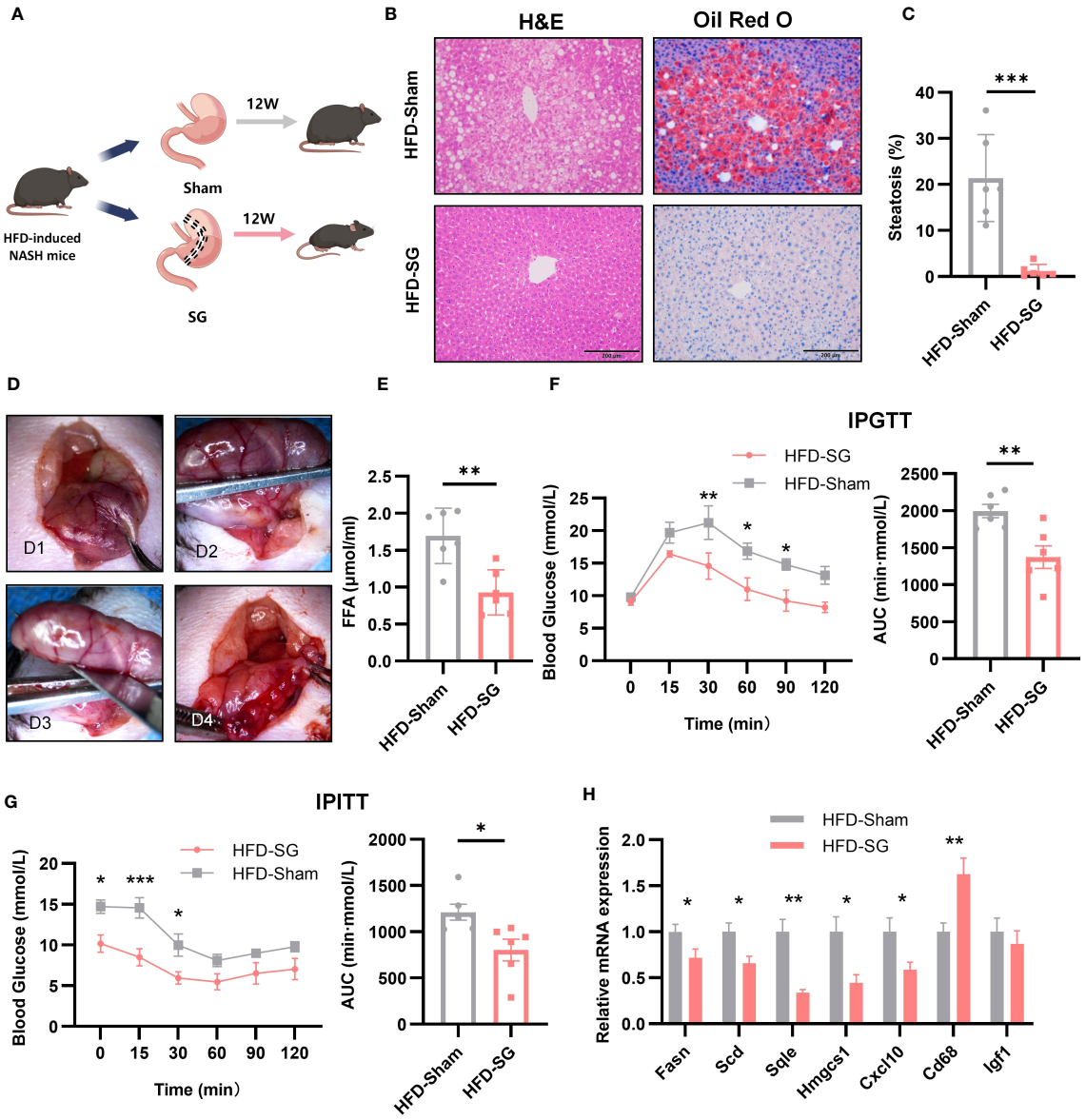

FIGURE 9
The expression of 7 key genes after SG. **(A)** Flow chart of SG (n=6/group). **(B)** HE staining and Oil Red O staining of liver tissue from sham and SG group (8 weeks post-surgery, n=6/group), Scale bar: 200mm. **(C)** Percentage of liver tissue with steatosis. **(D)** The main procedure of SG; a: Expose the body of stomach; b: Fix the gastric body with ophthalmic forceps; c: Excise the greater curvature of stomach; d: Suture stump. **(E)** IPGTT and AUC at 8 weeks post-surgery (n=6/group). **(F)** Serum FFA content at 8 weeks post-surgery (n=6/group). **(G)** IPITT and AUC at 8 weeks post-surgery (n=6/group). (H) Relative mRNA expression in the liver of 7 key genes by qPCR at 8 weeks post-surgery (n=6/group).

pro-inflammatory cytokines such as CXCL10, IL6, and TNFα, leading to M1 macrophage polarization and exacerbation of steatohepatitis alterations in hepatocytes (66). In CXCL10 knockout mice, hepatic inflammation, subsequent hepatic injury, and fibrosis were reduced (67). SG likely attenuates hepatocyte damage and liver tissue inflammation by reducing CXCL10 expression in mice (Figure 9H).

CD68 is used as a marker for macrophages, and its high expression is closely associated with hepatic inflammation (68). In the present study, different from the results from bioinformatics analysis, we have noticed that qPCR results have shown that there was an increase in CD68 expression in livers of NASH mice, when compared to that of Sham group (Figure 9H). There are two reasons to explain the difference. First, the objects of bioinformatics analysis and qPCR are so different. In the bioinformatics analysis, all databases are from patients, while qPCR results are obtained from experimental mice. Second, the time points of bioinformatics analysis and qPCR are quite different. The time point on patients for the comparison of CD68 expression levels in bioinformatics analysis is 52 weeks after bariatric surgery (SG or RYGB), while the time point on mice for the comparison of CD68 expression levels by qPCR is 12 weeks after SG surgery. It is deduced that NASH patients receiving surgery after more than one year have improved so greatly that CD68 expression might return to the normal level. Different from the long recovery course of patients, the livers of NASH mice after 12 weeks after SG operations have

been still suffered from inflammation attack, therefore it is reasonable for the absence of the decrease of CD68 expression. Our present result is consistent with previous study which has reported the increased expression of CD68 in adipose tissue of mice after SG (69). It is deduced that the increase of CD68 level could represent the presence of inflammatory state.

Insulin-like growth factor 1 (IGF1) is primarily produced by growth hormone (GH) stimulated hepatic production in adults (70). GH primarily affects metabolism by stimulating lipolysis in white adipose tissue, raising free fatty acid levels in the blood, blocking glucose oxidation, and decreasing insulin sensitivity in the liver and peripheral tissues (71). An increasing body of research indicates that IGF1 directly targets the liver, as well as hepatocytes, macrophages, and hematopoietic stem cells, through a variety of mechanisms that inhibit the progression of nonalcoholic fatty liver disease (72). It was verified in this experiment that IGF1 expression levels were reduced in NASH mice (Figure 8G). GH and IGF1 have also been reported to reduce oxidative stress in hepatocytes, suggesting that they have different effects on the multiple strikes of NASH (73). In diet-induced obese mice, the knockdown of IGF1 receptors in macrophage precursor cells led to an increase in M1 macrophages and induced metabolic dysfunction, suggesting a protective effect against inflammation in the IGF1 signaling pathway in macrophages (74). IGF1-induced insulin sensitization has been in rodent models of liver disease, including models of NAFLD and NASH, and has been demonstrated to have antifibrotic properties (73, 75). However, no significant changes in IGF1 were seen after SG, suggesting that the recovery of insulin sensitivity in animals is not dependent on IGF1 concentration.

In GSEA, FASN, SCD, HMGCS1, and SQLE high-expression groups are enriched in the 'cholesterol homeostasis' pathway. It is suggested that 'cholesterol homeostasis' is closely related to the development of NASH, and bariatric surgery may reduce lipid deposition by reducing the 'cholesterol homeostasis' pathway. The 'allograft rejection', 'IL2 STAT5 signaling', 'inflammatory response', 'interferon gamma response', and 'KRAS signaling up' pathways were enriched in the CD68 and CXCL10 high-expression groups (Figures 4C, F). It is suggested that the inflammatory pathway is closely related to the occurrence of NASH, and bariatric surgery may alleviate NASH by reducing the inflammation-related pathway.

NASH patients have increased *de novo* lipogenesis and increased fatty acid flux in the liver, leading to heightened production of lipotoxic substances that significantly contribute to hepatic inflammation and hepatocyte death associated with steatohepatitis (76). By down-regulating lipid metabolism-related genes (FASN, SCD, HMGCS), bariatric surgery reduces free fatty acid levels, restores insulin sensitivity, and reduces lipid deposition in the liver. Meanwhile, it may mitigate hepatocyte injury and liver tissue inflammation by down-regulating CXCL10 expression, thereby achieving the purpose of alleviating NASH. Recent data have revealed that myeloid cell-derived growth factor (MYDGF) alleviates NAFLD and inflammation in a manner involving IKKβ/NF-κB signaling, and serves as a factor involved in the crosstalk between the liver and bone marrow that regulates liver fat metabolism (77). Moreover, stem cell growth factor-beta (SCGF-β) has shown an activity on granulocyte/macrophage progenitor cells in combination with granulocyte macrophage colony-stimulating factor (GM-CSF) and macrophage colony-stimulating factor (M-CSF). In fact, in obesity patients with NAFLD, SCGF-β levels have been linked to insulin resistance and hepatic steatosis severity with the mediation role of CRP (78). In the present study, qPCR results have shown the increase of CD68 expression in livers of NASH mice receiving SG. We have discussed this might be due to the inflammatory infiltration of monocytes/macrophages into livers. This result is consistent with previous study that Da Riva et al. have reported that CD68-positivity could be detected in SCGF-positive areas, which has indicated the inflammatory infiltration state (79). It has been also noticed that Kim ML et al. have reported that the level of CXCL10 is elevated in sera from patients with acute rheumatic fever, and CXCL10 could bind to CXCR3 of T cells to activate the release of GM-CSF from T cells (80). This result is consistent with our present study that SG operation treatment could decrease the CXCL10 level of NASH mice. Therefore, growth factors, as key factors in NASH, may be potential therapeutic targets for NASH.

Bariatric surgery may be done by altering the expression of key genes (FASN, HMGCS1, SQLE, SCD, CXCL10, CD68, IGF1) to improve NASH. CeRNA network construction provides a new choice for regulating the expression of the key genes. In the future, the mRNA level of the target genes may be regulated by changing the level of related ceRNAs or microRNAs. The ultimate goal is to obtain remission of NASH without the use of a scalpel.

Limitations of this study

Although obvious changes in glucose and lipid metabolism were observed in HFD-NASH mice, the hepatic inflammation exhibited a mild phenotype. We verified that the key genes are limited to the mRNA level rather than the protein level, which does not reflect their final levels within the organism. Obesity, T2DM, sex and age may be the influential factors of NASH. However, this study did not account for potential confounding variables when screening DEGs. The ceRNA network construction only found microRNAs and ecRNAs that could regulate mRNA levels of key genes, but it was not verified in NASH mice and humans.

5 Conclusion

In this study, we obtained seven key genes (FASN, HMGCS1. SQLE, SCD1, CXCL10, CD68, IGF1) by analyzing transcriptomic information that may be the key to alleviating NASH after bariatric surgery. It was found that SG reduced FFA levels and lipid deposition in the liver by down-regulating lipid metabolism-related genes (FASN, SCD1, HMGCS1). Meanwhile, it may reduce hepatocyte injury and liver tissue inflammation by down-regulating CXCL10, to achieve the purpose of alleviating NASH. CeRNA network construction of the key genes provides a new choice for improving the NASH.

Data availability statement

The datasets presented in this study can be found in online repositories. The names of the repository/repositories and accession number(s) can be found in the article/Supplementary Material.

Ethics statement

The animal study was approved by Animal Welfare Ethics Committee of the Air Force Military Medical University. The study was conducted in accordance with the local legislation and institutional requirements.

Author contributions

XC: Data curation, Formal analysis, Methodology, Validation, Writing – original draft. SD: Data curation, Formal analysis, Methodology, Software, Writing – original draft. YS: Data curation, Methodology, Writing – original draft. YW: Conceptualization, Project administration, Supervision, Writing – review & editing. YY: Conceptualization, Funding acquisition, Project administration, Supervision, Writing – review & editing. YB: Formal analysis, Methodology, Writing – original draft.

Funding

The author(s) declare financial support was received for the research, authorship, and/or publication of this article. The General Programs of the National Natural Science Foundation of China (818704150); and the Xijing Hospital Boost Project (XJZT19Z29). both of them are chaired by YY.

Conflict of interest

The authors declare that the research was conducted in the absence of any commercial or financial relationships that could be construed as a potential conflict of interest.

Publisher's note

Supplementary material

The Supplementary Material for this article can be found online at: https://www.frontiersin.org/articles/10.3389/fendo.2024.1338889/full#supplementary-material

References

1. Younossi Z, Anstee QM, Marietti M, Hardy T, Henry L, Eslam M, et al. Global burden of NAFLD and NASH: trends, predictions, risk factors and prevention. *Nat Rev Gastroenterol Hepatol* (2018) 15(1):11–20. doi: 10.1038/nrgastro.2017.109

2. Younossi Z, Tacke F, Arrese M, Chander Sharma B, Mostafa I, Bugianesi E, et al. Global perspectives on nonalcoholic fatty liver disease and nonalcoholic steatohepatitis. *Hepatol (Baltimore Md)* (2019) 69(6):2672–82. doi: 10.1002/hep.30251

3. Adams LA, Lymp JF, St Sauver J, Sanderson SO, Lindor KD, Feldstein A, et al. The natural history of nonalcoholic fatty liver disease: a population-based cohort study. *Gastroenterol* (2005) 129(1):113–21. doi: 10.1053/j.gastro.2005.04.014

4. Sheka AC, Adeyi O, Thompson J, Hameed B, Crawford PA, Ikramuddin S. Nonalcoholic steatohepatitis: A review. *JAMA* (2020) 323(12):1175–83. doi: 10.1001/jama.2020.2298

5. Chalasani N, Younossi Z, Lavine JE, Charlton M, Cusi K, Rinella M, et al. The diagnosis and management of nonalcoholic fatty liver disease: Practice guidance from the American Association for the Study of Liver Diseases. *Hepatol (Baltimore Md)* (2018) 67(1):328–57. doi: 10.1002/hep.29367

6. Targher G, Corey KE, Byrne CD, Roden M. The complex link between NAFLD and type 2 diabetes mellitus - mechanisms and treatments. *Nat Rev Gastroenterol Hepatol* (2021) 18(9):599–612. doi: 10.1038/s41575-021-00448-y

7. Hossain N, Afendy A, Stepanova M, Nader F, Srishord M, Rafiq N, et al. Independent predictors of fibrosis in patients with nonalcoholic fatty liver disease. *Clin Gastroenterol Hepatol* (2009) 7(11):1224–9.E2. doi: 10.1016/j.cgh.2009.06.007

8. Powell EE, Wong VW-S, Rinella M. Non-alcoholic fatty liver disease. *Lancet (London England)* (2021) 397(10290):2212–24. doi: 10.1016/S0140-6736(20)32511-3

9. Petroni ML, Brodosi L, Bugianesi E, Marchesini G. Management of non-alcoholic fatty liver disease. *BMJ (Clinical Res ed)* (2021) 372:m4747. doi: 10.1136/bmj.m4747

10. Mingrone G, Panunzi S, De Gaetano A, Guidone C, Iaconelli A, Capristo E, et al. Metabolic surgery versus conventional medical therapy in patients with type 2 diabetes: 10-year follow-up of an open-label, single-centre, randomised controlled trial. *Lancet (London England)* (2021) 397(10271):293–304. doi: 10.1016/S0140-6736(20)32649-0

11. Lassailly G, Caiazzo R, Ntandja-Wandji L-C, Gnemmi V, Baud G, Verkindt H, et al. Bariatric surgery provides long-term resolution of nonalcoholic steatohepatitis and regression of fibrosis. *Gastroenterology* (2020) 159(4):1290–301.e5. doi: 10.1053/j.gastro.2020.06.006

12. Wang SH, Keenan BT, Wiemken A, Zang Y, Staley B, Sarwer DB, et al. Effect of weight loss on upper airway anatomy and the apnea-hypopnea index. The importance of tongue fat. *Am J Respir Crit Care Med* (2020) 201(6):718–27. doi: 10.1164/rccm.201903-0692OC

13. Courcoulas AP, Christian NJ, Belle SH, Berk PD, Flum DR, Garcia L, et al. Weight change and health outcomes at 3 years after bariatric surgery among individuals with severe obesity. *JAMA* (2013) 310(22):2416–25. doi: 10.1001/jama.2013.280928

14. Korenkov M, Sauerland S. Clinical update: bariatric surgery. *Lancet* (2007) 370 (9604):1988–90. doi: 10.1016/S0140-6736(07)61844-3

15. Brown WA, Shikora S, Liem R, Holland J, Campbell AB, Sprinkhuizen SM. *Seventh IFSO Global Registry Report*. Naples, Italy: The International Federation for the Surgery of Obesity and Metabolic Disorders. (2022).

16. Sutti S, Albano E. Adaptive immunity: an emerging player in the progression of NAFLD. *Nat Rev Gastroenterol Hepatol* (2020) 17(2):81–92. doi: 10.1038/s41575-019-0210-2

17. Wolf MJ, Adili A, Piotrowitz K, Abdullah Z, Boege Y, Stemmer K, et al. Metabolic activation of intrahepatic CD8+ T cells and NKT cells causes nonalcoholic steatohepatitis and liver cancer via cross-talk with hepatocytes. *Cancer Cell* (2014) 26 (4):549–64. doi: 10.1016/j.ccell.2014.09.003

18. Finelli C, Padula MC, Martelli G, Tarantino G. Could the improvement of obesity-related co-morbidities depend on modified gut hormones secretion? *World J Gastroenterol* (2014) 20(44):16649–64. doi: 10.3748/wjg.v20.i44.16649

19. Browning MG, Pessoa BM, Khoraki J, Campos GM. Changes in bile acid metabolism, transport, and signaling as central drivers for metabolic improvements after bariatric surgery. *Curr Obes Rep* (2019) 8(2):175–84. doi: 10.1007/s13679-019-00334-4

20. Dong TS, Katzka W, Yang JC, Chang C, Arias-Jayo N, Lagishetty V, et al. Microbial changes from bariatric surgery alters glucose-dependent insulinotropic polypeptide and prevents fatty liver disease. *Gut Microbes* (2023) 15(1):2167170. doi: 10.1080/19490976.2023.2167170

21. Cerreto M, Santopaolo F, Gasbarrini A, Pompili M, Ponziani FR. Bariatric surgery and liver disease: general considerations and role of the gut-liver axis. *Nutrients* (2021) 13(8):2649. doi: 10.3390/nu13082649

22. Verbeek J, Lannoo M, Pirinen E, Ryu D, Spincemaille P, Vander Elst I, et al. Roux-en-y gastric bypass attenuates hepatic mitochondrial dysfunction in mice with non-alcoholic steatohepatitis. *Gut* (2015) 64(4):673–83. doi: 10.1136/gutjnl-2014-306748

23. Lalloyer F, Mogilenko DA, Verrijken A, Haas JT, Lamazière A, Kouach M, et al. Roux-en-Y gastric bypass induces hepatic transcriptomic signatures and plasma metabolite changes indicative of improved cholesterol homeostasis. *J Hepatol* (2023) 79(4):898–909. doi: 10.1016/j.jhep.2023.05.012

24. Cabré N, Luciano-Mateo F, Fernández-Arroyo S, Baiges-Gayà G, Hernández-Aguilera A, Fibla M, et al. Laparoscopic sleeve gastrectomy reverses non-alcoholic fatty liver disease modulating oxidative stress and inflammation. *Metabol: Clin Experimental* (2019) 99:81–9. doi: 10.1016/j.metabol.2019.07.002

25. Costa V, Angelini C, De Feis I, Ciccodicola A. Uncovering the complexity of transcriptomes with RNA-Seq. *J Biomed Biotechnol* (2010) 2010:853916. doi: 10.1155/2010/853916

26. Cao S, Lin Y, Yang Z. Vaccinia virus transcriptome analysis by RNA sequencing. *Methods In Mol Biol (Clifton NJ)* (2019) 2023:157–70. doi: 10.1007/978-1-4939-9593-6_10

27. Ritchie ME, Phipson B, Wu D, Hu Y, Law CW, Shi W, et al. limma powers differential expression analyses for RNA-sequencing and microarray studies. *Nucleic Acids Res* (2015) 43(7):e47. doi: 10.1093/nar/gkv007

28. Love MI, Huber W, Anders S. Moderated estimation of fold change and dispersion for RNA-seq data with DESeq2. *Genome Biol* (2014) 15(12):550. doi: 10.1186/s13059-014-0550-8

29. Harris MA, Clark JI, Ireland A, Lomax J, Ashburner M, Collins R, et al. The gene ontology (GO) project in 2006. *Nucleic Acids Res* (2006) 34(Database issue):D322–D6. doi: 10.1093/nar/gkj021

30. Kanehisa M, Goto S. KEGG: kyoto encyclopedia of genes and genomes. *Nucleic Acids Res* (2000) 28(1):27–30. doi: 10.1093/nar/28.1.27

31. Shannon P, Markiel A, Ozier O, Baliga NS, Wang JT, Ramage D, et al. Cytoscape: a software environment for integrated models of biomolecular interaction networks. *Genome Res* (2003) 13(11):2498–504. doi: 10.1101/gr.1239303

32. Chin C-H, Chen S-H, Wu H-H, Ho C-W, Ko M-T, Lin C-Y. cytoHubba: identifying hub objects and sub-networks from complex interactome. *BMC Syst Biol* (2014) 8 Suppl 4(Suppl 4):S11. doi: 10.1186/1752-0509-8-S4-S11

33. Subramanian A, Tamayo P, Mootha VK, Mukherjee S, Ebert BL, Gillette MA, et al. Gene set enrichment analysis: a knowledge-based approach for interpreting genome-wide expression profiles. *Proc Natl Acad Sci U S A* (2005) 102(43):15545–50. doi: 10.1073/pnas.0506580102

34. Hänzelmann S, Castelo R, Guinney J. GSVA: gene set variation analysis for microarray and RNA-seq data. *BMC Bioinf* (2013) 14:7. doi: 10.1186/1471-2105-14-7

35. John B, Enright AJ, Aravin A, Tuschl T, Sander C, Marks DS. Human microRNA targets. *PloS Biol* (2004) 2(11):e363. doi: 10.1371/journal.pbio.0020363

36. Chen Y, Wang X. miRDB: an online database for prediction of functional microRNA targets. *Nucleic Acids Res* (2020) 48(D1):D127–D31. doi: 10.1093/nar/gkz757

37. Pottoo FH, Barkat MA, Harshita, Ansari MA, Javed MN, Sajid Jamal QM, et al. Nanotechnological based miRNA intervention in the therapeutic management of neuroblastoma. *Semin Cancer Biol* (2021) 69:100–8. doi: 10.1016/j.semcancer.2019.09.017

38. Furió-Tarí P, Tarazona S, Gabaldón T, Enright AJ, Conesa A. spongeScan: A web for detecting microRNA binding elements in lncRNA sequences. *Nucleic Acids Res* (2016) 44(W1):W176–W80. doi: 10.1093/nar/gkw443

39. Garibay D, Cummings BP. A Murine Model of Vertical Sleeve Gastrectomy. *J Vis Exp* (2017) 18(130):56534. doi: 10.3791/56534

40. Qi X, Zhang D-H, Wu N, Xiao J-H, Wang X, Ma W. ceRNA in cancer: possible functions and clinical implications. *J Med Genet* (2015) 52(10):710–8. doi: 10.1136/jmedgenet-2015-103334

41. Bartel DP. MicroRNAs: target recognition and regulatory functions. *Cell* (2009) 136(2):215–33. doi: 10.1016/j.cell.2009.01.002

42. Thomas M, Lieberman J, Lal A. Desperately seeking microRNA targets. *Nat Struct Mol Biol* (2010) 17(10):1169–74. doi: 10.1038/nsmb.1921

43. Paik JM, Golabi P, Younossi Y, Mishra A, Younossi ZM. Changes in the global burden of chronic liver diseases from 2012 to 2017: the growing impact of NAFLD. *Hepatol (Baltimore Md)* (2020) 72(5):1605–16. doi: 10.1002/hep.31173

44. Oseini AM, Sanyal AJ. Therapies in non-alcoholic steatohepatitis (NASH). *Liver Int* (2017) 37 Suppl 1(Suppl 1):97–103. doi: 10.1111/liv.13302

45. Hannah WN, Harrison SA. Effect of weight loss, diet, exercise, and bariatric surgery on nonalcoholic fatty liver disease. *Clin Liver Dis* (2016) 20(2):339–50. doi: 10.1016/j.cld.2015.10.008

46. Lassailly G, Caiazzo R, Buob D, Pigeyre M, Verkindt H, Labreuche J, et al. Bariatric surgery reduces features of nonalcoholic steatohepatitis in morbidly obese patients. *Gastroenterology* (2015) 149(2):379–88. doi: 10.1053/j.gastro.2015.04.014

47. Satriano L, Lewinska M, Rodrigues PM, Banales JM, Andersen JB. Metabolic rearrangements in primary liver cancers: cause and consequences. *Nat Rev Gastroenterol Hepatol* (2019) 16(12):748–66. doi: 10.1038/s41575-019-0217-8

48. Emma MR, Giannitrapani L, Cabibi D, Porcasi R, Pantuso G, Augello G, et al. Hepatic and circulating levels of PCSK9 in morbidly obese patients: Relation with severity of liver steatosis. *Biochim Et Biophys Acta Mol Cell Biol Lipids* (2020) 1865 (12):158792. doi: 10.1016/j.bbalip.2020.158792

49. Hua R, Wang G-Z, Shen Q-W, Yang Y-P, Wang M, Wu M, et al. Sleeve gastrectomy ameliorated high-fat diet (HFD)-induced non-alcoholic fatty liver disease and upregulated the nicotinamide adenine dinucleotide +/Sirtuin-1 pathway in mice. *Asian J Surg* (2021) 44(1):213–20. doi: 10.1016/j.asjsur.2020.05.030

50. Loftus TM, Jaworsky DE, Frehywot GL, Townsend CA, Ronnett GV, Lane MD, et al. Reduced food intake and body weight in mice treated with fatty acid synthase inhibitors. *Science* (2000) 288(5475):2379–81. doi: 10.1126/science.288.5475.2379

51. Benhammou JN, Ko A, Alvarez M, Kaikkonen MU, Rankin C, Garske KM, et al. Novel lipid long intervening noncoding RNA, oligodendrocyte maturation-associated long intergenic noncoding RNA, regulates the liver steatosis gene stearoyl-coenzyme A desaturase as an enhancer RNA. *Hepatol Commun* (2019) 3(10):1356–72. doi: 10.1002/hep4.1413

52. Chiappini F, Coilly A, Kadar H, Gual P, Tran A, Desterke C, et al. Metabolism dysregulation induces a specific lipid signature of nonalcoholic steatohepatitis in patients. *Sci Rep* (2017) 7:46658. doi: 10.1038/srep46658

53. Miyazaki M, Flowers MT, Sampath H, Chu K, Otzelberger C, Liu X, et al. Hepatic stearoyl-CoA desaturase-1 deficiency protects mice from carbohydrate-induced adiposity and hepatic steatosis. *Cell Metab* (2007) 6(6):484–96. doi: 10.1016/j.cmet.2007.10.014

54. Dobrzyn P, Dobrzyn A, Miyazaki M, Cohen P, Asilmaz E, Hardie DG, et al. Stearoyl-CoA desaturase 1 deficiency increases fatty acid oxidation by activating AMP-activated protein kinase in liver. *Proc Natl Acad Sci U S A* (2004) 101(17):6409–14. doi: 10.1073/pnas.0401627101

55. Jiang G, Li Z, Liu F, Ellsworth K, Dallas-Yang Q, Wu M, et al. Prevention of obesity in mice by antisense oligonucleotide inhibitors of stearoyl-CoA desaturase-1. *J Clin Invest* (2005) 115(4):1030–8. doi: 10.1172/JCI23962

56. Bhattacharya D, Basta B, Mato JM, Craig A, Fernández-Ramos D, Lopitz-Otsoa F, et al. Aramchol downregulates stearoyl CoA-desaturase 1 in hepatic stellate cells to attenuate cellular fibrogenesis. *JHEP Reports: Innovation In Hepatol* (2021) 3 (3):100237. doi: 10.1016/j.jhepr.2021.100237

57. Ratziu V, de Guevara L, Safadi R, Poordad F, Fuster F, Flores-Figueroa J, et al. Aramchol in patients with nonalcoholic steatohepatitis: a randomized, double-blind, placebo-controlled phase 2b trial. *Nat Med* (2021) 27(10):1825–35. doi: 10.1038/s41591-021-01495-3

58. Quintana AM, Hernandez JA, Gonzalez CG. Functional analysis of the zebrafish ortholog of HMGCS1 reveals independent functions for cholesterol and isoprenoids in craniofacial development. *PloS One* (2017) 12(7):e0180856. doi: 10.1371/journal.pone.0180856

59. Ma X, Bai Y, Liu K, Han Y, Zhang J, Liu Y, et al. Ursolic acid inhibits the cholesterol biosynthesis and alleviates high fat diet-induced hypercholesterolemia via irreversible inhibition of HMGCS1 in vivo. *Phytomedicine* (2022) 103:154233. doi: 10.1016/j.phymed.2022.154233

60. Li H, Xie Z, Lin J, Song H, Wang Q, Wang K, et al. Transcriptomic and metabonomic profiling of obesity-prone and obesity-resistant rats under high fat diet. *J Proteome Res* (2008) 7(11):4775–83. doi: 10.1021/pr800352k

61. Liu D, Wong CC, Fu L, Chen H, Zhao L, Li C, et al. Squalene epoxidase drives NAFLD-induced hepatocellular carcinoma and is a pharmaceutical target. *Sci Transl Med* (2018) 10(437):eaap9840. doi: 10.1126/scitranslmed.aap9840

62. Herrera-Marcos LV, Martínez-Beamonte R, Macías-Herranz M, Arnal C, Barranquero C, Puente-Lanzarote JJ, et al. Hepatic galectin-3 is associated with lipid droplet area in non-alcoholic steatohepatitis in a new swine model. *Sci Rep* (2022) 12 (1):1024. doi: 10.1038/s41598-022-04971-z

63. Liu D, Wong CC, Zhou Y, Li C, Chen H, Ji F, et al. Squalene epoxidase induces nonalcoholic steatohepatitis via binding to carbonic anhydrase III and is a therapeutic target. *Gastroenterology* (2021) 160(7):2467–82.e3. doi: 10.1053/j.gastro.2021.02.051

64. Marra F, Tacke F. Roles for chemokines in liver disease. *Gastroenterol* (2014) 147 (3):577–94.e1. doi: 10.1053/j.gastro.2014.06.043

65. Zhang X, Shen J, Man K, Chu ESH, Yau TO, Sung JCY, et al. CXCL10 plays a key role as an inflammatory mediator and a non-invasive biomarker of non-alcoholic steatohepatitis. *J Hepatol* (2014) 61(6):1365–75. doi: 10.1016/j.jhep.2014.07.006

66. Zhang X, Fan L, Wu J, Xu H, Leung WY, Fu K, et al. Macrophage p38α promotes nutritional steatohepatitis through M1 polarization. *J Hepatol* (2019) 71(1):163–74. doi: 10.1016/j.jhep.2019.03.014

67. Tomita K, Freeman BL, Bronk SF, LeBrasseur NK, White TA, Hirsova P, et al. CXCL10-Mediates Macrophage, but not Other Innate Immune Cells-Associated Inflammation in Murine Nonalcoholic Steatohepatitis. *Sci Rep* (2016) 6:28786. doi: 10.1038/srep28786

68. Patouraux S, Rousseau D, Bonnafous S, Lebeaupin C, Luci C, Canivet CM, et al. CD44 is a key player in non-alcoholic steatohepatitis. *J Hepatol* (2017) 67(2):328–38. doi: 10.1016/j.jhep.2017.03.003

69. Yeh C-L, Yang P-J, Lee P-C, Wu J-M, Chen P-D, Huang C-C, et al. Intravenous glutamine administration improves glucose tolerance and attenuates the inflammatory response in diet-induced obese mice after sleeve gastrectomy. *Nutrients* (2020) 12 (10):3192. doi: 10.3390/nu12103192

70. Takahashi Y. Nonalcoholic fatty liver disease and adult growth hormone deficiency: An under-recognized association? *Best Pract Res Clin Endocrinol Metab* (2023) 37(6):101816. doi: 10.1016/j.beem.2023.101816

71. Møller N, Jørgensen JOL. Effects of growth hormone on glucose, lipid, and protein metabolism in human subjects. *Endocr Rev* (2009) 30(2):152–77. doi: 10.1210/er.2008-0027

72. Takahashi Y. The role of growth hormone and insulin-like growth factor-I in the liver. *Int J Mol Sci* (2017) 18(7):1447. doi: 10.3390/ijms18071447

73. Nishizawa H, Takahashi M, Fukuoka H, Iguchi G, Kitazawa R, Takahashi Y. GH-independent IGF-I action is essential to prevent the development of nonalcoholic steatohepatitis in a GH-deficient rat model. *Biochem Biophys Res Commun* (2012) 423 (2):295–300. doi: 10.1016/j.bbrc.2012.05.115

74. Spadaro O, Camell CD, Bosurgi L, Nguyen KY, Youm Y-H, Rothlin CV, et al. IGF1 shapes macrophage activation in response to immunometabolic challenge. *Cell Rep* (2017) 19(2):225–34. doi: 10.1016/j.celrep.2017.03.046

75. Sanz S, Pucilowska JB, Liu S, Rodríguez-Ortigosa CM, Lund PK, Brenner DA, et al. Expression of insulin-like growth factor I by activated hepatic stellate cells reduces fibrogenesis and enhances regeneration after liver injury. *Gut* (2005) 54(1):134–41. doi: 10.1136/gut.2003.024505

76. Lambert JE, Ramos-Roman MA, Browning JD, Parks EJ. Increased *de novo* lipogenesis is a distinct characteristic of individuals with nonalcoholic fatty liver disease. *Gastroenterol* (2014) 146(3):726–35. doi: 10.1053/j.gastro.2013.11.049

77. Ding Y, Xu X, Meng B, Wang L, Zhu B, Guo B, et al. Myeloid-derived growth factor alleviates non-alcoholic fatty liver disease alleviates in a manner involving IKKβ/NF-κB signaling. *Cell Death Dis* (2023) 14(6):376. doi: 10.1038/s41419-023-05904-y

78. Tarantino G, Citro V, Balsano C, Capone D. Could SCGF-beta levels be associated with inflammation markers and insulin resistance in male patients suffering from obesity-related NAFLD? *Diagnostics (Basel Switzerland)* (2020) 10 (6):395. doi: 10.3390/diagnostics10060395

79. Da Riva L, Bozzi F, Mondellini P, Miccichè F, Fumagalli E, Vaghi E, et al. Proteomic detection of a large amount of SCGFα in the stroma of GIST's after imatinib therapy. *J Transl Med* (2011) 9:158. doi: 10.1186/1479-5876-9-158

80. Kim ML, Martin WJ, Minigo G, Keeble JL, Garnham AL, Pacini G, et al. Dysregulated IL-1β-GM-CSF axis in acute rheumatic fever that is limited by hydroxychloroquine. *Circulation* (2018) 138(23):2648–61. doi: 10.1161/CIRCULATIONAHA.118.033891

frontiers | Frontiers in Endocrinology

TYPE Original Research
PUBLISHED 26 February 2024
DOI 10.3389/fendo.2024.1334342

OPEN ACCESS

EDITED BY
Yayun Wang,
Air Force Medical University, China

REVIEWED BY
Søren Madsen,
The University of Sydney, Australia
Chunmei Wang,
Baylor College of Medicine, United States

*CORRESPONDENCE
Tongtong Zhang
163zttong@163.com
Yanjun Liu
liuyanjun@swjtu.edu.cn

RECEIVED 07 November 2023
ACCEPTED 09 January 2024
PUBLISHED 26 February 2024

CITATION
Wang Y, Yang C, Wen J, Ju L, Ren Z, Zhang T and Liu Y (2024) Whole-exome sequencing combined with postoperative data identify c.1614dup (CAMKK2) as a novel candidate monogenic obesity variant.
Front. Endocrinol. 15:1334342.
doi: 10.3389/fendo.2024.1334342

Whole-exome sequencing combined with postoperative data identify c.1614dup (CAMKK2) as a novel candidate monogenic obesity variant

Yan Wang[1,2], Chao Yang[3], Jun Wen[1], Lingling Ju[1,4], Zhengyun Ren[1,4], Tongtong Zhang[1,2]* and Yanjun Liu[1]*

[1]Center of Gastrointestinal and Minimally Invasive Surgery, Department of General Surgery, The Third People's Hospital of Chengdu, Affiliated Hospital of Southwest Jiaotong University, Chengdu, China, [2]Medical Research Center, The Third People's Hospital of Chengdu, Affiliated Hospital of Southwest Jiaotong University, Chengdu, China, [3]West China Second University Hospital, Sichuan University, Chengdu, China, [4]Institute of Biomedical Engineering, College of Medicine, Southwest Jiaotong University, Chengdu, China

Early-onset obesity is a rising health concern influenced by heredity. However, many monogenic obesity variants (MOVs) remain to be discovered due to differences in ethnicity and culture. Additionally, patients with known MOVs have shown limited weight loss after bariatric surgery, suggesting it can be used as a screening tool for new candidates. In this study, we performed whole-exome sequencing (WES) combined with postoperative data to detect candidate MOVs in a cohort of 62 early-onset obesity and 9 late-onset obesity patients. Our findings demonstrated that patients with early-onset obesity preferred a higher BMI and waist circumference (WC). We confirmed the efficacy of the method by identifying a mutation in known monogenic obesity gene, *PCSK1*, which resulted in less weight loss after surgery. 5 genes were selected for further verification, and a frameshift variant in *CAMKK2* gene: NM_001270486.1, c.1614dup, (p.Gly539Argfs*3) was identified as a novel candidate MOV. This mutation influenced the improvement of metabolism after bariatric surgery. In conclusion, our data confirm the efficacy of WES combined with postoperative data in detecting novel candidate MOVs and c.1614dup (CAMKK2) might be a promising MOV, which needs further confirmation. This study enriches the human monogenic obesity mutation database and provides a scientific basis for clinically accurate diagnosis and treatment.

KEYWORDS

monogenic obesity, WES, bariatric surgery, CAMKK2, weight loss

1 Introduction

The increase in obesity presents a significant health issue as it has become a major contributor to the global occurrence of chronic diseases, including type 2 diabetes, cardiovascular diseases and some types of cancer (1, 2). Of particular concern is early-onset obesity, which refers to obesity that develops during childhood or adolescence. The prevalence of early-onset obesity is on the rise in low-income and middle-income countries, as well as many high-income countries (3). The role of genetics in the transmission of early-onset obesity and its associated health conditions is undeniable. Through genome-wide association studies (GWAS) and whole-exome sequencing (WES), numerous genetic loci linked to obesity have been identified (4, 5). However, a significant portion of patients with obesity remains unexplained by the currently identified individual genes. This implies that numerous unknown genes are yet to be discovered, and this genetic diversity is especially enhanced by differences in ethnicity and culture.

Bariatric surgery has emerged as an effective treatment for severe obesity, leading to sustained weight loss over a 10-year period and improvements in comorbidities and quality of life (6). However, it has been reported that patients carrying known MOVs experience lower weight loss after undergoing bariatric surgery (7), suggesting long-term negative effects of MOVs on patients following bariatric surgery. We therefore wondered whether this could be used to screening novel candidate MOVs.

In the current study, we employed WES in combination with weight data obtained after bariatric surgery to identify candidate MOVs that are enriched in patients with early-onset obesity. We hypothesized that candidate MOVs would be selectively enriched in the cases and filtered out in the control group. Our study successfully identified *PCSK1*, a known monogenic obesity gene, in 4 patients who experienced less weight loss after surgery, thereby confirming the validity of our method. Additionally, our study provides evidence for another candidate MOV found in the coding sequence of the *CAMKK2* gene.

These findings highlight the potential of using WES combined with post-surgical weight data to identify and characterize candidate MOVs. By expanding our understanding of the genetic factors contributing to obesity, we can gain insights into the underlying mechanisms and potentially develop more personalized and targeted approaches for the management and treatment of obesity.

2 Methods

2.1 Subjects

Obese patients (BMI >30kg/m^2) who underwent bariatric surgery at the Gastrointestinal Minimally Invasive Center of the Third People's Hospital of Chengdu during years of 2021 to 2022 were selected. The early-onset obesity group included subjects who were obese before 10 years old while the control group were after, according to the criteria of the Working Group for Obesity in China (WGOC) (8). Finally, a total of 62 early-onset obesity and 9 controls were included. Patient blood samples were collected, and preoperative clinical data and postoperative follow-up information were recorded. All procedures involving human subjects were approved by the Ethics Committee of The Third People's Hospital of Chengdu. The clinical trial registration number is ChiCTR2300073353. The volunteers were provided with full information about the study, and their informed consent was obtained.

2.2 Whole-exome sequencing and variants analysis

Genomic DNA was isolated from peripheral blood using the Blood Genome DNA Extraction Kit (TIANGEN Biotech, Beijing, China) according to manufacturer's protocols. Whole-exome sequencing analysis was performed using the Illumina HiSeq2500 platform (Illumina San Diego, CA, USA) with 150 bp paired-end reads. All reads were mapped against the hg38 reference genome using the Burrow–Wheeler aligner (BWA). The identification of variants was performed using a custom pipeline that utilizes the GATK Best Practices workflow (9).

Variants were filtered according to minor allele frequency (MAF) ≥ 5% in the 1000 Genomes and Exome Aggregation Consortium (ExAC) databases. Variants showed in the controls and synonymous variants, assumed to be benign or likely benign, were also excluded. Frameshift, stop gain and stoploss were considered damaging. The nonsynonymous variants were predicted to be damaging by annotation in dbNSFP database. In detail, different prediction software (SIFT, Polyphen2_HDIV, Polyphen2_HVAR, LRT, MutationTaster, MutationAssessor, FATHMM, PROVEAN, MetaSVM, MetaLR, M-CAP, CADD, fathmm-MKL) were used to assign scores for the nonsynonymous variants. Considering that some software may lack annotations for certain mutations, for those with available scores, if half or more of the software predicts damaging, the variant is considered deleterious. Then, Criteria of the American College of Medical Genetics and Genomics (ACMG) were used to determine the pathogenicity of variants, building on the automatic classification provided by VarSome (https://varsome.com/). Finally, variants for further verification were selected based on mutation category and literature data.

2.3 Statistical analysis

The early-onset subjects were divided into groups of non-carriers and carriers depending on whether they carried the particular variant in each comparison, e.g., non-carriers of PCSK1 mutation vs carriers of PCSK1 mutation. In the postoperative period of bariatric surgery, patients' weight was followed up at 1 month, 3 months, 6 months, and 12 months, and the percent of weight loss was calculated. Independent *t* tests were conducted to compare the percentage of weight loss between the two groups at

each time point, and the *P* values were adjusted via the FDR. Paired *t* tests were used to compare HDL, LDL, TC and TG between baseline and 12 months after surgery. To compare the percentage changes in HDL, LDL, TC and TG from baseline to 12 months post-surgery between CAMKK2 non-carriers and carriers, independent *t* tests were also performed. A value of 0.05 was considered to be statistically significant. Statistical analyses were carried out with the use of IBM SPSS Statistics, GraphPad Prism 8 and R software.

3 Results

3.1 Clinical characteristics of patients

All individuals included in the whole exome sequencing (WES) and assessments were classified as obese (BMI >30 kg/m^2). Control subjects were selected from individuals who developed obesity after the age of 10 (n=9), while the early-onset obesity group consisted of individuals who developed obesity before the age of 10 (n=62). The clinical characteristics of both groups are summarized in Table 1.

The results showed a significant difference in BMI and waist circumference (WC) between the control and early-onset obesity groups ($P< 0.05$), with the latter exhibiting higher BMI and WC, suggesting that early-onset obesity has a more pronounced impact on overall weight gain compared to individuals who develop obesity later in life. However, there is no significant change in waist-hip ratio (WHR), visceral fat level (VFL), and percent body fat (PBF) between them, indicating that early-onset obesity has a greater impact on weight rather than on fat distribution, potentially influenced by genetic factors that influence appetite and energy homeostasis.

3.2 Identification of MOVs

WES was performed for 62 early-onset obesity and 9 late-onset obesity and an average sequencing depth of 100× was obtained. Variants were selected according to mutation damaging prediction software, the American College of Medical Genetics (ACMG) guidelines (10) and literature data for further analysis. Candidate MOVs were verified by the weight loss data after bariatric surgery, as previous study reported that MOVs lead to less weight loss after bariatric surgery (7).

TABLE 1 Clinical information of individuals with obesity.

Subject	Control (n=9)	Early-onset obesity (n=62)	*P* value
Male/Female	4/5	29/33	
Age (years)	30.00 ± 5.94	28.84 ± 8.25	
Hypertension	1	10	
Diabetes	2	13	
BMI (kg/m^2)	33.52 ± 3.54	40.13 ± 5.95	0.002
WC (cm)	110.64 ± 8.20	121.21 ± 12.69	0.02
WHR	0.99 ± 0.04	1.01 ± 0.07	
VFL	17.89 ± 2.67	19.10 ± 1.87	
PBF (%)	42.91 ± 7.00	44.85 ± 5.78	

A total of 567 variants (variant frequency ≥5%) predicted as deleterious were identified in patients with early-onset obesity (including nonsynonymous SNVs and frameshift Indels). 11 were predicted pathogenic (P) or likely pathogenic (LP) and 60 were considered variants of uncertain significance (VUS) according to ACMG guidelines (Supplementary Table 1). We found 1 missense variant in the *PCSK1* gene (c.242G>A) (Table 2) that was already known to be associated with monogenic early-onset obesity (11, 12), which mutation led to less weight loss after bariatric surgery (7). We also found 5 genes (2 frameshift insertion, 2 frameshift deletion and 1 stop-loss) reported associating with obesity, adipogenesis or previously linked to obesity-associated traits by genome-wide association studies: *SLC25A5* (13), *AIM2* (14), *SNX16* (15), *CAMKK2* (16–18), *PDE11A* (19) (Table 2) and they were selected for further verification.

To test the validity of the post-operative data to identify candidate MOVs, analysis was first performed on PCSK1 mutation carriers, and the results showed that the PCSK1 mutation resulted in less weight loss with a significant difference (FDR<0.05) (Figure 1), indicating that the method is effective. Therefore, to validate whether other gene variants are candidates, analysis were performed between non-carriers and carriers of each variant, including c.450del (SLC25A5), c.1029dup (AIM2), c.1033T>C (SNX16), c.1614dup (CAMKK2), c.20_21del (PDE11A). Compared to the non-carriers, CAMKK2 variant carriers exhibited poorer weight loss with a significant difference (FDR<0.001) (Figure 2), with no overlapping individuals with PCSK1 variant carriers, indicating that the effect of the CAMKK2 variant on weight loss is independent. AIM2 variant carriers also showed less weight loss from 1 month until 12 months after surgery, but similar with other three gene variants (c.450del (SLC25A5), c.1033T>C (SNX16), c.20_21del (PDE11A) carriers, the difference was not statistically significant compared to the non-carriers group (Supplementary Figure 1). In order to rule out other genetic mutations carried by CAMKK2 mutation carriers resulting in less weight loss, we took the intersection of all the mutations carried by the 8 CAMKK2 mutation carriers, and none of the mutations were screened. Therefore, we consider c.1614dup (CAMKK2) might be a promising MOV but needs further confirmation.

The calcium/calmodulin dependent protein kinase kinase 2 (CAMKK2) is a member of the serine/threonine protein kinase family and Ca(2+)/calmodulin-dependent protein kinase subfamily requiring the presence of calcium and calmodulin to be active. The c.1614dup (CAMKK2) variant involves the insertion of an A base at position 1615, which is identical to position 1614. This results in the mutation of glycine to arginine at position 539 of the CAMKK2 protein and a premature truncation from 556 amino acids to 540 amino acids. It is important to note that this mutation is predicted to cause nonsense-mediated mRNA decay (NMD), a process by which mRNAs that contain premature termination codons are degraded, indicating that even though it only reduces 16 amino acids, it is critical for the stability of this protein.

TABLE 2 Variants selected for further analysis.

Gene	Transcript	Variant	Protein	dbSNP	1000G	ACMG classification	ACMG tags	Carriers/ Total
SLC25A5	NM_001152.5	c.450del	p. Ala150fs*64	rs759019641	.	LP	PVS1, PP5	9/62
AIM2	NM_004833.3	c.1029dup	p. *344Ileext*3	rs1557889335	0.0129792	LP	PM4, PM2, BP4	4/62
SNX16	NM_152836.3	c.1033T>C	p. *345Glnext*15	rs150053915	0.00199681	LP	PM4, PM2, BP4	4/62
CAMKK2	NM_001270486.1	c.1614dup	p. Gly539Argfs*3	NA	.	VUS	PM2	8/62
PDE11A	NM_001077197.2	c.20_21del	p. Arg7Thrfs*30	rs202117698	0.00219649	VUS	PVS1, PP5, BS2	4/62
PCSK1	NM_000439.5	c.242G>A	p. Arg81Lys	NA	.	VUS	PM2	4/62

*means change in a stop codon. NA, Not Available.

3.3 CAMKK2 variant influences metabolism improvement after bariatric surgery

To evaluate the effect of c.1614dup (CAMKK2) on metabolism after bariatric surgery, we compared lipid levels between baseline and 12 months post-surgery between carriers and non-carriers of the CAMKK2 mutation (Figure 3A), and compared their percentage change from baseline to 12 months after surgery (Figure 3B). Final data were collected from 43 non-carriers and 7 carriers of the mutation due to loss of follow-up in some patients. Both groups showed a statistically significant increase in HDL cholesterol levels (mean HDL levels increased from 1.15mmol/L to 1.44mmol/L in CAMKK2 mutation non-carriers, FDR = 0, and from 1.17mmol/L to 1.30mmol/L in CAMKK2 carriers, FDR = 0.038) (Figure 3A), and there was a significant difference in the percentage change between the two groups (CAMKK2 non-mutation carriers 27.3%, CAMKK2 mutation carriers 11.5%, FDR = 0.046) (Figure 3B). LDL cholesterol was down-regulated in both groups. However, the changes between baseline and 12 months after surgery were statistically significant in CAMKK2 mutation non-carriers but not in carriers (Figure 3A), likely due to the limitation of the sample size. Furthermore, there was no significant difference in the percentage change between the two groups (Figure 3B). Meanwhile, both groups exhibited a statistically significant decrease in triglyceride (TG) levels (Figure 3A) and the percentage decrease was greater in individuals without the CAMKK2 mutation (29.5%) compared to those with the mutation (14%) (FDR = 0.029) (Figure 3B). However, no significant changes in total cholesterol (TC) levels were observed in either group (Figure 3A) or in percentage change between the two groups (Figure 3B). The results indicate that patients, regardless of whether they carry the CAMKK2 mutation or not, experience improved metabolism after undergoing bariatric surgery. However, the degree of improvement varies, with non-carriers of the CAMKK2 mutation showing significant changes in elevated levels of HDL and reduced levels of TG compared to carriers of the CAMKK2 mutation.

4 Discussion

Identifying the underlying causes of early-onset obesity is a challenging task due to the complex interplay of genetic and

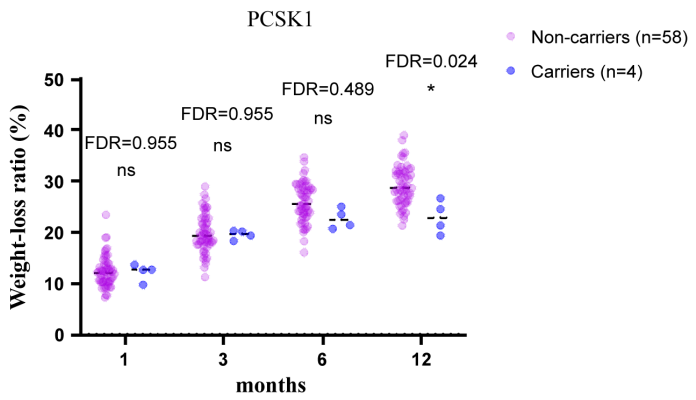

FIGURE 1
12-month weight-loss ratio for obese individuals with/without the PCSK1 mutation after bariatric surgery. PCSK1 variant led to less weight loss after bariatric surgery compared with PCSK1 non-carriers. Independent *t* tests were conducted at 1, 3, 6, 12 months, respectively, and the *P* values were adjusted via the FDR. *FDR<0.05, ns, no significance.

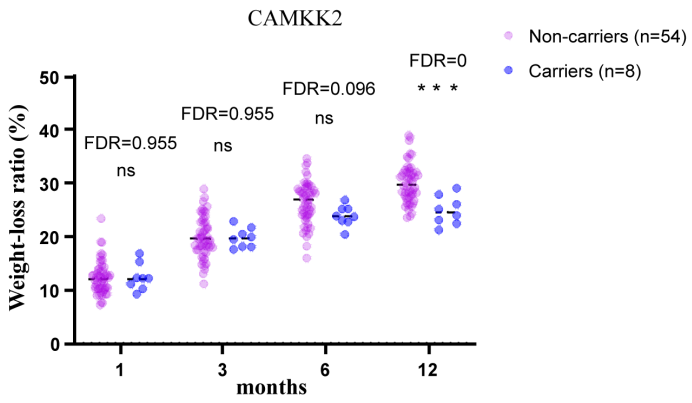

FIGURE 2
12-month postoperative weight-loss ratio in obese patients with/without CAMKK2 mutation. CAMKK2 variant carriers exhibited poorer weight loss after bariatric surgery compared with CAMKK2 non-carriers. Independent *t* tests were performed at each time point and the *P* values were adjusted via the FDR. ***FDR<0.001, ns, no significance.

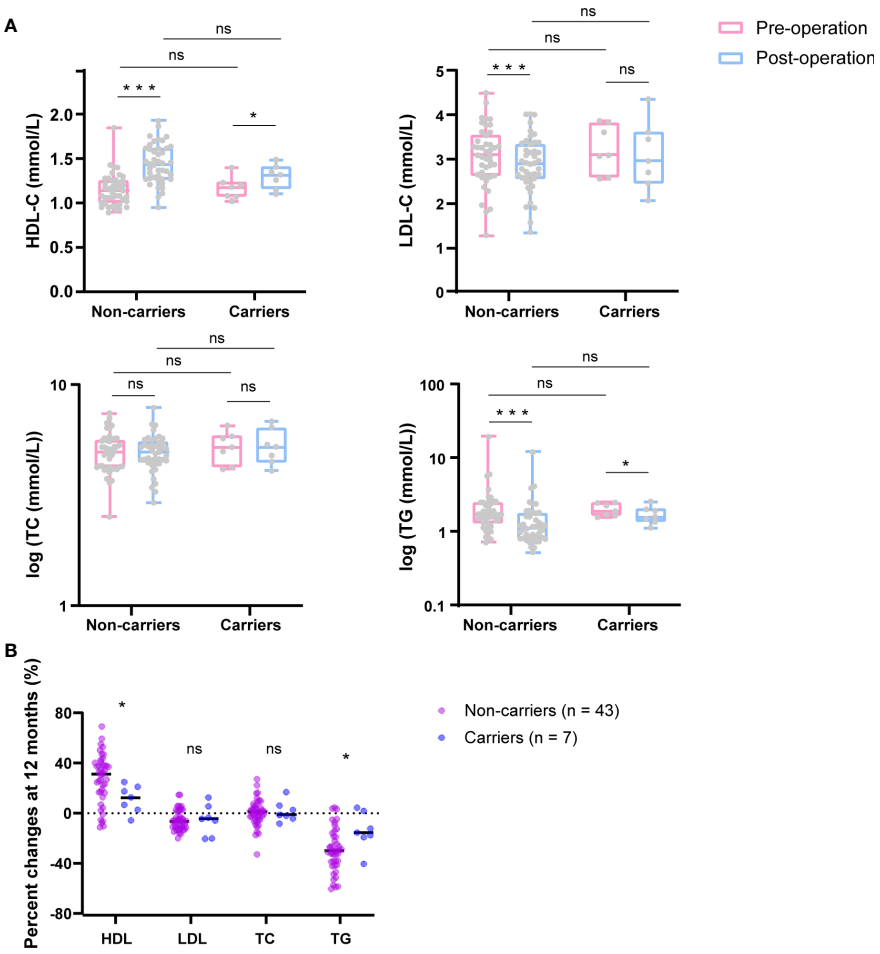

FIGURE 3
CAMKK2 variant influences metabolism improvement after bariatric surgery. **(A)** Changes in HDL, LDL, TC, and TG after bariatric surgery (12months) (blue) compared with baseline (pink) between CAMKK2 mutation non-carriers (n = 43) and carriers (n = 7). **(B)** Percentage changes from baseline to 12 months post-surgery of HDL, LDL, TC and TG. TC and TG were logarithmically transformed using GraphPad Prism 8. Compared *t* tests and independent *t* tests were performed, and the *P* values were adjusted via the FDR. *FDR<0.05, ***FDR<0.001, ns, no significance.

environmental factors. WES has emerged as an effective tool for detecting novel candidate genes associated with these disorders. In a study conducted by Li et al., the researchers investigated whether MOVs influence the effectiveness of bariatric surgery (7). Similarly, the long-term outcomes of bariatric surgery were evaluated in patients with bi-allelic mutations in known monogenic obesity genes such as *POMC*, *LEPR*, and *MC4R* (20). The findings from both studies suggested that carriers of monogenic obesity gene mutations exhibit less weight loss after bariatric surgery, indicating that bariatric surgery could potentially be used as a screening method for detecting MOVs following WES analysis. In the present study, WES was performed on a cohort of 62 individuals with early-onset obesity and 9 individuals with late-onset obesity. This analysis led to the identification of a known monogenic obesity gene, *PCSK*, with a mutation that was associated with less weight loss in our study. This finding further validated the effectiveness of using WES combined with postoperative data as a method for detecting candidate MOVs. Then, we selected 5 variants in genes previously reported to be associated with obesity, adipogenesis or linked to obesity-associated traits by genome-wide association studies (*SLC25A5*, *AIM2*, *SNX16*, *CAMKK2* and *PDE11A*) for further analysis to identify candidate MOVs. In combination with weight data after bariatric surgery, we finally identified c.1614dup (CAMKK2) as a novel candidate MOV.

CAMKK2 is expressed both in hypothalamus (17) and preadipocytes (16). It plays a key role in the calcium/calmodulin-dependent (CaM) kinase cascade through the phosphorylation of the downstream kinases, including CaMKI, CaMKIV and AMP-activated protein kinase (AMPK) (17, 21–23). Among these, AMPK is a key regulator of cellular energy balance, which is involved in the leptin-melanocortin signaling pathway (24). CAMKK2 null mice developed obesity, insulin resistance, and less glucose tolerance with standard chow whereas displayed a considerably smaller increase in adiposity and adipocyte size with high-fat diet compared with WT mice by regulating NPY and therefore affecting appetite (17). NPY is a known appetite regulator and its mutation led to obesity and metabolic syndrome (25). *In vitro*, inhibition or deletion of CAMKK2 in preadipocytes promoted their differentiation into mature adipocytes, which could be rescued by AMPK activation (16). These studies suggest that the CAMKK2 variant carriers identified in this study may have followed a normal diet structure instead of a high-fat diet, which surprisingly lead to weight gain. After bariatric surgery, all patients, including CAMKK2 variant carriers, are instructed to follow a specific dietary structure, which is more closely aligned with a standard diet, rather than a high-fat diet, leading to suboptimal weight loss.

Among the other genes variants that lacked statistical significance, AIM2 necessitates further validation. AIM2, a member of the IFN-inducible HIN200 protein family (26), is a cytoplasmic double-stranded DNA sensor and a tumor suppressor (27, 28). AIM2 knockout mice exhibited increased both subcutaneous and visceral adiposity compared to WT, with no differences in food intake. For the reason, AIM2 null mice showed a reduction in energy expenditure and impaired function of their brown adipose tissue. Furthermore, AIM2 knockout led to insulin resistance and glucose intolerant (14). AIM2 variants have not been reported to cause obesity yet, and in our study, a frameshift variant of AIM2 was found in 4 patients who had a family history of obesity. Although their weight loss after bariatric surgery did not reach statistical significance, it is important to note that the sample size was limited, suggesting additional studies with larger sample sizes or different populations may help to clarify whether AIM2 is a candidate monogenic obesity gene.

Furthermore, in 70 genes predicted pathology, likely pathology and variants of uncertain significance, MPP2 is predominantly expressed in the brain (Genotype-Tissue Expression), which is an established key region in the regulation of energy homeostasis and food intake. However, its role in obesity or metabolic disorders has not been reported and need to be further explored in the future.

In summary, the present investigation indicates that individuals with early-onset obesity have significantly higher BMI and waist circumstance (WC) compared to subjects with late-onset obesity. This data verified the efficiency of WES combined with postoperative data to identify candidate monogenic obesity genes and also identified c.1614dup (CAMKK2) as a promising MOV in a cohort of patients experiencing early-onset obesity. Further research with larger sample sizes is needed to confirm these findings and to determine the long-term effects of the c.1614dup (CAMKK2) variant on metabolism.

5 Conclusions

WES combined with weight data following bariatric surgery is an effective strategy for identifying novel candidate MOVs and c.1614dup (CAMKK2) might be a new MOV.

Data availability statement

The datasets presented in this study can be found in online repositories. The accession number is PRJNA1041755 (https://www.ncbi.nlm.nih.gov/bioproject/PRJNA1041755).

Ethics statement

The studies involving humans were approved by The Ethics Committee of The Third People's Hospital of Chengdu. The studies were conducted in accordance with the local legislation and institutional requirements. Written informed consent for participation in this study was provided by the participants' legal guardians/next of kin.

Author contributions

YW: Investigation, Validation, Writing – original draft, Visualization, Writing – review & editing. CY: Data curation, Validation, Writing – review & editing. JW: Resources, Writing – review & editing. LJ: Investigation, Writing – review & editing. ZR: Resources, Writing – review & editing. TZ: Funding acquisition, Supervision, Writing – review & editing, Project administration. YL: Funding acquisition, Supervision, Writing – review & editing, Project administration.

Funding

The author(s) declare financial support was received for the research, authorship, and/or publication of this article. This work was supported by The National Natural Science Foundation of China (82370884, 82170887).

Acknowledgments

The authors thank all patients involved in this project.

Conflict of interest

The authors declare that the research was conducted in the absence of any commercial or financial relationships that could be construed as a potential conflict of interest.

Publisher's note

Supplementary material

The Supplementary Material for this article can be found online at: https://www.frontiersin.org/articles/10.3389/fendo.2024.1334342/full#supplementary-material

References

1. Piché ME, Tchernof A, Després JP. Obesity phenotypes, diabetes, and cardiovascular diseases. *Circ Res* (2020) 126(11):1477–500. doi: 10.1161/CIRCRESAHA.120.316101

2. Lega IC, Lipscombe LL. Review: diabetes, obesity, and cancer-pathophysiology and clinical implications. *Endocrine Rev* (2020) 41(1):bnz014. doi: 10.1210/endrev/bnz014

3. Jebeile H, Kelly AS, O'Malley G, Baur LA. Obesity in children and adolescents: epidemiology, causes, assessment, and management. *Lancet Diabetes endocrinol* (2022) 10(5):351–65. doi: 10.1016/S2213-8587(22)00047-X

4. Loos RJF, Yeo GSH. The genetics of obesity: from discovery to biology. *Nat Rev Genet* (2022) 23(2):120–33. doi: 10.1038/s41576-021-00414-z

5. Littleton SH, Berkowitz RI, Grant SFA. Genetic determinants of childhood obesity. *Mol diagnosis Ther* (2020) 24(6):653–63. doi: 10.1007/s40291-020-00496-1

6. Nguyen NT, Kim E, Vu S, Phelan M. Ten-year outcomes of a prospective randomized trial of laparoscopic gastric bypass versus laparoscopic gastric banding. *Ann surgery* (2018) 268(1):106–13. doi: 10.1097/SLA.0000000000002348

7. Li Y, Zhang H, Tu Y, Wang C, Di J, Yu H, et al. Monogenic obesity mutations lead to less weight loss after bariatric surgery: a 6-year follow-up study. *Obes Surg* (2019) 29(4):1169–73. doi: 10.1007/s11695-018-03623-4

8. Group of China Obesity Task Force. Body mass index reference norm for screening overweight and obesity in Chinese children and adolescents. *Chin J Epidemiol* (2004) 25:97–102.

9. Venselaar H, Te Beek TA, Kuipers RK, Hekkelman ML, Vriend G. Protein structure analysis of mutations causing inheritable diseases. An e-Science approach with life scientist friendly interfaces. *BMC Bioinf* (2010) 11:548. doi: 10.1186/1471-2105-11-548

10. Richards S, Aziz N, Bale S, Bick D, Das S, Gastier-Foster J, et al. Standards and guidelines for the interpretation of sequence variants: a joint consensus recommendation of the American College of Medical Genetics and Genomics and the Association for Molecular Pathology. *Genet Med* (2015) 17(5):405–24. doi: 10.1038/gim.2015.30

11. Folon L, Baron M, Toussaint B, Vaillant E, Boissel M, Scherrer V, et al. Contribution of heterozygous PCSK1 variants to obesity and implications for precision medicine: a case-control study. *Lancet Diabetes endocrinol* (2023) 11(3):182–90. doi: 10.1016/S2213-8587(22)00392-8

12. Ramos-Molina B, Martin MG, Lindberg I. PCSK1 variants and human obesity. *Prog Mol Biol Trans science* (2016) 140:47–74. doi: 10.1016/bs.pmbts.2015.12.001

13. Zhu S, Wang W, Zhang J, Ji S, Jing Z, Chen YQ. Slc25a5 regulates adipogenesis by modulating ERK signaling in OP9 cells. *Cell Mol Biol letters* (2022) 27(1):11. doi: 10.1186/s11658-022-00314-y

14. Gong Z, Zhang X, Su K, Jiang R, Sun Z, Chen W, et al. Deficiency in AIM2 induces inflammation and adipogenesis in white adipose tissue leading to obesity and insulin resistance. *Diabetologia* (2019) 62(12):2325–39. doi: 10.1007/s00125-019-04983-x

15. Wu Y, Wang W, Jiang W, Yao J, Zhang D. An investigation of obesity susceptibility genes in Northern Han Chinese by targeted resequencing. *Medicine* (2017) 96(7):e6117. doi: 10.1097/MD.0000000000006117

16. Lin F, Ribar TJ, Means AR. The Ca2+/calmodulin-dependent protein kinase kinase, CaMKK2, inhibits preadipocyte differentiation. *Endocrinology* (2011) 152(10):3668–79. doi: 10.1210/en.2011-1107

17. Anderson KA, Ribar TJ, Lin F, Noeldner PK, Green MF, Muehlbauer MJ, et al. Hypothalamic CaMKK2 contributes to the regulation of energy balance. *Cell Metab* (2008) 7(5):377–88. doi: 10.1016/j.cmet.2008.02.011

18. Najar MA, Rex DAB, Modi PK, Agarwal N, Dagamajalu S, Karthikkeyan G, et al. A complete map of the Calcium/calmodulin-dependent protein kinase kinase 2 (CAMKK2) signaling pathway. *J Cell communication Signaling* (2021) 15(2):283–90. doi: 10.1007/s12079-020-00592-1

19. Ohlsson T, Lindgren A, Engström G, Jern C, Melander O. A stop-codon of the phosphodiesterase 11A gene is associated with elevated blood pressure and measures of obesity. *J hypertension* (2016) 34(3):445–51; discussion 51. doi: 10.1097/HJH.0000000000000821

20. Poitou C, Puder L, Dubern B, Krabusch P, Genser L, Wiegand S, et al. Long-term outcomes of bariatric surgery in patients with bi-allelic mutations in the POMC, LEPR, and MC4R genes. *Surg Obes related Dis* (2021) 17(8):1449–56. doi: 10.1016/j.soard.2021.04.020

21. Ye C, Zhang D, Zhao L, Li Y, Yao X, Wang H, et al. CaMKK2 suppresses muscle regeneration through the inhibition of myoblast proliferation and differentiation. *Int J Mol Sci* (2016) 17(10):1695. doi: 10.3390/ijms17101695

22. Matsushita M, Nairn AC. Characterization of the mechanism of regulation of Ca2+/ calmodulin-dependent protein kinase I by calmodulin and by Ca2+/calmodulin-dependent protein kinase kinase. *J Biol Chem* (1998) 273(34):21473–81. doi: 10.1074/jbc.273.34.21473

23. Marcelo KL, Means AR, York B. The ca(2+)/calmodulin/caMKK2 axis: nature's metabolic camshaft. *Trends Endocrinol metabolism: TEM* (2016) 27(10):706–18. doi: 10.1016/j.tem.2016.06.001

24. Pollard AE, Martins L, Muckett PJ, Khadayate S, Bornot A, Clausen M, et al. AMPK activation protects against diet induced obesity through Ucp1-independent thermogenesis in subcutaneous white adipose tissue. *Nat Metab* (2019) 1(3):340–9. doi: 10.1038/s42255-019-0036-9

25. Olza J, Gil-Campos M, Leis R, Rupérez AI, Tojo R, Cañete R, et al. Influence of variants in the NPY gene on obesity and metabolic syndrome features in Spanish children. *Peptides* (2013) 45:22–7. doi: 10.1016/j.peptides.2013.04.007

26. Cresswell KS, Clarke CJ, Jackson JT, Darcy PK, Trapani JA, Johnstone RW. Biochemical and growth regulatory activities of the HIN-200 family member and putative tumor suppressor protein, AIM2. *Biochem Biophys Res Commun* (2005) 326(2):417–24. doi: 10.1016/j.bbrc.2004.11.048

27. Hornung V, Ablasser A, Charrel-Dennis M, Bauernfeind F, Horvath G, Caffrey DR, et al. AIM2 recognizes cytosolic dsDNA and forms a caspase-1-activating inflammasome with ASC. *Nature* (2009) 458(7237):514–8. doi: 10.1038/nature07725

28. Roberts TL, Idris A, Dunn JA, Kelly GM, Burnton CM, Hodgson S, et al. HIN-200 proteins regulate caspase activation in response to foreign cytoplasmic DNA. *Science* (2009) 323(5917):1057–60. doi: 10.1126/science.1169841

frontiers | Frontiers in Endocrinology

TYPE Original Research
PUBLISHED 11 March 2024
DOI 10.3389/fendo.2024.1355703

OPEN ACCESS

EDITED BY
Kaixiong Tao,
Huazhong University of Science and Technology, China

REVIEWED BY
Ying Qing,
City of Hope, United States
Yanmin Wang,
California Medical Innovations Institute, United States

*CORRESPONDENCE
Shaozhuang Liu
liushaozhuang@sdu.edu.cn
Xin Huang
huangxinsdu@163.com

†These authors have contributed equally to this work and share first authorship

RECEIVED 14 December 2023
ACCEPTED 22 February 2024
PUBLISHED 11 March 2024

CITATION
Zhao Y, Xiong S, Liu T, Shu J, Zhu T, Li S, Zhong M, Zhao S, Huang X and Liu S (2024) Total weight loss rather than preoperative body mass index correlates with remission of irregular menstruation after sleeve gastrectomy in patients with polycystic ovary syndrome.
Front. Endocrinol. 15:1355703.
doi: 10.3389/fendo.2024.1355703

Total weight loss rather than preoperative body mass index correlates with remission of irregular menstruation after sleeve gastrectomy in patients with polycystic ovary syndrome

Yian Zhao[1†], Sisi Xiong[1†], Teng Liu[1], Jiaxin Shu[1], Tao Zhu[1], Shumin Li[2], Mingwei Zhong[3], Shigang Zhao[4], Xin Huang[1*] and Shaozhuang Liu[1*]

[1]Division of Bariatric and Metabolic Surgery, Department of General Surgery, Qilu Hospital of Shandong University, Jinan, China, [2]Center for Reproductive Medicine, Renji Hospital, School of Medicine, Shanghai Jiao Tong University, Shanghai, China, [3]Division of Bariatric and Metabolic Surgery, Department of General Surgery, the First Affiliated Hospital of Shandong First Medical University, Jinan, China, [4]Center for Reproductive Medicine, Cheeloo College of Medicine, Shandong University, Jinan, China

Introduction: Polycystic ovary syndrome (PCOS) is the most common endocrinopathy affecting reproductive-aged women. Some retrospective studies with small sample sizes have reported that bariatric metabolic surgery is effective in remission of irregular menstruation in patients with PCOS and obesity. However, the correlation between preoperative body mass index (BMI), postoperative weight loss, and remission of irregular menstruation in patients with obesity and PCOS after sleeve gastrectomy (SG) is lack of consensus.

Methods: We enrolled 229 participants with obesity and PCOS who underwent SG. All patients were followed up for one year after surgery. Remission of irregular menstruation was defined as a spontaneous consecutive six-month menstrual cycle in one year. Subgroup analysis was conducted using tertiles of preoperative BMI and postoperative total weight loss (TWL)% to determine their correlation with the remission of irregular menstruation after SG.

Results: 79.03% (181/229) patients achieved remission of irregular menstruation one year after SG with a TWL% of 33.25 ± 0.46%. No significant difference was detected in the remission rate among the subgroups with different BMI (P=0.908). TWL% was correlated with the remission of irregular menstruation (OR 1.78, 95% CI 1.18-2.69, P<0.05).

Conclusions: SG had a significant effect on the remission of irregular menstruation in patients with obesity and PCOS. Preoperative BMI did not emerge as a decisive factor correlated with remission; instead, TWL% showed potential as a key factor.

KEYWORDS

obesity, total weight loss, polycystic ovary syndrome, sleeve gastrectomy, irregular menstruation

1 Introduction

Polycystic ovary syndrome (PCOS) is the most common endocrinopathy affecting reproductive-aged women with a 10%-13% prevalence (1), accounting for nearly 80% of infertility cases (2). The clinical presentation of PCOS is complex, with reproductive, metabolic, and psychological features that impact across the lifespan (3). Among the typical characteristics of PCOS, irregular menstruation is a key concern for patients because of infertility and an increased risk of endometrial cancer. PCOS is strongly associated with obesity and other metabolic disorders. More than 60% of women with PCOS are estimated to be overweight or obese (4). Obesity further amplifies and worsens all the metabolic and reproductive outcomes of PCOS (5).

Weight management is recommended as the mainstay treatment for PCOS (1), and symptoms commonly improve with 5%-10% weight loss (6). However, when combined with morbid obesity, the required 25%-50% weight loss is difficult to achieve, depending on lifestyle or medical treatment (7). In addition, patients with PCOS and obesity tend to respond poorly to pharmacological treatments for ovarian stimulation and assisted reproductive technology (8). Therefore, the traditional treatment methods for patients with PCOS and morbid obesity have encountered dilemmas.

As the most effective and reliable treatment for morbid obesity, bariatric metabolic surgery (BMS) also results in greater improvement in obesity-related comorbidities, including type 2 diabetes, hypertension, dyslipidemia, sleep apnea, and osteoarthritis, than non-surgical treatment (9). Sleeve gastrectomy (SG) is the most common bariatric metabolic procedure, accounting for more than 60% of both total and primary procedures globally (10). Previous studies with small sample sizes reported that BMS was effective for PCOS in terms of improving ovulatory dysfunction, hyperandrogenism, and infertility (11–13). However, BMS is still conditionally recommended for patients with PCOS and obesity in the 2023 International Assessment and Management of PCOS owing to the absence of high-level evidence (1). Moreover, although a correlation between PCOS and obesity has been confirmed, there is no consensus on whether the degree of preoperative obesity influences PCOS improvement after BMS. Further research is required to elucidate the effect of postoperative weight loss on the prognosis of postoperative PCOS.

To confirm the efficacy of SG in patients with PCOS and obesity, we conducted a prospective multi-center cohort named "Sleeve Gastrectomy for Obese Polycystic Ovary Syndrome" (SGOP). Based on the subdatasets of the SGOP cohort, the current study aimed to investigate the correlation of preoperative BMI and postoperative weight loss with remission of irregular menstruation after SG.

2 Materials and methods

2.1 Study design and patients

Beginning in January 2020, patients in the SGOP cohort were prospectively recruited at Qilu Hospital of Shandong University (Center A) in Jinan, Shandong province and First Affiliated Hospital of Shandong First Medical University (Center B) in Jinan, Shandong province. Among the SGOP serial studies, the SGOP-01 study aimed to compare the efficacy of SG with that of drug therapy, and was registered in the Chinese Clinical Trial Registry with the identification number ChiCTR1900026845.

A subset of patients from the SGOP-01 study was recruited for the current study. The current study was approved by the Medical Ethics Committee of Qilu Hospital of Shandong University. The inclusion criteria of this study were as follows: (1) BMI≥32.5 kg/m^2 or BMI≥27.5kg/m^2 combined with diabetes or two components of metabolic syndrome, (2) aged 18–42 years, and (3) PCOS with irregular menstruation. PCOS was diagnosed based on the 2003 Rotterdam criteria (14). Patients who received pharmacological treatment for PCOS, had previously undergone BMS, had incomplete preoperative data, or had poorly controlled psychological disorders were excluded.

All patients were followed up for at least one year after SG. Remission of irregular menstruation was defined as a spontaneous consecutive six-month menstrual cycle (21-35 days) in one year after SG.

2.2 Procedure and follow-up

All SG procedures at each center were performed by the same experienced bariatric and metabolic teams. The surgical process was consistent with that previously described (15). All sleeve gastrectomy at each center was performed laparoscopically by the same experienced bariatric and metabolic teams. Briefly, the greater curvature was dissected free from the momentum starting 2–4 cm from the pylorus and up to the angle of His, with a tubular sleeve created using a 36-Fr bougie. All the patients received suggestions for postoperative diet and exercise. Weight reduction and menstrual status were recorded each month after SG. The total weight loss (TWL)% was calculated to evaluate weight loss.

2.3 Biochemical analysis

Sex hormone, thyroid function, blood lipid analysis, and fasting plasma glucose (FPG) levels were measured using a Roche Cobas 8000 modular analyzer system (Roche Diagnostics, IN, USA). Plasma insulin and C-peptide levels were determined using a two-site enzymatic assay with a Tosoh 2000 Autoanalyzer (Tosoh Corp., Tokyo, Japan). Homeostatic model assessment of insulin resistance (HOMA-IR) was performed as follows: fasting insulin (mU/mL) × FPG (mmol/L)/22.5 (16).

2.4 Oral glucose tolerance test

After fasting overnight, the participants underwent a 2-h oral glucose tolerance test (OGTT) (75 g of glucose in 250 mL of water). Blood samples were collected in chilled EDTA tubes at 0, 30, 60, and

120 min after glucose intake. The areas under the curve (AUC) of glucose and insulin levels during the OGTT were calculated using the trapezoidal method.

2.5 Body composition via dual-energy X-ray absorptiometry

Body composition was determined via DEXA using the HOLOGIC DELPHI system with QDR software, v.11.1 (Hologic, Bedford, MA, USA). Four trained and certified personnel performed whole-body scans. Body fat ratio was calculated as fat volume/body volume, and body lean percentage was calculated as lean mass/body mass.

2.6 Statistical analysis

Statistical analyses were performed using IBM SPSS Statistics Version 25.0 for Windows (SPSS Inc, Chicago, IL, USA). Continuous variables are presented as the mean ± SEM, or as the median with the interquartile range. One-way analysis of variance (ANOVA), the Kruskal Wallis H test, t-test and the Mann-Whitney U test were used to compare continuous variables and differences in mean values. The chi-square test was used to compare differences in menstrual outcomes among the groups. The TWL% changes over time among groups were analyzed using two-way ANOVA, followed by the Bonferroni *post hoc* test, and the results were reported as ^{A}P by group, ^{B}P over time, and ^{C}P due to the interaction of the two factors. Univariate logistic regression analysis was performed to assess the correlation between TWL% and remission of irregular menstruation. In all analyses, $P<0.05$ was considered statistically significant.

3 Results

3.1 Participants

Between January 8, 2020, and July 1, 2022, a total of 229 patients (mean [SEM] age, 28.68 [0.35] years; mean [SEM] BMI, 40.91 [0.44] kg/m^2) with oligo-/anovulatory PCOS and obesity underwent SG in centers A and B (Figure 1). All patients completed at least one-year follow-up.

3.2 Participants' baseline characteristics

All participants were divided according to tertiles of baseline BMI (group A, ≤37.65 kg/m^2; group B, >37.66, ≤42.98 kg/m^2; group C, >42.99 kg/m^2), and participants' characteristics are shown in Table 1. The waist-hip ratio (WHR), body fat ratio, and body lean percentage were significantly different among groups A, B, and C ($P<0.05$). No significant differences were detected among the three groups with respect to glycolipid metabolism, thyroid function, or sex hormone levels, except anti-mullerian hormone (AMH) ($P<0.01$). As BMI increased, AMH levels decreased, and there was a significant difference between groups A and C ($P<0.01$).

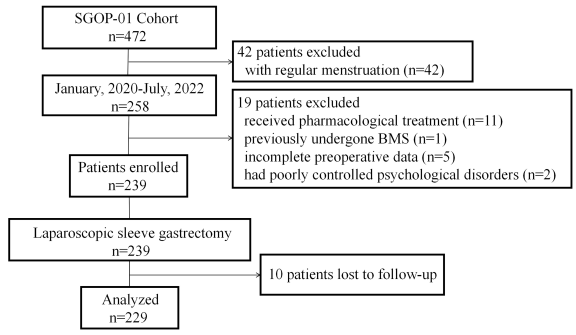

FIGURE 1
Flowchart of study participants.

3.3 Weight loss effect after SG

The mean (± SEM) TWL% at 1, 3, 6, and 12 months after SG were 12.27 ± 0.21%, 21.90 ± 0.33%, 29.46 ± 0.40%, and 33.25 ± 0.46%, respectively. Overall, TWL% showed an upward trend within 1 year after SG. There were no significant differences among the three groups at 1,3,6, and 12 months after SG (Figure 2). The results indicated that the preoperative BMI did not correlate with postoperative weight loss effect.

3.4 Remission of irregular menstruation after SG

After SG, 79.03% (181/229) and 20.97% (48/229) of the patients did and did not achieve remission of irregular menstruation in the one-year follow-up, respectively (Figure 3). It follows that SG achieved significant remission of irregular menstruation in patients with oligo-/anovulatory PCOS. Patients who achieved remission seven months after SG initiated menstruation within the first month after surgery. Regular menstrual cycles were initiated within the first and third months in 31.0% (71/229) and 60.7% (139/229) of patients, respectively. Interestingly, the patients who did not initiate regular menstruation within six months after SG continued to face this challenge for up to one year after SG. Therefore, the effect of SG on menstrual remission can be observed in the early postoperative period, and most patients with oligo-/anovulatory PCOS are sensitive to SG.

3.5 Correlation between preoperative BMI and remission of irregular menstruation after SG

The remission rates of irregular menstruation in groups A, B, and C were 80.52%, 77.63%, and 78.95%, respectively. No significant

10.3389/fendo.2024.1355703

TABLE 1 Baseline characteristic of participants with obesity and oligo-/anovulatory polycystic ovary syndrome.

Variables	Total Participants (n=229)	Group A (n=77) BMI ≤ 37.65 kg/m^2	Group B (n=76) BMI ≥ 37.66, ≤ 42.98 kg/m^2	Group C (n=76) BMI ≥ 42.99 kg/m^2	*P* Value
Age, years	28.68 ± 0.35	28.88 ± 0.54	28.46 ± 0.67	28.70 ± 0.63	0.89
BMI, kg/m^2	40.31(35.96, 44.64)	35.05(32.99, 35.96)	40.32(39.05, 41.74)**	46.40(44.86, 50.78)$^{\#\#, \&\&}$	<0.01
WHR	0.94 ± 0.01	0.93 ± 0.01	0.94 ± 0.01	0.96 ± 0.01$^{\#}$	0.04
Body fat ratio, %	43.75 ± 0.31	41.54 ± 0.44	43.95 ± 0.54**	45.78 ± 0.50$^{\#\#, \&}$	<0.01
Body lean percentage, %	51.71 ± 0.33	54.66 ± 0.36	51.81 ± 0.60**	48.64 ± 0.50$^{\#\#, \&\&}$	<0.01
Testosterone, nmol/L	1.76 ± 0.05	1.74 ± 0.09	1.83 ± 0.09	1.69 ± 0.09	0.56
Estradiol, pmol/L	140.00(62.48, 195.10)	123.40(59.34, 174.44)	134.05(62.18, 213.30)	145.60(80.51, 193.35)	0.56
Progesterone, nmol/L	0.42(0.16, 0.77)	0.50(0.19, 1.03)	0.42(0.16, 0.78)	0.38(0.16, 0.70)	0.30
Prolactin, uIU/ml	283.90 (213.40, 411.70)	283.90(200.13, 391.35)	265.45(227.51, 457.28)	288.15(203.80, 408.20)	0.53
AMH, ng/ml	4.91 ± 0.19	5.67 ± 0.36	4.97 ± 0.34	4.07 ± 0.25$^{\#\#}$	<0.01
LH, mIU/ml	8.38 ± 0.31	8.58 ± 0.61	8.30 ± 0.56	8.25 ± 0.44	0.90
FSH, mIU/ml	5.08 ± 0.11	4.99 ± 0.19	4.91 ± 0.19	5.34 ± 0.17	0.22
LH/FSH	1.70 ± 0.06	1.81 ± 0.13	1.72 ± 0.10	1.59 ± 0.08	0.38
FT3, pmol/L	5.07 ± 0.07	5.09 ± 0.16	5.09 ± 0.08	5.04 ± 0.09	0.94
FT4, pmol/L	15.26 ± 0.19	15.58 ± 0.40	14.87 ± 0.28	15.32 ± 0.32	0.32
TSH, uIU/ml	2.99 ± 0.44	2.47 ± 0.19	2.68 ± 0.18	3.83 ± 1.29	0.40
FPG, mmol/L	6.43 ± 0.20	6.36 ± 0.36	6.26 ± 0.35	6.66 ± 0.33	0.69
Fasting C-peptide, ng/ml	3.60 ± 0.14	3.45 ± 0.23	3.60 ± 0.28	3.75 ± 0.21	0.69
Fasting insulin, uIU/ml	33.99 ± 2.22	32.84 ± 3.08	38.14 ± 5.46	31.02 ± 2.31	0.40
$HbA1_{c,}$ %	6.49 ± 0.10	6.41 ± 0.20	6.34 ± 0.17	6.73 ± 0.16	0.25
HOMA-IR	6.87(4.63, 11.46)	6.91(4.13, 11.03)	6.70(4.36, 10.62)	7.37(5.34, 11.85)	0.32
$AUC_{glucose}$	21.28 ± 0.55	20.97 ± 0.93	20.88 ± 1.01	22.00 ± 0.90	0.66
$AUC_{insulin}$	231.14 ± 8.13	235.51 ± 15.36	246.02 ± 12.54	211.83 ± 14.07	0.22
Triglyceride, mmol/L	1.59(1.23, 2.33)	1.80(1.31, 2.85)	1.56(1.27, 2.24)	1.53(1.05, 2.00)	0.08
Total cholesterol, mmol/L	4.80 ± 0.06	4.80 ± 0.11	4.73 ± 0.09	4.87 ± 0.11	0.63
HDL-C, mmol/L	1.05(0.94, 1.16)	1.03(0.91, 1.14)	1.05(0.95, 1.17)	1.06(0.95, 1.17)	0.87
Non-HDL-C, mmol/L	3.64(3.16, 4.22)	3.72(3.16, 4.29)	3.59(3.25, 4.01)	3.66(3.13, 4.44)	0.84
NEFA, umol/dL	68.71 ± 1.35	65.10 ± 2.65	68.73 ± 1.88	72.34 ± 2.39	0.09

Data are presented as mean ± SE, or median (25th percentile, 75th percentile). *P < 0.05, **P < 0.01 Group A vs. Group B;#P < 0.05, ##P < 0.01 Group A vs. Group C;&P < 0.05, &&P < 0.01 Group B vs. Group C.

WHR, waist hip ratio; AMH, anti-mullerian hormone; LH, luteinizing hormone; FSH, follicle-stimulating hormone; FT3, free triiodothyronine; FT4, free thyroxine; TSH, thyroid stimulating hormone; FPG, fasting plasma glucose; HbA1c, glycated hemoglobin; HOMA-IR, homeostatic model assessment of insulin resistance; AUC, area under the curve; HDL-C, high density lipoprotein-cholesterol; NEFA, nonesterified fatty acid.

difference was detected among groups A, B, and C with respect to the remission rate (Figure 4A). Furthermore, there was no significant difference between patients with remission and without remission with respect to preoperative BMI (Figure 5A). Thus, there was no correlation between preoperative BMI and postoperative remission of irregular menstruation in patients with PCOS and obesity.

3.6 Correlation between TWL% and remission of irregular menstruation after SG

To further investigate the correlation between weight loss effect and remission of irregular menstruation, all participants were

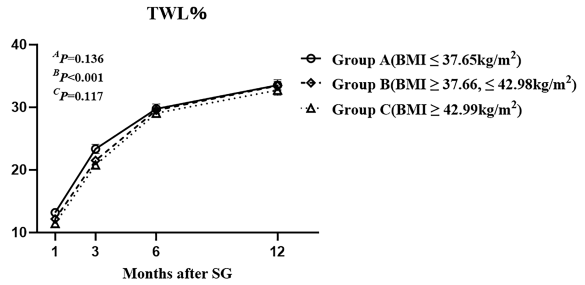

FIGURE 2
The total weight loss percentage of the three groups with different class of preoperative body mass index up to one year after sleeve gastrectomy. Total weight loss percentage was defined as weight loss/baseline weight *100%. ^{A}P by group, ^{B} P over time, and ^{C}P due to the interaction of the two factors.

divided according to tertiles of TWL% at one year after SG (group D, ≤30.27%; group E >30.28%, ≤35.71%; group F >35.72%). The chi-square test results showed that there was a significant difference among groups D, E, and F with respect to remission rate (P<0.05) (Figure 4B). The result of univariate logistic regression analysis confirmed that TWL% at one year after SG [odds ratio (OR) 1.78, 95% confidence interval (CI) 1.18-2.69, P < 0.05] was a potential key factor that impacted remission of irregular menstruation after SG. And patients with remission of irregular menstruation had a higher TWL% at one year after SG compared to patients without remission (P<0.05) (Figure 5B).

4 Discussion

The principal finding of the current study is that SG is effective in the treatment of PCOS with a 79.03% remission of irregular menstruation one year after surgery. Furthermore, TWL%, rather than preoperative BMI, correlated with the remission after SG.

Irregular menstruation is a key concern in patients with PCOS even beyond infertility partially because of the increased risk of endometrial cancer (17). This study showed that 79.03% (181/229) of the patients achieved remission of irregular menstruation after SG, which is similar to that of a previous Chinese single-center study (78% remission rate) and higher than that of a study from Iran (66% remission rate) (18, 19). Another Chinese study by Meili Cai et al. (20) reported that 78.56% of patients achieved remission of irregular menstruation within six months after SG. The definition of remission in the study above required a consecutive three-month menstrual cycle (20). Limited by small sample sizes and inconsistency of remission standard of aforementioned studies, although the efficacy of BMS in the treatment of PCOS has been elucidated, it is underemphasized in present PCOS treatment guidelines. Our study, based on a prospective PCOS cohort with largest sample size, further confirmed that SG is effective in the treatment of irregular menstruation in Chinese patients with PCOS.

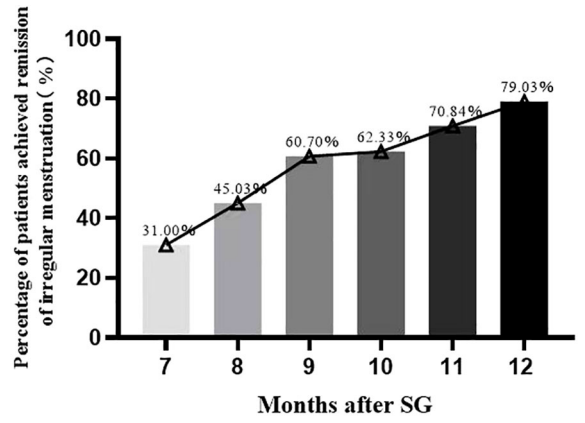

FIGURE 3
The percentage of patients achieved remission of irregular menstruation after sleeve gastrectomy.

Considering that patients with PCOS and obesity have a more severe phenotype than those with PCOS and normal weight, including more severe menstrual irregularities and infertility (7, 21), it is reasonable to hypothesize that differences exist in menstrual remission after SG among patients with different preoperative body mass index (BMI) classes. To investigate this issue, we divided patients the into three groups (A, B, and C) according to tertiles of preoperative BMI. Surprisingly, our results indicated that no significant differences were detected among the three groups with respect to the remission rate. Obesity is the most common cause of insulin resistance and compensatory hyperinsulinemia, which are the primary pathological features of PCOS. Previous studies have demonstrated that insulin resistance plays a role in determining the degree of menstrual irregularity in patients with PCOS (22, 23). However, in the current study, for PCOS patients with an average BMI of 40.91 kg/m^2, no significant differences were observed in HOMA-IR and $AUC_{insulin}$ of OGTT values among the different BMI groups; therefore, it is reasonable for these patients to have a similar response to SG in the remission of irregular menstruation. This result further confirms that although obesity plays an important role in the occurrence and development of PCOS, the degree of obesity is not a key factor determining postoperative menstrual outcomes in patients undergoing SG.

Effective and sustained weight loss is the most fundamental change after SG. The follow-up results of this study also showed that patients with PCOS and obesity achieved an average TWL% of 33.25 ± 0.46% (with the range of 16.91% to 58.95%) 1 year after SG. This result was similar to that of a Chinese study (n=41) focusing on patients with PCOS and obesity, with an approximate TWL% of 33.38% (18). Furthermore, our study showed that the greater the TWL% achieved one year after SG, the greater the likelihood of remission of irregular menstruation. Hu et al. (18) concluded that endpoint BMI, rather than baseline BMI, is associated with the remission of irregular menstruation after SG. However, for patients with PCOS and obesity with an average BMI of 40.91 kg/m^2 and a maximum BMI of 73.35kg/m^2, it is unrealistic to simply pursue endpoint BMI without considering the difficulty of weight loss caused by baseline BMI. In our opinion, TWL%, which could reflect the magnitude of weight loss and concomitant metabolic changes,

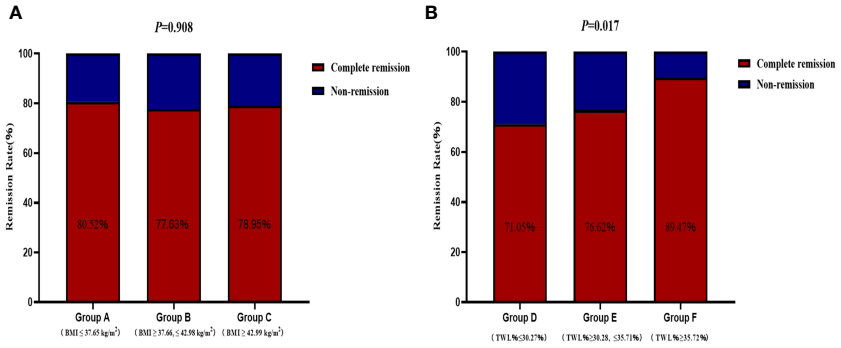

FIGURE 4
The correlations between remission of irregular menstruation and preoperative body mass index **(A)** and total weight lossp ercentage **(B)** at one year after sleeve gastrectomy.

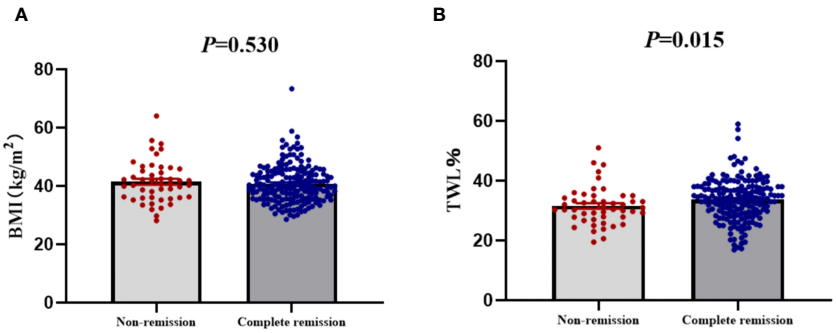

FIGURE 5
The compare of preoperative body mass index **(A)** and total weight loss percentage **(B)** between patients with complete remission and non-remission of irregular menstruation one year after sleeve gastrectomy.

should be a better index for predicting remission of irregular menstruation after SG than the endpoint BMI.

BMS is superior to drug therapy for reducing hyperinsulinemia, and improving insulin sensitivity (24), both of which are optimal for treating PCOS. Improvement in insulin resistance, reduction of inflammatory markers, and loss of abdominal fat caused by sufficient weight loss can disrupt the vicious feedback cycle among obesity, inflammatory adipokines, and hyperinsulinemia, thereby improving menstrual irregularity (25–28). However, it is noteworthy that 60.7% of patients initiated regular menstruation within the third month after SG without sufficient weight loss, indicating the existence of a weight loss-independent effect of SG, which was similar to the mechanisms of diabetes remission after BMS.

To our knowledge, our study elucidated the correlation of postoperative menstrual remission with TWL% and preoperative BMI in patients with PCOS and obesity based on a multi-center cohort with the largest sample sizes. However, the participants were divided into groups based on tertiles of preoperative BMI and TWL% rather than international or Asian standards, which may limit the generalizability of the study results. Furthermore, a longer follow-up period is required to evaluate long-term effects and pregnancy outcomes.

The present study further confirmed that SG has a significant effect on menstruation remission in patients with obesity and PCOS. Preoperative BMI was not a decisive factor that correlated with remission; instead, TWL% emerged as a potential key factor.

Data availability statement

The original contributions presented in the study are included in the article/supplementary material, further inquiries can be directed to the corresponding authors.

Ethics statement

The studies involving humans were approved by the Medical Ethics Committee of Qilu Hospital of Shandong University. The studies were conducted in accordance with the local legislation and institutional requirements. The participants provided their written informed consent to participate in this study.

Author contributions

YZ: Data curation, Formal analysis, Investigation, Methodology, Project administration, Software, Writing – original draft, Validation. SX: Data curation, Formal analysis, Writing – original draft. TL: Formal analysis, Writing – original draft, Methodology, Project administration, Software, Validation. JS: Formal analysis, Investigation, Methodology, Writing – original draft. TZ: Data curation, Methodology, Writing – original draft. SML: Supervision, Writing – review & editing. MZ: Supervision, Writing – review & editing. SZ: Conceptualization, Supervision, Writing – review & editing. XH: Writing – review & editing, Funding acquisition, Project administration, Validation. SZL: Writing – review & editing, Conceptualization, Funding acquisition, Project administration, Resources, Supervision, Validation, Visualization.

Funding

The author(s) declare financial support was received for the research, authorship, and/or publication of this article. This study was funded by grants from the National Natural Science Foundation of China (82100853), the Natural Science Foundation of Shandong Province of China (ZR2019MH013, ZR2021QH028), the Clinical Research Project of Shandong University (2020SDUCRCC024), and the Bethune Charitable Foundation (HZB-20190528-9).

Acknowledgments

The authors thank the nursing staff of the Department of General Surgery, Qilu Hospital of Shandong University and First Affiliated Hospital of Shandong First Medical University, for their expert assistance in performing the study, and all the patients included and their families for their cooperation.

Conflict of interest

The authors declare that the research was conducted in the absence of any commercial or financial relationships that could be construed as a potential conflict of interest.

Publisher's note

References

1. Teede HJ, Tay CT, Laven J, Dokras A, Moran LJ, Piltonen TT, et al. Recommendations from the 2023 international evidence-based guideline for the assessment and management of polycystic ovary syndrome†. *Hum Reprod.* (2023) 38:1655–79. doi: 10.1210/clinem/dgad463

2. Zhang J, Bao Y, Zhou X, Zheng L. Polycystic ovary syndrome and mitochondrial dysfunction. *Reprod Biol Endocrinol.* (2019) 17:67. doi: 10.1186/s12958-019-0509-4

3. Joham AE, Norman RJ, Stener-Victorin E, Legro RS, Franks S, Moran LJ, et al. Polycystic ovary syndrome. *Lancet Diabetes Endocrinol.* (2022) 10:668–80. doi: 10.1016/S2213-8587(22)00163-2

4. Teede HJ, Tay CT, Joham AE. Polycystic ovary syndrome: an intrinsic risk factor for diabetes compounded by obesity. *Fertil Steril.* (2021) 115:1449–50. doi: 10.1016/j.fertnstert.2021.03.024

5. Legro RS. Obesity and PCOS: implications for diagnosis and treatment. *Semin Reprod Med.* (2012) 30:496–506. doi: 10.1055/s-00000072

6. Teede H, Deeks A, Moran L. Polycystic ovary syndrome: a complex condition with psychological, reproductive and metabolic manifestations that impacts on health across the lifespan. *BMC Med.* (2010) 8:41. doi: 10.1186/1741-7015-8-41

7. Glueck CJ, Goldenberg N. Characteristics of obesity in polycystic ovary syndrome: Etiology, treatment, and genetics. *Metabolism.* (2019) 92:108–20. doi: 10.1016/j.metabol.2018.11.002

8. Balen AH, Morley LC, Misso M, Franks S, Legro RS, Wijeyaratne CN, et al. The management of anovulatory infertility in women with polycystic ovary syndrome: an analysis of the evidence to support the development of global WHO guidance. *Hum Reprod Update.* (2016) 22:687–708. doi: 10.1093/humupd/dmw025

9. Arterburn DE, Telem DA, Kushner RF, Courcoulas AP. Benefits and risks of bariatric surgery in adults: A review. *JAMA.* (2020) 324:879–87. doi: 10.1001/jama.2020.12567

10. IFSO. 7th IFSO Global Registry Report. Available online at: https://www.ifso.com/pdf/ifso-7th-registry-report-2022.

11. Yue W, Huang X, Zhang W, Li S, Liu X, Zhao Y, et al. Metabolic surgery on patients with polycystic ovary syndrome: A systematic review and meta-analysis. *Front Endocrinol (Lausanne).* (2022) 13:848947. doi: 10.3389/fendo.2022.848947

12. Luo P, Su Z, Li P, Wang G, Li W, Sun X, et al. Effects of sleeve gastrectomy on patients with obesity and polycystic ovary syndrome: a meta-analysis. *Obes Surg.* (2023) 33:2335–41. doi: 10.1007/s11695-023-06617-z

13. Tian Z, Zhang YC, Wang Y, Chang XH, Zhu HL, Zhao Y. Effects of bariatric surgery on patients with obesity and polycystic ovary syndrome: a meta-analysis. *Surg Obes Relat Dis.* (2021) 17:1399–408. doi: 10.1016/j.soard.2021.04.009

14. Rotterdam ESHRE/ASRM-Sponsored PCOS consensus workshop group. Revised 2003 consensus on diagnostic criteria and long-term health risks related to polycystic ovary syndrome (PCOS). *Hum Reprod.* (2004) 19:41–7. doi: 10.1093/humrep/deh098

15. Huang X, Zhao Y, Liu T, Wu D, Shu J, Yue W, et al. β-cell function and insulin dynamics in obese patients with and without diabetes after sleeve gastrectomy. *Diabetes.* (2023), db221048. doi: 10.2337/figshare.23152325.v1

16. Matthews DR, Hosker JP, Rudenski AS, Naylor BA, Treacher DF, Turner RC. Homeostasis model assessment: insulin resistance and beta-cell function from fasting plasma glucose and insulin concentrations in man. *Diabetologia.* (1985) 28:412–9. doi: 10.1007/BF00280883

17. Gibson-Helm M, Teede H, Dunaif A, Dokras A. Delayed diagnosis and a lack of information associated with dissatisfaction in women with polycystic ovary syndrome. *J Clin Endocrinol Metab.* (2017) 102:604–12. doi: 10.1210/jc.2016-2963

18. Hu L, Ma L, Xia X, Ying T, Zhou M, Zou S, et al. Efficacy of bariatric surgery in the treatment of women with obesity and polycystic ovary syndrome. *J Clin Endocrinol Metab.* (2022) 107:e3217–29. doi: 10.1210/clinem/dgac294

19. Alamdari NM, Sadegh GHM, Farsi Y, Besharat S, Hajimirzaie SH, Abbasi M. The impact of sleeve gastrectomy on polycystic ovarian syndrome: a single-center 1-year cohort study. *Ir J Med Sci.* (2023). doi: 10.1007/s11845-023-03488-2

20. Cai M, Zhang Y, Gao J, Dilimulati D, Bu L, Cheng X, et al. Predictive factors of menstrual recovery after laparoscopic sleeve gastrectomy in polycystic ovary syndrome women with obesity. *Diabetes Metab Syndr Obes.* (2023) 16:1755–66. doi: 10.2147/DMSO.S411573

21. Glueck CJ, Goldenberg N, Pranikoff J, Khan Z, Padda J, Wang P. Effects of metformin-diet intervention before and throughout pregnancy on obstetric and neonatal outcomes in patients with polycystic ovary syndrome. *Curr Med Res Opin.* (2013) 29:55–62. doi: 10.1185/03007995.2012.755121

22. Niu J, Lu M, Liu B. Association between insulin resistance and abnormal menstrual cycle in Chinese patients with polycystic ovary syndrome. *J Ovarian Res*. (2023) 16:45. doi: 10.1186/s13048-023-01122-4

23. Ezeh U, Ezeh C, Pisarska MD, Azziz R. Menstrual dysfunction in polycystic ovary syndrome: association with dynamic state insulin resistance rather than hyperandrogenism. *Fertil Steril*. (2021) 115:1557–68. doi: 10.1016/j.fertnstert.2020.12.015

24. Schauer PR, Bhatt DL, Kirwan JP, Wolski K, Brethauer SA, Navaneethan SD, et al. Bariatric surgery versus intensive medical therapy for diabetes–3-year outcomes. *N Engl J Med*. (2014) 370:2002–13. doi: 10.1056/NEJMoa1401329

25. Holte J, Bergh T, Berne C, Wide L, Lithell H. Restored insulin sensitivity but persistently increased early insulin secretion after weight loss in obese women with polycystic ovary syndrome. *J Clin Endocrinol Metab*. (1995) 80:2586–93. doi: 10.1210/jcem.80.9.7673399

26. Huber-Buchholz MM, Carey DG, Norman RJ. Restoration of reproductive potential by lifestyle modification in obese polycystic ovary syndrome: role of insulin sensitivity and luteinizing hormone. *J Clin Endocrinol Metab*. (1999) 84:1470–4. doi: 10.1210/jc.84.4.1470

27. Escobar-Morreale HF, Botella-Carretero JI, Alvarez-Blasco F, Sancho J, San Millán JL. The polycystic ovary syndrome associated with morbid obesity may resolve after weight loss induced by bariatric surgery. *J Clin Endocrinol Metab*. (2005) 90:6364–9. doi: 10.1210/jc.2005-1490

28. Abiad F, Khalife D, Safadi B, Alami R, Awwad J, Khalifeh F, et al. The effect of bariatric surgery on inflammatory markers in women with polycystic ovarian syndrome. *Diabetes Metab Syndr*. (2018) 12:999–1005. doi: 10.1016/j.dsx.2018.06.013

frontiers | Frontiers in Endocrinology

TYPE Original Research
PUBLISHED 03 April 2024
DOI 10.3389/fendo.2024.1343738

OPEN ACCESS

EDITED BY
Yayun Wang,
Air Force Medical University, China

REVIEWED BY
Jarlei Fiamoncini,
University of São Paulo, Brazil
Lihua Jin,
Beckman Research Institute, City of Hope, United States
Wendong Huang,
Beckman Research Institute, City of Hope, United States
Akira Umemura,
Iwate Medical University, Japan

*CORRESPONDENCE
Hong Chang Tan
gmsthch@nus.edu.sg

†These authors share first authorship

RECEIVED 24 November 2023
ACCEPTED 15 March 2024
PUBLISHED 03 April 2024

CITATION
Tan HC, Hsu JW, Tai ES, Chacko S, Kovalik J-P and Jahoor F (2024) The impact of obesity-associated glycine deficiency on the elimination of endogenous and exogenous metabolites via the glycine conjugation pathway. *Front. Endocrinol.* 15:1343738. doi: 10.3389/fendo.2024.1343738

The impact of obesity-associated glycine deficiency on the elimination of endogenous and exogenous metabolites via the glycine conjugation pathway

Hong Chang Tan[1*†], Jean W. Hsu[2†], E Shyong Tai[3], Shaji Chacko[2], Jean-Paul Kovalik[4] and Farook Jahoor[2]

[1]Department of Endocrinology, Singapore General Hospital, Singapore, Singapore, [2]Children's Nutrition Research Center, Agricultural Research Service, U.S. Department of Agriculture, and Department of Pediatrics, Baylor College of Medicine, Houston, TX, United States, [3]Department of Medicine, Yong Loo Lin School of Medicine, National University Health System, Singapore, Singapore, [4]Cardiovascular and Metabolic Disorders Program, Duke-NUS Medical School, Singapore, Singapore

Background: Glycine is an integral component of the human detoxification system as it reacts with potentially toxic exogenous and endogenously produced compounds and metabolites via the glycine conjugation pathway for urinary excretion. Because individuals with obesity have reduced glycine availability, this detoxification pathway may be compromised. However, it should be restored after bariatric surgery because of increased glycine production.

Objective: To examine the impact of obesity-associated glycine deficiency on the glycine conjugation pathway. We hypothesize that the synthesis rates of acylglycines from endogenous and exogenous sources are significantly reduced in individuals with obesity but increase after bariatric surgery.

Methods: We recruited 21 participants with class III obesity and 21 with healthy weight as controls. At baseline, [1,2-$^{13}C_2$] glycine was infused to study the glycine conjugation pathway by quantifying the synthesis rates of several acylglycines. The same measurements were repeated in participants with obesity six months after bariatric surgery. Data are presented as mean ± standard deviation, and *p*-value< 0.05 is considered statistically significant.

Results: Baseline data of 20 participants with obesity were first compared to controls. Participants with obesity were significantly heavier than controls (mean BMI 40.5 ± 7.1 vs. 20.8 ± 2.1 kg/m^2). They had significantly lower plasma glycine concentration (168 ± 30 vs. 209 ± 50 μmol/L) and slower absolute synthesis rates of acetylglycine, isobutyrylglycine, tigylglycine, isovalerylglycine, and hexanoylglycine. Pre- and post-surgery data were available for 16 participants with obesity. Post-surgery BMI decreased from 40.9 ± 7.3 to 31.6 ± 6.0 kg/m^2. Plasma glycine concentration increased from 164 ± 26 to 212 ± 38 μmol/L) and was associated with significantly higher rates of excretion of acetylglycine, isobutyrylglycine, tigylglycine, isovalerylglycine, and hexanoylglycine. Benzoic acid (a xenobiotic dicarboxylic acid) is excreted as benzoylglycine; its synthesis

rate was significantly slower in participants with obesity but increased after bariatric surgery.

Conclusion: Obesity-associated glycine deficiency impairs the human body's ability to eliminate endogenous and exogenous metabolites/compounds via the glycine conjugation pathway. This impairment is ameliorated when glycine supply is restored after bariatric surgery. These findings imply that dietary glycine supplementation could treat obesity-associated metabolic complications due to the accumulation of intramitochondrial toxic metabolites.

Clinical trial registration: https://clinicaltrials.gov/study/NCT04660513, identifier NCT04660513.

KEYWORDS

glycine deficiency, class III obesity, glycine conjugation, acylglycine, bariatric surgery

1 Introduction

Obesity leads to systemic derangement in the metabolism of various nutrients, including amino acids. In individuals with obesity, plasma concentrations of several amino acids, such as the branched-chain acids (BCAAs), phenylalanine, and tyrosine, are consistently elevated. By contrast, the plasma concentration of glycine is significantly reduced (1–6). Glycine is traditionally categorized as a nutritionally non-essential amino acid, meaning the human body's glycine requirement can be met through food intake plus endogenous synthesis from other precursors. Yet, in obesity, a state of nutrient oversupply, the supply of this amino acid seems to be deficient. The reason for obesity-associated glycine deficiency was previously unknown until we reported that it is due to impaired *de novo* glycine synthesis secondary to insulin resistance (6). Interestingly, *de novo* glycine synthesis rate increased, and glycine deficiency was corrected in individuals with class III obesity following weight loss after bariatric surgery (6).

Glycine is central to human metabolism and is required in large amounts by the human body. Glycine serves as a substrate to support the synthesis of proteins and is the precursor of several critical biomolecules such as purine, creatine, porphyrin, and glutathione. It is also a primary donor of 1-carbon, essential for various methylation, redox, and biosynthetic reactions (7, 8). In addition, glycine is an integral component of the human detoxification system via the glycine conjugation pathway (7–9). The glycine conjugation pathway is a phase II detoxification system in the liver and is catalyzed by the enzyme *glycine N-acyltransferase*. It involves the transfer of acyl groups from acylCoA (from endogenously or exogenously derived organic acids) in the mitochondria to glycine to form their respective acylglyicine conjugates for urinary excretion (7–9).

The importance of glycine conjugation as an alternative route for the elimination of toxic metabolites is exemplified in patients with inborn errors of metabolism (IEM), who accumulate a large amount of intramitochondrial acylCoAs due to defects in fatty acid and/or amino acid oxidation (10). Similarly, in obesity, the accelerated turnover rates of substrates result in an increased influx of substrates into the mitochondria for oxidation and/or clearance. However, mitochondrial capacity may not increase in tandem. When the influx of substrates exceeds mitochondrial oxidative capacity, these intermediates accumulate as intramitochondrial acylCoAs (11, 12), and the glycine conjugation pathway may be activated as an alternative detoxification pathway (7–9). Since glycine availability is rate limiting for the glycine conjugation reaction (9, 13) and glycine is deficient in patients with obesity, the glycine conjugation pathway may be impaired.

2 Aim and hypothesis

Our understanding of the impact of obesity-associated glycine deficiency on the glycine conjugation pathway is limited. Furthermore, it is unclear whether glycine deficiency in individuals with obesity affects the elimination of both endogenous and exogenous metabolites. Our aim in this study is to test the hypothesis that compared to healthy weight individuals, acylglycine synthesis rates are significantly reduced in individuals with class III obesity but will be restored six months after bariatric surgery. Further, obesity-associated glycine deficiency affects the elimination of both endogenous and exogenous metabolites. To achieve our aim, we utilized stable-isotope tracer methods to study the glycine conjugation pathway by quantifying the synthesis and excretion rates of several endogenously and exogenously derived acylglycines in participants with class III obesity and healthy weight. We then repeated the measurements in the same individuals with class III obesity six months after bariatric surgery.

3 Methods

3.1 Subjects

This study was approved by the SingHealth Centralized Institutional Review Board (CIRB Ref: 2018/2714), and all participants provided written informed consent. We recruited 21 participants with class III obesity and 21 with normal weight. Participants with class III obesity were recruited from patients attending the Singapore General Hospital's obesity clinic who were scheduled for bariatric surgery. They were recruited if they were between 21 and 65 years old and had a BMI ≥ 32.5 kg/m^2 with obesity-related complications. They were excluded if they were receiving insulin treatment, consumed excessive alcohol (> 1 drink/day for females or > 2 drinks/day for males), received systemic corticosteroid treatment, or had existing cardiovascular, kidney, or liver disorders. Individuals with a healthy weight (BMI< 25 kg/m^2) were recruited from our healthy volunteer database. These participants were excluded if they had diabetes mellitus or any significant chronic illness.

All eligible participants underwent stable-isotope tracer studies at baseline. Participants with obesity then underwent bariatric surgery and returned six months later for the same stable-isotope studies to measure the post-surgery changes from baseline.

3.2 Stable-isotope infusion

[1,2-$^{13}C_2$] glycine (99 atom% ^{13}C) was used to study the glycine conjugation pathway by quantifying the synthesis rates of several acylglycines. The tracer was purchased as a sterile and pyrogen-free compound (Cambridge Isotope Laboratories, MA) and reconstituted within 24 hours of the intravenous infusion.

Participants were admitted to the SingHealth Investigational Medical Unit one day before the stable-isotope infusion. They were asked to refrain from smoking, drinking coffee and alcohol, and vigorous exercise (more than 1 hour of high-intensity physical activity) during the 24 hours before the study. Dinner was prepared by the hospital's kitchen, with the calories kept similar to their habitual intake. Meal energy composition consisted of 55% from carbohydrates, 33% from fat %, and 15% from protein. Both groups' total daily protein intake, hence dietary glycine, was similar. Subjects also drank 200 mL of zero-calorie soda containing benzoic acid and fasted from 10:00 PM onwards.

After an 8-hour overnight fast, two intravenous cannulas were inserted into opposite arms; one for the infusion of tracers and the other for blood draws. A hand warmer was used to arterialize the venous blood collected. After collecting baseline blood and urine samples for metabolite analysis and background isotopic enrichments (IEs), a primed-constant infusion of [1,2-$^{13}C_2$] glycine (Prime=8 μmol·kgFFM^{-1}, Infusion=8 μmol·kgFFM^{-1}·h^{-1}) was started and maintained for the next 7 hours. Blood samples were collected hourly from the 4th to 6th hour of infusion and every 15 minutes during the last hour. Urine samples were collected at baseline (from 10 PM until the start of the infusion) and at 2, 4, 5, 6, and 7 hours.

3.3 Laboratory analyses

3.3.1 Plasma amino acid and acylcarnitine profiling

Plasma amino acid (AA) concentrations were measured by ultra-high performance liquid chromatography (ACQUITY H-Class System, Waters Corporation, MA, USA) using pre-column derivatization with 6-aminoquinolyl-N-hydroxysuccinimidyl carbamate (Waters AccQ×Tag™ assay kit, MA, USA) and norvaline (Sigma Aldrich, MO, USA) as internal standard. Plasma samples were deproteinized with 10% sulfosalicylic acid dihydrate and derivatized using AccQ-Fluor ™ derivative reagent. The derivatized AAs were separated using gradient-based ACQUITY UPLC BEH C18 column (130 Å, 1.7 μM, 2.1 mm x 150 mm) with ACQUIT UPLC Tunable UV (TUV) detector (6). Total plasma cysteine (cystine plus cysteine) concentration was measured by *in vitro* isotope dilution as described previously (14). A known quantity of U-$^{13}C_3$-cysteine (Cambridge Isotope Laboratories Inc.) was added as an internal standard to the baseline plasma samples; dithiothreitol (60 mmol/L in 0.1 mol sodium tetraborate/L) was added to convert cystine to cysteine Cysteine was then alkylated by adding iodoacetamide (0.5 mol/L) in 0.1 mol ammonium bicarbonate/L. Alkylated cysteine was converted into its DANS [5-(dimethylamino)-1-napthalene sulfonamide] derivative and analyzed by liquid chromatography–mass spectrometry. The ions were then analyzed by SRM mode. The transitions observed were: m/z 412 to 170 & 415 to 170.

Acylcarnitines are formed by the conjugation of acylCoAs with free carnitine in the mitochondria and exported back into the plasma. Therefore, the measurement of acylcarnitines in the plasma pool reflects the intramitochondrial content of their respective acylCoAs. In addition, plasma concentrations of acylcarnitines of different chain lengths correspond to their respective acylCoAs. Short-chain acylcarnitines (C3-C5) are derived from the metabolism of amino acids such as the BCAAs. In contrast, medium-chain acylcarnitines (C6-C12) and long-chain acylcarnitines (C14-C22) reflect oxidation of medium and long-chain fatty acids, respectively. Acetylcarnitine (C2) represents intra-mitochondrial acetylCoA, the final common metabolic product of substrate oxidation.

In this study we measured the plasma concentrations of acetylcarnitine (C2), propionylcarnitine (C3), butyrylcarnitine (C4), and isovalerylcarnitine (C5), octanoylcarnitine (C8), myristoylcarnitine (C14) and palmitoylcarnitine (C16) by *in vivo* isotope dilution using internal standards from labelled carnitine standards set B (NSK-B, Cambridge Isotope Laboratories Inc.) and analyzed by LC tandem MS (TSQ Altis; Thermo Scientific) as previously described (5). The ions were then analyzed by SRM mode, and the transitions observed were: Acetylcarnitine m/z 204 to 85 & 207 to 85; Propionylcarnitine m/z 218 to 85 & 221 to 85; Butyrylcarnitine m/z 232 to 85 & 235 to 85; Isovalerylcarnitine m/z 246 to 85 & 255 to 85; Octanoylcarnitine m/z 288 to 85 & 291 to 85; Myristoylcarnitine m/z 372 to 85 & 381 to 85; Palmitoylcarnitine m/z 400 to 85 & 403 to 85.

3.3.2 Acylglycine profiling

Urine collected from 10:00 PM until the end of the study was pooled and used to measure concentrations of various acylglycines. Acetylglycine is derived from acetylCoA, while isobutyrylglycine, tigylglycine, and isovalerylglycine are formed from glycine conjugation with their BCAA-derived acylCoAs. Hexanoylglycine and octanoylglycine are synthesized from medium-chain fatty acid acylCoA. To estimate the ability of the glycine conjugating pathway to eliminate exogenously derived compounds, we measured bezoylglycine (hippuric acid), which is formed by the conjugation of benzoic acid (consumed from the diet soda of the evening meal) with glycine. The internal standards ($^{2}H_5$-acetylglycine, $^{2}H_2$-isobutyrylglycine, $^{13}C_2$,^{15}N-tigylglycine, $^{13}C_2$,^{15}N- isovalerylglycine, $^{13}C_2$,^{15}N- hexanoylglycine, $^{2}H_2$-octanoylglycine, $^{2}H_2$- bezoylglycine) used were from Cambridge Isotope Laboratories Inc. The urinary acylglycine was butylated according to the method of Hobert et al. (15) & Fisher et al. (16) and analyzed by LC tandem MS (TSQ Altis, Thermo Scientific). The ions were then analyzed by SRM mode. The transitions observed were: Acetylglycine m/z 174 to 76 & 179 to 79; Isobutyrylglycine m/z 202 to 76 & 204 to 78; Tigylglycine m/z 214 to 83 & 217 to 83; Isovalerylglycine m/z 216 to 76 & 219 to 79; Hexanoylglycine m/z 230 to 76 & 233 to 79; Octanoylglycine m/z 258 to 76 & 260 to 78; and Benzoylglycine m/z 236 to 105 & 241 to 110. Urine acylglycine concentrations were corrected for renal function and expressed as mmol/mol creatinine (crt).

3.3.3 Isotopic enrichments

Intracellular glycine isotopic enrichment was measured in red blood cells (RBC) using liquid chromatography-tandem mass spectroscopy (LC-MS/MS). Briefly, RBC free glycine was converted into its DANS [5-(dimethylamino)-1-napthalene sulfonamide] derivative and analyzed using a Kinetex C18 2.6µ 100 × 2.1 mm column (Phenomenex, Torrance, CA) on a triple quadrupole mass spectrometer (TSQ Altis; Thermo Scientific, San Jose, CA). The ions were then analyzed by SRM (selected reaction monitoring) mode. The transitions observed were precursor ions m/z 309, and 311 to product ion m/z 170.

IEs of various acylglycines in urine were measured using liquid chromatography-tandem mass spectroscopy (LC-MS/MS). Acylglycine was butylated and analyzed using an Omega C18 2.6µ 100 × 2.1 mm column (Phenomenex, Torrance, CA) on a triple quadrupole mass spectrometer (TSQ Altis; Thermo Scientific, San Jose, CA). The ions were then analyzed by SRM mode. The transitions observed were: Acetylglycine m/z 174 to 76 & 176 to 78; Isobutyrylglycine m/z 202 to 76 & 204 to 78; Benzoylglycine m/z 236 to 105 & 238 to 105; Tigylglycine m/z 214 to 83 & 216 to 83; Isovalerylglycine m/z 216 to 76 & 218 to 78; and Hexanoylglycine m/z 230 to 76 & 232 to 78; Octanoylglycine m/z 258 to 76 & 260 to 78; and Benzoylglycine m/z 236 to 105 & 238 to 105.

3.3.4 Acylglycine kinetics

The kinetics of octanoylglycine was excluded because its urinary isotopic enrichments were too low to be measured reliably.

The fractional (FRS) and absolute (ASR) synthesis rates of acetylglycine, isobutyrylglycine, tigylglycine, isovalerylglycine, octanoylglycine, hexanoylglycine, and benzoylglycine were estimated according to the precursor-product equations:

$$FSR_{acylglycine}(\%\ pool/d) = \Delta IE_{acylglycine} / IE_{RBC} x\ 24\ (hr)$$

Where $\Delta\ IE_{acylglycine}$ = isotopic enrichment slope of acylglycine (%/h) based on the M+2 enrichment of acyglycine from time 0 to 7 hour. IE_{RBC} = m+2 enrichment of RBC free glycine (used as a proxy for intracellular glycine enrichment) during the final hour of infusion.

The ASR of acylglycines were calculated as described below and expressed as mmol/mol crt/day:

$$ASR_{acylglycine}\ (\text{mmol/mol crt/day}) = FSR_{acylglycine} x\ \text{urine acylglycine concentration}$$

3.4 Statistics

Our previous study indicated that bariatric surgery increases plasma glycine concentration by 26 mmol/L (standard deviation = 26) (6, 17, 18). We hypothesized that this increase will result in a significant improvement in acylglycine synthesis rate, hence, we will need to recruit 21 subjects with class III obesity for a power of more than 80% at a 0.05 significance level. Therefore, 21 normal-weight participants were recruited as controls to compare the differences in acylglycine kinetics at baseline. The distribution of continuous data was first examined, and data with a normal distribution were presented as mean ± standard deviation. Data that did not follow a normal distribution was presented as medians with interquartile range. Statistical differences in metabolic parameters between participants with class III obesity and healthy weight were sought using the unpaired t-test. If the residuals did not follow a normal distribution, the Mann–Whitney U test was used.

Similarly, significant changes in metabolic parameters after bariatric surgery were tested using the paired *t*-test. Wilcoxon's Signed Rank test was used if the residuals did not follow a normal distribution. To examine the relationship between glycine availability and glycine conjugation pathway, linear regression was performed with benzoylglycine ASR as the dependent variable and plasma glycine concentration as the independent variable. P values< 0.05 were considered statistically significant. Statistical testing was performed using STATA version 17 (Stata Corp) and Prism version 9 (GraphPad Software Inc.).

4 Results

4.1 Baseline characteristics, plasma amino acid concentration, and plasma acylcarnitines

One healthy weight control and one participant with obesity were excluded because their urine samples were not collected due to menstruation. Results from 20 participants with healthy weight and 20 participants with obesity (n = 20) with complete data were

analyzed. Participants with healthy weight and obesity were not different in age (40 ± 10 vs. 41 ± 9 years, p = 0.726), and there was an equal number of females (n = 16 in each group). Participants with obesity were significantly heavier than controls, with a body weight of 104.9 ± 15.6 vs. 56.4 ± 8.8 kg, p< 0.0001, and body mass index of 40.5 ± 7.1 vs. 20.8 ± 2.1 kg/m^2, p< 0.0001.

Compared to healthy weight controls, participants with obesity had significantly lower plasma concentrations of glycine and serine (Table 1). By contrast, plasma concentrations of several nutritionally non-essential amino acids (cysteine, tyrosine, alanine, aspartate, and glutamate) and nutritionally essential amino acids (leucine, isoleucine, valine, methionine, phenylalanine, and lysine) were significantly higher in those with obesity (Table 1).

Participants with class III obesity also had significantly higher plasma concentrations of propionylcarnitine (C3), butyrylcarnitine (C4), isovalerylcarnitine (C5), and myristoylcarnitine (C14) compared to healthy weight controls. However, there were no statistically significant differences in the plasma concentrations of acetylcarnitine (C2), octanoylcarnitine (C8), and palmitoylcarnitine (C16) between the two groups (Table 2).

TABLE 1 Plasma amino acid concentration of participants with healthy weight and class III obesity.

(μmol/L)	Healthy weight (n = 20)	Class III Obesity (n = 20)	*P* value
Nutritionally non-essential amino acids			
Glycine	209 ± 50	168 ± 30	0.0034
Serine	122 ± 14	105 ± 18	0.0023
Glutamine	452 ± 74	471 ± 56	0.3546
Total Cysteine	272 ± 39	338 ± 49	<0.0001
Tyrosine	50 ± 10	66 ± 8	<0.0001
Arginine	77 (66-89)	78 (72-97)	0.6017
Proline	131 (103-164)	149 (128-173)	0.2315
Alanine	227 (189-269)	314 (289-341)	<0.0001
Asparagine	35 ± 6	35 ± 6	0.8330
Aspartate	2 ± 1	3 ± 1	0.0030
Glutamate	27 ± 15	54 ± 24	0.0001
Nutritionally essential amino acids			
Leucine	110 ± 17	137 ± 26	0.0004
Isoleucine	52 ± 9.3	68 ± 13	0.0001
Valine	209 ± 34	253 ± 43	0.0008
Methionine	19 (12-22)	21 (20-24)	0.0080
Phenylalanine	56 ± 6	66 ± 8	<0.0001
Threonine	104 ± 25	116 ± 39	0.1733
Lysine	163 ± 32	202 ± 31	0.0004
Histidine	75 ± 9	70 ± 10	0.0642
Tryptophan	39 ± 7	39 ± 6	0.9313

Values are presented as median (inter-quartile range) or mean ± standard deviation. P value< 0.05 is considered as statistically significant.

4.2 Baseline acylglycine concentrations and kinetics

Compared to healthy weight controls, participants with obesity had significantly lower urine concentrations of acetylglycine [0.54 (0.30-0.90) vs. 1.02 (0.55-1.96) mmol/mol crt, p = 0.0143] (Figure 1A), isobutyrylglycine [0.37 (0.30-0.55) vs. 0.73 (0.53-0.89) mmol/mol crt, p = 0.0004] (Figure 1B), tigylglycine [0.57 (0.48-0.71) vs. 1.04 (0.86-1.60) mmol/mol crt, p< 0.0001] (Figure 1C), and isovalerylglycine [0.37 (0.26-0.46) vs. 0.74 (0.46-0.83) mmol/mol crt, p< 0.0001] (Figure 1D). There were no significant between-group differences in the urine concentration of hexanoylglycine [0.32 (0.15-0.26) vs. 0.26 (0.20-0.38) mmol/mol crt, p = 0.1493] (Figure 1E) or octanoylglycine [0.32 (0.15-0.26) vs. 0.26 (0.20-0.38) mmol/mol crt, p = 0.0821] (Figure 1F). Interestingly, the FSR and ASR of acetylglycine, isobutyrylglycine, tigylglycine, isovalerylglycine, and hexanoylglycine were also significantly slower in participants with obesity than healthy weight controls (Table 3).

4.3 Post-surgery changes in clinical parameters, plasma amino acids, and plasma acylcarnitines

Four participants with obesity were lost to follow-up, and the baseline sample for one individual was not available. Hence, paired results (before and after bariatric surgery) of 16 participants with obesity were analyzed. These participants underwent bariatric surgery (14 sleeve gastrectomy and 2 Roux-en-Y gastric bypass) and returned for their follow-up visit at a median of 6.5 (5.9-8.9) months. They experienced significant reductions in body weight from 106.1 ± 16.5 to 82.0 ± 13.7 kg, p< 0.0001, and BMI from 40.9 ± 7.3 to 31.6 ± 6.0 kg/m^2, p< 0.0001. Post-surgery plasma glycine and serine concentrations increased significantly. In contrast, the plasma concentrations of the nutritionally non-essential amino acids, tyrosine, proline, aspartate, and glutamate, and nutritionally essential amino acids, isoleucine, valine, methionine, and phenylalanine decreased significantly (Table 4).

The plasma concentrations of propionylcarnitine, butyrylcarnitine, and isovalerylcarnintine decreased significantly post-surgery, while plasma acetylcarnitine concentration increased significantly. No statistically significant changes in octanoylcarnitine, myristoylcarnintine, and palmitoylcarnitine were observed (Table 5).

10.3389/fendo.2024.1343738

TABLE 2 Plasma acylcarnitine concentration of participants with healthy weight and class III obesity.

(μmol/L)	Healthy weight (n = 20)	Class III Obesity (n = 20)	*P* value
Acetylcarnitine (C2)	13.09 ± 3.63	15.49 ± 6.23	0.1446
Propionylcarnitine (C3)	0.35 ± 0.13	0.45 ± 0.15	0.0376
Butyrylcarnitine (C4)	0.065 (0.051-0.076)	0.126 (0.090-0.213)	<0.0001
Isovalerylcarnitine (C5)	0.056 ± 0.033	0.094 ± 0.051	0.0092
Octanoylcarnitine (C8)	0.107 (0.090-0.162)	0.115 (0.089-0.163)	0.8201
Myristoylcarnitine (C14)	0.020 ± 0.004	0.027 ± 0.009	0.0046
Palmitoylcarnitine (C16)	0.121 ± 0.022	0.135 ± 0.029	0.1115

Values are presented as median (inter-quartile range) or mean ± standard deviation. P value < 0.05 is considered as statistically significant.

4.4 Acylglycine concentration and kinetics

After bariatric surgery, there were significant increases in the urinary concentrations of acetylglycine from 0.54 (0.32-1.00) to 1.10 (0.61-1.63) mmol/mol crt, p = 0.0063 (Figure 2A), isobutyrylglycine from 0.40 ± 0.18 to 0.64 ± 0.31 mmol/mol crt, p = 0.0036 (Figure 2B), tigylglycine from 0.62 ± 0.29 to 1.01 ± 0.47 mmol/mol crt (Figure 2C), isovalerylglycine from 0.38 ± 0.18 to 0.54 ± 0.29 mmol/mol crt, p = 0.0214 (Figure 2D), and hexanoylglycine from 0.22 ± 0.11 to 0.30 ± 0.13 mmol/mol crt, p = 0.0050 (Figure 2E). However, urine octanoylglycine concentration was not significantly different from baseline (Figure 2F). Acetylglycine ASR increased significantly post-surgery, but the post-surgery increase in its FSR did not reach statistical significance (Table 6). On the other hand, FSRs and ASRs of isobutyrylglycine, tigylcine, isovalerylglycine, and hexanoylglycine were significantly higher post-surgery (Table 6).

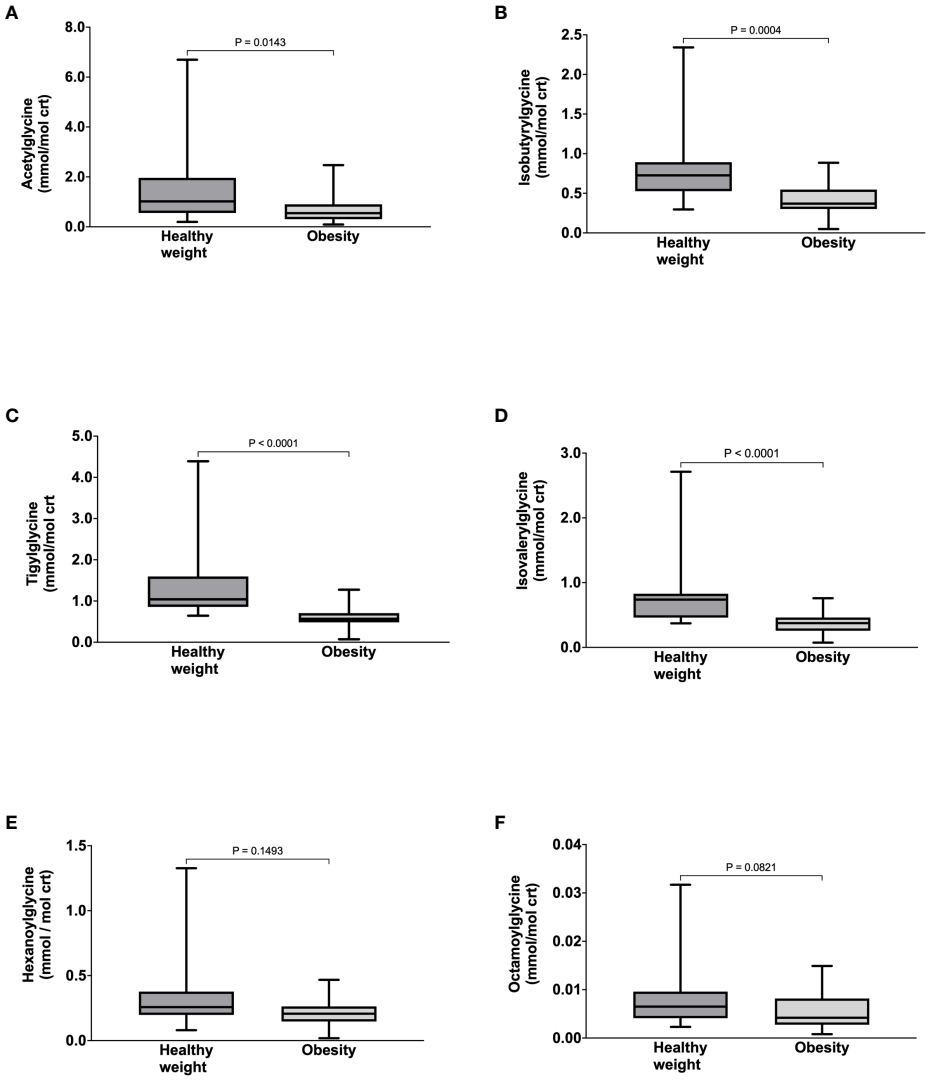

FIGURE 1
Urine concentrations of Acetyglglycine **(A)**, Isobutyrylglycine **(B)**, Tigylglycine **(C)**, Isovalerylglycine **(D)**, Hexaoylglycine **(E)**, and Octanoylglycine **(F)** in participants with healthy weight and class III obesity.

10.3389/fendo.2024.1343738

TABLE 3 Acylglycine kinetics of participants with healthy weight and class III obesity.

	Healthy weight (n = 20)	Class III Obesity (n = 20)	*P* value
Acetylglycine			
FSR (% pool/day)	433 ± 107	316 ± 107	0.0014
ASR (mmol/mol crt/day)	4.70 (2.44-6.13)	1.52 (0.92-3.71)	0.0018
Isobutyrylglycine			
FSR (% pool/day)	448 ± 94	385 ± 102	0.0509
ASR (mmol/mol crt/day)	3.46 (2.26-4.11)	1.49 (0.99-1.49)	<0.0001
Tigylglycine			
FSR (% pool/day)	565 ± 127	443 ± 89	0.0012
ASR (mmol/mol crt/day)	6.96 (4.26-9.09)	2.35 (1.99-3.76)	<0.0001
Isovalerylglycine			
FSR (% pool/day)	606 ± 126	435 ± 77	<0.0001
ASR (mmol/mol crt/day)	4.53 (2.76-5.41)	1.53 (1.27-1.93)	<0.0001
Hexanoylglycine			
FSR (% pool/day)	436 ± 91	340 ± 79	0.0010
ASR (mmol/mol crt/day)	1.19 (0.88-1.51)	0.62 (0.45-1.09)	0.0143

Values are presented as median (inter-quartile range) or mean ± standard deviation. P value< 0.05 is considered statistically significant. FSR, Fractional Synthesis Rate; ASR, Absolute Synthesis Rate; crt, creatinine.

4.5 Benzoylglycine concentration and kinetics

Compared to healthy weight controls, the urine concentration of benzoylglycine was significantly lower in participants with obesity (63 ± 34 vs. 112 ± 45 mmol/mol crt, p = 0.0004) (Figure 3A) due to significantly slower FSR (363 ± 112 vs. 521 ± 128% pool/day, p = 0.0002) (Figure 3B) and ASR (211 ± 104 vs. 557 ± 256 mmol/mol crt/day, p < 0.0001) (Figure 3C). Following surgery, urine benzoylglycine concentration increased from 59.7 (38.3-100.60) to 127.4 (70.0 -152.2) mmol/mol crt (p = 0.0063) (Figure 3D). There were similar significant increases in benzoylglycine FSR (368 ± 121 to 492 ± 83% pool/day) (Figure 3E), and ASR [232 (146-299) to 554 (352-912) mmol/mol crt/day, p = 0.0003] (Figure 3F). Regression analysis also showed a significant association between plasma glycine concentration and benzoylglycine ASR (model R^2 = 0.16, Beta coefficient = 3.81, p = 0.0021) (Figure 4).

5 Discussion

Our study examined the impact of obesity-associated glycine deficiency on the glycine conjugation pathway. Whereas substrate turnover rates are increased in individuals with obesity leading to the accumulation of metabolically toxic intramitochondral aylCoAs, paradoxically plasma glycine concentration is decreased. We found that in patients with class III obesity, the elimination rate of various endogenously produced metabolites and exogenous benzoic acid as acylglycines was impaired. Following bariatric surgery, however, glycine availability improved, and this was associated with increased synthesis and excretion of these acylglycines.

Participants with obesity in our study had higher plasma concentrations of amino acids such as the BCAAs, aromatic amino acids, and alanine compared to healthy weight controls. By contrast, glycine and serine plasma concentrations were significantly lower. These findings are consistent with those reported in earlier studies by us and others (1–6); and such changes in amino acid profile are independent predictors of adverse cardiometabolic outcomes (17, 18). The reasons why the plasma concentration of glycine is reduced while other amino acids, such as the BCAAs, are elevated in individuals with obesity have been elusive. However, we recently showed, using isotopically labelled tracers, that the lower plasma glycine concentration in individuals with obesity can be explained by the slower rate of *de novo* glycine synthesis (6) and elevated BCAAs can be attributed to an accelerated rate of protein breakdown in skeletal muscles due to insulin resistance (4, 5). Glycine and serine are interconvertible via *serine hydroxymethytransferase*, which explains why glycine and serine trend in the same direction (19, 20). Our results also showed significantly higher plasma concentrations of glycine and serine post-surgery, which is due to faster rates of *de novo* glycine synthesis from reduced insulin resistance (6). Similarly, improved insulin-mediated suppression of skeletal muscle breakdown and BCAA oxidation (5, 21, 22) leads to lower post-surgery concentrations of BCAAs (except leucine), aromatic amino acids, methionine, proline, alanine, aspartate, and glutamate. The interaction between BCAA and glycine metabolism has been studied in animal models of obesity, which found that glycine participates in the disposal of excess nitrogen from skeletal muscle BCAA oxidation via the urea cycle, and glycine deficiency may also contribute to higher BCAA levels in obesity. Pharmacologic inhibition of BCAA oxidation increases skeletal muscle and plasma glycine levels and improves insulin resistance (23). However, dietary glycine supplementation lowered BCAAs in the muscle but did not improve insulin resistance. Extrapolating such findings directly to humans is challenging but provides a framework to test additional hypotheses in future studies.

The concentrations of acylcarnitines in plasma reflect the amount and types of acylCoAs in the mitochondria and provide

TABLE 4 Plasma amino acid concentrations of participants with class III obesity before and six months after bariatric surgery.

(μmol/L)	Pre-surgery (n = 16)	Post-surgery (n = 16)	*P* value
Nutritionally non-essential amino acids			
Glycine	164 ± 26	212 ± 38	<0.0001
Serine	103 ± 19	114 ± 21	0.0166
Glutamine	468 ± 51	470 ± 49	0.8338
Total Cysteine	337 ± 48	337 ± 32	0.9713
Tyrosine	66 ± 8	51 ± 5	<0.0001
Arginine	83 ± 18	85 ± 14	0.6178
Proline	144 ± 22	129 ± 18	0.0119
Alanine	312 ± 28	250 ± 34	<0.0001
Asparagine	34 ± 6	36 ± 8	0.4716
Aspartate	3 ± 1	2 ± 1	0.0020
Glutamate	54 ± 26	32 ± 18	0.0005
Nutritionally essential amino acids			
Leucine	134 ± 21	123 ± 16	0.1105
Isoleucine	66 ± 10	56 ± 6	0.0007
Valine	248 ± 38	224 ± 22	0.0262
Methionine	20 (20-23)	19 (17-20)	<0.0001
Phenylalanine	67 ± 8	57 ± 6	0.0001
Threonine	111 ± 30	101 ± 25	0.2628
Lysine	197 ± 30	182 ± 25	0.0783
Histidine	69 ± 8	75 ± 8	0.0779
Tryptophan	40 ± 7	37 ± 3	0.0947

Values are presented as median (inter-quartile range) or mean ± standard deviation. P value< 0.05 is considered as statistically significant.

an overview of substrate metabolism at the cellular level. In this study, the higher plasma concentrations of propionylcarnitine (C3), butyrylcarnitine (C4), and isovalerylcarnitine (C5) in individuals with obesity compared to controls indicate the higher turnover rates and oxidation of BCAAs. Similarly, the higher plasma myristoylcarnitine (C14) in participants with obesity indicates accelerated rates of lipolysis and free fatty acid oxidation. Although the higher acetylcarnitine, octanoylcarnitine, and palmitoylcarnitine concentrations in individuals with obesity did not achieve statistical significance, our overall findings are consistent with the notion that obesity is associated with faster substrate turnover rates resulting in the intramitochondrial production and accumulation of various amino acid and lipid oxidation intermediates (11, 12). The reduction of BCAA-derived acylcarnitines: propionylcarnitine (C3), butyrylcarnitine (C4), and isovlearylcarnitine (C5) after bariatric surgery indicates a decrease in BCAA flux from muscle protein breakdown and its oxidation rate following improvement in insulin resistance (3, 5, 21). The lack of statistically significant reductions in medium or long-chain acylcarnitines after surgery indicate that free fatty acid flux and oxidation remained elevated. These findings are expected as post-surgery dietary calorie intake remains low during the first six months after bariatric surgery (5, 9, 21). In this state of negative calorie balance, the body's energy requirement is dependent on the oxidation of fatty acids mobilized from adipose tissue (24, 25). This interpretation is supported by the higher post-surgery concentration of acetylcarnitine, which reflects the elevated intramitochondrial acetylCoAs generated as the final product of fatty acid beta-oxidation. Ketone bodies generated from acetylCoA can be further utilized by various organs as an energy source. Oxidative stress levels are increased in individuals with obesity due to higher production of reactive oxygen species as a byproduct of accelerated free fatty oxidation. However, this is less of a concern post-surgery despite a reliance on lipid oxidation, as multiple studies have demonstrated a reduction in oxidative stress post-bariatric surgery (26, 27). Weight loss stabilizes 12 months after bariatric surgery (5, 9, 21), and during this phase, the associated changes in nutrient intake will need to be considered for any additional alterations in metabolite levels.

We measured the urine concentrations and synthesis rates of various acylglycines to examine the ability of the glycine conjugation pathway to eliminate potentially toxic endogenously derived metabolites. The decrease in urine isobutyrylglycine and isovalerylglycine have been described in individuals with obesity (5). However, this is the first human study to use stable isotope tracers to confirm the impact of obesity-associated glycine deficiency on the glycine conjugation pathway. We found that at baseline, urine concentrations of acetylglycline and BCAA-derived acylglycines (isobutyrylglycine, tigylglycine, and isovalerylglycine) were significantly lower in individuals with obesity compared to healthy weight controls. The lower concentrations of medium-chain fatty acid-derived acylglycines (hexanoylglycine and octanoylglycine) were not statistically significant. Nonetheless, the kinetic data showed significantly slower synthesis rates for acetyglcyine, BCAA-derived acylglycines, and medium-chain fatty acid-derived acylglycines in participants with obesity than healthy weight controls. Post-bariatric surgery, the urine concentrations and synthesis rates of acylglycines derived from acetylCoA, BCAAs, and medium-chain fatty acids increased significantly.

To examine whether obesity-associated glycine deficiency impairs the clearance of metabolites from exogenous sources, we measured the urine concentration and synthesis rate of benzoylglycine, also known as hippuric acid. Benzoic acid, a carboxylic acid used as a food preservative and a by-product of gut microbiome metabolism, is conjugated with glycine and excreted as bezoylglycine (9, 13). This pathway is linked to glycine homeostasis as glycine used to form benzoylglycine cannot be recycled and could drain the glycine pool (28). We found lower urine concentration and synthesis of benzoylglycine in individuals with obesity compared to controls. When glycine availability improved after bariatric surgery, synthesis and urine excretion of benzoylglycine increased. Regression analysis further revealed that a 16% variance in benzoic acid elimination can be attributed to glycine availability. These findings are consistent with our hypothesis that obesity-associated glycine deficiency impairs

10.3389/fendo.2024.1343738

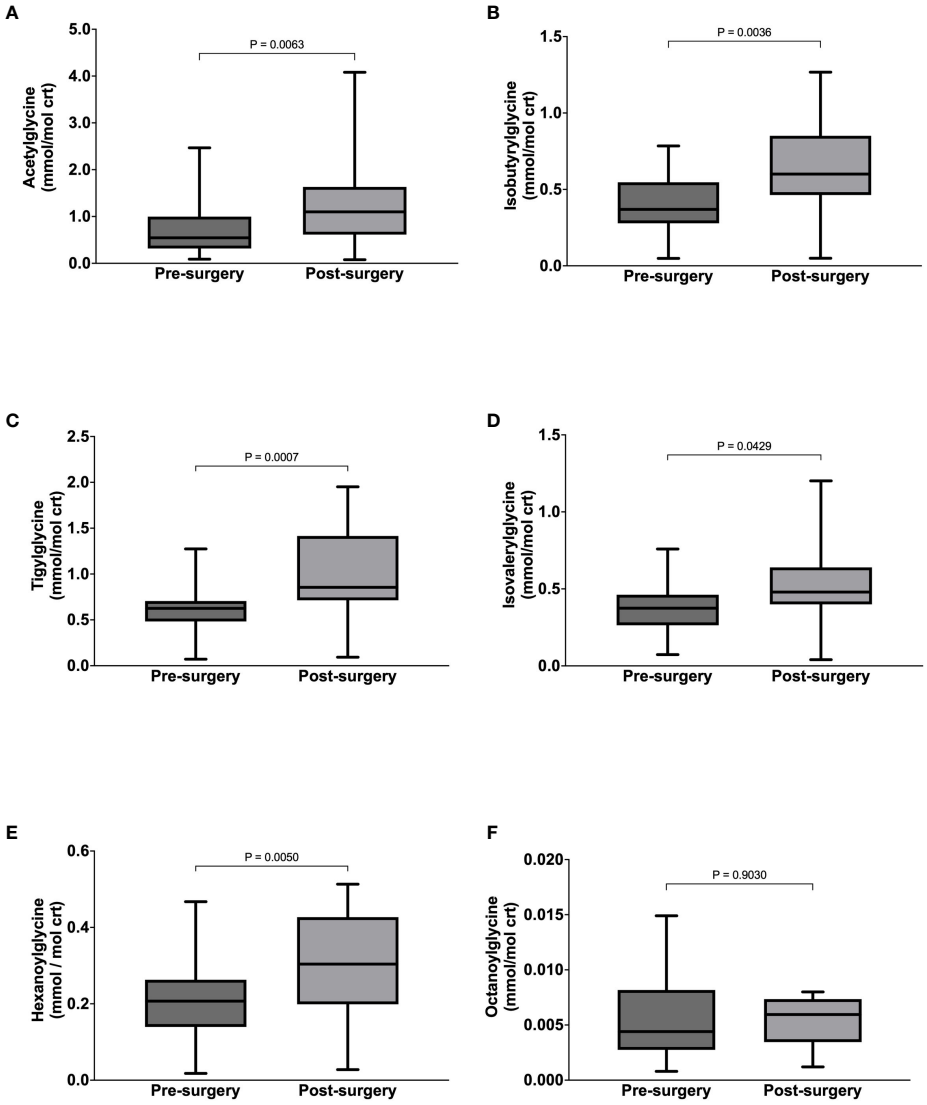

FIGURE 2
Urine concentrations of Acetyglglycine **(A)**, Isobutyrylglycine **(B)**, Tigylglycine **(C)**, Isovalerylglycine **(D)**, Hexaoylglycine **(E)**, and Octanoylglycine **(F)** in participants with class III obesity before and six months after bariatric surgery.

TABLE 5 Plasma acylcarnitine concentrations of participants with class III obesity before and six months after bariatric surgery.

μmol/L	Pre-surgery (n = 16)	Post-surgery (n = 16)	*P* value
Acetylcarnitine (C2)	14.83 ± 5.72	17.94 ± 6.83	0.0435
Propionylcarnitine (C3)	0.44 ± 0.14	0.34 ± 0.07	0.0045
Butyrylcarnitine (C4)	0.13 ± 0.05	0.09 ± 0.06	0.0006
Isovalerylcarnitine (C5)	0.09 ± 0.05	0.05 ± 0.02	0.0162
Octanoylcarnitine (C8)	0.13 ± 0.05	0.12 ± 0.04	0.3453
Myristoylcarnitine (C14)	0.03 ± 0.01	0.02 ± 0.01	0.0737
Palmitoylcarnitine (C16)	0.14 ± 0.03	0.14 ± 0.04	0.9584

Values are presented as median (inter-quartile range) or mean ± standard deviation. P value< 0.05 is considered as statistically significant.

the glycine conjugation pathway and compromises the elimination of endogenous and exogenous metabolites as acylglycines.

Our findings have several potential clinical implications. The accumulation of incompletely oxidized substrates in metabolically active organs such as the skeletal muscle, heart, and liver can lead to mitochondrial stress and organ dysfunction (11, 12). Therefore, methods that enhance the elimination of excess metabolites via glycine conjugation could be developed to treat various obesity-related metabolic complications. Supplementation with dietary glycine is an antidote for humans with isovaleryl-CoA dehydrase deficiency by increasing organic acid excretion as acylglycine (29). Since the glycine conjugation reaction occurs primarily in the liver, patients with metabolic liver disease may benefit the most from such treatment. Oral glycine supplementation in high-fat diet Zucker-Fatty Rats enhanced urine acylglycine excretion, reduced serum triglycerides, and decreased hepatic short- and medium-

TABLE 6 Acylglycine kinetics of participants with class III obesity before and six months after bariatric surgery.

	Pre-surgery (n = 16)	Post-surgery (n = 16)	*P* value
Acetylglycine			
FSR (% pool/day)	317 ± 112	365 ± 83	0.0775
ASR (mmol/mol crt/day)	1.52 (0.92-1.52)	3.92 (2.29-6.19)	0.0013
Isobutyrylglycine			
FSR (% pool/day)	378 ± 94	448 ± 93	0.0098
ASR (mmol/mol crt/day)	1.48 ± 0.70	2.75 ± 1.14	0.0002
Tigylglycine			
FSR (% pool/day)	442 ± 89	510 ± 80	0.0433
ASR (mmol/mol crt/day)	2.72 ± 1.28	5.18 ± 2.43	0.0002
Isovalerylglycine			
FSR (% pool/day)	429 ± 78	554 ± 97	0.0002
ASR (mmol/mol crt/day)	1.63 ± 0.68	3.00 ± 1.63	0.0016
Hexanoylglycine			
FSR (% pool/day)	342 ± 78	413 ± 62	0.0013
ASR (mmol/mol crt/day)	0.79 ± 0.52	1.25 ± 0.59	0.0004

Values presented as median (inter-quartile range) or mean ± standard deviation. P value< 0.05 is considered as statistical significant. FSR, Fractional Synthesis Rate; ASR, Absolute Synthesis Rate; crt, creatinine.

chain acylCoAs. However, the actual metabolic benefit at the organ level remains to be determined (23). Another study also showed that glycine supplementation in animals with non-alcoholic hepatic liver disease lowered serum triglycerides, hepatic steatosis, and inflammation (30). However, whether these improvements were attributable to the glycine conjugation pathway or other mechanisms was unclear. Further studies in humans are needed to examine the effectiveness of glycine supplements to improve glycine conjugation as a treatment for specific obesity-related metabolic complications. The impaired elimination of benzoic acid in patients with obesity indicates that the detoxification of xenobiotic metabolites via glycine conjugation is compromised. Humans in the industrialized world are exposed to various chemicals in the environment, food, and consumer products. Some of these molecules are regarded as endocrine-disrupting chemicals and may contribute to various endocrine disorders (31). Thus, individuals with class III obesity may be more susceptible to various environmental toxins due to glycine deficiency, but this hypothesis needs to be tested in future studies.

Our study has several limitations. We reported the effect of glycine deficiency on the glycine conjugation pathway and discussed its metabolic implications when this detoxification system is compromised. However, glycine plays a central role in various human metabolic reactions. Our understanding of the metabolic consequence of glycine deficiency is incomplete without examining its impact on other physiologically important pathways, such as 1-carbon cycle metabolism, glutathione biosynthesis, glycine-mediated signaling pathways, and gut microbiome. For example, higher glycine availability could modulate the gut microbiome population, although the causal relationship between gut microbiome and disease pathogenesis remains complex (30). We could not measure the urine concentrations and synthesis rates of long-chain fatty acids-derived acylglycines due to technical

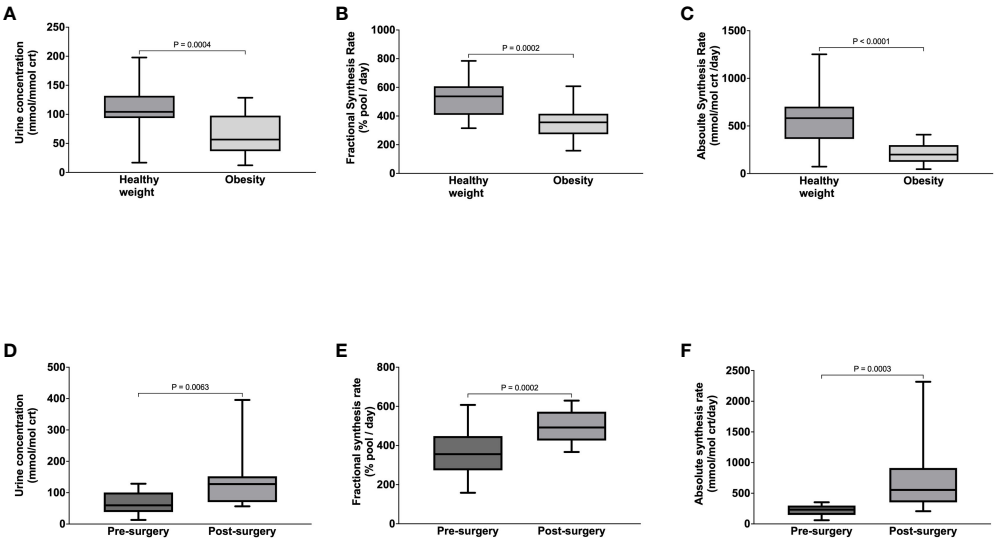

FIGURE 3
Benzoylglycine urine concentration **(A)**, Fractional Synthesis Rate **(B)**, Absolute Synthesis rate **(C)** in participants with healthy weight and class III obesity, and Benzoylglycine urine concentration **(D)**, Fractional Synthesis Rate **(E)**, and Absolute Synthesis rate **(F)** in participants with class III obesity before and six months after bariatric surgery.

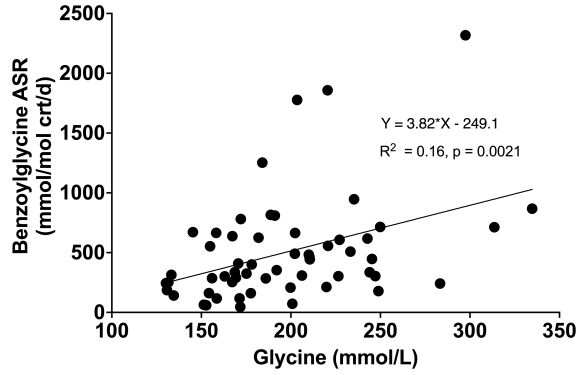

FIGURE 4
Relationship between plasma glycine concentration with benzoylglycine absolute synthesis rate (ASR).

difficulties in preparing its internal standards. However, the glycine conjugation pathway may also have greater selectivity for acylCoAs of short and medium-chain lengths. We studied and reported the improvement in the glycine conjugation pathway by correcting glycine deficiency in individuals who underwent bariatric surgery. However, bariatric surgery also changes body weight, body composition, diet, and physical activity levels. It is unclear whether these contemporaneous changes confound our measured outcomes and should be controlled for in future studies.

6 Conclusion

Obesity-associated glycine deficiency impairs the human body's ability to eliminate endogenous and exogenous metabolites via the glycine conjugation pathway. However, this impairment can be ameliorated by correcting glycine deficiency with weight loss secondary to bariatric surgery.

Data availability statement

The raw data supporting the conclusions of this article will be made available by the authors, without undue reservation.

Ethics statement

The studies involving humans were approved by SingHealth Centralized Institutional Review Board. The studies were conducted in accordance with the local legislation and institutional requirements. The participants provided their written informed consent to participate in this study.

Author contributions

HT: Conceptualization, Data curation, Formal analysis, Funding acquisition, Investigation, Methodology, Project administration, Resources, Visualization, Writing – original draft, Writing – review & editing. JH: Conceptualization, Formal Analysis, Methodology, Writing – original draft. ET: Supervision, Writing – review & editing. SC: Writing – review & editing, Methodology. JK: Writing – review & editing. FJ: Methodology, Writing – review & editing, Conceptualization, Supervision.

Funding

The author(s) declare that financial support was received for the research, authorship, and/or publication of this article. This study was supported by the National Medical Research Council Transition Award (grant reference: NRMC/TA/0063/2018 and Khoo Mentored Research Award (grant reference: Duke-NUS-KMRA/2020/0013).

Acknowledgments

The authors would like to thank Vieon Wu and the SingHealth Investigational Medical Unit for their support in conducting the metabolic studies, and the clinical teams (Drs Lim Chong Hong, Alvin Eng, Eugene Lim, Chan Weng Hoong, Jeremy Tan, Sonali Ganguly, and Lee Phong Ching) for providing clinical and surgical support.

Conflict of interest

The authors declare that the research was conducted in the absence of any commercial or financial relationships that could be construed as a potential conflict of interest.

Publisher's note

References

1. Felig P, Marliss E, Cahill GF Jr. Plasma amino acid levels and insulin secretion in obesity. *N Engl J Med*. (1969) 281:811–6.

2. Newgard CB, An J, Bain JR, Muehlbauer MJ, Stevens RD, Lien LF, et al. A branched-chain amino acid-related metabolic signature that differentiates obese and lean humans and contributes to insulin resistance. *Cell Metab*. (2009) 9:311–26.

3. Yao J, Kovalik JP, Lai OF, Lee PC, Eng A, Chan WH, et al. Comprehensive assessment of the effects of sleeve gastrectomy on glucose, lipid, and amino acid metabolism in asian individuals with morbid obesity. *Obes Surg*. (2019) 29:149–58.

4. Tan HC, Hsu JW, Khoo CM, Tai ES, Yu S, Chacko S, et al. Alterations in branched-chain amino acid kinetics in nonobese but insulin-resistant Asian men. *Am J Clin Nutr*. (2018) 108:1220–8.

5. Tan HC, Hsu JW, Kovalik JP, Eng A, Chan WH, Khoo CM, et al. Branched-chain amino acid oxidation is elevated in adults with morbid obesity and decreases significantly after sleeve gastrectomy. *J Nutr*. (2020) 150:3180–9.

6. Hong Chang Tan JWH, Shyong Tai E, Chacko S, Wu V, Lee CF, Kovalik J-P, et al. De novo glycine synthesis is reduced in adults with morbid obesity and increases following bariatric surgery. *Fronters Endocrinol*. (2022) 13.

7. Alves A, Bassot A, Bulteau AL, Pirola L, Morio B. Glycine metabolism and its alterations in obesity and metabolic diseases. *Nutrients*. (2019) 11.

8. Adeva-Andany M, Souto-Adeva G, Ameneiros-Rodriguez E, Fernandez-Fernandez C, Donapetry-Garcia C, Dominguez-Montero A. Insulin resistance and glycine metabolism in humans. *Amino Acids*. (2018) 50:11–27.

9. Badenhorst CP, van der Sluis R, Erasmus E, van Dijk AA. Glycine conjugation: importance in metabolism, the role of glycine N-acyltransferase, and factors that influence interindividual variation. *Expert Opin Drug Metab Toxicol*. (2013) 9:1139–53.

10. Bonafe L, Troxler H, Kuster T, Heizmann CW, Chamoles NA, Burlina AB, et al. Evaluation of urinary acylglycines by electrospray tandem mass spectrometry in mitochondrial energy metabolism defects and organic acidurias. *Mol Genet Metab*. (2000) 69:302–11.

11. Koves TR, Ussher JR, Noland RC, Slentz D, Mosedale M, Ilkayeva O, et al. Mitochondrial overload and incomplete fatty acid oxidation contribute to skeletal muscle insulin resistance. *Cell Metab*. (2008) 7:45–56.

12. Muoio DM, Newgard CB. Mechanisms of disease:Molecular and metabolic mechanisms of insulin resistance and beta-cell failure in type 2 diabetes. *Nat Rev Mol Cell Biol*. (2008) 9:193–205.

13. Gregus Z, Fekete T, Varga F, Klaassen CD. Dependence of glycine conjugation on availability of glycine: role of the glycine cleavage system. *Xenobiotica*. (1993) 23:141–53.

14. Badaloo A, Hsu JW, Taylor-Bryan C, Green C, Reid M, Forrester T, et al. Dietary cysteine is used more efficiently by children with severe acute malnutrition with edema compared with those without edema. *Am J Clin Nutr*. (2012) 95:84–90.

15. Hobert JA, Liu A, Pasquali M. Acylglycine analysis by ultra-performance liquid chromatography-tandem mass spectrometry (UPLC-MS/MS). *Curr Protoc Hum Genet*. (2016) 91:17 25 1–17 25 12.

16. Fisher L, Davies C, Al-Dirbashi OY, Ten Brink HJ, Chakraborty P, Lepage N. A novel method for quantitation of acylglycines in human dried blood spots by UPLC-tandem mass spectrometry. *Clin Biochem*. (2018) 54:131–8.

17. Wang TJ, Larson MG, Vasan RS, Cheng S, Rhee EP, McCabe E, et al. Metabolite profiles and the risk of developing diabetes. *Nat Med*. (2011) 17:448–53.

18. Floegel A, Stefan N, Yu Z, Muhlenbruch K, Drogan D, Joost HG, et al. Identification of serum metabolites associated with risk of type 2 diabetes using a targeted metabolomic approach. *Diabetes*. (2013) 62:639–48.

19. Gregory JF 3rd, Cuskelly GJ, Shane B, Toth JP, Baumgartner TG, Stacpoole PW. Primed, constant infusion with [2H3]serine allows in *vivo* kinetic measurement of serine turnover, homocysteine remethylation, and transsulfuration processes in human one-carbon metabolism. *Am J Clin Nutr*. (2000) 72:1535–41.

20. Lamers Y, Williamson J, Gilbert LR, Stacpoole PW, Gregory JF 3rd. Glycine turnover and decarboxylation rate quantified in healthy men and women using primed, constant infusions of [1,2-(13)C2]glycine and [(2)H3]leucine. *J Nutr*. (2007) 137:2647–52.

21. Tan HC, Khoo CM, Tan MZ, Kovalik JP, Ng AC, Eng AK, et al. The effects of sleeve gastrectomy and gastric bypass on branched-chain amino acid metabolism 1 year after bariatric surgery. *Obes Surg*. (2016) 26:1830–5.

22. Tan HC, Yew TW, Chacko S, Tai ES, Kovalik JP, Ching J, et al. Comprehensive assessment of insulin resistance in non-obese Asian Indian and Chinese men. *J Diabetes Investig*. (2018) 9:1296–303.

23. White PJ, Lapworth AL, McGarrah RW, Kwee LC, Crown SB, Ilkayeva O, et al. Muscle-liver trafficking of BCAA-derived nitrogen underlies obesity-related glycine depletion. *Cell Rep*. (2020) 33:108375.

24. Bruss MD, Khambatta CF, Ruby MA, Aggarwal I, Hellerstein MK. Calorie restriction increases fatty acid synthesis and whole body fat oxidation rates. *Am J Physiol Endocrinol Metab*. (2010) 298:E108–16.

25. Tan HC, Shumbayawonda E, Beyer C, Cheng LT, Low A, Lim CH, et al. Multiparametric magnetic resonance imaging and magnetic resonance elastography to evaluate the early effects of bariatric surgery on nonalcoholic fatty liver disease. *Int J BioMed Imaging*. (2023) 2023:4228321.

26. Metere A, Graves CE, Pietraforte D, Casella G. The effect of sleeve gastrectomy on oxidative stress in obesity. *Biomedicines*. (2020) 8.

27. Bankoglu EE, Seyfried F, Arnold C, Soliman A, Jurowich C, Germer CT, et al. Reduction of DNA damage in peripheral lymphocytes of obese patients after bariatric surgery-mediated weight loss. *Mutagenesis*. (2018) 33:61–7.

28. Beyoglu D, Idle JR. The glycine deportation system and its pharmacological consequences. *Pharmacol Ther*. (2012) 135:151–67.

29. Naglak M, Salvo R, Madsen K, Dembure P, Elsas L. The treatment of isovaleric acidemia with glycine supplement. *Pediatr Res*. (1988) 24:9–13.

30. Rom O, Liu Y, Liu Z, Zhao Y, Wu J, Ghrayeb A, et al. Glycine-based treatment ameliorates NAFLD by modulating fatty acid oxidation, glutathione synthesis, and the gut microbiome. *Sci Transl Med*. (2020) 12.

31. Diamanti-Kandarakis E, Bourguignon JP, Giudice LC, Hauser R, Prins GS, Soto AM, et al. Endocrine-disrupting chemicals: an Endocrine Society scientific statement. *Endocr Rev*. (2009) 30:293–342.

frontiers | Frontiers in Endocrinology

TYPE Original Research
PUBLISHED 15 August 2024
DOI 10.3389/fendo.2024.1431728

OPEN ACCESS

EDITED BY
Kaixiong Tao,
Huazhong University of Science and Technology, China

REVIEWED BY
Yiping Wei,
Peking University Hospital of Stomatology, China
Ying Qing,
Beckman Research Institute, City of Hope, United States

*CORRESPONDENCE
Xin Huang
huangxinsdu@163.com
Xiaole Hu
hxllks@163.com

RECEIVED 12 May 2024
ACCEPTED 29 July 2024
PUBLISHED 15 August 2024

CITATION
Bi X, Zhao P, Liu T, Zhu T, Li Y, Xiong S, Liu S, Hu X and Huang X (2024) Impact of sleeve gastrectomy on the periodontal status of patients with and without type 2 diabetes: a 1-year prospective real-world study.
Front. Endocrinol. 15:1431728.
doi: 10.3389/fendo.2024.1431728

Impact of sleeve gastrectomy on the periodontal status of patients with and without type 2 diabetes: a 1-year prospective real-world study

Xiaocheng Bi[1], Peikai Zhao[2,3], Teng Liu[2,4], Tao Zhu[2,3], Yuxuan Li[2,3], Sisi Xiong[2,3], Shaozhuang Liu[2,4], Xiaole Hu[5]* and Xin Huang[2,4]*

[1]Department of Periodontology, School and Hospital of Stomatology, Cheeloo College of Medicine, Shandong University & Shandong Key Laboratory of Oral Tissue Regeneration and Shandong Engineering Research Center of Dental Materials and Oral Tissue Regeneration and Shandong Provincial Clinical Research Center for Oral Diseases, Jinan, Shandong, China, [2]Division of Bariatric and Metabolic Surgery, Department of General Surgery, Qilu Hospital of Shandong University, Jinan, Shandong, China, [3]The First Clinical College, Shandong University, Jinan, Shandong, China, [4]State Key University Laboratory of Diabetes and Obesity Surgery, Shandong University, Jinan, Shandong, China, [5]Department of Operating Room, Qilu Hospital of Shandong University, Jinan, Shandong, China

Background: Periodontitis is a chronic inflammatory disease potentially associated with obesity and type 2 diabetes (T2D). Sleeve gastrectomy (SG) has shown substantial effect on weight loss and treatment of T2D. However, there is no direct evidence comparing the impact of SG on the periodontal status of patients with and without T2D.

Objectives: To determine the impact of SG on the periodontal status of patients with and without T2D in a real-world setting.

Methods: In a prospective and two-armed cohort design, participants who were scheduled for SG at an affiliated hospital between April 2022 and December 2022 were approached for eligibility. After a clinical evaluation and oral examination, those with periodontitis were included and further divided into the DM group (diabetic) and the Control group (non-diabetic) with a 1-year follow-up after surgery. The primary outcome was the periodontal status of patients at 12 months after SG. The secondary outcomes included weight loss, diabetes remission, and alterations in inflammatory markers for up to 1 year after SG.

Results: Fifty-seven and 49 patients were included in the DM and the Control group, respectively. Before surgery, patients in the DM group had further worsened periodontal condition compared with those in the Control group. Accompanied by weight loss and glucose reduction, patients in both groups demonstrated significant decreases in plaque index (PLI) and bleeding index (BI) with no alterations in probing depth or clinical attachment loss for up to 1 year after SG. Even patients in the DM group achieved less TWL% (32.79 $\pm$ 6.20% vs. 37.95 $\pm$ 8.34, $P<0.01$), their periodontal condition had more substantial improvement with no significant difference in PLI and BI between groups at 1 year after SG. We also observed a significant reduction in the levels of high sensitive C-reactive protein and interleukin-6 in both groups at 1 year after SG.

Conclusion: Both patients with and without T2D demonstrated improved periodontal status for up to 1 year after SG. Patients with T2D achieved less weight loss but a more substantial improvement in periodontal condition. The significant reduction in inflammatory biomarkers contributed to the improvement of periodontal status after SG.

KEYWORDS

type 2 diabetes, periodontitis, obesity, sleeve gastrectomy, prospective studies

1 Introduction

The prevalence of obesity and type 2 diabetes (T2D) continues to increase significantly in developed and developing countries. According to the latest survey, 42% of adults are with overweight or obesity globally (1), and approximately 537 million adults are affected by T2D worldwide (2).

Periodontitis is a non-communicable disease characterized by pathological loss of the periodontal ligament and alveolar bone (3). Severe periodontitis affects 11.2% of the world's population, being the 6th most prevalent disease worldwide and the primary cause of tooth loss (4). Treatment of periodontitis aims to prevent further disease progression, reduce the risk of tooth loss, possibly restore lost periodontal tissue, and maintain a healthy periodontium (5).

Patients with obesity are considered a risk group for periodontitis. However, the importance of oral health in patients with obesity, especially those with morbid obesity, is commonly overlooked due to their other life-threatening comorbidities. The limited available evidence has demonstrated the periodontitis prevalence in patients with obesity and eligible for bariatric/metabolic surgery (BMS) ranges between 45% and 70% (6–8). In addition, there is an evident bidirectional relationship between T2D and periodontitis. Patients with T2D are reported to have significantly worse periodontal status and a 34% greater risk of developing periodontitis (9). Likewise, severe periodontitis increases the incidence of T2D by 53% (9). However, when we focus on the patients with T2D and eligible for BMS, there has been no direct evidence on their periodontal health status.

BMS has shown substantial effect on weight loss and the treatment of T2D (10, 11). Sleeve gastrectomy (SG) is the most commonly performed bariatric/metabolic procedure, accounting for approximately 62.5% of all primary BMS worldwide (12). Changes induced by surgery, including weight loss, a decrease in blood glucose, a reduction in systemic inflammation, alterations in eating habits and dietary choices, and remodeling of the oral microbiota, could have a significant impact on the periodontal status of patients. However, there has been no consensus in terms of the impact of BMS on periodontal conditions. Some studies have demonstrated an improvement in periodontal status following BMS (13, 14), whereas others have shown a progress in periodontal degradation after BMS (6, 15). Furthermore, it is unclear whether there is difference in the impact of SG on the periodontal status of patients with and without T2D.

Based on a prospective cohort of patients scheduled for SG, the main aim of the current study was to determine the impact of SG on the periodontal status of patients with and without T2D in a real-world setting.

2 Research design and methods

2.1 Study design and patients

This prospective, longitudinal, two-armed cohort study was approved by the Ethics Committee on Scientific Research of Shandong University Qilu Hospital (KYLL-202111-137-1), registered at the Chinese Clinical Trial Registry (www.chictr.org.cn) with the identification number ChiCTR2200060644 (diabetic cohort) and ChiCTR2200058242 (non-diabetic cohort), and conducted in accordance with the standards set by the Declaration of Helsinki.

From April 2022 to December 2022, candidates were approached for eligibility if they were scheduled for SG at Qilu Hospital of Shandong University. SG was indicated if a patient had a body mass index (BMI) ≥ 32.5 kg/m^2, or BMI ≥ 28 kg/m^2 with obesity-related complications or with more than 2 metabolic syndrome components, and there were no other contraindications for general anesthesia or the surgical procedure.

The inclusion criteria of the current study were (1) body mass index (BMI) ≥ 32.5 kg/m^2 (2); aged 18-60 years (3); with a diagnosis of periodontitis identified as a threshold of interproximal clinical attachment loss (CAL) of ≥2 mm, or ≥3 mm at ≥2 non-adjacent teeth (16) (4); at least 16 remaining teeth (5); agree to participate in this study and sign the informed consent form.

The key exclusion criteria included individuals (1) with active smoking within the past 6 months (2); were pregnant or still in lactation (3); had a history of radiotherapy to the head and neck (4); with long-term use of nonsteroidal anti-inflammatory drugs or corticosteroids (5); with any periodontal therapy less than 6 months before the study (6); had acute infection of the affected tooth (7);

had poor anesthesia or surgery tolerance because of severe cardiopulmonary dysfunction; and (8) who were unwilling to comply with follow-up visits.

Among patients included, individuals with T2D were assigned to the DM group if they had a fasting plasma glucose (FPG) level ≥7.0 mmol/l or a glycated hemoglobin (HbA1c) level ≥6.5% (10). Participants without diabetes were included and assigned to the Control group if their FPG was <6.1 mmol/L and their HbA1c level was <6.0% without taking any anti-diabetes medications or insulin.

2.2 Baseline measurements and biochemical analysis

Clinical determinations, including demographic features, anthropometric measurements, and laboratory test results, were obtained at baseline before surgery. Blood lipid profiles and plasma glucose levels were measured using a Roche Cobas 8000 modular analyzer system (Roche Diagnostics, IN, USA). Plasma insulin levels were determined by a two-site enzymometric assay using a Tosoh 2000 auto-analyzer (Tosoh Corp., Tokyo, Japan). The levels of inflammatory markers, including high sensitivity C-reactive protein (hs-CRP), interleukin-6 (IL-6), and tumor necrosis factor alpha (TNF-α), were determined with high sensitivity enzyme linked immunosorbent assay kits (R&D Systems). The homeostatic model assessment of insulin resistance (HOMA-IR) was calculated as fasting insulin (mU/mL) × FPG (mmol/L)/ 22.5 (17).

2.3 Oral clinical evaluation

The oral clinical examination was performed by an experienced periodontist. The following periodontal parameters were recorded for all the teeth during each examination: probing depth (PD), bleeding index (BI), plaque index (PLI), and CAL. PD was determined by measuring the distance from the gingival margin to the bottom of the gingival crevice in millimeters (14). CAL was measured as the distance from the cement–enamel junction to the bottom of the gingival crevice in millimeters (14). PLI used the standard proposed by Silness and Loe (18). The scoring method of BI was in accordance with the standard proposed by Mazza in 1981 (19).

PD and CAL were measured at six sites (mesiobuccal, midbuccal, distobuccal, distolingual, midlingual and mesiolingual) for all present teeth (except for third molars) to the nearest millimeter using a graded probe (Hu-Friedy, Chicago, IL). BI and PLI were measured at two sites (midbuccal and midlingual) per tooth.

2.4 Procedure

All SG operations were performed by the same experienced surgical team as described previously (10). In brief, a tubular sleeve of stomach was created by dissecting the greater curvature starting 2–4 cm from the pylorus and extending up to the angle of His.

2.5 Follow-up and outcomes

Suggestions for diet and physical activities but not oral hygiene were provided at the time of discharge. A reassessment of periodontal status was performed by the same examiner at 6 and 12 months after SG. The primary outcome of the current study was the periodontal condition of patients at 12 months after SG. The secondary outcomes included weight loss, diabetes remission, and alterations in inflammatory markers for up to 1 year after SG. The weight loss effect was evaluated by both percentage of total weight loss (TWL%) and excess weight loss (EWL%), which was calculated as reported previously (20). Diabetes remission was defined as HbA1c < 6.5% and the absence of antidiabetes medications for at least 2 months (21).

2.6 Statistical analysis

SPSS version 26.0 (SPSS Inc., Chicago, IL, USA) was used for the statistical analysis. Continuous variables are presented as the mean ± standard deviation (SD). The unpaired t tests or Mann–Whitney tests was used to compare the mean values between baseline and after surgery and also between the two groups. The levels of TWL% and EWL% over time after surgery were analyzed using two-way (repeated-measures) ANOVA, followed by the Bonferroni *post hoc* test, and the results are reported as ${}^{A}P$ by group, ${}^{B}P$ over time, and ${}^{C}P$ due to the interaction of the two factors. The data of a small number of patients who were lost to follow-up were omitted from subsequent analysis. A P value less than 0.05 indicated a statistically significant difference.

3 Results

3.1 Patient characteristics

From April 2022 to December 2022, 284 patients scheduled for SG were approached for eligibility. 73 and 60 patients were enrolled (as shown in Figure 1) from the diabetic and non-diabetic cohort, respectively. After exclusion, the remaining 57 and 49 patients were included in the DM and the Control group, and 51 (92.73%) and 41 (83.67%) of which completed the 12-month follow-up, respectively (Figure 1). The baseline characteristics of the patients included are detailed in Table 1. No significant difference was detected between the DM and the Control groups in age, sex, BMI, obesity comorbidities, or tooth brushing habits. In the DM group, 42.11% of the patients were already on treatment for T2D, and only 4 patients were receiving insulin therapy.

3.2 Effects of SG on weight loss

The TWL% and EWL% continued to increase for up to 1 year after SG in both groups (Figure 2). Although both groups had comparable EWL% after surgery (${}^{A}P = 0.733$), patients in the DM group achieved less TWL% at 12 months after SG (32.79 ± 6.20% vs. 37.95 ± 8.34, $P < 0.01$).

10.3389/fendo.2024.1431728

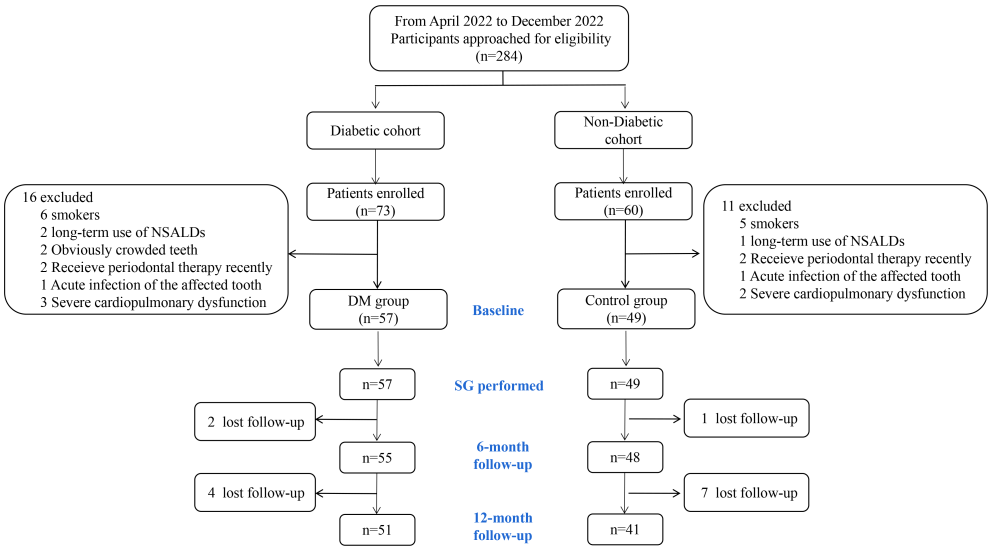

FIGURE 1
Flowchart of participants. NSALD, non-steroidal anti-inflammatory drug; SG, sleeve gastrectomy.

3.3 Effects of SG on glucose homeostasis

At baseline, patients in the DM group demonstrated higher levels of HbA1c, FPG, and HOMA-IR than those in the Control group (Table 2). After surgery, both groups showed a significant decrease in HbA1c, FPG, fasting insulin, and HOMA-IR. At 12 months after surgery, 48 of the 51 patients (94.11%) achieved remission of diabetes, and the remaining 3 patients still needed oral medication. No significant difference was detected between groups at 12 months after SG except lower level of FPG in the Control group (4.06 ± 0.56 vs. 4.49 ± 0.59, $P < 0.01$).

3.4 Effects of SG on blood lipid profiles

Before surgery, patients in the DM group showed significantly higher level of triglycerides than those in the Control group (2.42 ± 1.34 vs. 1.49 ± 0.60, $P < 0.01$, Table 3). Patients in both the DM group and the Control group showed an increased level of high-density lipoprotein-cholesterol (HDL-c) as well as decreased levels of triglycerides, low-density lipoprotein-cholesterol (LDL-c), and nonesterified fatty acids (NEFA) after SG. No significant difference was detected in level of total cholesterol between baseline and 6 or 12 months after SG in neither group. At 12 months after SG, patients in the Control group achieved better improvement in levels of total cholesterol (4.25 ± 1.17 vs. 4.84 ± 0.96, $P < 0.05$) and LDL-c (2.35 ± 0.77 vs. 2.76 ± 0.38, $P < 0.01$) compared with those in the DM group.

3.5 Impact of SG on the periodontal status of patients

At baseline, patients in the DM group had higher levels of PD (4.10 ± 1.08 vs. 3.68 ± 0.87, $P < 0.05$), BI (2.67 ± 0.68 vs. 2.13 ± 0.71,

TABLE 1 Baseline characteristics of patients.

Parameters	DM (n = 57)	Control (n = 49)	*P* value
Age (years)	32.16 ± 6.50	31.73 ± 6.44	0.733
Sex			0.728
Female	33 (57.89)	30 (61.22)	
Male	24 (42.11)	19 (38.78)	
BMI (kg/m^2)	42.48 ± 7.33	41.87 ± 7.63	0.676
BMI-based classes, n (%)			0.900
32.5 ≤ BMI < 37.5	17 (29.82)	15 (30.61)	
37.5 ≤ BMI < 50	30 (52.63)	27 (55.10)	
BMI ≥ 50	10 (17.54)	7 (14.29)	
Obesity comorbidities			
Hypertension, n (%)	22 (38.60)	17 (34.69)	0.678
Obstructive sleep, n (%) apnea-hypopnea syndrome, n (%)	34 (59.65)	26 (53.06)	0.495
Tooth brushing			0.859
≤1 time/day	16 (28.07)	13 (26.53)	
≥2 times/day	41 (71.93)	36 (73.47)	
Fasting plasma glucose (mmol/L)	8.49 ± 3.39	5.04 ± 0.54	< 0.001
HbA1c (%)	7.71 ± 2.24	5.37 ± 0.28	< 0.001
Diabetes treatment, n (%)	24 (42.11)	–	–
On insulin therapy, n (%)	4 (7.02)	–	–

Data are presented as mean ± SD or n (%). P value refers to the statistical difference DM vs. Control.
BMI, body mass index; HbA1c, glycated hemoglobin.

10.3389/fendo.2024.1431728

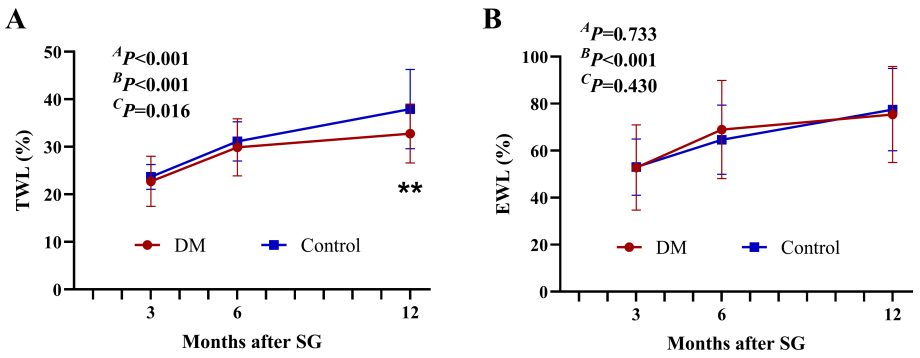

FIGURE 2
Weight-loss effect after SG. The TWL% **(A)** and EWL% **(B)** after SG. **P < 0.01 DM vs. Control. ^{A}P by group, ^{B}P over time, and ^{C}P due to the interaction of the two factors in the two-way ANOVA. TWL%, percentage of total weight loss; EWL%, percentage of excess weight loss; SG, sleeve gastrectomy.

P < 0.01), and CAL (2.04 ± 0.96 vs. 1.69 ± 0.61, P < 0.05) than those in the Control group (Table 4), indicating the worse periodontal condition in patients with T2D than those without. No significant difference was detected in the level of PLI between the two groups before surgery. Compared with those at baseline, significantly lower PLI and BI values were detected after SG in both the DM and the Control group. No statistically significant change was observed in PD or CAL after SG neither in the DM group nor in the Control group. At 12 months after SG, the DM group had similar levels of PLI, BI, and CAL but higher level of PD (4.08 ± 0.92 vs. 3.63 ± 1.03, P < 0.05) compared with the Control group.

3.6 Changes in inflammatory markers after SG

As shown in Table 5, the DM group showed higher levels of hs-CRP and IL-6 compared with the Control group at baseline. However, significant difference was detected only in IL-6 (4.21 ± 2.11 vs. 3.36 ± 1.91, P < 0.05). Both groups showed significantly lower levels of hs-CRP and IL-6 as well as similar level of TNF-α after SG than at baseline. At 12 months after SG, no significant difference was detected between the two groups in levels of hs-CRP, IL-6, or TNF-α.

TABLE 2 Glucose homeostasis before and after SG.

Parameters	Baseline		6 months after SG			12 months after SG		
	n	Mean ± SD	n	Mean ± SD	^{a}P value	n	Mean ± SD	^{b}P value
HbA1c (%)								
DM	57	7.71 ± 2.24**	55	5.02 ± 0.82	< 0.001	51	5.06 ± 0.87	< 0.001
Control	49	5.37 ± 0.28	48	5.11 ± 0.21	< 0.001	41	5.03 ± 0.24	< 0.001
FPG (mmol/L)								
DM	57	8.49 ± 3.39**	55	4.66 ± 0.67**	< 0.001	51	4.49 ± 0.59**	< 0.001
Control	49	5.04 ± 0.54	48	4.28 ± 0.70	< 0.001	41	4.06 ± 0.56	< 0.001
Fasting insulin (mIU/L)								
DM	57	32.54 ± 24.53	55	10.05 ± 7.53	< 0.001	51	7.54 ± 4.90	< 0.001
Control	49	26.52 ± 12.52	48	8.97 ± 5.42	< 0.001	41	6.77 ± 4.02	< 0.001
HOMA-IR								
DM	57	12.23 ± 10.31**	55	1.97 ± 1.12	< 0.001	51	1.46 ± 0.75	< 0.001
Control	49	5.91 ± 3.98	48	1.71 ± 0.79	< 0.001	41	1.22 ± 0.41	< 0.001

Data are presented as mean ± SD. [a]P value refers to the statistical difference 6 months after SG vs. baseline. [b]P value refers to the statistical difference 12 months after SG vs. baseline. **P < 0.01 DM vs. control.
HbA1c, glycated hemoglobin; FPG, fasting plasma glucose; HOMA-IR, the homeostatic model assessment of insulin resistance.

10.3389/fendo.2024.1431728

TABLE 3 Lipid profiles before and after SG.

Parameters	Baseline		6 months after SG			12 months after SG		
	n	Mean ± SD	n	Mean ± SD	[a]*P* value	n	Mean ± SD	[b]*P* value
Triglycerides (mmol/L)								
DM	57	2.42 ± 1.34**	55	1.17 ± 0.45	< 0.001	51	0.89 ± 0.31	< 0.001
Control	49	1.49 ± 0.60	48	1.01 ± 0.42	< 0.001	41	0.87 ± 0.45	< 0.001
Total cholesterol (mmol/L)								
DM	57	5.19 ± 1.45	55	4.96 ± 1.22	0.367	51	4.84 ± 0.96*	0.147
Control	49	4.76 ± 1.28	48	4.92 ± 1.21	0.528	41	4.25 ± 1.17	0.052
LDL-c (mmol/L)								
DM	57	3.03 ± 0.85	55	3.11 ± 1.03	0.654	51	2.76 ± 0.38**	0.039
Control	49	2.97 ± 0.89	48	2.93 ± 0.86	0.822	41	2.35 ± 0.77	< 0.001
HDL-c (mmol/L)								
DM	57	1.13 ± 0.49	55	1.30 ± 0.34	0.036	51	1.43 ± 0.22	< 0.001
Control	49	1.15 ± 0.47	48	1.31 ± 0.54	0.123	41	1.41 ± 0.38	0.005
NEFA (umol/dL)								
DM	57	83.92 ± 28.02	55	75.06 ± 20.02	0.058	51	58.73 ± 18.45	< 0.001
Control	49	85.65 ± 37.06	48	77.46 ± 32.11	0.247	41	62.44 ± 31.46	0.002

Data are presented as mean ± SD. [a]P value refers to the statistical difference 6 months after SG vs. baseline. [b]P value refers to the statistical difference 12 months after SG vs. baseline. *P < 0.05, **P < 0.01 DM vs. control.
LDL-c, low-density lipoprotein-cholesterol; HDL-c, high-density lipoprotein-cholesterol; NEFA, nonesterified fatty acids.

4 Discussion

Obesity and T2D are two of the most common chronic diseases worldwide. Cross-sectional studies supported that there was a strong connection between periodontitis and obesity or T2D (9). As the most commonly performed BMS procedure, SG has been confirmed to be more effective than conventional medical therapy for long-term weight loss and control of T2D (22, 23). However,

TABLE 4 Comparison of periodontal status before and after SG.

Parameters	Baseline		6 months after SG			12 months after SG		
	n	Mean ± SD	n	Mean ± SD	[a]*P* value	n	Mean ± SD	[b]*P* value
PLI								
DM	57	2.20 ± 0.43	55	1.74 ± 0.37	< 0.001	51	1.78 ± 0.35	< 0.001
Control	49	2.05 ± 0.37	48	1.79 ± 0.44	0.002	41	1.85 ± 0.32	0.008
PD (mm)								
DM	57	4.10 ± 1.08*	55	4.12 ± 0.96	0.918	51	4.08 ± 0.92*	0.918
Control	49	3.68 ± 0.87	48	3.77 ± 0.92	0.622	41	3.63 ± 1.03	0.803
BI								
DM	57	2.67 ± 0.68**	55	2.09 ± 0.49	< 0.001	51	2.05 ± 0.48	< 0.001
Control	49	2.13 ± 0.71	48	1.82 ± 0.52	0.016	41	1.88 ± 0.39	0.047
CAL (mm)								
DM	57	2.04 ± 0.96*	55	2.05 ± 1.12	0.960	51	2.02 ± 1.14	0.921
Control	49	1.69 ± 0.61	48	1.75 ± 0.73	0.661	41	1.66 ± 0.57	0.811

Data are presented as mean ± SD. [a]P value refers to the statistical difference 6 months after SG vs. baseline. [b]P value refers to the statistical difference 12 months after SG vs. baseline. *P < 0.05, **P < 0.01 DM vs. control.
PLI, plaque index; PD, probing depth; BI, bleeding index; CAL, clinical attachment loss.

10.3389/fendo.2024.1431728

TABLE 5 Levels of inflammatory markers before and after SG.

Parameters	Baseline		6 months after SG			12 months after SG		
	n	Mean ± SD	n	Mean ± SD	[a]*P* value	n	Mean ± SD	[b]*P* value
hs-CRP (mg/L)								
DM	57	12.37 ± 9.14	55	5.65 ± 4.43	< 0.001	51	5.17 ± 4.51	< 0.001
Control	49	9.51 ± 7.27	48	4.93 ± 3.72	<0.001	41	5.21 ± 4.01	< 0.001
IL-6 (pg/ml)								
DM	57	4.21 ± 2.11*	55	2.79 ± 1.61	< 0.001	51	2.93 ± 1.95	0.002
Control	49	3.36 ± 1.91	48	2.65 ± 1.29	0.035	41	2.37 ± 1.34	< 0.001
TNF-α (pg/ml)								
DM	57	11.01 ± 7.43	55	10.54 ± 8.24	0.752	51	11.36 ± 6.41	0.795
Control	49	11.73 ± 6.86	48	11.46 ± 7.16	0.850	41	11.23 ± 5.25	0.697

Data are presented as mean ± SD. [a]P value refers to the statistical difference 6 months after SG vs. baseline. [b]P value refers to the statistical difference 12 months after SG vs. baseline. *P < 0.05 DM vs. control.
hs-CRP, high sensitive C-reactive protein; IL-6, interleukin-6; TNF-α, tumour necrosis factor alpha.

further studies are needed to elucidate the impact of SG on the periodontal status of patients with and without T2D.

The principal findings of the present study were as follows: 1. For patients with obesity and scheduled for SG, those with T2D had further worsened periodontal status compared with those without; 2. Both patients with and without T2D demonstrated improved periodontal status for up to 1 year after SG, accompanied by weight loss and glucose reduction; 3. Even patients with T2D achieved less TWL% after surgery than those without, their periodontal condition had more substantial improvement with no significant difference in PLI and BI between groups at 1 year after SG; 4. The significant reduction in the inflammatory biomarkers, including hs-CRP and IL-6, contributed to the improvement of periodontal status after SG in both groups.

The patients in the present study consisted of mainly females, with a mean age of approximately 32 years. Previous studies have confirmed that tobacco smoking has a detrimental effect on the incidence and progression of periodontitis (24), so participants with active smoking within the past 6 months were excluded from the current study. 28.07% of patients with T2D and 24.40% of patients without T2D had a tooth brushing ≤1 time/day, indicating a low level of attention to oral hygiene in the patients included. In addition, only 42.11% of patients with T2D were already on treatment, suggesting the poor awareness towards personal health among the participants.

Our study further confirmed the weight loss effect of SG with more than 30% TWL at 1 year after surgery in both groups. A previous meta-analysis including 6235 Asian patients reported 32.1% TWL at 1 year after SG (25). Our previous research demonstrated that, male and female patients with balanced baseline BMI could achieve comparable TWL% for up to 1 year after SG (20). In addition, out results showed that patients with T2D achieved less TWL% after surgery than those without, which is similar to our previous report (10). Another study performed by Diedisheim et al. demonstrated subjects with obesity and T2D who have poor pre-operative glycemic control displayed reduced weight-loss and less improvement in body composition compared to patients with obesity but without T2D (26). These results suggest that even though the rapid and sustained weight loss effect of BMS has been confirmed, glycemic control prior to surgery is an important factor to be taken into account in the expectation of the weight loss outcome after surgery.

Previous studies have confirmed that T2D is associated with a higher prevalence, incidence, severity, and progression of periodontitis (9, 27, 28). Patients with poorly controlled diabetes have more serious clinical symptoms of periodontitis compared with those without diabetes or well controlled diabetes (29, 30). A study from Italian participants demonstrated that the probability of severe periodontitis in patients increased by approximately 60% for 1 unit of increase in serum HbAlc (30). However, it should be noted that the evidence abovementioned focused on the general population, with some overweight individuals involved at most. There has been no evidence yet for patients with pathological obesity, especially those who meet the indications for BMS. The present study filled in the blank of this area that we demonstrated more serious clinical symptoms of periodontitis (with higher PD, BI, and CAL) in patients scheduled for SG with T2D compared with those without diabetes. PLI is a parameter that closely related to the individual oral hygiene habits (31). There was no significant difference in tooth brushing between the DM group and the Control group, and that could be the reason why there was similar levels of PLI between groups at baseline. The plausible pathogenic mechanisms of T2D promoting the susceptibility of periodontitis included microbiome factors, enhanced inflammatory response via cytokines or adipokines, host immune factors, and oxidative stress (32).

In addition to the improvements in systemic conditions (glucose homeostasis, insulin sensitivity, and plasma lipid profiles), the present study revealed a positive impact of SG on periodontal status in both the DM and the Control group characterized by a decrease in periodontal inflammation and an improvement of oral hygiene situation, which was reflected by the

decrease in BI and PLI, respectively. Jaiswal et al. reported improvements in the bleeding score and PLI 6 months after BMS and attributed to changes in diet and oral hygiene instructions provided to patients before surgery (13). However, another prospective study conducted by Sales-Peres et al. demonstrated significantly increased gingival bleeding and unaltered CAL 6 months after BMS, suggesting the deterioration of periodontal conditions after bariatric surgery (33). The discrepancy among studies may be attributed to differences in individual characteristics and oral hygiene intervention. As far as we know, there has been no existing evidence comparing the periodontal status between patients with and without diabetes after BMS. Our results confirmed that both patients with and without T2D could benefit from SG in terms of periodontal status in the absence of any instructions for oral hygiene. In addition, our results showed no obvious change in PD or CAL after SG. The reason could be that these parameters often change only after periodontal surgical treatment (13), which was not involved in this study.

The real mechanisms underlying the improvement in periodontal status after SG in patients with T2D are not well understood. Both obesity and T2D are characterized by persistent, low-grade inflammation (34). Low–grade systemic inflammation has also been proposed as a potential causative factor for periodontitis (35). The most important mediators related to this association are TNF–α and IL–6, which may alter the activities of leukocytes, osteoblasts and osteoclasts, causing periodontal tissue destruction (36). The present study demonstrated significant higher level of IL-6 in the DM group before surgery. The result is consistent with a previous report by Rodrigues et al., in which they found higher levels of IL-6 and hs-CRP in patients with T2D, especially in those with BMI > 30 kg/m^2 (37). In addition, our study demonstrated a significantly decrease in levels of hs-CRP and IL-6 after SG than at baseline in both groups. Mallipedhi et al. investigated changes in inflammatory markers after SG in patients with impaired glucose homeostasis and T2D, and reached the same conclusion as ours (38). In addition, they also observed a significant improvement in leptin as well as unaltered adiponectin and IL-10 after SG.

The major strengths of the current study are that we compared the impact of SG on the periodontal status of patients with and without T2D based on a prospective cohort in a real-world setting. However, this study has several limitations. First, information on individual oral habits after surgery was not involved. However, with no additional instructions for oral hygiene was provided at the time of discharge or in the process of follow-up, the possible individual behavioral changes should originate from the surgery or its related other improvements. Second, the generalizability of the results is limited by the single-center design and the relatively short 1-year follow-up period.

5 Conclusion

In conclusion, both patients with and without T2D demonstrated improved periodontal status for up to 1 year after SG. Patients with T2D achieved less weight loss but a more substantial improvement in periodontal condition. The significant reduction in inflammatory biomarkers contributed to the improvement of periodontal status after SG.

Data availability statement

The raw data supporting the conclusions of this article will be made available by the authors, without undue reservation.

Ethics statement

The studies involving humans were approved by Ethics Committee on Scientific Research of Shandong University Qilu Hospital. The studies were conducted in accordance with the local legislation and institutional requirements. The participants provided their written informed consent to participate in this study.

Author contributions

XB: Formal analysis, Methodology, Resources, Writing – original draft. PZ: Data curation, Formal analysis, Methodology, Writing – original draft. TL: Data curation, Formal analysis, Project administration, Writing – original draft. TZ: Data curation, Methodology, Software, Writing – original draft. YL: Data curation, Resources, Writing – original draft. SX: Data curation, Methodology, Writing – original draft. SL: Conceptualization, Investigation, Supervision, Visualization, Writing – review & editing. XLH: Conceptualization, Investigation, Supervision, Visualization, Writing – review & editing. XH: Conceptualization, Funding acquisition, Investigation, Supervision, Validation, Visualization, Writing – review & editing.

Funding

The author(s) declare financial support was received for the research, authorship, and/or publication of this article. This study was funded by the National Natural Science Foundation of China Grants (82100853), the Natural Science Foundation of Shandong Province of China (ZR2021QH028).

Acknowledgments

The authors thank the nursing staff of the Department of General Surgery, Qilu Hospital of Shandong University, for their expert assistance in performing the study, and all the patients included and their families for their cooperation.

Conflict of interest

The authors declare that the research was conducted in the absence of any commercial or financial relationships that could be construed as a potential conflict of interest.

Publisher's note

References

1. The World Obesity Federation. *World obesity atlas* (2024). Available online at: https://www.worldobesity.org/resources/resource-library/world-obesity-atlas-2024.

2. Ahmad E, Lim S, Lamptey R, Webb DR, Davies MJ. Type 2 diabetes. *Lancet*. (2022) 400:1803–20. doi: 10.1016/S0140-6736(22)01655-5

3. Slots J. Periodontitis: facts, fallacies and the future. *Periodontol 2000*. (2017) 75:7–23. doi: 10.1111/prd.12221

4. Tonetti MS, Jepsen S, Jin L, Otomo-Corgel J. Impact of the global burden of periodontal diseases on health, nutrition and wellbeing of mankind: A call for global action. *J Clin Periodontol*. (2017) 44:456–62. doi: 10.1111/jcpe.12732

5. Graziani F, Karapetsa D, Alonso B, Herrera D. Nonsurgical and surgical treatment of periodontitis: how many options for one disease? *Periodontol 2000*. (2017) 75:152–88. doi: 10.1111/prd.12201

6. de Moura-Grec PG, Yamashita JM, Marsicano JA, Ceneviva R, de Souza Leite CV, de Brito GB, et al. Impact of bariatric surgery on oral health conditions: 6-months cohort study. *Int Dent J*. (2014) 64:144–9. doi: 10.1111/idj.12090

7. Pataro AL, Costa FO, Cortelli SC, Cortelli JR, Dupim Souza AC, Nogueira Guimarães Abreu MH, et al. Influence of obesity and bariatric surgery on the periodontal condition. *J Periodontol*. (2012) 83:257–66. doi: 10.1902/jop.2011.100782

8. Čolak D, Cmok Kučič A, Pintar T, Gašpirc B, Gašperšič R. Periodontal and systemic health of morbidly obese patients eligible for bariatric surgery: a cross-sectional study. *BMC Oral Health*. (2022) 22:174. doi: 10.1186/s12903-022-02207-0

9. Wu CZ, Yuan YH, Liu HH, Li SS, Zhang BW, Chen W, et al. Epidemiologic relationship between periodontitis and type 2 diabetes mellitus. *BMC Oral Health*. (2020) 20:204. doi: 10.1186/s12903-020-01180-w

10. Huang X, Zhao Y, Liu T, Wu D, Shu J, Yue W, et al. β-cell function and insulin dynamics in obese patients with and without diabetes after sleeve gastrectomy. *Diabetes*. (2024) 73:572–84. doi: 10.2337/db22-1048

11. Huang X, Liu T, Zhong M, Cheng Y, Hu S, Liu S. Predictors of glycemic control after sleeve gastrectomy versus Roux-en-Y gastric bypass: A meta-analysis, meta-regression, and systematic review. *Surg Obes Relat Dis*. (2018) 14:1822–31. doi: 10.1016/j.soard.2018.08.027

12. Brown WA, Liem R, Al-Sabah S, Anvari M, Boza C, Cohen RV, et al. Metabolic bariatric surgery across the IFSO chapters: key insights on the baseline patient demographics, procedure types, and mortality from the eighth IFSO global registry report. *Obes Surg*. (2024) 34:1764–77. doi: 10.1007/s11695-024-07196-3

13. Jaiswal GR, Jain VK, Dhodapkar SV, Kumathalli KI, Kumar R, Nemawat A, et al. Impact of bariatric surgery and diet modification on periodontal status: A six month cohort study. *J Clin Diagn Res*. (2015) 9:ZC43–5. doi: 10.7860/JCDR/2015/14663.6489

14. Arboleda S, Pianeta R, Vargas M, Lafaurie GI, Aldana-Parra F, Chaux CF. Impact of bariatric surgery on periodontal status in an obese cohort at one year of follow-up. *Med Int (Lond)*. (2021) 1:4. doi: 10.3892/mi.2021.4

15. Marsicano JA, Sales-Peres A, Ceneviva R, de C Sales-Peres SH. Evaluation of oral health status and salivary flow rate in obese patients after bariatric surgery. *Eur J Dent*. (2012) 6:191–7.

16. Papapanou PN, Sanz M, Buduneli N, Dietrich T, Feres M, Fine DH, et al. Periodontitis: Consensus report of workgroup 2 of the 2017 World Workshop on the Classification of Periodontal and Peri-Implant Diseases and Conditions. *J Periodontol*. (2018) 89 Suppl 1:S173–82. doi: 10.1002/JPER.17-0721

17. Matthews DR, Hosker JP, Rudenski AS, Naylor BA, Treacher DF, Turner RC. Homeostasis model assessment: insulin resistance and beta-cell function from fasting plasma glucose and insulin concentrations in man. *Diabetologia*. (1985) 28:412–9. doi: 10.1007/BF00280883

18. Zarabadipour M, Makhlooghi Sari M, Moghadam A, Kazemi B, Mirzadeh M. Effects of educational intervention on dental plaque index in 9-year-old children. *Int J Dent*. (2022) 2022:7339243. doi: 10.1155/2022/7339243

19. Mazza JE, Newman MG, Sims TN. Clinical and antimicrobial effect of stannous fluoride on periodontitis. *J Clin Periodontol*. (1981) 8:203–12. doi: 10.1111/j.1600-051X.1981.tb02031.x

20. Shu J, Zhu T, Xiong S, Liu T, Zhao Y, Huang X, et al. Sex dimorphism in the effect and predictors of weight loss after sleeve gastrectomy. *Front Endocrinol (Lausanne)*. (2024) 14:1333051. doi: 10.3389/fendo.2023.1333051

21. Lean ME, Leslie WS, Barnes AC, Brosnahan N, Thom G, McCombie L, et al. Primary care-led weight management for remission of type 2 diabetes (DiRECT): an open-label, cluster-randomised trial. *Lancet*. (2018) 391:541–51. doi: 10.1016/S0140-6736(17)33102-1

22. Mingrone G, Panunzi S, De Gaetano A, Guidone C, Iaconelli A, Capristo E, et al. Metabolic surgery versus conventional medical therapy in patients with type 2 diabetes: 10-year follow-up of an open-label, single-centre, randomised controlled trial. *Lancet*. (2021) 397:293–304. doi: 10.1016/S0140-6736(20)32649-0

23. Courcoulas AP, Patti ME, Hu B, Arterburn DE, Simonson DC, Gourash WF, et al. Long-term outcomes of medical management vs bariatric surgery in type 2 diabetes. *JAMA*. (2024) 331:654–64. doi: 10.1001/jama.2024.0318

24. Leite FRM, Nascimento GG, Scheutz F, López R. Effect of smoking on periodontitis: A systematic review and meta-regression. *Am J Prev Med*. (2018) 54:831–41. doi: 10.1016/j.amepre.2018.02.014

25. Jaruvongvanich V, Wongjarupong N, Vantanasiri K, Samakkarnthai P, Ungprasert P. Midterm outcome of laparoscopic sleeve gastrectomy in asians: a systematic review and meta-analysis. *Obes Surg*. (2020) 30:1459–67. doi: 10.1007/s11695-019-04332-2

26. Diedisheim M, Poitou C, Genser L, Amouyal C, Bouillot JL, Ciangura C, et al. Weight loss after sleeve gastrectomy: does type 2 diabetes status impact weight and body composition trajectories? *Obes Surg*. (2021) 31:1046–54. doi: 10.1007/s11695-020-05075-1

27. Genco RJ, Borgnakke WS. Diabetes as a potential risk for periodontitis: association studies. *Periodontol 2000*. (2020) 83:40–5. doi: 10.1111/prd.12270

28. Graves DT, Ding Z, Yang Y. The impact of diabetes on periodontal diseases. *Periodontol 2000*. (2020) 82:214–24. doi: 10.1111/prd.12318

29. Singh M, Bains VK, Jhingran R, Srivastava R, Madan R, Maurya SC, et al. Prevalence of periodontal disease in type 2 diabetes mellitus patients: A cross-sectional study. *Contemp Clin Dent*. (2019) 10:349–57. doi: 10.4103/ccd.ccd_652_18

30. Romano F, Perotto S, Mohamed SEO, Bernardi S, Giraudi M, Caropreso P, et al. Bidirectional association between metabolic control in type-2 diabetes mellitus and periodontitis inflammatory burden: A cross-sectional study in an italian population. *J Clin Med*. (2021) 10:1787. doi: 10.3390/jcm10081787

31. Soldo M, Matijević J, Malčić Ivanišević A, Čuković-Bagić I, Marks L, Nikolov Borić D, et al. Impact of oral hygiene instructions on plaque index in adolescents. *Cent Eur J Public Health*. (2020) 28:103–7. doi: 10.21101/cejph.a5066

32. Zhao M, Xie Y, Gao W, Li C, Ye Q, Li Y. Diabetes mellitus promotes susceptibility to periodontitis-novel insight into the molecular mechanisms. *Front Endocrinol (Lausanne)*. (2023) 14:1192625. doi: 10.3389/fendo.2023.1192625

33. Sales-Peres SHC, Sales-Peres MC, Ceneviva R, Bernabé E. Weight loss after bariatric surgery and periodontal changes: a 12-month prospective study. *Surg Obes Relat Dis*. (2017) 13:637–42. doi: 10.1016/j.soard.2016.08.007

34. Cox AJ, West NP, Cripps AW. Obesity, inflammation, and the gut microbiota. *Lancet Diabetes Endocrinol*. (2015) 3:207–15. doi: 10.1016/S2213-8587(14)70134-2

35. Genco RJ, Grossi SG, Ho A, Nishimura F, Murayama Y. A proposed model linking inflammation to obesity, diabetes, and periodontal infections. *J Periodontol*. (2005) 76:2075–84. doi: 10.1902/jop.2005.76.11-S.2075

36. Noh MK, Jung M, Kim SH, Lee SR, Park KH, Kim DH, et al. Assessment of IL-6, IL-8 and TNF-α levels in the gingival tissue of patients with periodontitis. *Exp Ther Med*. (2013) 6:847–51. doi: 10.3892/etm.2013.1222

37. Rodrigues KF, Pietrani NT, Bosco AA, Campos FMF, Sandrim VC, Gomes KB. IL-6, TNF-α, and IL-10 levels/polymorphisms and their association with type 2 diabetes mellitus and obesity in Brazilian individuals. *Arch Endocrinol Metab*. (2017) 61:438–46. doi: 10.1590/2359-3997000000254

38. Zhu C, Mei F, Gao J, Zhou D, Lu L, Qu S. Changes in inflammatory markers correlated with increased testosterone after laparoscopic sleeve gastrectomy in obese Chinese men with acanthosis nigricans. *J Dermatol*. (2019) 46:338–42. doi: 10.1111/1346-8138.14783

frontiers | Frontiers in Endocrinology

TYPE Original Research
PUBLISHED 14 October 2024
DOI 10.3389/fendo.2024.1440250

OPEN ACCESS

EDITED BY
Yayun Wang,
Air Force Medical University, China

REVIEWED BY
Giovanni Casella,
Sapienza University of Rome, Italy
Diego Moriconi,
University of Pisa, Italy

*CORRESPONDENCE
Anca Elena Sirbu
anca.sirbu@umfcd.ro

RECEIVED 29 May 2024
ACCEPTED 25 September 2024
PUBLISHED 14 October 2024

CITATION
Popa MM, Sirbu AE, Malinici EA, Copaescu C and Fica S (2024) Obesity-related renal dysfunction: gender-specific influence of visceral adiposity and early impact of metabolic and bariatric surgery.
Front. Endocrinol. 15:1440250.
doi: 10.3389/fendo.2024.1440250

Obesity-related renal dysfunction: gender-specific influence of visceral adiposity and early impact of metabolic and bariatric surgery

Miruna Maria Popa[1,2], Anca Elena Sirbu[1,2]*, Elisabeta Andreea Malinici[1,2], Catalin Copaescu[3] and Simona Fica[1,2]

[1]Department of Endocrinology, Carol Davila University of Medicine and Pharmacy, Bucharest, Romania, [2]Department of Endocrinology and Diabetes, Elias Emergency University Hospital, Bucharest, Romania, [3]General Surgery Department, Ponderas Hospital, Bucharest, Romania

Introduction: Renal dysfunction is a recognized complication of obesity with an incompletely characterized pathophysiology. Improvement of glomerular filtration rate (GFR) after metabolic and bariatric surgery (MBS) has been reported across all classes of renal function. Inter-gender differences with regard to correlates of renal function have been described, but the influence of body composition is an understudied area. We aimed to explore determinants of renal function in obesity and to assess its variations after MBS, with a focus on body composition parameters in males and females, respectively.

Materials, methods: We conducted a retrospective study on 196 patients who underwent laparoscopic sleeve gastrectomy, evaluated preoperatively and 6 months after the intervention. Recorded data included clinical and biochemical assessment, as well as body composition estimation via dual-energy X-ray absorptiometry. Serum creatinine-based formulas were used for the estimation of GFR.

Results: We included a total of 196 patients (80 males and 116 females), with a mean age of 41.43 ± 10.79. Median baseline body mass index was 42.6 (6.61) kg/m^2 and 6 months excess weight loss (EWL) reached 71.43 ± 17.18%, in females, estimated GFR correlated negatively with visceral adipose tissue (VAT) mass (rho=-.368) and this correlation was stronger in females with type 2 diabetes mellitus. Moreover, women in the third VAT mass tertile were 5 times more likely to have reduced GFR compared to the first tertile. Renal function improved after MBS across all classes of filtration. In males, this improvement correlated with EWL (rho=.358) and lean mass variation (rho=-.412), while in females it correlated with VAT mass variation (rho=-.266).

Conclusions: Our results are consistent with previous findings on the positive impact of MBS on renal function and suggest a more prominent impact of visceral adiposity on GFR in females.

KEYWORDS

obesity, renal dysfunction, metabolic and bariatric surgery, sleeve gastrectomy, visceral adiposity, body composition

1 Introduction

Obesity is a multisystem disease, that has undoubtedly reached pandemic proportions. In 2020, there were over 800 million adults living with obesity worldwide and current trends predict a prevalence of over 1.5 billion in 2035 (1). Parallelling the obesity epidemic, chronic kidney disease is also a major cause of morbi-mortality worldwide (2). Multiple epidemiologic studies have shown that excessive body weight is a risk factor for both the onset and the progression of kidney disease across all ages and across a wide range of co-existing pathologies (3–9).

A more in-depth analysis of this relationship reveals that the two entities are, in fact, intertwined, involving complex and multilayered mechanisms of augmenting the detrimental effects of one another (3, 10–12). Thus, research in the field of obesity-related renal dysfunction is challenging and the issue remains incompletely explored, despite the fact that the interest in this topic dates from decades ago (13). The diversity of body composition among patients with similar body mass index (BMI), including varying proportions of adipose tissue components (e.g. visceral vs subcutaneous adiposity) is widely acknowledged (14). The distinct influences body compartments exert on renal parameters might prove useful in shedding more light on this adipo-renal relationship.

Metabolic and bariatric surgery (MBS) is currently the most effective intervention in severe obesity, with clear benefits on related comorbidities (15). Among these, the postoperative improvement of renal function has been reported in the past years and a number of authors regard MBS as a short and long-term renoprotective intervention (16). Specifically, MBS is associated with improved glomerular filtration rate (GFR), decreased albuminuria and a lower rate of progression to end-stage-renal disease upon follow-up (17, 18).

In the current study, we aimed to explore baseline determinants of renal function, focusing on body composition parameters, as well as short-term postoperative dynamics in patients with obesity undergoing laparoscopic sleeve gastrectomy (LSG).

2 Methods

We conducted a retrospective study on a cohort of adult patients with obesity who benefited from LSG at an International Federation for the Surgery of Obesity and Metabolic Disorders (IFSO) accredited Center of Excellence in Romania. The study followed the standards of the Helsinki Committee for Human Rights and the design received approval from the local ethics committee. All patients provided written informed consent. Evaluations were performed preoperatively and 6 months after the intervention.

Inclusion criteria consisted of adult age (>18 years old) and meeting the indication for MBS as per guideline recommendations (19). Exclusion criteria were represented by previous bariatric therapy, documented kidney disease, family history positive for hereditary kidney disease, usage of nephrotoxic medication during the past year and excessive alcohol consumption (defined as 5 or more drinks on any day or 15 or more per week for men and 4 or more on any day or 8 or more drinks per week for women) (20). Of the 268 patients initially included, 33 had incomplete baseline evaluation, while an additional 39 were either lost to follow-up or had incomplete evaluation during their second visit. Consequently, 196 patients were analyzed in the present study.

2.1 Clinical and biological evaluation

Body weight and height were measured (both at baseline and postoperatively) using a standardized digital scale with fixed stadiometer. BMI was calculated as weight (in kilograms) divided by the square of height (in meters). Excess weight loss percentage (%EWL) was calculated as [(Baseline BMI – Postoperative BMI)/(Baseline BMI – 25)] × 100, as defined in literature (21). Arterial blood pressure (ABP) was assessed in-office, at brachial artery level, with the patient in seating position, using an electronic sphygmomanometer. Hypertension (HTN) was defined as systolic ABP ≥140 mmHg, diastolic ABP ≥90 mmHg, or antihypertensive medication use following a previously established diagnosis. Postoperative improvement of ABP was defined as normalized ABP with consistent or de-escalated medical treatment. Diabetes was defined per American Diabetes Association criteria (22) or by the use of anti-hyperglycemic drugs or medical nutritional therapy following a previously established positive diagnosis. Improvement of glycemic control was defined as improved glycated hemoglobin by at least 0.5% and/or de-escalation of medical treatment.

Both pre- and postoperative assays were performed in the same laboratory. Creatinine was determined through colorimetric enzymatic assay and glomerular filtration rate was estimated (eGFR) using the CKD Epidemiology Collaboration (CKD-EPI) 2021 serum creatinine-based formula, adjusted for standard body surface area of 1.73 m^2 (23).

Classes of renal function were defined as: hyperfiltration (≥ 125), normal function (90-124), mild dysfunction (60-89), mild-to-moderate dysfunction (45-59 ml/min/1.73 m^2), in accordance with KDIGO guidelines and commonly employed hyperfiltration cut-off values (24–26). Renal function was also estimated using the formula proposed by Basolo and colleagues (eGFR = 53 + 0.7 × (140 − Age) × Weight/(96xSCr) × (0.85 if female)), aimed at characterizing hyperfiltration (27).

2.2 Scan procedure—dual-energy x-ray absorptiometry

Whole body DXA scans using Lunar iDXA Forma (GE Healthcare) were performed to estimate total and regional body composition. Visceral adipose tissue (VAT) mass was quantified using the CoreScan™ application. Appendicular skeletal mass index (ASMI) was calculated as the sum of upper and lower extremities lean mass expressed in kilograms over the square of height expressed in meters. Quality assurance and control procedures were carried out in accordance with manufacturer indications. All scans were performed by an ISCD-certified DXA technologist, using the same software for analysis.

2.3 Statistical analysis

Statistical analysis was performed using IBM®SPSS® v. 26.0. Parameter variations were defined as $value_{6\ months} - value_{baseline}$. Qualitative data was reported as frequency (percentage). Quantitative data was assessed with *Komologorov-Smirnov* test and normally distributed data was reported as mean ± standard deviation (SD), while parameters with non-normal distribution were described by median and inter-quartile range (IQR). Subsequently, independent and paired *t Student* tests were performed to compare normally distributed parameters, while *Mann-Whitney U* and *Wilcoxon Signed Rank* test were employed for non-normally distributed data. Bivariate correlations were explored using *Pearson's r* and *Spearman's rho*, respectively. Binary and linear adjusted regression models were employed to further explore the predictive value of parameters. Confounders were included as covariates in binary and multinominal regression, in order to validate the results. All analyses were 2-tailed, with a cut-off *p* value of less than 0.05 for statistical significance.

3 Results

The study included a total of 196 patients (80 males and 116 females), with ages ranging from 19 to 68 and a mean of 41.43 ± 10.79, slightly lower in males versus females (p=.08). The diagnosis of obesity had been established for an average of 18.21 ± 10.51 years, similar between the two genders. Median baseline BMI was 42.6 (6.61) kg/m^2 and 6 months EWL reached 71.43 ± 17.18%, with no inter-gender differences.

T2DM and HTN baseline prevalences were 18.9% and 49.5%, with 6 months de-escalation of treatment reported in 51.3% and 43.2% of patients, respectively. Fasting plasma glucose, as well as total cholesterol, VLDL-cholesterol and triglycerides levels showed significant decline at 6 months.

TABLE 1 Pre- and postoperative values of selected parameters.

	Males, n=80			Females, n=116		
Parameter*	Preoperative	6 months	P value	Preoperative	6 months	P value
BMI	43.78 ± 4.84	30.61 ± 4.11	<.001	41.79 (6.44)	30.31 (4.63)	<.001
Creatinine	1 (0.2)	1 (0.2)	<.001	0.9 (0.2)	0.8 (0.1)	<.001
eGFR (creatinine)	93.94 (19.87)	102.48 (23.36)	<.001	83.15 (17.96)	89.59 (20.17)	<.001
Total cholesterol (mg/dl)	198 (66)	175 (42.74)	<.001	199.15 ± 37.79	192.32 ± 35.37	.03
HDL-cholesterol (mg/dl)	47.8 (13.5)	49.9 (11.3)	NS	56.47 ± 10.19	57.2 ± 10.34	NS
LDL-cholesterol (mg/dl)	106.7 (56)	107.4 (43.4)	NS	112.6 (38.7)	113.6 (42.9)	NS
VLDL-cholesterol (mg/dl)	32 (20.6)	20.6 (8.6)	<.001	24.5 (15.2)	17.9 (7.4)	<.001
Triglycerides (mg/dl)	163.5 (110)	104.5 (43)	<.001	122 (70)	89 (36)	<.001
Fasting plasma glucose (mg/dl)	93.5 (22)	79 (14)	<.001	94 (21)	79 (12)	<.001
Total fat mass (kg)	62.07 (15.71)	30.89 (11.81)	<.001	59.89 (14.11)	34.17 (9.89)	<.001
Total lean mass (kg)	71.82 ± 7.29	62.16 ± 6.71	<.001	52.22 ± 5.57	45.28 ± 5.09	<.001
VAT mass (kg)	4.4 (1.56)	1.58 (0.76)	<.001	2.38 (1.01)	1.06 (0.57)	<.001
ASMI (kg/m^2)	10.49 ± 1.09	8.92 ± 0.89	<.001	8.79 ± 0.9	7.57 ± 0.77	<.001

* values are expressed either as mean ± SD, or as median (interquartile range), depending on the type of distribution.
BMI, body mass index, EWL, excess weight loss, eGFR, estimated glomerular filtration rate (determined by CKD-EPI 2021 creatinine-based formula); VAT, visceral adipose tissue; ASMI, appendicular skeletal muscle index.

Males tended to demonstrate greater 6 months percentual variations of body composition compartments - with the exception of total lean mass variation, which was similar between the two genders. Table 1 summarizes the evolution of aforementioned parameters in males and females respectively.

Analysis of gender-specific determinants of renal function revealed a number of differences. Specifically, in females, eGFR correlated negatively with VAT mass (rho=-.368, p<.001), uric acid (rho=-.396, p<.001), glycemia (rho=-.419, p<.001) and VLDL-cholesterol (rho=-.239, p=.001). eGFR-VAT mass correlation was present irrespective of T2DM status, but was stronger in females with T2DM (rho=-.529, p=0.02). None of these results were replicable in males. Moreover, when dividing females according to menopause status (75% premenopausal, 25% postmenopausal), all of the correlations were lost in postmenopausal state.

To further explore the relationship between renal filtration and visceral adiposity, we compared renal function across VAT mass tertiles in females. Women in the third VAT mass tertile were 5 times more likely to have eGFR<90ml/min/1.73m^2 compared to the first tertile (OR=5.2, 95%CI = [1.29,20.99], p=0.02), in a model adjusted for BMI, number of years living with obesity, ASMI, T2DM and smoking status. However, the model lost significance when also accounting for menopausal state. It should be noted that patients demonstrating hyperfiltration were excluded from this analysis in order to ensure adequate comparison.

Stratification of baseline eGFR by standard classes of renal function revealed a very small prevalence of hyperfiltration in our group (1%), with the majority of patients demonstrating mild renal dysfunction (54.6%), followed by normal function (40.3%) and mild-to-moderate dysfunction (4.1%). Postoperatively, renal filtration improved across all defined classes, as depicted in Figure 1. Specific variations (expressed ml/min/1.73m^2) were as follows: an increase from 55.01 (8.4) to 68.63 (20.97) in mild-to-moderate dysfunction class and from 79.35 (11.26) to 88.06 (19.64) in mild dysfunction class patients. In normal function class, baseline and 6 months eGFR values were 98.88 (13.75) and 106.92 (18.87), respectively (p=0.09). Finally, in the two cases exhibiting renal hyperfiltration per standard criteria, eGFR decreased postoperatively. The alternative approach of Basolo et al. (27) for evaluating hyperfiltration in patients with obesity determined the reclassification of 151 patients (77%) as exhibiting hyperfiltration and showed a significant postoperative reduction in their eGFR (145.1 (25.08) vs. 120.64 (28.55), p<.001) (Figure 2). We also considered a surrogate marker, eGFR/ASMI (aimed at controlling for postoperative muscle mass loss) and confirmed a similar pattern.

Finally, we analyzed correlates of renal function variation in all patients exhibiting either increase or decrease of eGFR. Inter-gender differences were evident once more. In males, eGFR variation correlated (p<.001 for all) with EWL (rho=.358) (Figure 3), lean mass (rho=-.412) and ASMI (rho=-.374) variations; in females, on the other hand, eGFR variation only correlated (p=0.01) with VAT mass (rho=-.266) (Figure 4) and LDL (rho=-.279) variations. VAT mass variation was an independent predictor (β=-.246, p=.02) of eGFR variation in females in a model adjusted for baseline eGFR, menopause status, EWL, ASMI variation, LDL variation and additionally for the improvement of both T2DM and HTN (model data: R=.6, R^2=.36, p<.001). Conversely, in males, EWL was an independent predictor of eGFR variation (β=.32, p=.01) in an equivalent model – adjusted for baseline eGFR, ASMI variation, VAT mass variation and for the improvement of T2DM and HTN (model data: R=.63, R^2=.4, p<.001).

4 Discussion

In the present study we investigated the relationship between creatinine-based estimated glomerular filtration rate and DXA-evaluated body composition, as well as basic biochemical parameters in a cohort of patients with severe obesity undergoing LSG. Gender-oriented analysis identified interesting differences in the factors influencing renal function in males vs. females, both at baseline, as well as when considering early (6 months) postoperative variation.

Estimation of renal function by means of serum creatinine levels is currently the most widespread method used in clinical practice for both screening and monitoring and it also constitutes the basis of renal function staging (28). The CKD-EPI formula is believed to yield more accurate results and is, hence, favored by

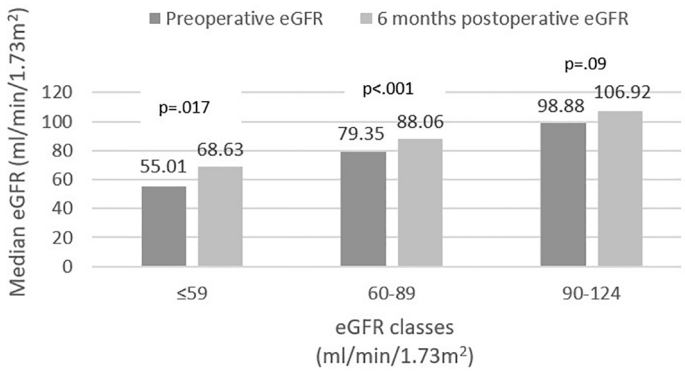

FIGURE 1
CKD-EPI (2021) estimated glomerular filtration rate (eGFR) variation.

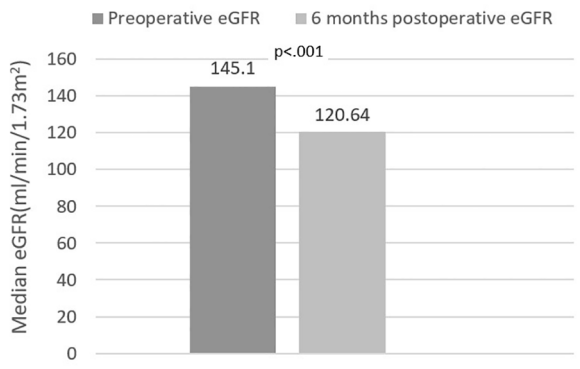

FIGURE 2
Estimated glomerular filtration rate (eGFR) variation in hyperfiltration class [eGFR formula - Basolo et al. (27)].

profile societies (23, 24, 28, 29). Its main limitations derive from the influence of muscle mass and dietary protein intake on serum creatinine levels (30), from the delayed increase in creatinine compared to the onset of renal function decline (31) and from the fact that the equations were developed on a population mainly in the normal BMI range (32). These lead to inaccuracies both in the general population with obesity, as well as in assessing the dynamics after MBS (31–35). Various means of resolving these shortcomings have been proposed in literature, with mostly unsatisfying results. The most popular is de-adjusting from standard body surface area (BSA) of 1.73m^2 and adjusting for calculated BSA (de-indexed equations). However, this method consistently overestimates renal function, since muscle mass, and not total body mass is actually the main contributor to the estimation bias (36, 37). In this regard, Nankivell and colleagues demonstrated that ASMI constitutes the best correlate of eGFR error (34). Considering these results, we used the eGFR provided by CKD-EPI (2021) formula, adjusted for standard body surface area and corrected our analyses for ASMI and ASMI variation in order to provide accuracy. Through this, we were able to stratify patients in classes of renal function and assess their dynamics in compliance with guideline recommendations and

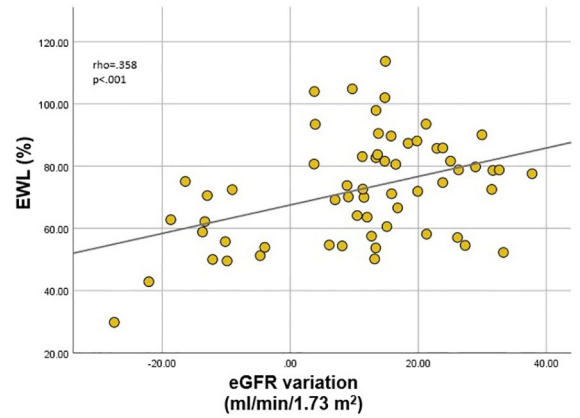

FIGURE 3
Correlation between estimated glomerular filtration rate (eGFR) variation and excess weight loss (EWL) in males.

in line with standard clinical practice. Renal dysfunction is reported to be more prevalent among persons with obesity (11, 38, 39) and our results are in line with previous findings, with the majority of patients exhibiting mild or mild-to-moderate dysfunction at baseline. An ample study, with an 8 million person-year follow-up, elegantly demonstrated that the risk of end-stage CKD progressively increases with the increase of BMI. Particularly, patients with severe obesity had a 7-fold increase in risk compared to normal weight controls (4). Additionally, in a more recent meta-analysis comprising a total of 3 million patients, obesity was associated with an almost two fold increase in the risk of renal function decline) over a 10 year follow-up (6). The largest epidemiologic study regarding CKD in the general Romanian population reported a cumulative prevalence of reduced kidney function (defined as eGFR<60ml/min/1.73m^2) of 3.76% (40). Comparatively, in our cohort, mild-to-moderate renal dysfunction had a prevalence of 4.1%. However, the majority of our patients (56.4%) exhibited mild dysfunction, on which the aforementioned study did not report.

Postoperatively, we identified significant increase in eGFR in patients exhibiting subnormal renal function at baseline; this was paralleled by a statistically insignificant (p=.09) less ample eGFR increase in patients classified as having normal baseline renal function (Figure 1). Interestingly, the patients exhibiting hyperfiltration, demonstrated postoperative decrease of eGFR; however, the very small number of subjects pertaining to this category precludes these results from being statistically relevant. Based on the assumption that currently used formulas underestimate the prevalence of renal hyperfiltration (36, 41), Basolo and colleagues devised a new formula, specifically aimed at more accurately identifying hyperfiltration in patients with obesity (27). Using this approach, we reclassified the majority of the patients (77%) as exhibiting hyperfiltration and confirmed a significant postoperative decrease of eGFR in this class (Figure 2). However, the authors specifically excluded patients with renal dysfunction from their original analysis; therefore, while these results provide further confirmation of eGFR improvement across all renal function classes, re-thinking the stratification of all patients based on the proposed formula is likely to be inaccurate. These outcomes were also confirmed by the comparable variation of eGFR/ASMI [analogous to the procedure employed by Favre and colleagues who used eGFR over lean body mass in their study (42)]. There is currently a robust body of literature with similar results, pointing to the beneficial role of MBS-induced weight loss on renal function (16–18, 33, 43–45). Improvement of GFR and proteinuria are evident in the first months-to-years following surgery, but positive effects have been recorded up to 15 years postoperatively (43).

Obesity negatively impacts renal dynamics through a combination of direct and indirect mechanism; of the latter, the two most important are HTN and T2DM, both of which are widely recognized complications of obesity and also major risk factors for the development of kidney disease. However, direct pathogenic ways, occurring even in the absence of overt HTN/T2DM are believed to be of equal importance. These include hemodynamic alterations and increased sodium reabsorption (leading to initial hyperfiltration, followed by GFR decline), adipokine and cytokine dysregulation,

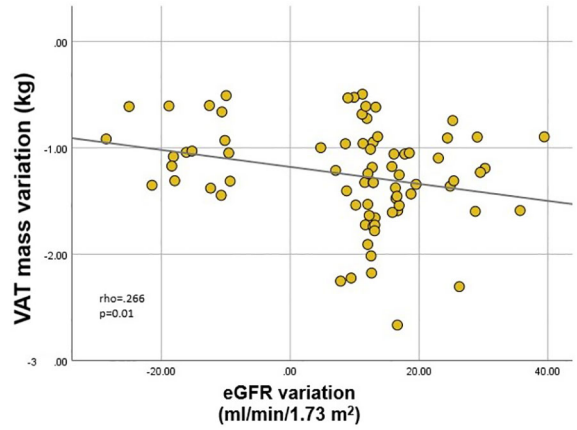

FIGURE 4
Correlation between estimated glomerular filtration rate (eGFR) variation and visceral adipose tissue (VAT) mass variation in females.

insulin resistance, oxidative stress and direct lipotoxicity (3, 10–12). Visceral adipose tissue (VAT) is recognized as the metabolically active, pathogenic compartment, linked to aforementioned alterations (46), as opposed to subcutaneous adipose tissue (SAT), which serves as a buffer for excess energy and has positive metabolic impact (47, 48). Obesity-related adipose tissue dysfunction is characterized by chronic inflammation and M1-polarized macrophage infiltration and activation, all of which occur predominantly in VAT (47, 49). Kidney morphology and physiology (e.g. high vascularization, not paralleled by equally effective local anti-inflammatory guards) determine increased renal sensitivity towards inflammation-induced damage (50). Studies have tied various pro-inflammatory molecules (e.g. tumor necrosis factor-alpha (TNF-α), interleukins 1β and 6 (IL-1β, IL-6) etc.) to the onset of chronic kidney disease (CKD) (50). A landmark study including over 3000 patients revealed that higher circulating TNF-α and fibrinogen levels are associated with more rapid decline of eGFR in patients with established CKD (51). More recently, involvement of TNF-α in renal fibrosis, as well as the benefits of its inhibition have been described in murine aristolochic acid-induced nephropathy (considered superior to previously employed murine models) (52). Moriconi et al. aimed to assess the relationship between IL-1β/Caspase-1, insulin sensitivity and early-stage obesity-related renal damage, namely hyperfiltration. Apart from demonstrating the capacity of IL-1β to predict hyperfiltration in patients with severe obesity, their study had another valuable result – patients in whom GFR did not normalize after MBS also showed failure to normalize circulating IL-1β/Caspase-1 levels (53). These results suggest a pathogenic role of the inflammasome in kidney dysfunction, as well as the potential for achieving renoprotection through targeted anti-inflammatory therapy, in concert with weight reduction. Similar strategies are being considered in diabetic kidney disease, in which renal benefits of medication with potential anti-inflammatory effect (e.g. type 2 sodium-glucose cotransporter inhibitors, glucagon-like peptide-1 receptor agonists, renin-angiotensin-aldosterone system (RAAS) inhibitors) are evidently superior to those of medication that solely achieves tight glycemic control or reduction of arterial blood pressure (54).

Apart from the mechanisms detailed above, it is noteworthy that peri- and intrarenal accumulation of VAT also increases local pressure, activating sympathetic and RAA systems and directly contributes to glomerular lesions (55, 56). In line with these concepts, central adiposity (i.e. various estimates of VAT), perirenal adipose tissue and renal sinus fat exhibit a stronger correlation with the occurrence of obesity-related renal complications than BMI or subcutaneous adipose tissue (57). In a multicentric study using bioelectrical impedance analysis aimed to assess the ability of various obesity indicators to predict renal impairment (GFR decline/new-onset proteinuria) during a 6-year follow-up, only visceral fat area (with a cut-off of 100 cm^2) proved to be a sensitive marker (58). Kataoka and colleagues found that VAT to SAT ratio serves as a predictor of eGFR decline in CKD patients, with a greater impact in females and in patients with lower absolute values of VAT (59). Interestingly, the relationship between VAT mass and CKD development seems to be stronger in patients with lower body weight. In a large scale cohort study (11000 subjects, 5.6-year follow-up), VAT was a predictor of CKD onset only in patients with normal BMI (60).

Accurate estimation of VAT mass has been a topic of great interest in the past years and surrogate markers such as lipid accumulation product (LAP), visceral adiposity index (VAI) (61), novel VAI (NVAI) (62), Chinese-population specific cVAI (63) and, more recently, the metabolic score for visceral fat (METS-VF) (64) have been widely used in studies of obesity-related renal affliction. However, DXA has the advantage of providing a direct and accurate assessment of body composition and the CoreScan™ application has been validated against MRI and CT, with satisfactory concordance (65).

In a meta-analysis including seven studies, Fang and colleagues concluded that VAI is a useful tool for predicting CKD (area under the curve 0.77, prediction rate of 73% when considering a 50% pre-test probability) (66). Another ample study revealed that both LAP and VAI are associated with increase odds of CKD incidence (61). Interestingly, in our study, the correlation between eGFR and VAT mass, along with various other markers of lipotoxicity and inflammation (uric acid, VLDL-cholesterol) was only apparent in females, and not in males. Moreover, when analyzing VAT mass tertiles, the odds of reduced eGFR (<90ml/min/1.73m^2) was 5 times higher in women in the third VAT mass tertile compared to those in the first one, in a model adjusted for major confounders. This is in line with other reported findings. For example, in an ample community-based study in Taiwan, involving approximately 2000 subjects, VAI was significantly associated with the presence of CKD in females, but not in males (67). In another large study, comprising 5355 subjects, Xu and colleagues demonstrated a negative correlation between eGFR and CVAI and found CVAI to more accurately predict renal dysfunction in females compared to males (63). Similarly, in a study involving 400 middle-aged and elderly subjects, VAI was an independent predictor of CKD in females, but not in males (68). Another interesting study based on the KORA cohort, revealed a negative association between cystatin-based

eGFR and MRI estimated VAT only in women. However, the authors found no correlation between creatinine-based eGFR and VAT (69). Similarly, in a study including approximately 35000 participants from the NHANES database, no association between VAI and eGFR could be established; nevertheless, visceral adiposity was associated with increased odds of chronic kidney disease and albuminuria in females (70).

In contrast, a number of studies reported negative correlation between VAT and renal function in males, rather than in females. For example, in a longitudinal study including almost 7000 non-diabetic patients, VAI was found to be an independent predictor of renal function decline only in men over a period of follow-up of 8.6 years (71). Similarly, in a cross-sectional study conducted by Seong et al. and including almost 5000 subjects, VAI and LAP correlated with CKD exclusively in males (72). Yu and colleagues found METS-VF to be an independent predictor of CKD, exhibiting superiority to other obesity indices in both sexes, but more prominently in men (73).

Males and females differ not only in body size, but also in body composition. Men tend to have higher BMIs, as well as a higher absolute value of VAT and VAT: SAT ratio when compared to premenopausal women (74, 75). Similarly, male and female kidneys show differences that go beyond size, namely in histology and physiology (76, 77). For example, inter-gender variability in the abundance and functionality of renal transporters has been described (77), explaining differences in water and solute handling (e.g. a more rapid and efficient natriuretic response to high salt diet in females (78)). These provide a basis for the discrepancies in CKD evolution (known to be slower in premenopausal women than in men (77)) on one hand, and might explain the gender-specific renal-VAT interaction, on the other. Gonadal hormones are likely to have the greatest impact on these dissimilarities, influencing both body composition parameters and renal function directly. Estrogen promotes expansion of SAT, rather than VAT, reduces RAAS activation, promotes nitric oxide-mediated vasodilation and attenuates inflammation (75, 79). Of note, three types of renal estrogen receptors have been described and estrogen is believed to also exert its direct renoprotective actions, of which we mention attenuation of glomerular hypertrophy, reduction of mesangial expansion and decrease of fibrosis, mainly via ERα (80–83).

Menopause brings about a reversal of the female "advantage" in adiposity polarization and CKD progression, further supporting the central protective role of estrogen (81). The global consequences of estrogen decline (e.g. inflammatory milieu alterations (84)) further enhance the negative renal impact. In line with these findings, in our study, menopause status influenced all preoperative correlates of renal function. An ample prospective study, with a 15-year follow-up, interestingly showed that women with low estimated endogenous estrogen exposure had a higher risk of developing CKD later in life (79), while, in a nationwide Korean study, the use of menopausal hormone therapy was associated with a reduced risk of end-stage renal disease (83). However, in the context of obesity, conflicting results have been reported, with a number of deleterious effects especially in female subjects (85–87). Moreover, the dysregulation of systems involved in estrogen-mediated renal protection (e.g. RAAS) (88) might render estrogen less effective in the context of obesity (75). In their studies on murine models, Rodríguez-Rodríguez and colleagues elegantly assessed the combined renal effects of obesity and menopause. Ovariectomized obese mice had the most detrimental metabolic and renal responses to obesogenic diet and also exhibited the most severe lipotoxic and inflammatory profile in renal tissue (81, 91). These results suggest concerted deleterious renal effects of obesity and menopause and highlight the importance of weight control in menopause and perimenopausal transition as a renoprotective measure.

Another noteworthy result of our research is the stronger eGFR-VAT mass correlation in female patients with obesity and T2DM versus female patients with obesity, but no T2DM diagnosis. A very recent study by Liu and colleagues using DXA scans to quantify visceral adiposity in patients with T2DM, revealed additive interaction between diabetes and visceral adiposity on the occurrence of albuminuria. Higher visceral adiposity was also found to induce a stronger correlation between T2DM and albuminuria (89).

There are multiple hypotheses regarding post-MBS renal function improvement, derived from the positive impact on all aforementioned obesity-related dysregulations. Most of the studies found that improvement of renal filtration does not correlate with the degree of weight loss, but rather with the amelioration of metabolic profile and comorbidities, as a consequence of VAT and ectopic adipose tissue reduction (35, 43, 44, 90). However, we revealed a positive correlation between eGFR variation and EWL in male patients with obesity, paralleled by negative correlations with lean mass and ASMI reductions (which may be considered logical in light of the influence on creatinine). These results were not replicated in females. Instead, similar to the baseline strong influence of visceral adiposity, VAT mass variation proved to be an independent predictor of eGFR variation in a model adjusted for the main confounders. Interestingly, this held significance regardless of menopause status, suggesting beneficial effects of VAT mass reduction in both states.

To our knowledge, no other studies have reported on the correlation between DXA-estimated VAT and GFR dynamics before and after MBS, neither globally, nor through gender-oriented analysis. The availability of DXA also provides an additional strength of our study, namely the possibility to assess and adjust for the influence of ASMI. The main limitations stem from the inherent issues with creatinine-based eGFR, as discussed above. Although ideal, direct measurement or GFR is unfeasible in clinical practice. However, estimating GFR via equations based on both creatinine and cystatin C might increase reliability (31, 32). Secondly, albuminuria was not assessed in our cohort and therefore we could solely analyze renal function, rather than chronic kidney disease. Finally, while benefiting from a fairly ample evaluation, there are still confounders that should be considered when interpreting these results, such as dietary intake, physical activity levels, and socioeconomic status, which may influence both obesity (along with body composition parameters) and renal function (including the estimation of GFR).

The present study concentrated on the early impact of MBS on renal function. Added value would be provided by long-term

assessment. However, the most significant improvement in GFR seems to occur in the early postoperative timeframe (6-12 months), as pointed out by a meta-analysis by Huang et al. (17). Finally, our results should be confirmed on larger and more diverse cohorts, since we included a fairly low number of patients pertaining to the same ethnic group.

5 Conclusion

In the current study, we demonstrated a positive impact of MBS on obesity-related renal dysfunction and outlined gender-specific determinants of baseline eGFR and of postoperative eGFR variation. Our results suggest a stronger impact of visceral adiposity and lipotoxicity on renal pathology in females with obesity. This warrants further exploration, as it may guide future personalized therapeutic approaches.

Data availability statement

The raw data supporting the conclusions of this article will be made available by the authors, without undue reservation.

Ethics statement

The studies involving humans were approved by Carol Davila University Ethics Committee. The studies were conducted in accordance with the local legislation and institutional requirements. The participants provided their written informed consent to participate in this study.

Author contributions

MP: Writing – review & editing, Writing – original draft, Visualization, Software, Resources, Methodology, Investigation, Formal analysis, Data curation, Conceptualization. AS: Writing – review & editing, Writing – original draft, Visualization, Validation, Supervision, Formal analysis, Conceptualization. EM: Writing – review & editing, Writing – original draft, Validation, Resources, Methodology, Investigation, Formal analysis, Data curation. CC: Writing – review & editing, Writing – original draft, Resources, Conceptualization. SF: Writing – review & editing, Writing – original draft, Visualization, Validation, Supervision, Resources, Conceptualization.

Funding

The author(s) declare that no financial support was received for the research, authorship, and/or publication of this article.

Acknowledgments

Publication of this paper was supported by the University of Medicine and Pharmacy Carol Davila, through the institutional program Publish not Perish.

Conflict of interest

The authors declare that the research was conducted in the absence of any commercial or financial relationships that could be construed as a potential conflict of interest.

Publisher's note

All claims expressed in this article are solely those of the authors and do not necessarily represent those of their affiliated organizations, or those of the publisher, the editors and the reviewers. Any product that may be evaluated in this article, or claim that may be made by its manufacturer, is not guaranteed or endorsed by the publisher.

References

1. World Obesity Federation. *World Obesity Atlas*. London: World Obesity Federation (2024). Available at: https://data.worldobesity.org/publications/?cat=22.

2. Bello AK, Okpechi IG, Levin A, Ye F, Damster S, Arruebo S, et al. An update on the global disparities in kidney disease burden and care across world countries and regions. *Lancet Glob Heal.* (2024) 12:e382–95. doi: 10.1016/S2214-109X(23)00570-3

3. Tsuboi N, Okabayashi Y. The renal pathology of obesity: structure-function correlations. *Semin Nephrol.* (2021) 41:296–306. doi: 10.1016/j.semnephrol.2021.06.002

4. Hsu Cy, McCulloch CE, Iribarren C, Darbinian J, Go AS. Body mass index and risk for end-stage renal disease. *Ann Intern Med.* (2006) 144:21–8. doi: 10.7326/0003-4819-144-1-200601030-00006

5. Garofalo C, Borrelli S, Minutolo R, Chiodini P, De Nicola L, Conte G. A systematic review and meta-analysis suggests obesity predicts onset of chronic kidney disease in the general population. *Kidney Int.* (2017) 91:1224–35. doi: 10.1016/j.kint.2016.12.013

6. Pinto KRD, Feckinghaus CM, Hirakata VN. Obesity as a predictive factor for chronic kidney disease in adults: systematic review and meta-analysis. *Braz J Med Biol Res = Rev Bras Pesqui medicas e Biol.* (2021) 54:e10022. doi: 10.1590/1414-431X202010022

7. Wang S, Qin A, Dong L, Tan J, Zhou X, Qin W. Association of obesity with the development of end stage renal disease in IgA nephropathy patients. *Front Endocrinol (Lausanne).* (2023) 14:1094534. doi: 10.3389/fendo.2023.1094534

8. Munkhaugen J, Lydersen S, Widerøe TE, Hallan S. Prehypertension, obesity, and risk of kidney disease: 20-year follow-up of the HUNT I study in Norway. *Am J Kidney Dis Off J Natl Kidney Found.* (2009) 54:638–46. doi: 10.1053/j.ajkd.2009.03.023

9. Mohammedi K, Chalmers J, Herrington W, Li Q, Mancia G, Marre M, et al. Associations between body mass index and the risk of renal events in patients with type 2 diabetes. *Nutr Diabetes.* (2018) 8:7. doi: 10.1038/s41387-017-0012-y

10. Zhu Q, Scherer PE. Immunologic and endocrine functions of adipose tissue: implications for kidney disease. *Nat Rev Nephrol.* (2018) 14:105–20. doi: 10.1038/nrneph.2017.157

11. Nawaz S, Chinnadurai R, Al-Chalabi S, Evans P, Kalra PA, Syed AA, et al. Obesity and chronic kidney disease: A current review. *Obes Sci Pract.* (2023) 9:61–74. doi: 10.1002/osp4.629

12. Lakkis JI, Weir MR. Obesity and kidney disease. *Prog Cardiovasc Dis*. (2018) 61:157–67. doi: 10.1016/j.pcad.2018.07.005

13. Kambham N, Markowitz GS, Valeri AM, Lin J, D'Agati VD. Obesity-related glomerulopathy: an emerging epidemic. *Kidney Int*. (2001) 59:1498–509. doi: 10.1046/j.1523-1755.2001.0590041498.x

14. Camhi SM, Bray GA, Bouchard C, Greenway FL, Johnson WD, Newton RL, et al. The relationship of waist circumference and BMI to visceral, subcutaneous, and total body fat: sex and race differences. *Obesity*. (2011) 19:402–8. doi: 10.1038/oby.2010.248

15. Liao J, Yin Y, Zhong J, Chen Y, Chen Y, Wen Y, et al. Bariatric surgery and health outcomes: An umbrella analysis. *Front Endocrinol (Lausanne)*. (2022) 13:1016613. doi: 10.3389/fendo.2022.1016613

16. Friedman AN, Cohen RV. Bariatric surgery as a renoprotective intervention. *Curr Opin Nephrol Hypertens*. (2019) 28:537–44. doi: 10.1097/MNH.0000000000000539

17. Huang H, Lu J, Dai X, Li Z, Zhu L, Zhu S, et al. Improvement of renal function after bariatric surgery: a systematic review and meta-analysis. *Obes Surg*. (2021) 31:4470–84. doi: 10.1007/s11695-021-05630-4

18. Moriconi D, Nannipieri M, Dadson P, Rosada J, Tentolouris N, Rebelos E. The beneficial effects of bariatric-surgery-induced weight loss on renal function. *Metabolites*. (2022) 12:967. doi: 10.3390/metabo12100967

19. Eisenberg D, Shikora SA, Aarts E, Aminian A, Angrisani L, Cohen RV, et al. 2022 American society of metabolic and bariatric surgery (ASMBS) and international federation for the surgery of obesity and metabolic disorders (IFSO) indications for metabolic and bariatric surgery. *Obes Surg*. (2023) 33:3–14. doi: 10.1007/s11695-022-06332-1

20. National Institute on Alcohol Abuse and Alcoholism. *Drinking levels defined* . Available online at: https://www.niaaa.nih.gov/alcohol-health/overview-alcohol-consumption/moderate-binge-drinking. (Accessed March 26, 2024).

21. Montero PN, Stefanidis D, Norton HJ, Gersin K, Kuwada T. Reported excess weight loss after bariatric surgery could vary significantly depending on calculation method: a plea for standardization. *Surg Obes Relat Dis Off J Am Soc Bariatr Surg*. (2011) 7:531–4. doi: 10.1016/j.soard.2010.09.025

22. American Diabetes Association Professional Practice Committee. 2. Diagnosis and classification of diabetes: standards of care in diabetes—2024. *Diabetes Care*. (2023) 47:S20–42. doi: 10.2337/dc24-S002

23. Inker LA, Eneanya ND, Coresh J, Tighiouart H, Wang D, Sang Y, et al. New creatinine- and cystatin C–based equations to estimate GFR without race. *N Engl J Med*. (2021) 385:1737–49. doi: 10.1056/nejmoa2102953

24. Levin A, Stevens PE, Bilous RW, Coresh J, De Francisco ALM, De Jong PE, et al. KDIGO 2012 clinical practice guideline for the evaluation and management of chronic kidney disease: Chapter 1: Definition and classification of CKD. *Kidney Int Suppl*. (2013) 3:19–62. doi: 10.1038/KISUP.2012.64

25. Cachat F, Combescure C, Cauderay M, Girardin E, Chehade H. A systematic review of glomerular hyperfiltration assessment and definition in the medical literature. *Clin J Am Soc Nephrol*. (2015) 10:382–9. doi: 10.2215/CJN.03080314

26. Helal I, Fick-Brosnahan GM, Reed-Gitomer B, Schrier RW. Glomerular hyperfiltration: Definitions, mechanisms and clinical implications. *Nat Rev Nephrol*. (2012) 8:293–300. doi: 10.1038/nrneph.2012.19

27. Basolo A, Salvetti G, Giannese D, Genzano SB, Ceccarini G, Giannini R, et al. Obesity, hyperfiltration, and early kidney damage: A new formula for the estimation of creatinine clearance. *J Clin Endocrinol Metab*. (2023) 108:3280–6. doi: 10.1210/clinem/dgad330

28. Levey AS, Coresh J, Tighiouart H, Greene T, Inker LA. Measured and estimated glomerular filtration rate: current status and future directions. *Nat Rev Nephrol*. (2020) 16:51–64. doi: 10.1038/s41581-019-0191-y

29. Lemoine S, Guebre-Egziabher F, Sens F, Nguyen-Tu MS, Juillard L, Dubourg L, et al. Accuracy of GFR estimation in obese patients. *Clin J Am Soc Nephrol*. (2014) 9:720–7. doi: 10.2215/CJN.03610413

30. Kashani K, Rosner MH, Ostermann M. Creatinine: From physiology to clinical application. *Eur J Intern Med*. (2020) 72:9–14. doi: 10.1016/j.ejim.2019.10.025

31. Zou LX, Sun L, Nicholas SB, Lu Y, SS K, Hua R. Comparison of bias and accuracy using cystatin C and creatinine in CKD-EPI equations for GFR estimation. *Eur J Intern Med*. (2020) 80:29–34. doi: 10.1016/j.ejim.2020.04.044

32. Friedman AN, Moe S, Fadel WF, Inman M, Mattar SG, Shihabi Z, et al. Predicting the glomerular filtration rate in bariatric su. *Am J Nephrol*. (2014) 39:8–15. doi: 10.1159/000357231

33. Clerte M, Wagner S, Carette C, Brodin-Sartorius A, Vilaine É, Alvarez JC, et al. The measured glomerular filtration rate (mGFR) before and 6 months after bariatric surgery: A pilot study. *Nephrol Ther*. (2017) 13:160–7. doi: 10.1016/j.nephro.2016.10.002

34. Nankivell BJ, Nankivell LFJ, Elder GJ, Gruenewald SM. How unmeasured muscle mass affects estimated GFR and diagnostic inaccuracy. *EClinicalMedicine*. (2020) 29–30:1–9. doi: 10.1016/j.eclinm.2020.100662

35. Rothberg AE, McEwen LN, Herman WH. Severe obesity and the impact of medical weight loss on estimated glomerular filtration rate. *PloS One*. (2020) 15:e0228984. doi: 10.1371/journal.pone.0228984

36. Delanaye P, Krzesinski JM. Indexing of renal function parameters by body surface area: intelligence or folly? *Nephron Clin Pract*. (2011) 119:c289–92. doi: 10.1159/000330276

37. Donadio C, Moriconi D, Berta R, Anselmino M. Estimation of urinary creatinine excretion and prediction of renal function in morbidly obese patients: new tools from body composition analysis. *Kidney Blood Press Res*. (2017) 42:629–40. doi: 10.1159/000481630

38. Hojs R, Ekart R, Bevc S, Vodošek Hojs N. Chronic kidney disease and obesity. *Nephron*. (2023) 147:660–4. doi: 10.1159/000531379

39. Sharma I, Liao Y, Zheng X, Kanwar YS. New pandemic: obesity and associated nephropathy. *Front Med*. (2021) 8:673556. doi: 10.3389/fmed.2021.673556

40. Moţa E, Popa SG, Moţa M, Mitrea A, Penescu M, Tuţă L, et al. Prevalence of chronic kidney disease and its association with cardio-metabolic risk factors in the adult Romanian population: the PREDATORR study. *Int Urol Nephrol*. (2015) 47:1831–8. doi: 10.1007/s11255-015-1109-7

41. Chang AR, Zafar W, Grams ME. Kidney function in obesity-challenges in indexing and estimation. *Adv Chronic Kidney Dis*. (2018) 25:31–40. doi: 10.1053/j.ackd.2017.10.007

42. Favre G, Anty R, Canivet C, Clément G, Ben-Amor I, Tran A, et al. Determinants associated with the correction of glomerular hyper-filtration one year after bariatric surgery. *Surg Obes Relat Dis*. (2017) 13:1760–6. doi: 10.1016/j.soard.2017.07.018

43. Shulman A, Andersson-Assarsson JC, Sjöström CD, Jacobson P, Taube M, Sjöholm K, et al. Remission and progression of pre-existing micro- and macroalbuminuria over 15 years after bariatric surgery in Swedish Obese Subjects study. *Int J Obes*. (2021) 45:535–46. doi: 10.1038/s41366-020-00707-z

44. Bilha SC, Nistor I, Nedelcu A, Kanbay M, Scripcariu V, Timofte D, et al. The effects of bariatric surgery on renal outcomes: a systematic review and meta-analysis. *Obes Surg*. (2018) 28:3815–33. doi: 10.1007/s11695-018-3416-4

45. Friedman AN, Wahed AS, Wang J, Courcoulas AP, Dakin G, Hinojosa MW, et al. Effect of bariatric surgery on CKD risk. *J Am Soc Nephrol*. (2018) 29:1289–300. doi: 10.1681/ASN.2017060707

46. Stefan N. Causes, consequences, and treatment of metabolically unhealthy fat distribution. *Lancet Diabetes Endocrinol*. (2020) 8:616–27. doi: 10.1016/S2213-8587(20)30110-8

47. Chait A, den Hartigh LJ. Adipose tissue distribution, inflammation and its metabolic consequences, including diabetes and cardiovascular disease. *Front Cardiovasc Med*. (2020) 7:22. doi: 10.3389/fcvm.2020.00022

48. Vela-Bernal S, Facchetti R, Dell'Oro R, Quarti-Trevano F, Lurbe E, Mancia G, et al. Anthropometric measures of adiposity as markers of kidney dysfunction: A cross-sectional study. *High Blood Press Cardiovasc Prev*. (2023) 30:467–74. doi: 10.1007/s40292-023-00600-6

49. Arabi T, Shafqat A, Sabbah BN, Fawzy NA, Shah H, Abdulkader H, et al. Obesity-related kidney disease: Beyond hypertension and insulin-resistance. *Front Endocrinol (Lausanne)*. (2022) 13:1095211. doi: 10.3389/fendo.2022.1095211

50. Kadatane SP, Satariano M, Massey M, Mongan K, Raina R. The role of inflammation in CKD. *Cells*. (2023) 12:1581. doi: 10.3390/cells12121581

51. Amdur RL, Feldman HI, Gupta J, Yang W, Kanetsky P, Shlipak M, et al. Inflammation and progression of CKD: the CRIC study. *Clin J Am Soc Nephrol*. (2016) 11:1546–56. doi: 10.2215/CJN.13121215

52. Taguchi S, Azushima K, Yamaji T, Urate S, Suzuki T, Abe E, et al. Effects of tumor necrosis factor-α inhibition on kidney fibrosis and inflammation in a mouse model of aristolochic acid nephropathy. *Sci Rep*. (2021) 11:23587. doi: 10.1038/s41598-021-02864-1

53. Moriconi D, Antonioli L, Masi S, Bellini R, Pellegrini C, Rebelos E, et al. Glomerular hyperfiltration in morbid obesity: Role of the inflammasome signalling. *Nephrology*. (2022) 27:673–80. doi: 10.1111/nep.14077

54. Donate-Correa J, Ferri CM, Sánchez-Quintana F, Pérez-Castro A, González-Luis A, Martín-Núñez E, et al. Inflammatory cytokines in diabetic kidney disease: pathophysiologic and therapeutic implications. *Front Med*. (2020) 7:628289. doi: 10.3389/fmed.2020.628289

55. Grigoraş A, Balan RA, Căruntu ID, Giuşcă SE, Lozneanu L, Avadanei RE, et al. Perirenal adipose tissue-current knowledge and future opportunities. *J Clin Med*. (2021) 10:1291. doi: 10.3390/jcm10061291

56. Spit KA, Muskiet MHA, Tonneijck L, Smits MM, Kramer MHH, Joles JA, et al. Renal sinus fat and renal hemodynamics: a cross-sectional analysis. *MAGMA*. (2020) 33:73–80. doi: 10.1007/s10334-019-00773-z

57. Xu S, Ma J, Zheng Y, Ren R, Li W, Zhao W, et al. Para-perirenal fat thickness is associated with reduced glomerular filtration rate regardless of other obesity-related indicators in patients with type 2 diabetes mellitus. *PloS One*. (2023) 18:1–15. doi: 10.1371/journal.pone.0293464

58. Miyasato Y, Oba K, Yasuno S, Matsuyama Y, Masuda I. Associations between visceral obesity and renal impairment in health checkup participants: a retrospective cohort study. *Clin Exp Nephrol*. (2020) 24:935–45. doi: 10.1007/s10157-020-01921-9

59. Kataoka H, Mochizuki T, Iwadoh K, Ushio Y, Kawachi K, Watanabe S, et al. Visceral to subcutaneous fat ratio as an indicator of a ≥30% eGFR decline in chronic kidney disease. *PloS One*. (2020) 15:e0241626. doi: 10.1371/journal.pone.0241626

60. Lee J, Min S, Oh SW, Oh S, Lee YH, Kwon H, et al. Association of intraabdominal fat with the risk of incident chronic kidney disease according to body mass index among Korean adults. *PloS One*. (2023) 18:1–14. doi: 10.1371/journal.pone.0280766

61. Bullen AL, Katz R, Kumar U, Gutierrez OM, Sarnak MJ, Kramer HJ, et al. Lipid accumulation product, visceral adiposity index and risk of chronic kidney disease. *BMC Nephrol*. (2022) 23:1–11. doi: 10.1186/s12882-022-03026-9

62. Sun Y, Yan Y, Liao Y, Chu C, Guo T, Ma Q, et al. The new visceral adiposity index outperforms traditional obesity indices as a predictor of subclinical renal damage in Chinese individuals: a cross-sectional study. *BMC Endocr Disord*. (2023) 23:78. doi: 10.1186/s12902-023-01330-5

63. Xu Y, Wang XY, Liu H, Jin D, Song X, Wang S, et al. A novel clinical diagnostic marker predicting the relationship between visceral adiposity and renal function evaluated by estimated glomerular filtration rate (eGFR) in the Chinese physical examination population. *Lipids Health Dis*. (2023) 22:1–11. doi: 10.1186/s12944-023-01783-6

64. Bello-Chavolla OY, Antonio-Villa NE, Vargas-Vázquez A, Viveros-Ruiz TL, Almeda-Valdes P, Gomez-Velasco D, et al. Metabolic Score for Visceral Fat (METS-VF), a novel estimator of intra-abdominal fat content and cardio-metabolic health. *Clin Nutr*. (2020) 39:1613–21. doi: 10.1016/j.clnu.2019.07.012

65. Kaul S, Rothney MP, Peters DM, Wacker WK, Davis CE, Shapiro MD, et al. Dual-energy X-ray absorptiometry for quantification of visceral fat. *Obesity*. (2012) 20:1313–8. doi: 10.1038/oby.2011.393

66. Fang T, Zhang Q, Wang Y, Zha H. Diagnostic value of visceral adiposity index in chronic kidney disease: a meta-analysis. *Acta Diabetol*. (2023) 60:739–48. doi: 10.1007/s00592-023-02048-5

67. Huang J, Zhou C, Li Y, Zhu S, Liu A, Shao X, et al. Visceral adiposity index, hypertriglyceridemic waist phenotype and chronic kidney disease in a southern Chinese population: a cross-sectional study. *Int Urol Nephrol*. (2015) 47:1387–96. doi: 10.1007/s11255-015-1040-y

68. Chen IJ, Hsu LT, Lu MC, Chen YJ, Tsou MT, Chen JY. Gender differences in the association between obesity indices and chronic kidney disease among middle-aged and elderly Taiwanese population: A community-based cross-sectional study. *Front Endocrinol (Lausanne)*. (2021) 12:737586. doi: 10.3389/fendo.2021.737586

69. Mueller-Peltzer K, von Krüchten R, Lorbeer R, Rospleszcz S, Schulz H, Peters A, et al. Adipose tissue is associated with kidney function parameters. *Sci Rep*. (2023) 13:1–8. doi: 10.1038/s41598-023-36390-z

70. Qin Z, Chen X, Sun J, Jiang L. The association between visceral adiposity index and decreased renal function: A population-based study. *Front Nutr*. (2023) 10:1076301. doi: 10.3389/fnut.2023.1076301

71. Mousapour P, Barzin M, Valizadeh M, Mahdavi M, Azizi F, Hosseinpanah F. Predictive performance of lipid accumulation product and visceral adiposity index for renal function decline in non-diabetic adults, an 8.6-year follow-up. *Clin Exp Nephrol*. (2020) 24:225–34. doi: 10.1007/s10157-019-01813-7

72. Seong JM, Lee JH, Gi MY, Son YH, Moon AE, Park CE, et al. Gender difference in the association of chronic kidney disease with visceral adiposity index and lipid accumulation product index in Korean adults: Korean National Health and Nutrition Examination Survey. *Int Urol Nephrol*. (2021) 53:1417–25. doi: 10.1007/s11255-020-02735-0

73. Yu P, Meng X, Kan R, Wang Z, Yu X. Association between metabolic scores for visceral fat and chronic kidney disease: A cross-sectional study. *Front Endocrinol (Lausanne)*. (2022) 13:1052736. doi: 10.3389/fendo.2022.1052736

74. Al-Chalabi S, Syed AA, Kalra PA, Sinha S. Mechanistic links between central obesity and cardiorenal metabolic diseases. *Cardiorenal Med*. (2024) 14:12–22. doi: 10.1159/000535772

75. Kataoka H, Nitta K, Hoshino J. Visceral fat and attribute-based medicine in chronic kidney disease. *Front Endocrinol (Lausanne)*. (2023) 14:1097596. doi: 10.3389/fendo.2023.1097596

76. Layton AT, Sullivan JC. Recent advances in sex differences in kidney function. *Am J Physiol Renal Physiol United States*. (2019) 316:F328–31. doi: 10.1152/ajprenal.00584.2018

77. McDonough AA, Harris AN, Xiong LI, Layton AT. Sex differences in renal transporters: assessment and functional consequences. *Nat Rev Nephrol*. (2024) 20:21–36. doi: 10.1038/s41581-023-00757-2

78. Veiras LC, Girardi ACC, Curry J, Pei L, Ralph DL, Tran A, et al. Sexual dimorphic pattern of renal transporters and electrolyte homeostasis. *J Am Soc Nephrol*. (2017) 28:3504–17. doi: 10.1681/ASN.2017030295

79. Farahmand M, Ramezani Tehrani F, Khalili D, Cheraghi L, Azizi F. Endogenous estrogen exposure and chronic kidney disease; a 15-year prospective cohort study. *BMC Endocr Disord*. (2021) 21:155. doi: 10.1186/s12902-021-00817-3

80. Ma HY, Chen S, Du Y. Estrogen and estrogen receptors in kidney diseases. *Ren Fail*. (2021) 43:619–42. doi: 10.1080/0886022X.2021.1901739

81. Afonso-Alí A, Porrini E, Teixido-Trujillo S, Pérez-Pérez JA, Luis-Lima S, Acosta-González NG, et al. The role of gender differences and menopause in obesity-related renal disease, renal inflammation and lipotoxicity. *Int J Mol Sci*. (2023) 24:12984. doi: 10.3390/ijms241612984

82. Singh AP, Singh M, Kaur T, Buttar HS, Ghuman SS, Pathak D. *Estradiol Benzoate Ameliorates Obesity-Induced Renal Dysfunction in Male Rats: Biochemical and Morphological Observations BT - Biochemistry of Cardiovascular Dysfunction in Obesity*. Tappia PS, Bhullar SK, Dhalla NS, editors. Cham: Springer International Publishing (2020) p. 367–84. doi: 10.1007/978-3-030-47336-5_19

83. Ahn SY, Choi YJ, Kim J, Ko GJ, Kwon YJ, Han K. The beneficial effects of menopausal hormone therapy on renal survival in postmenopausal Korean women from a nationwide health survey. *Sci Rep*. (2021) 11:15418. doi: 10.1038/s41598-021-93847-9

84. Opoku AA, Abushama M, Konje JC. Obesity and menopause. *Best Pract Res Clin Obstet Gynaecol*. (2023) 88:102348. doi: 10.1016/j.bpobgyn.2023.102348

85. Stevenson FT, Wheeldon CM, Gades MD, Kaysen GA, Stern JS, van Goor H. Estrogen worsens incipient hypertriglyceridemic glomerular injury in the obese Zucker rat. *Kidney Int*. (2000) 57:1927–35. doi: 10.1046/j.1523-1755.2000.00042.x

86. Sun L, Chao F, Luo B, Ye D, Zhao J, Zhang Q, et al. Impact of estrogen on the relationship between obesity and renal cell carcinoma risk in women. *EBioMedicine*. (2018) 34:108–12. doi: 10.1016/j.ebiom.2018.07.010

87. Gades MD, Stern JS, van Goor H, Nguyen D, Johnson PR, Kaysen GA. Estrogen accelerates the development of renal disease in female obese Zucker rats. *Kidney Int*. (1998) 53:130–5. doi: 10.1046/j.1523-1755.1998.00746.x

88. Vargas-Castillo A, Tobon-Cornejo S, Del Valle-Mondragon L, Torre-Villalvazo I, Schcolnik-Cabrera A, Guevara-Cruz M, et al. Angiotensin-(1-7) induces beige fat thermogenesis through the Mas receptor. *Metabolism*. (2020) 103:154048. doi: 10.1016/j.metabol.2019.154048

89. Liu Y, Zhao D, Chai S, Zhang X. Association of visceral adipose tissue with albuminuria and interaction between visceral adiposity and diabetes on albuminuria. *Acta Diabetol*. (2024) 61:909–16. doi: 10.1007/s00592-024-02271-8

90. Gong X, Zeng X, Fu P. The impact of weight loss on renal function in individuals with obesity and type 2 diabetes: a comprehensive review. *Front Endocrinol (Lausanne)*. (2024) 15:1320627. doi: 10.3389/fendo.2024.1320627

91. Rodríguez-Rodríguez AE, Donate-Correa J, Luis-Lima S, Díaz-Martín L, Rodríguez-González C, Pérez-Pérez JA, et al. Obesity and metabolic syndrome induce hyperfiltration, glomerulomegaly, and albuminuria in obese ovariectomized female mice and obese male mice. *Menopause* (2021) 28(11):1296–306. doi: 10.1097/GME.0000000000001842

frontiers | Frontiers in Endocrinology

TYPE Review
PUBLISHED 29 October 2024
DOI 10.3389/fendo.2024.1463567

OPEN ACCESS

EDITED BY
Yayun Wang,
Air Force Medical University, China

REVIEWED BY
Francesca Abbatini,
Azienda Sanitaria Locale Roma 6, Italy
Jingyan Tian,
Shanghai Jiao Tong University, China

*CORRESPONDENCE
Hua Meng
menghuade@hotmail.com

RECEIVED 12 July 2024
ACCEPTED 08 October 2024
PUBLISHED 29 October 2024

CITATION
Liu G, Wang P, Ran S, Xue X and Meng H (2024) Surgical treatment strategies for gastroesophageal reflux after laparoscopic sleeve gastrectomy. *Front. Endocrinol.* 15:1463567. doi: 10.3389/fendo.2024.1463567

Surgical treatment strategies for gastroesophageal reflux after laparoscopic sleeve gastrectomy

Genzheng Liu, Pengpeng Wang, Shuman Ran, Xiaobin Xue and Hua Meng*

Department of General Surgery and Obesity and Metabolic Disease Center, China–Japan Friendship Hospital, Beijing, China

Bariatric surgery has emerged as an effective therapeutic approach for combating obesity. As the most commonly performed bariatric surgery, laparoscopic sleeve gastrectomy (LSG) has a long-term and effective outcome in weight reduction. However, studies have reported an increased incidence of gastroesophageal reflux disease (GERD) among patients after LSG. For those who fail to respond to conventional oral acid-suppressing medication, surgical intervention comes into consideration. The most commonly performed revisional surgery for sleeve gastrectomy is the Roux-en-Y gastric bypass, which can effectively alleviate the symptoms of reflux in patients and also continues to promote weight loss in patients who have not achieved satisfactory results or have experienced weight regain. In addition to this established procedure, innovative techniques such as laparoscopic magnetic sphincter augmentation (MSA) are being explored. MSA is less invasive, has good reflux treatment outcomes, and its safety and efficacy are supported by the literature, making it a promising tool for the future treatment of gastroesophageal reflux. This article also explores the role of endoscopic interventions for GERD treatment of post-sleeve gastrectomy patients. Although these methods have shown some therapeutic effect, their efficacy still requires further study due to a lack of support from more clinical data. For patients with preoperative hiatal hernia or gastroesophageal reflux symptoms, some experts now consider performing LSG combined with hiatal hernia repair or fundoplication to alleviate or prevent postoperative reflux symptoms. Both of these surgical approaches have demonstrated favorable outcomes; however, the addition of fundoplication requires further investigation regarding its long-term effects and potential postoperative complications. This article gathers and examines the current laparoscopic and endoscopic treatments for refractory gastroesophageal reflux following LSG, as well as the concurrent treatment of LSG in patients with preoperative gastroesophageal reflux or hiatal hernia.

KEYWORDS

laparoscopic sleeve gastrectomy, gastroesophageal reflux, surgical treatment, refractory gastroesophageal reflux, revision surgery

1 Introduction

Obesity has emerged as a critical global health concern. Between 1975 and 2014, the prevalence of obesity among adult men surged from 3.2% to 10.8%, while the prevalence among women increased from 6.4% to 14.9% (1). In China, the percentage of overweight adults has climbed to 34.8%, with an obesity rate of 14.1% (2). Bariatric surgery, with its significant weight loss outcomes, long-term stability, and high remission rate for obesity-related complications, has increasingly become one of the weight loss options for obese individuals. Laparoscopic sleeve gastrectomy (LSG) has become the most commonly performed bariatric procedure due to its relative simplicity and positive outcomes. In the United States, LSG accounts for approximately 57.4% of all bariatric surgeries (3). Despite its popularity, recent research suggests that LSG may exacerbate postoperative gastroesophageal reflux or lead to *de novo* reflux episodes (4). A meta-analysis encompassing 22 studies revealed a 35% incidence of gastroesophageal reflux following LSG (5). In the long-term follow-up after LSG, the incidence of new-onset gastroesophageal reflux is 20.0% to 24.8% (6, 7). However, some studies have reported even higher rates, with the incidence of postoperative reflux potentially ranging from 50% to 53.8%, and the rate of new-onset reflux reaching up to 42.3% to 73% (8–10). This discrepancy may be attributed to demographic differences or variations in dietary habits.

Currently, when addressing gastroesophageal reflux in patients post-LSG, the predominant approach, considering safety and the desire to minimize postoperative patient trauma, remains focused on dietary and lifestyle adjustments, in conjunction with the administration of antacid and acid-suppressing pharmaceuticals. However, there is no unified treatment guideline in the academic community for dealing with persistent gastroesophageal reflux that is unresponsive to long-term acid suppression therapy after LSG.

This article reviews the possible mechanism and the currently available treatment strategies for gastroesophageal reflux after LSG, including non-surgical treatment, surgical treatment and concurrent surgical treatment.

2 Mechanisms of gastroesophageal reflux after LSG

The potential factors contributing to gastroesophageal reflux after LSG surgery include reduced gastric compliance, elevated intra-gastric pressure, and the disruption of the anti-reflux barrier, such as an enlarged His angle and decreased lower esophageal sphincter pressure. Other factors may include the presence of a hiatal hernia, gastric sleeve torsion, stenosis, etc. (11) Quero et al. (12) employed magnetic resonance imaging, high-resolution manometry, and dynamic pH impedance measurement to evaluate the structure and function of the gastroesophageal junction and stomach before and after LSG. Their research revealed that the His angle increased from 36° to 51° following LSG, with 78% of patients exhibiting an enlarged His angle. Postoperatively, the average length of the lower esophageal sphincter decreased by 1cm, and the mean intra-gastric pressure rose from 21.3 mmHg preoperatively to 33.5 mmHg postoperatively. Similar results have been reported by Mion, Balla, Poggi, and others (13–15). Furthermore, studies have indicated that the morphology of the residual stomach after LSG also plays a role in reflux dynamics (16).

3 Non-surgical treatment of GERD after LSG

For patients with gastroesophageal reflux who have not undergone surgery, conventional treatment methods include: 1. Dietary and lifestyle interventions, which involve avoiding foods that may trigger reflux (such as coffee, alcohol, chocolate, high-fat foods, etc.) and highly irritating foods (such as citrus, carbonated beverages, spicy foods, etc.), as well as losing weight, quitting smoking, elevating the head of the bed, and avoiding lying flat after meals. 2. The use of antacid and gastric mucosal protective agents, such as aluminum magnesium carbonate suspension. 3. The use of acid suppressants, including H2 receptor antagonists (such as cimetidine), proton pump inhibitors (such as omeprazole), and potassium-competitive acid blockers (such as vonoprazan) (17).

In the study by Peterli et al. (18), at the five-year follow-up, out of 101 patients who underwent LSG, 7 experienced reflux esophagitis that was unresponsive to proton pump inhibitor (PPI) treatment, and 1 had developed *de novo* Barrett mucosa. All of these patients eventually converted to RYGB. In another study by Paulina et al. (19), a ten-year follow-up found that as many as 64.4% of patients still required oral PPIs after LSG. For patients who remain dependent on medication long-term or for those whose symptoms are not adequately controlled by drugs, it becomes imperative to explore additional surgical or endoscopic intervention strategies.

4 Surgical treatment of GERD after LSG

4.1 Roux-en-Y gastric bypass

The most common reason for revision surgery after LSG is poor weight loss, weight regain, or severe gastroesophageal reflux, with RYGB being the most frequently performed revisional procedure following LSG (20). Both the American Gastroenterological Association and the American Society for Gastrointestinal and Endoscopic Surgeons consider RYGB to be the preferred surgery for obese patients with gastroesophageal reflux (21, 22). In a study by Mandalosso et al. (23), 53 patients were monitored for an average of 39 months to assess the changes in esophageal and extraesophageal symptoms before and after RYGB. The results showed that 83% of patients with typical reflux symptoms prior to surgery experienced significant improvement postoperatively.

Huynh et al. (24) utilized the Gastroesophageal Reflux Disease - Health-Related Quality of Life (GERD-HRQL) score to evaluate the quality of life in 41 patients who underwent RYGB following LSG.

The average GERD-HRQL score plummeted from 31.5 before the revision surgery to 5.6 at 6 months post-RYGB, and it still remained 7.3 at 15 months. In a retrospective study by Felsenreich and others (25), among the 45 patients who converted from LSG to RYGB, 36 had preoperative GERD, and 6 had Barrett's esophagus. Following the RYGB, Barrett's esophagus was fully resolved in 4 patients, and symptoms of gastroesophageal reflux improved in 23 patients (63.9%). A similar study by Dayan (26) found that out of 47 patients with GERD who underwent RYGB as a revisional procedure after LSG, 43 (91.5%) experienced relief from their reflux symptoms. Insufficient weight loss is also a critical indication for revisional surgery following RYGB. In the study by Antonio et al. (27), the percentage of excess weight loss at 1, 3, and 5 years post-bypass was 40.3%, 34.3%, and 23.2%, respectively, for the group with poor weight reduction. In a separate study enrolling 97 individuals, those who underwent RYGB revisional surgery achieved an average weight loss of 11.1 ± 12.9 kg. For patients who underwent surgery to address reflux, 80.2% experienced overall symptom improvement following the revision, and 19.4% were able to cease PPI therapy postoperatively. However, the majority of patients (80.5%) still required oral PPIs at the last follow-up (average 16.5 ± 19.56 months). The incidence of complications classified as Clavien–Dindo grade III or higher was 7.21%, including grade IV complications accounting for 2.06% of the cases (with an average follow-up of 16.5 ± 19.56 months) (27, 28). In contrast, the reported short-term complication rate for primary RYGB surgery is 6.3% (29), and the 10-year complication rate is 24.4%, with an incidence of Clavien–Dindo grade III or higher complications at 18.5% (19). However, the sample sizes for RYGB revisional surgery studies are relatively small, and there is a scarcity of longer-term follow-up data. Consequently, further research is needed to compare the incidence of complications.

It is evident that RYGB has a favorable therapeutic effect in the treatment of gastroesophageal reflux and insufficient weight loss after LSG. Moreover, the complication rate of RYGB revisional surgery does not appear to be significantly higher than that of the primary RYGB. For patients who continue to struggle with refractory reflux symptoms after LSG, RYGB remains the preferred option for surgical revision. However, it is worth noting that some studies have identified an increased likelihood of experiencing weak acid reflux following RYGB (30).

4.2 Magnetic sphincter augmentation

MSA is a novel anti-reflux surgical technique, a method that utilizes the LINX Reflux Management System to achieve the goal of preventing reflux. The LINX device is a ring-like construct formed from a series of titanium beads, each embedded with a magnetic core and interconnected by independent titanium arms. This device is implanted laparoscopically around the lower esophageal sphincter to enhance its capability (31).

A meta-analysis encompassing three studies has revealed that patients who underwent MSA experienced an average reduction of 17.5 points in their GERD-HRQL scores, signifying MSA's viability as a treatment for refractory GERD following bariatric surgery (32). In a clinical study by Patel et al. (33) that included 22 individuals, 82% of patients were able to cease using acid-suppressing medication after MSA, with average postoperative GERD-HRQL scores dropping from 43.8 preoperatively to 16.7 postoperatively, 77% of patients were "satisfied" with the MSA surgery, while 14% were "dissatisfied." The main reason for dissatisfaction was the persistent need for acid suppressants to control reflux symptoms, and a few other patients experienced dysphagia after MSA. Other studies have also reported similar results, showing significant improvements in GERD-HRQL scores after MSA, with proton pump inhibitor discontinuation rates ranging from 69.2% to 90.0% (34–36). The study by Khaitan et al. (37) noted that common adverse events following MSA included dysphagia (16.7%), pain (10.0%), and nausea (6.7%). The research also compared the treatment differences of MSA surgery between patients with a history of weight loss surgery and those without gastric surgery, suggesting similar therapeutic effects in both groups (35, 36).

Based on the current results, MSA is a safe and effective surgical treatment for refractory gastroesophageal reflux following weight loss surgery. It can effectively alleviate reflux symptoms, allowing the majority of patients to avoid long-term oral acid suppression medication and improve their quality of life.

4.3 Antireflux mucosectomy

Antireflux mucosectomy is an endoscopic treatment technique first reported by Inoue and colleagues for the treatment of refractory GERD. It involves the use of endoscopic mucosal resection or endoscopic submucosal dissection to remove mucosal tissue at the gastroesophageal junction. As the mucosa heals, submucosal fibrosis and scarring develop, creating a postoperative antireflux barrier. Their study also suggests that ARMs may effectively improve symptoms and DeMeester scores in patients with GERD (38).

Zhu and colleagues (39) have reviewed the therapeutic outcomes of ARMs in recent studies. Analysis of six studies that recorded GERD-HRQL scores revealed varying degrees of improvement in patients following ARMs. In seven studies involving 24-hour esophageal pH monitoring, DeMeester scores significantly improved postoperatively, and the average time of esophageal acid exposure was greatly reduced. These findings confirm the efficacy of ARMs in the treatment of refractory GERD. They also highlighted common postoperative complications, mainly including dysphagia (11.4%) and bleeding (5%).

In a case study, Patil et al. (40) employed ARMs to treat a patient experiencing refractory GERD after LSG. The patient's DeMeester score dramatically decreased from 159 to 13.8, and the 24-hour pH measurement of acid reflux time was reduced from 25% to 4.5%. Additionally, the GREDQ score fell from 10 to 7, allowing for the discontinuation of acid suppressants postoperatively. Debourdeau and colleagues (41) found similar results in their study of six patients who underwent ARMs after bariatric surgery, with the average GERD-HRQL score dropping from 30.6 to 6.8 at three months postoperatively. However, three patients still required

ongoing acid suppressant therapy, and complications such as esophageal stricture and gastrointestinal bleeding were observed in one patient each.

ARMs demonstrate promising efficacy in the management of refractory GERD. While more clinical evidence is needed to support its use in patients with refractory GERD following weight loss surgery, the current studies suggest that ARMs can be an effective treatment option. Nonetheless, caution must be exercised to monitor and manage potential postoperative complications.

4.4 Endoscopic radiofrequency therapy

Endoscopic radiofrequency therapy is a treatment method that utilizes the Stretta device, which primarily consists of a catheter with four nickel-titanium needle electrodes and a guide wire. During treatment, the device is positioned at the gastroesophageal junction, and heat energy is released within a 2cm range above and below the squamocolumnar junction, with the temperature maintained at 85°C. To prevent overheating, cold water is used to cool the tissue, ensuring that the mucosal temperature stays below 30°C for a period of 2 minutes. This process ultimately induces scar formation in the lower esophageal sphincter through heat stimulation, thereby increasing the pressure in the lower esophageal sphincter. Additionally, the radiofrequency energy can disrupt the intramuscular vagal ganglia in the esophagus, preventing vagally induced transient lower esophageal sphincter relaxation, thus achieving the therapeutic goal (42, 43).

In a study that followed 83 patients for 4 years, the proportion of patients using acid suppressants decreased from 100% at baseline to 29.4% at 12 months, 12.1% at 36 months, and 13.75% at 48 months after radiofrequency treatment. Concomitantly, there was a marked improvement in both the symptoms score and the quality of life score for gastroesophageal reflux (44).

In a retrospective study involving 15 patients, the efficacy of radiofrequency treatment for gastroesophageal reflux after LSG was assessed. At the six-month post-treatment mark, a majority of patients (66.7%) expressed dissatisfaction, and only a fifth (20%) had ceased using acid suppressants. Additionally, two patients (13.3%) required a subsequent RYGB surgery at eight months post-treatment to address persistent reflux symptoms (45). Therefore, the therapeutic role of radiofrequency treatment in patients with reflux after LSG requires further investigation.

4.5 Other treatment modalities

A study comparing the conversion from LSG to One-Anastomosis Gastric Bypass (OAGB) versus RYGB surgery revealed that OAGB may offer superior outcomes in terms of acid exposure and DeMeester scores, even though it was associated with a higher prevalence of reflux symptoms in the OAGB group (25). Additional studies suggest that OAGB might be as effective as RYGB in addressing reflux following LSG. Data from Rheinwalt's research indicate that the rates of GERD remission after converting from LSG to RYGB and OAGB were 89% and 87%, respectively (46). Dayan et al. (26) found that 77.4% of patients who underwent conversion to OAGB after LSG experienced a resolution of reflux symptoms and were able to discontinue acid suppressants, with their average GERD-HRQL score plummeting from 9.6 preoperatively to 1.7 postoperatively.

Endoscopic interventions that are commonly used for GERD in patients who have not had gastric surgery have not yet been widely adopted for the treatment of post-LSG reflux. These include procedures such as transoral incisionless fundoplication and transoral endoscopic cardial plication. Given the uncertain safety profile of these methods, further study is required to determine their safety and therapeutic effectiveness in the context of post-LSG reflux management.

5 Concurrent surgical treatment and prevention of reflux during LSG

5.1 LSG combined with hiatal hernia repair

Excessive body weight is significantly associated with the presence of hiatal hernia and esophagitis (47). Furthermore, central obesity and hiatal hernia can lead to an increase in GERD (48). A meta-analysis of 18 studies suggests that LSG combined with Hiatal Hernia Repair (HHR) results in a 68% reduction in GERD symptoms, as well as significant improvements in esophagitis and GERD- HRQL. However, the article also notes that there is no significant difference between LSG + HHR and LSG alone in terms of new-onset GERD, with postoperative incidence rates of new GERD at 12.0% and a recurrence rate of hiatal hernia at 11.0% (49). Additionally, another study that included 91 patients and completed a 7-year follow-up found that among patients with preoperative gastroesophageal reflux, 60% experienced relief from their symptoms. Nevertheless, 30.6% of patients reported postoperative reflux symptoms, with 15.9% experiencing persistent GERD and 14.8% experiencing new-onset GERD (50).

In the study by Perez et al. (51), they utilized Propensity Score Matched Analysis to examine patients from The Metabolic and Bariatric Surgery Accreditation and Quality Improvement (MBSAQIP) database. They found that LSG + HHR had a similar risk of death, postoperative bleeding, leakage, or reoperation within 30 days after surgery when compared to LSG alone. However, the risk of postoperative pneumonia (0.45% vs 0.15%) and readmission rates (4.69% vs 3.58%) were higher after LSG+HHR.

HHR encompasses three primary techniques: posterior repair with mesh (PRM), posterior repair (PR), and anterior repair (AR). Ehlers and colleagues (52) conducted an analysis of data from the Michigan Bariatric Surgery Collaborative (MBSC) spanning from 2008 to 2019, revealing that PR was the most frequently performed procedure, constituting 78% of the cases. The severity of heartburn at baseline was assessed using the GERD- HRQL scale, with the PRM group exhibiting the highest scores (PRM 1.40 versus PR 1.20 versus AR 0.99). However, the PR cohort had the lowest average heartburn severity score at one year postoperatively (PR 0.81 vs PRM 0.84 vs AR 0.96). Patients across all three surgical groups

reported high levels of satisfaction at the one-year postoperative follow-up, with no statistically significant differences in satisfaction among the groups. Additionally, there were no significant differences in the incidence of bleeding, leakage, or surgical complications at 30 days postoperatively across the three cohorts. In a separate study based on the same database covering the period from 2015 to 2019, Hider and associates (53) focused solely on the comparison between PR and AR. They found that patients undergoing PR had a higher rate of improvement in GERD symptoms (69.5% vs 64.0%) and a lower rate of new symptoms at one year (28.2% vs 30.2%). Conversely, patients receiving AR had higher rates of bleeding and readmission.

In conclusion, the combination of LSG and HHR has been shown to substantially reduce GERD symptoms in patients with a minimal risk of complications. Performing HHR concurrently with LSG is deemed a safe surgical practice, and within the HHR techniques, posterior repair seems to be the preferred approach. A panel of 50 experts from across 25 nations engaged in a discourse on LSG and GERD, with 80% of the experts supporting the concurrent repair of large hiatal hernias during LSG, and 66.7% supporting the concurrent repair of small hiatal hernias (54).

5.2 LSG combined with fundoplication

Fundoplication has long been the standard approach for surgical treatment of GERD. This procedure involves using either a portion of the stomach fundus (Dor 180°, Toupet 270°) or the entire fundus (Rossetti, Nissen 360°) to wrap around the lower esophageal sphincter (LES), providing structural support to enhance its ability to prevent reflux. Studies conducted by Capua and associates have shown that the combination of LSG and Rossetti fundoplication can significantly elevate LES pressure in patients following surgery (55). In a survey of 50 experts, 77.3% reported using LSG along with an anti-reflux procedure (either anterior or posterior fundoplication) in patients with GERD symptoms (54).

Olmi and colleagues performed surgery using LSG combined with a modified Rossetti fundoplication on 220 patients, of which 68.5% had preoperative reflux symptoms. Following the procedure, 98.5% of the patients reported no reflux symptoms and were not reliant on PPI medication. Among those with preoperative esophagitis, 96.9% experienced relief, and all four patients with Barrett's esophagus showed improvement. The incidence of Clavien–Dindo grade III or higher complications was 6.9%, primarily due to fundus perforations (56). In another study involving 56 patients, the postoperative GERD outcomes of LSG and LSGFD were compared. Patients without preoperative reflux symptoms were placed in the LSG group, while those with reflux symptoms were assigned to the LSGFD group. At 12 months postoperatively, the incidence of new-onset GERD following LSG was 52.2%, which reduced to 30.4% at an average follow-up of 34 months. In the LSGFD group, 86.4% experienced relief from reflux symptoms at 12 months, and 90.9% did so at an average follow-up of 34 months. There were no notable disparities between the two groups in terms of weight loss and postoperative complications (57).

In a meta-analysis encompassing five studies, researchers reviewed the current evidence and outcomes of LSGFD. They discovered that LSGFD resulted in superior GERD relief postoperatively but may lead to a lower percentage of total weight loss and a higher incidence of postoperative complications (OR=2.56) (58).

LSGFD is evidently effective in the prevention and treatment of GERD, but it also comes with an increased risk of postoperative complications. Currently, there is a scarcity of literature comparing the outcomes of LSG and LSGFD, and the clinical application of LSGFD requires careful assessment of the risks versus benefits by the surgeon. In the comparison between LSG+HHR and LSGFD, both procedures are effective in alleviating and preventing GERD following LSG. LSGFD demonstrates a stronger advantage in managing reflux, but it also has a higher overall complication rate (59).

5.3 The impact of LSG surgical technique

The LSG surgical procedure can also impact postoperative GERD. Currently, the main disagreement among surgeons focuses on the distance between the resection line and the pylorus, as well as the sizes of the bougie.

A meta-analysis based on randomized controlled trials compared four RCT studies that described post-operative GERD and the distance between the resection line and the pylorus. It found that, in the late postoperative period, GERD was significantly reduced in the group where the resection was performed 6cm from the pylorus, compared to 2cm from the pylorus (OR=0.40) (60). However, an earlier meta-analysis showed no statistical difference in the incidence of new-onset GERD between antral resection (with the staple line starting 2-3 cm from the pylorus) and antral preservation (>5 cm from the pylorus) (61). Another study, based on an observational cohort, a shorter distance to the pylorus was found to be a predictor of postoperative GERD relief, while a shorter distance to the angle of His was a risk factor for new-onset GERD. But they did not find a correlation between the distance to the pylorus and the occurrence of GERD (62). Currently, there is still controversy over how far from the pylorus the resection should begin. Forty-one experts from China, Japan, and South Korea discussed postoperative GERD following LSG in Shanghai (63), with 70.7% of the experts agreeing that starting the resection 4-6 cm from the pylorus and reasonably preserving the antrum during surgery could effectively reduce the incidence of postoperative GERD.

Additionally, the choice of bougie size is quite controversial. In a meta-analysis conducted by Yao Wang and associates (64), bougie sizes were classified into two groups: less than or equal to 36Fr, and greater than 36Fr. They found that the smaller bougie group had better weight loss outcomes without increasing the risk of postoperative leaks or GERD. In another network meta-analysis, the bougie sizes were divided into four groups: XL (> 40 Fr), L (36–40 Fr), M (33–36 Fr), and S (< 32 Fr) (65). They discovered that the

S and M size bougies were more effective in reducing excess weight, and the M size bougie had lower rates of postoperative leaks and overall complications. However, an earlier systematic review that included 112 studies found that bougies ≥40 Fr reduced the risk of leaks (OR = 0.53). The distance from the pylorus was found to have no impact on leaks or the percentage of excess weight loss (66). In the Shanghai conference (63), considering that excessive resection of the fundus may lead to rapid gastric emptying, affecting patients' dietary control and weight loss outcomes, 85.4% of experts agreed to recommend the use of 36~38Fr bougies to ensure surgical effectiveness while reducing the incidence of postoperative GERD.

6 Conclusion

The high incidence of gastroesophageal reflux after LSG has become a significant challenge for post-operative patients. Currently, the primary approach to managing reflux after LSG is through conservative medical interventions. When faced with persistent gastroesophageal reflux that does not respond to acid suppressants for over three months, the prevailing recommendation within the medical community is to transition to Roux-en-Y gastric bypass (RYGB) surgery. The revised RYGB surgery has proven effective in controlling post-LSG reflux symptoms and enhancing patients' quality of life. In recent times, innovative surgical techniques have been gaining traction as a means to address the symptoms of refractory gastroesophageal reflux in patients after LSG. Laparoscopic magnetic sphincter augmentation, for instance, has shown promise in mitigating acid reflux symptoms and reducing the duration of esophageal acid exposure. Additionally, other endoscopic treatments have yielded positive therapeutic outcomes. Nevertheless, the long-term safety and effectiveness of these interventions for post-LSG reflux remain to be fully validated through future research. For patients who are found to have hiatal hernia during preoperative evaluation, concurrent repair of the hiatal hernia during LSG can be contemplated. This approach significantly reduces the probability of postoperative GERD and has a relatively low incidence of postoperative complications, making it a safe and effective surgical option. For those with preoperative gastroesophageal reflux, LSGFG can be considered to forestall the onset of postoperative GERD. However, this procedure may introduce additional surgical risk, and the decision to proceed with LSGFG should be made following thorough consideration by the surgical team.

Author contributions

GL: Writing – review & editing, Writing – original draft, Investigation. PW: Methodology, Investigation, Writing – review & editing. SR: Writing – review & editing. XX: Writing – review & editing. HM: Writing – review & editing, Resources, Project administration, Funding acquisition.

Funding

The author(s) declare financial support was received for the research, authorship, and/or publication of this article. This research was funded by the National High Level Hospital Clinical Research Funding (2023-NHLHCRF-YS-0103), National High Level Hospital Clinical Research Funding (2023-NHLHCRF-YYPP-TS-02), Beijing Demonstration Program of Research Ward (2022-YJXBF-03-02), Beijing Natural Science Foundation (7242125), National Natural Science Foundation of China (82470857), China-Japan Friendship Hospital Talent Introduction Project (No.2018-RC-1), "Kunlun Talents · High-end Innovation and Entrepreneurial Talents" project of Qinghai Province (202308210043).

Conflict of interest

The authors declare that the research was conducted in the absence of any commercial or financial relationships that could be construed as a potential conflict of interest.

Publisher's note

References

1. Blüher M. Obesity: global epidemiology and pathogenesis. *Nat Rev Endocrinol*. (2019) 15:288–98. doi: 10.1038/s41574-019-0176-8

2. Chen K, Shen Z, Gu W, Lyu Z, Qi X, Mu Y, et al. Prevalence of obesity and associated complications in China: A cross-sectional, real-world study in 15. *8 million adults. Diabetes Obes Metab*. (2023) 25:3390–9. doi: 10.1111/dom.15238

3. Clapp B, Ponce J, Corbett J, Ghanem OM, Kurian M, Rogers AM, et al. American Society for Metabolic and Bariatric Surgery 2020 estimate of metabolic and bariatric procedures performed in the United States. *Surg Obes Relat Dis*. (2022) 18(9):1134–40. doi: 10.1016/j.soard.2022.06.284

4. Znamirowski P, Kołomańska M, Mazurkiewicz R, Tymchyshyn O, Nawacki Ł. GERD as a complication of laparoscopic sleeve gastrectomy for the treatment of obesity: A systematic review and meta-analysis. *J Pers Med*. (2023) 13:1243. doi: 10.3390/jpm13081243

5. Trujillo AB, Sagar D, Amaravadhi AR, Muraleedharan D, Malik MZ, Effa-Ababio K, et al. Incidence of post-operative gastro-esophageal reflux disorder in patients undergoing laparoscopic sleeve gastrectomy: A systematic review and meta-analysis. *Obes Surg*. (2024) 34(5):1874–84. doi: 10.1007/s11695-024-07163-y

6. Hajibandeh S, Hajibandeh S, Ghassemi N, Evans D, Cheruvu CVN. Meta-analysis of long-term *de novo* acid reflux–related outcomes following sleeve gastrectomy: evidence against the need for routine postoperative endoscopic surveillance. *Curr Obes Rep*. (2023) 12:395–405. doi: 10.1007/s13679-023-00521-4

7. Yeung KTD, Penney N, Ashrafian L, Darzi A, Ashrafian H. Does sleeve gastrectomy expose the distal esophagus to severe reflux?: A systematic review and meta-analysis. *Ann Surg*. (2020) 271:257. doi: 10.1097/SLA.0000000000003275

8. Borbély Y, Schaffner E, Zimmermann L, Huguenin M, Plitzko G, Nett P, et al. *De novo* gastroesophageal reflux disease after sleeve gastrectomy: role of preoperative silent reflux. *Surg Endosc*. (2019) 33:789–93. doi: 10.1007/s00464-018-6344-4

9. Mandeville Y, Van Looveren R, Vancoillie PJ, Verbeke X, Vandendriessche K, Vuylsteke P, et al. Moderating the enthusiasm of sleeve gastrectomy: up to fifty percent of reflux symptoms after ten years in a consecutive series of one hundred laparoscopic sleeve gastrectomies. *Obes Surg*. (2017) 27:1797–803. doi: 10.1007/s11695-017-2567-z

10. Huh YJ, Park JS, Lee S, Han SM. Impacts of sleeve gastrectomy on gastroesophageal reflux disease in severely obese Korean patients. *Asian J Surg*. (2023) 46:244–9. doi: 10.1016/j.asjsur.2022.03.047

11. Stenard F, Iannelli A. Laparoscopic sleeve gastrectomy and gastroesophageal reflux. *World J Gastroenterol*. (2015) 21:10348–57. doi: 10.3748/wjg.v21.i36.10348

12. Quero G, Fiorillo C, Dallemagne B, Mascagni P, Curcic J, Fox M, et al. The causes of gastroesophageal reflux after laparoscopic sleeve gastrectomy: quantitative assessment of the structure and function of the esophagogastric junction by magnetic resonance imaging and high-resolution manometry. *Obes Surg*. (2020) 30:2108–17. doi: 10.1007/s11695-020-04438-y

13. Mion F, Tolone S, Garros A, Savarino E, Pelascini E, Robert M, et al. High-resolution impedance manometry after sleeve gastrectomy: increased intragastric pressure and reflux are frequent events. *Obes Surg*. (2016) 26:2449–56. doi: 10.1007/s11695-016-2127-y

14. Balla A, Meoli F, Palmieri L, Corallino D, Sacchi MC, Ribichini E, et al. Manometric and pH-monitoring changes after laparoscopic sleeve gastrectomy: a systematic review. *Langenbecks Arch Surg*. (2021) 406:2591–609. doi: 10.1007/s00423-021-02171-3

15. Poggi L, Bernui GM, Romani DA, Gavidia AF, Poggi LA. Persistent and *de novo* GERD after sleeve gastrectomy: manometric and pH-impedance study findings. *Obes Surg*. (2023) 33(1):87–93. doi: 10.1007/s11695-022-06126-5

16. Grover K, Khaitan L. Magnetic sphincter augmentation as treatment of gastroesophageal reflux disease after sleeve gastrectomy. *Dis Esophagus*. (2023) 36: doad030. doi: 10.1093/dote/doad030

17. Katzka DA, Kahrilas PJ. Advances in the diagnosis and management of gastroesophageal reflux disease. *BMJ*. (2020) 371:m3786. doi: 10.1136/bmj.m3786

18. Peterli R, Wölnerhanssen BK, Peters T, Vetter D, Kröll D, Borbély Y, et al. Effect of laparoscopic sleeve gastrectomy vs laparoscopic roux-en-Y gastric bypass on weight loss in patients with morbid obesity: the SM-BOSS randomized clinical trial. *JAMA*. (2018) 319:255–65. doi: 10.1001/jama.2017.20897

19. Salminen P, Grönroos S, Helmiö M, Hurme S, Juuti A, Juusela R, et al. Effect of Laparoscopic Sleeve Gastrectomy vs Roux-en-Y Gastric Bypass on Weight Loss, Comorbidities, and Reflux at 10 Years in Adult Patients With Obesity: The SLEEVEPASS Randomized Clinical Trial. *JAMA Surg*. (2022) 157:656–66. doi: 10.1001/jamasurg.2022.2229

20. Guan B, Chong TH, Peng J, Chen Y, Wang C, Yang J. Mid-long-term revisional surgery after sleeve gastrectomy: a systematic review and meta-analysis. *Obes Surg*. (2019) 29:1965–75. doi: 10.1007/s11695-019-03842-3

21. Stefanidis D, Hope WW, Kohn GP, Reardon PR, Richardson WS, Fanelli RD, et al. Guidelines for surgical treatment of gastroesophageal reflux disease. *Surg Endosc*. (2010) 24:2647–69. doi: 10.1007/s00464-010-1267-8

22. Katz PO, Gerson LB, Vela MF. Guidelines for the diagnosis and management of gastroesophageal reflux disease. *Am J Gastroenterol*. (2013) 108:308–328;quiz 329. doi: 10.1038/ajg.2012.444

23. Madalosso CAS, Gurski RR, Callegari-Jacques SM, Navarini D, Mazzini G, Pereira M da S. The impact of gastric bypass on gastroesophageal reflux disease in morbidly obese patients. *Ann Surg*. (2016) 263:110. doi: 10.1097/SLA.0000000000001139

24. Huynh D, Mazer L, Tung R, Cunneen S, Shouhed D, Burch M. Conversion of laparoscopic sleeve gastrectomy to Roux-en-Y gastric bypass: patterns predicting persistent symptoms after revision. *Surg Obes Related Diseases*. (2021) 17:1681–8. doi: 10.1016/j.soard.2021.05.025

25. Felsenreich DM, Steinlechner K, Langer FB, Vock N, Eichelter J, Bichler C, et al. Outcome of sleeve gastrectomy converted to roux-en-Y gastric bypass and one-anastomosis gastric bypass. *Obes Surg*. (2022) 32:643–51. doi: 10.1007/s11695-021-05866-0

26. Dayan D, Kanani F, Bendayan A, Nizri E, Lahat G, Abu-Abeid A. The effect of revisional one anastomosis gastric bypass after sleeve gastrectomy on gastroesophageal reflux disease, compared with revisional roux-en-Y gastric bypass: symptoms and quality of life outcomes. *Obes Surg*. (2023) 33:2125–31. doi: 10.1007/s11695-023-06636-w

27. D'Urso A, Vix M, Perretta S, Ignat M, Scheer L, Mutter D. Indications and long-term outcomes of conversion of sleeve gastrectomy to roux-en-Y gastric bypass. *Obes Surg*. (2021) 31:3410–8. doi: 10.1007/s11695-021-05444-4

28. Strauss AL, Triggs JR, Tewksbury CM, Soriano I, Wernsing DS, Dumon KR, et al. Conversion to Roux-En-Y Gastric Bypass: a successful means of mitigating reflux after laparoscopic sleeve gastrectomy. *Surg Endosc*. (2023) 37:5374–9. doi: 10.1007/s00464-023-10024-x

29. Hedberg S, Thorell A, Österberg J, Peltonen M, Andersson E, Näslund E, et al. Comparison of sleeve gastrectomy vs roux-en-Y gastric bypass. *JAMA Netw Open*. (2024) 7:e2353141. doi: 10.1001/jamanetworkopen.2023.53141

30. Rebecchi F, Allaix ME, Ugliono E, Giaccone C, Toppino M, Morino M. Increased esophageal exposure to weakly acidic reflux 5 years after laparoscopic roux-en-Y gastric bypass. *Ann Surg*. (2016) 264:871–7. doi: 10.1097/SLA.0000000000001775

31. Riva CG, Asti E, Lazzari V, Aquilino K, Siboni S, Bonavina L. Magnetic sphincter augmentation after gastric surgery. *JSLS*. (2019) 23:e2019.00035. doi: 10.4293/JSLS.2019.00035

32. Rausa E, Manfredi R, Kelly ME, Bianco F, Aiolfi A, Bonitta G, et al. Magnetic sphincter augmentation placement for recalcitrant gastroesophageal reflux disease following bariatric procedures: A systematic review and bayesian meta-analysis. *J Laparoendoscopic Advanced Surg Techniques*. (2021) 31:1034–9. doi: 10.1089/lap.2020.0763

33. Patel SH, Smith B, Polak R, Pomeranz M, Patel PV, Englehardt R. Laparoscopic magnetic sphincter augmentation device placement for patients with medically-refractory gastroesophageal reflux after sleeve gastrectomy. *Surg Endosc*. (2022) 36:8255–60. doi: 10.1007/s00464-022-09261-3

34. Broderick RC, Smith CD, Cheverie JN, Omelanczuk P, Lee AM, Dominguez-Profeta R, et al. Magnetic sphincter augmentation: a viable rescue therapy for symptomatic reflux following bariatric surgery. *Surg Endosc*. (2020) 34:3211–5. doi: 10.1007/s00464-019-07096-z

35. Leeds SG, Ngov A O, Ogola G, Ward MA. Safety of magnetic sphincter augmentation in patients with prior bariatric and anti-reflux surgery. *Surg Endosc*. (2021) 35:5322–7. doi: 10.1007/s00464-020-08025-1

36. Kuckelman JP, Phillips CJ, Derickson MJ, Faler BJ, Martin MJ. Esophageal magnetic sphincter augmentation as a novel approach to post-bariatric surgery gastroesophageal reflux disease. *Obes Surg*. (2018) 28:3080–6. doi: 10.1007/s11695-018-3292-y

37. Khaitan L, Hill M, Michel M, Chiasson P, Woodworth P, Bell R, et al. Feasibility and efficacy of magnetic sphincter augmentation for the management of gastroesophageal reflux disease post-sleeve gastrectomy for obesity. *Obes Surg*. (2023) 33:387–96. doi: 10.1007/s11695-022-06381-6

38. Inoue H, Ito H, Ikeda H, Sato C, Sato H, Phalanusitthepha C, et al. Anti-reflux mucosectomy for gastroesophageal reflux disease in the absence of hiatus hernia: a pilot study. *Ann Gastroenterol*. (2014) 27:346–51.

39. Zhu X, Shen J. Anti-reflux mucosectomy (ARMS) for refractory gastroesophageal reflux disease. *Eur J Med Res*. (2024) 29:185. doi: 10.1186/s40001-024-01789-5

40. Patil G, Iyer A, Dalal A, Maydeo A. Antireflux mucosectomy for managing reflux symptoms in an obese patient post laparoscopic sleeve gastrectomy. *Scand J Gastroenterol*. (2019) 54:1494–7. doi: 10.1080/00365521.2019.1697895

41. Debourdeau A, Vitton V, Monino L, Barthet M, Gonzalez JM. Antireflux mucosectomy band (ARM-b) in treatment of refractory gastroesophageal reflux disease after bariatric surgery. *Obes Surg*. (2020) 30:4654–8. doi: 10.1007/s11695-020-04753-4

42. Kahrilas PJ. Radiofrequency energy treatment of GERD. *Gastroenterology*. (2003) 125:970–3. doi: 10.1016/S0016-5085(03)01132-6

43. Triadafilopoulos G, DiBaise JK, Nostrant TT, Stollman NH, Anderson PK, Edmundowicz SA, et al. Radiofrequency energy delivery to the gastroesophageal junction for the treatment of GERD. *Gastrointestinal Endoscopy*. (2001) 53:407–15. doi: 10.1067/mge.2001.112843

44. Reymunde A, Santiago N. Long-term results of radiofrequency energy delivery for the treatment of GERD: sustained improvements in symptoms, quality of life, and drug use at 4-year follow-up. *Gastrointestinal Endoscopy*. (2007) 65:361–6. doi: 10.1016/j.gie.2006.06.036

45. Khidir N, Angrisani L, Al-Qahtani J, Abayazeed S, Bashah M. Initial experience of endoscopic radiofrequency waves delivery to the lower esophageal sphincter (Stretta procedure) on symptomatic gastroesophageal reflux disease post-sleeve gastrectomy. *Obes Surg*. (2018) 28:3125–30. doi: 10.1007/s11695-018-3333-6

46. Rheinwalt KP, Schipper S, Plamper A, Alizai PH, Trebicka J, Brol MJ, et al. Roux-en-Y versus one anastomosis gastric bypass as redo-operations following sleeve gastrectomy: A retrospective study. *World J Surg*. (2022) 46:1. doi: 10.1007/s00268-021-06424-6

47. Wilson LJ, Ma W, Hirschowitz BI. Association of obesity with hiatal hernia and esophagitis. *Am J Gastroenterol*. (1999) 94:2840–4. doi: 10.1111/j.1572-0241.1999.01426.x

48. Lee YY, Wirz AA, Whiting JGH, Robertson EV, Smith D, Weir A, et al. Waist belt and central obesity cause partial hiatus hernia and short-segment acid reflux in asymptomatic volunteers. *Gut*. (2014) 63:1053–60. doi: 10.1136/gutjnl-2013-305803

49. Chen W, Feng J, Wang C, Wang Y, Yang W, Dong Z, et al. Effect of concomitant laparoscopic sleeve gastrectomy and hiatal hernia repair on gastroesophageal reflux disease in patients with obesity: a systematic review and meta-analysis. *Obes Surg*. (2021) 31:3905–18. doi: 10.1007/s11695-021-05545-0

50. Angrisani L, Santonicola A, Borrelli V, Iovino P. Sleeve gastrectomy with concomitant hiatal hernia repair in obese patients: long-term results on gastroesophageal reflux disease. *Surg Obes Relat Dis*. (2020) 16:1171–7. doi: 10.1016/j.soard.2020.04.049

51. Perez SC, Ericksen F, Richardson N, Thaqi M, Wheeler AA. Propensity score matched analysis of laparoscopic revisional and conversional sleeve gastrectomy with

concurrent hiatal hernia repair. *Surg Endosc*. (2024) 38(7):3866–74. doi: 10.1007/s00464-024-10902-y

52. Ehlers AP, Bonham AJ, Ghaferi AA, Finks JF, Carlin AM, Varban OA. Impact of hiatal hernia repair technique on patient-reported gastroesophageal reflux symptoms following laparoscopic sleeve gastrectomy. *Surg Endosc*. (2022) 36:6815–21. doi: 10.1007/s00464-021-08970-5

53. Hider AM, Bonham AJ, Carlin AM, Finks JF, Ghaferi AA, Varban OA, et al. Impact of concurrent hiatal hernia repair during laparoscopic sleeve gastrectomy on patient-reported gastroesophageal reflux symptoms: a state-wide analysis. *Surg Obes Relat Dis*. (2023) 19:619–25. doi: 10.1016/j.soard.2022.12.021

54. Assalia A, Gagner M, Nedelcu M, Ramos AC, Nocca D. Gastroesophageal reflux and laparoscopic sleeve gastrectomy: results of the first international consensus conference. *Obes Surg*. (2020) 30:3695–705. doi: 10.1007/s11695-020-04749-0

55. Di Capua F, Cesana GC, Uccelli M, De Carli SM, Giorgi R, Ferrari D, et al. Sleeve gastrectomy with rossetti fundoplication increases lower esophageal sphincter tone preventing gastroesophageal reflux disease: high-resolution manometry assessment. *J Laparoendosc Adv Surg Tech A*. (2023) 33:44–51. doi: 10.1089/lap.2022.0123

56. Olmi S, Uccelli M, Cesana GC, Ciccarese F, Oldani A, Giorgi R, et al. Modified laparoscopic sleeve gastrectomy with Rossetti antireflux fundoplication: results after 220 procedures with 24-month follow-up. *Surg Obes Relat Dis*. (2020) 16:1202–11. doi: 10.1016/j.soard.2020.03.029

57. Aili A, Maimaitiming M, Maimaitiyusufu P, Tusuntuoheti Y, Li X, Cui J, et al. Gastroesophageal reflux related changes after sleeve gastrectomy and sleeve gastrectomy with fundoplication: A retrospective single center study. *Front Endocrinol (Lausanne)*. (2022) 13:1041889. doi: 10.3389/fendo.2022.1041889

58. Loo JH, Chue KM, Lim CH, Toh BC, Kariyawasam GMD, Ong LWL, et al. Effectiveness of sleeve gastrectomy plus fundoplication versus sleeve gastrectomy alone for treatment of patients with severe obesity: a systematic review and meta-analysis. *Surg Obes Relat Dis*. (2024) 20:532–43. doi: 10.1016/j.soard.2023.12.007

59. Castagneto-Gissey L, Russo MF, D'Andrea V, Genco A, Casella G. Efficacy of sleeve gastrectomy with concomitant hiatal hernia repair versus sleeve–fundoplication on gastroesophageal reflux disease resolution: systematic review and meta-analysis. *J Clin Med*. (2023) 12:3323. doi: 10.3390/jcm12093323

60. Diab ARF, Kim A, Remmel S, Sandstrom R, Docimo S, Sujka JA, et al. Antral preservation in sleeve gastrectomy appears to protect against prolonged vomiting and gastroesophageal reflux disease. A meta-analysis of randomized controlled trials. *Obes Surg*. (2023) 33:4103–14. doi: 10.1007/s11695-023-06884-w

61. McGlone ER, Gupta AK, Reddy M, Khan OA. Antral resection versus antral preservation during laparoscopic sleeve gastrectomy for severe obesity: Systematic review and meta-analysis. *Surg Obes Relat Dis*. (2018) 14:857–64. doi: 10.1016/j.soard.2018.02.021

62. Lyyjynen HS, Andersen JR, Liem RSL, Mala T, Nienhuijs SW, Ottosson J, et al. Surgical aspects of sleeve gastrectomy are related to weight loss and gastroesophageal reflux symptoms. *Obes Surg*. (2024) 34:902–10. doi: 10.1007/s11695-023-07018-y

63. Chinese Society for Metabolic and Bariatric Surgery(CSMBS), Chinese Society for Gastroesophageal Reflux Disease (CSGERD), Japanese Society for Treatment of Obesity(JSTO) and Korean Society for Metabolic and Bariatric Surgery (KSMBS). Shanghai consensus on the diagnosis and treatment of gastroesophageal reflux disease in patients undergoing sleeve gastrectomy(2024 edition). *Zhonghua Wei Chang Wai Ke Za Zhi*. (2024) 27:863–78. doi: 10.3760/cma.j.cn441530-20240819-00290

64. Wang Y, Yi XY, Gong Ll, Li Q, Zhang J, Wang Zh. The effectiveness and safety of laparoscopic sleeve gastrectomy with different sizes of bougie calibration: A systematic review and meta-analysis. *Int J Surg*. (2018) 49:32–8. doi: 10.1016/j.ijsu.2017.12.005

65. Chang PC, Chen KH, Jhou HJ, Chen PH, Huang CK, Lee CH, et al. Promising effects of 33 to 36 Fr. bougie calibration for laparoscopic sleeve gastrectomy: a systematic review and network meta-analysis. *Sci Rep*. (2021) 11:15217. doi: 10.1038/s41598-021-94716-1

66. Parikh M, Issa R, McCrillis A, Saunders JK, Ude-Welcome A, Gagner M. Surgical strategies that may decrease leak after laparoscopic sleeve gastrectomy: a systematic review and meta-analysis of 9991 cases. *Ann Surg*. (2013) 257:231–7. doi: 10.1097/SLA.0b013e31826cc714

frontiers | Frontiers in Endocrinology

TYPE Original Research
PUBLISHED 08 January 2025
DOI 10.3389/fendo.2024.1456885

OPEN ACCESS

EDITED BY
Yayun Wang,
Air Force Medical University, China

REVIEWED BY
Emanuel Vamanu,
University of Agricultural Sciences and Veterinary Medicine, Romania
Wendong Huang,
City of Hope, United States
Haiming Fang,
Second Hospital of Anhui Medical University, China

*CORRESPONDENCE
Liangping Wu
drwulp@163.com
Hongbin Zhang
zhangwater@hotmail.com

†These authors have contributed equally to this work and share first authorship

RECEIVED 29 June 2024
ACCEPTED 17 December 2024
PUBLISHED 08 January 2025

CITATION
Li H, He J, Hou J, He C, Dai X, Song Z, Liu Q, Wang Z, Huang H, Ding Y, Qi T, Zhang H and Wu L (2025) Intestinal rearrangement of biliopancreatic limbs, alimentary limbs, and common limbs in obese type 2 diabetic mice after duodenal jejunal bypass surgery. *Front. Endocrinol.* 15:1456885. doi: 10.3389/fendo.2024.1456885

Intestinal rearrangement of biliopancreatic limbs, alimentary limbs, and common limbs in obese type 2 diabetic mice after duodenal jejunal bypass surgery

Heng Li[1,2†], Jipei He[3†], Jie Hou[1], Chengjun He[1], Xiaojiang Dai[1], Zhigao Song[4], Qing Liu[5], Zixin Wang[1], Hongyan Huang[1], Yunfa Ding[1], Tengfei Qi[1], Hongbin Zhang[3,6*] and Liangping Wu[1,7*]

[1]Department of Metabolic Surgery, Jinshazhou Hospital of Guangzhou University of Chinese Medicine, Guangzhou, China, [2]Department of Endocrinology and Metabolism, Third Affiliated Hospital of Sun Yat-Sen University, Guangzhou, China, [3]Department of Basic Medical Research, General Hospital of Southern Theater Command of People's Liberation Army (PLA), Guangzhou, China, [4]Department of Cardiovascular Surgery, Zhujiang Hospital of Southern Medical University, Guangzhou, China, [5]Zhongshan Institute for Drug Discovery, Shanghai Institute of Materia Medica, Chinese Academy of Sciences, Guangzhou, China, [6]School of Laboratory Medicine and Biotechnology, Southern Medical University, Guangzhou, China, [7]Guangzhou Hualiang Qingying Biotechnology Co. Ltd, Guangzhou, China

Bariatric surgery is an effective treatment for type 2 Diabetes Mellitus (T2DM), yet the precise mechanisms underlying its effectiveness remain incompletely understood. While previous research has emphasized the role of rearrangement of the gastrointestinal anatomy, gaps persist regarding the specific impact on the gut microbiota and barriers within the biliopancreatic, alimentary, and common limbs. This study aimed to investigate the effects of duodenal-jejunal bypass (DJB) surgery on obese T2DM mice. We performed DJB and SHAM surgery in obese T2DM mice to investigate changes in the gut microbiota and barrier across different intestinal limbs. The effects on serum metabolism and potential associations with T2DM improvement were also investigated. Following DJB surgery, there was an increased abundance of commensals across various limbs. Additionally, the surgery improved intestinal permeability and inflammation in the alimentary and common limbs, while reducing inflammation in the biliopancreatic limbs. Furthermore, DJB surgery also improved T2DM by increasing L-glutamine, short-chain fatty acids, and bile acids and decreasing branched-chain amino acids. This study underscores the role of intestinal rearrangement in reshaping gut microbiota composition and enhancing gut barrier function, thereby contributing to the amelioration of T2DM following bariatric surgery, and providing new insights for further research on bariatric surgery.

KEYWORDS

duodenal jejunal bypass, type 2 diabetes mellitus, gut microbiota, gut barrier, metabonomics, bariatric surgery

1 Introduction

Bariatric surgery is increasingly performed worldwide to treat morbid obesity and is also known as metabolic surgery due to its beneficial metabolic effects, especially with respect to improvement in type 2 Diabetes Mellitus (T2DM) (1). In T2DM, relative insulin deficiency resulting from β-cell dysfunction is a key factor contributing to disease development, often in conjunction with insulin resistance (2). With the evolution of metabolic surgery, it has emerged as a viable long-term intervention for treating diabetes (3).

Roux-en-Y gastric bypass (RYGB) is a highly effective treatment for severe obesity and type 2 diabetes. By inducing alterations in the anatomical structure of the gastrointestinal tract, RYGB modifies the gut microbiota and diminishes systemic endotoxemia (4, 5). Anatomical rearrangement of the gastrointestinal tract likely alters the composition of the luminal milieu, consequently influencing downstream signaling pathways that regulate host energy balance and metabolism (1). Previous studies have highlighted the importance of jejunal and duodenal nutrient sensing in blood glucose homeostasis (6) with studies indicating that nutrient infusion bypassing the duodenum enhances insulin sensitivity (7). Rubino et al. have identified the proximal jejunum's involvement in the pathogenesis of T2DM (8). However, the mechanisms underlying these effects are not fully understood. To address these knowledge gaps, we adopted the recently developed duodenojejunal bypass (DJB) mouse model. DJB is a metabolic procedure involving the exclusion of nutrients from the duodenum and proximal jejunum, followed by jejunal Roux-en-Y reconstruction and early nutrient delivery to the distal small bowel (9). Intestinal remodeling following DJB surgery preserves the physiological structure of the stomach and provides an avenue for investigating the mechanism by which the proximal jejunum improves metabolism.

Combining 16S rRNA gene sequencing with metabolomics is considered a reliable method for analyzing structural changes in the gut microbiota and the metabolic profiles of the gut microbiota and the host (10). The gut microbiota is crucial for many biological functions in the body, including intestinal development, barrier integrity and function, metabolism, and the immune system (11, 12). In healthy individuals, the intestinal barrier consists of a cohesive layer of epithelial cells connected by tight junctions (TJ) (13). However, metabolites originating from the gut microbiota can enter the circulatory system, breaching the intestinal barrier to influence distal organs and potentially impact the progression of T2D (10). Increasing evidence has shown compositional differences in the gut microbiota and their metabolic characteristics, as well as the relationship between the intestinal microbiota and metabolism in T2D patients and healthy individuals (14). In this study, we used 16S rRNA gene sequencing and metabolomics to analyze the changes in the proximal gut microbiota and serum metabolism, aiming to elucidate their contributions to the DJB effect. The proximal jejunum was surgically treated in three separate sections, each of which may contribute to different local responses of the gut microbiota.

2 Materials and methods

2.1 Animals

Twenty 8-week-old male C57BL/6J mice were purchased from China Yaokang Cavens Laboratory Animal Center, housed in a specific pathogen-free (SPF) laboratory, and subjected to a light/dark cycle for 12 hours. Temperature was maintained at 22 ± 2℃ and humidity 55–65%. For six weeks, the mice were provided water and a diet containing 60% of calories from fat. To induce diabetes, intraperitoneal streptozotocin (40 mg/kg) was administered at week 7 for 5 consecutive days. Among the twenty mice, fourteen mice were screened for random blood glucose > 16.7 mmol/L and were randomly assigned to DJB (n=9) and SHAM (n=5) surgery groups. Six mice were excluded from the experiment due to substandard blood glucose. Nine mice underwent DJB surgery, five mice survived.

2.2 Surgical procedure

The DJB surgical procedures were performed as described in the Supplementary Material. For SHAM surgery, gastrointestinal transection and re-anastomosis are performed at a similar site as DJB (Figure 1).

2.3 Measurement of food intake, body weight, and blood glucose

The mice were allowed to recover for 1 week after surgery. Mice were individually housed in cages, and food intake was measured by weighing the amount of solid food before and after 24 hours. The body weights and random blood glucose levels of the mice were recorded before and 8 weeks after surgery. The mice were allowed to fast for 8 hours before the oral glucose tolerance test (OGTT) experiment in the 8th week after surgery, wherein an oral bolus of 20% D-glucose (2 g/kg) was administered to the mice, and blood glucose levels were measured at 0, 15, 30, 60, 90, 120, 150, and 180 min after gavage. Blood glucose levels were measured in blood collected from the tail vein using a handheld AccuChek Performa Glucometer (Roche).

2.4 Sample collection

At 8 weeks post-surgery, the mice were fasted overnight, and then euthanized to collect blood samples, which were stored at room temperature for 2-4 h, and then centrifuged at 3000 rpm for 10 min to extract the sera. Carefully collected intestinal contents and intestinal tissues of the biliopancreatic limb (BP limb), alimentary limb (A limb), common limb (C limb), caecum limb (CA limb), and colon limb (COL limb) were promptly frozen in liquid nitrogen and stored at −80°C. Representative sections of the

10.3389/fendo.2024.1456885

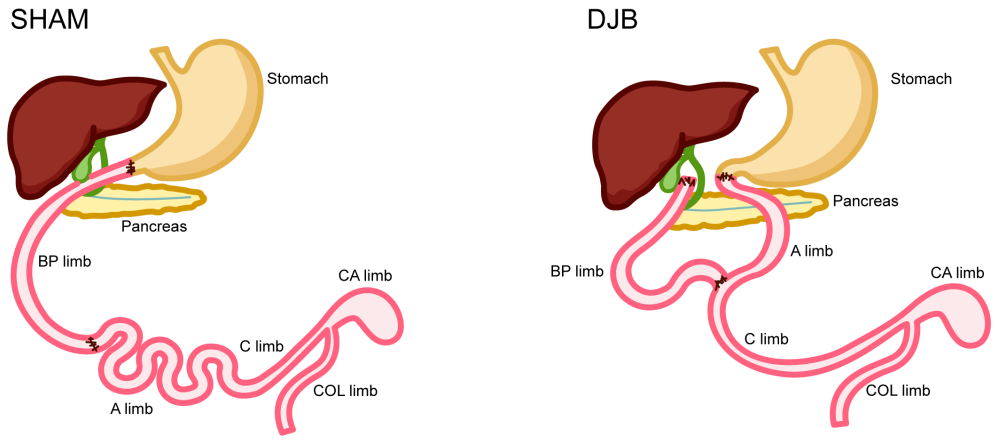

FIGURE 1
Operations and intestinal sampling locations. SHAM operation. Duodenal jejunal bypass (DJB) operation. BP limb, biliopancreatic limb; A limb, alimentary limb; C limb, common limb; CA limb, caecum limb; COL limb, colon limb.

intestinal segments were also collected from the SHAM animals for comparison. Histological analysis was performed on intestinal tissues.

2.5 RNA extraction and quantitative real time–ploymerase chain reaction (qRT-PCR)

Total RNA was extracted from intestinal tissues using an EZ-press RNA Purification Kit (EZ Bioscience, Shanghai, China) and reverse transcribed into cDNA using an EZscript Reverse Transcription Mixture (EZ Bioscience, Shanghai, China) according to the manufacturer's protocol. qRT-PCR was performed using the SYBR Green Master Mix (EZBioscience, Shanghai, China). The results were normalized as relative values of GAPDH mRNA, and the data were analyzed according to $2^{-\Delta\Delta CT}$. The primer sequences are listed in Supplementary Table 1.

2.6 Hematoxylin-eosin staining and immunohistochemistry

A hematoxylin and eosin (HE) staining kit (Beyotime Biotechnology, Shanghai, China) was used to stain the mouse intestinal tracts. The tissues were fixed with 4% paraformaldehyde for 24 hours and dehydrated with ethanol. The tissues were cleaned with xylene, embedded in paraffin, cut into 5 μm slices, dewaxed and dehydrated, and stained with hematoxylin for 5 min and eosin for 3 min. Morphology of the small intestine was observed under a microscope, and immunohistochemical (IHC) analysis was performed as previously described (15).

2.7 Immunofluorescence

Paraffin sections (4 μm thick) were dewaxed, rehydrated, treated with ethylenediamine tetraacetic acid antigen recovery solution (Beyotime, China), and blocked with 5% goat serum at 37℃ for 1 h. Subsequently, the sections were incubated with a primary antibody (anti-ZO-1and anti-Claudin-5; Abcam) at 4°C overnight, followed by Alexa Fluor 488 goat-anti-rabbit immunoglobulin G (Cell Signaling Technology) and Alexa Fluor 555 goat-anti-mouse IgG (Cell Signaling Technology) for 1 h at 37° C. Finally, the slices were cleaned and reverse-stained with DAPI (Cell Signaling Technology) using a 20× lens to obtain 3–5 images per slice.

2.8 Enzyme-linked immunosorbent assay (ELISA)

Sera were stored at −80°C until analysis. Serum cytokines interleukin-1 β (IL-1β), interleukin-6 (IL-6), tumor necrosis factor-α (TNF-α), and glucagon-like peptide 1 (GLP-1) were measured using ELISA kits according to the manufacturer's instructions (Ray Biotech, USA).

2.9 Metabolomic analysis

Based on previous studies, we performed a metabolomic analysis of serum content using liquid chromatography-mass spectrometry (LC-MS/MS) (16).

2.10 16S rRNA gene sequencing analysis

Absolute quantification of 16S rRNA amplicon sequencing was performed by Majorbio Bio-Pharm Technology Co., Ltd. (Shanghai, China). Total microbial genomic DNA was extracted using E.Z.N.A.® soil DNA Kit (Omega Bio-Tek, Norcross, GA, U.S.) according to the manufacturer's instructions. The V3-V4 hypervariable portions of the bacterium 16S rRNA gene were amplified using a thermocycler PCR system (GeneAmp 9700, ABI,

USA) with primers 338F (5′-ACTCCTACGGGAGGCAGCAG-3′) and 806R (5′-GGACTACHVGGGTWTCTAAT-3′). Purified amplicons were pooled in equimolar amounts and paired-end sequenced on an Illumina PE250 platform (Illumina, San Diego, CA, USA) according to the standard protocols of Majorbio Bio-Pharm Technology Co. Ltd. (Shanghai, China). Raw sequencing reads were deposited in the NCBI under the BioProject ID PRJNA1087303.

2.11 Statistical analysis

Data were analyzed using GraphPad Prism software and expressed as the mean ± standard deviation (SD). The area under the curve was calculated using the trapezoidal rule. All images were analyzed using Image-Pro Plus 6.0 (Media Cybernetics, USA). An unpaired Student's *t*-test was used to determine the significance of the intergroup differences, and values of $P< 0.05$ were considered significant. The Majorbio I-Sanger Cloud Platform (www.i-sanger.com) was utilized to examine the 16S rRNA gene sequencing data.

3 Results

3.1 Effects of DJB on obese T2D mice model

Within 8 weeks of DJB, no significant differences in body weight were observed (Figure 2A), nor in food intake (Figure 2B) in both DJB and SHAM animals; however, a notable weight control effect was evident after DJB surgery. As anticipated, significant reductions were observed in blood glucose levels and the area under the OGTT curve indicating improved glucose tolerance (Figures 2C-E). GLP-1 levels were also significantly elevated (Figure 2F) in DJB animals than in SHAM animals. These findings underscore significant improvements in glucose tolerance and insulin sensitivity following DJB surgery.

3.2 DJB modulated gut microbiota composition in obese T2D mice

In this study, we analyzed the 16S ribosomal RNA (rRNA) sequences of proximal (BP, A, and C limbs) and distal (CA and COL limbs) gut samples. Bioinformatic analysis of the resulting sequences for operational taxonomic units (OTUs) at 97% similarity revealed no differences in the alpha-diversity indices (Shannon, Simpson, Ace, and Chao) of the gut microbiota in the DJB and SHAM groups ($P > 0.05$, Figure 3A). Beta diversity, assessed using a hierarchical clustering tree, showed that the gut microbiota was distinctly clustered among the proximal and distal samples at the OTU level. (Figure 3B). Principal coordinate analysis (PCoA) was analyzed at the OTU level in the distal region ($P < 0.05$; Figure 3C) and proximal ($P < 0.05$, Figure 3D) samples, suggesting a significant difference in the intestinal microbiome composition between the DJB and SHAM groups. Furthermore, 411 and 604 OTUs were found in the distal (Figure 3E) and proximal regions (Figure 3F), as shown in the Venn diagram. Overall, our results indicated that the proximal and distal gut microbiota play different roles after DJB surgery.

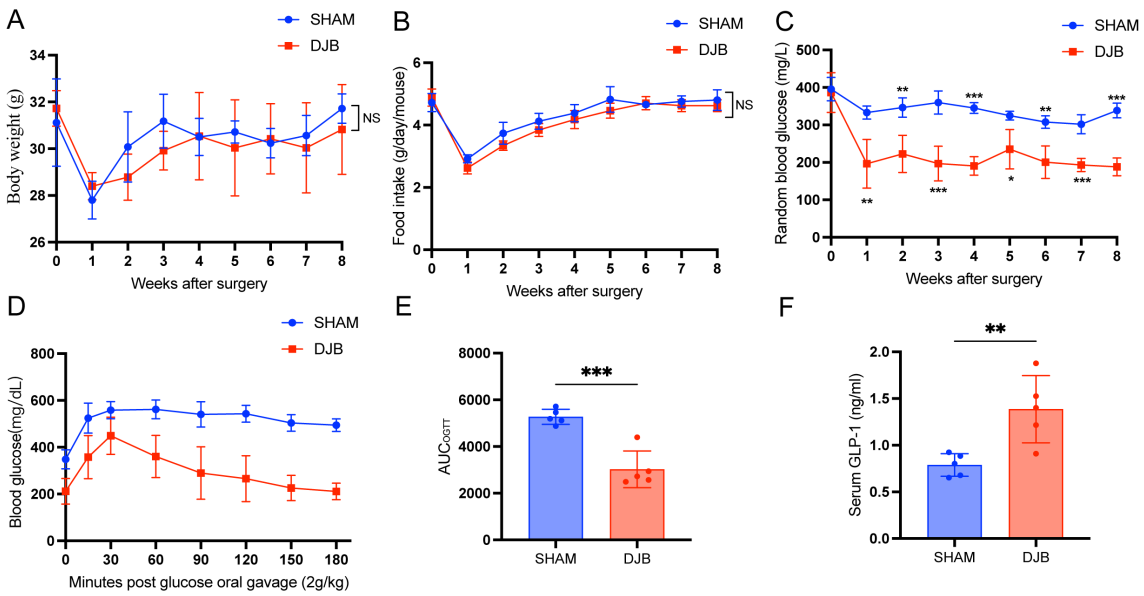

FIGURE 2
DJB improved glucose metabolism in mice with T2D. **(A)** Body weight. **(B)** Food intake. **(C)** Random blood glucose. **(D, E)** Oral glucose tolerance test (OGTT) and area under the curve (AUC). **(F)** The quantitative levels of GLP-1 in serum between DJB and SHAM groups detected by ELISA. The data are shown as mean ± SD, n=5. Statistical analyses were performed by a two-tailed, unpaired Student's t-test. *$P < 0.05$, **$P < 0.01$, ***$P < 0.001$. OGTT, oral glucose tolerance test; AUC_{OGTT}, the area under the OGTT curve; GLP-1, glucagon-like peptide 1; NS, no significance.

10.3389/fendo.2024.1456885

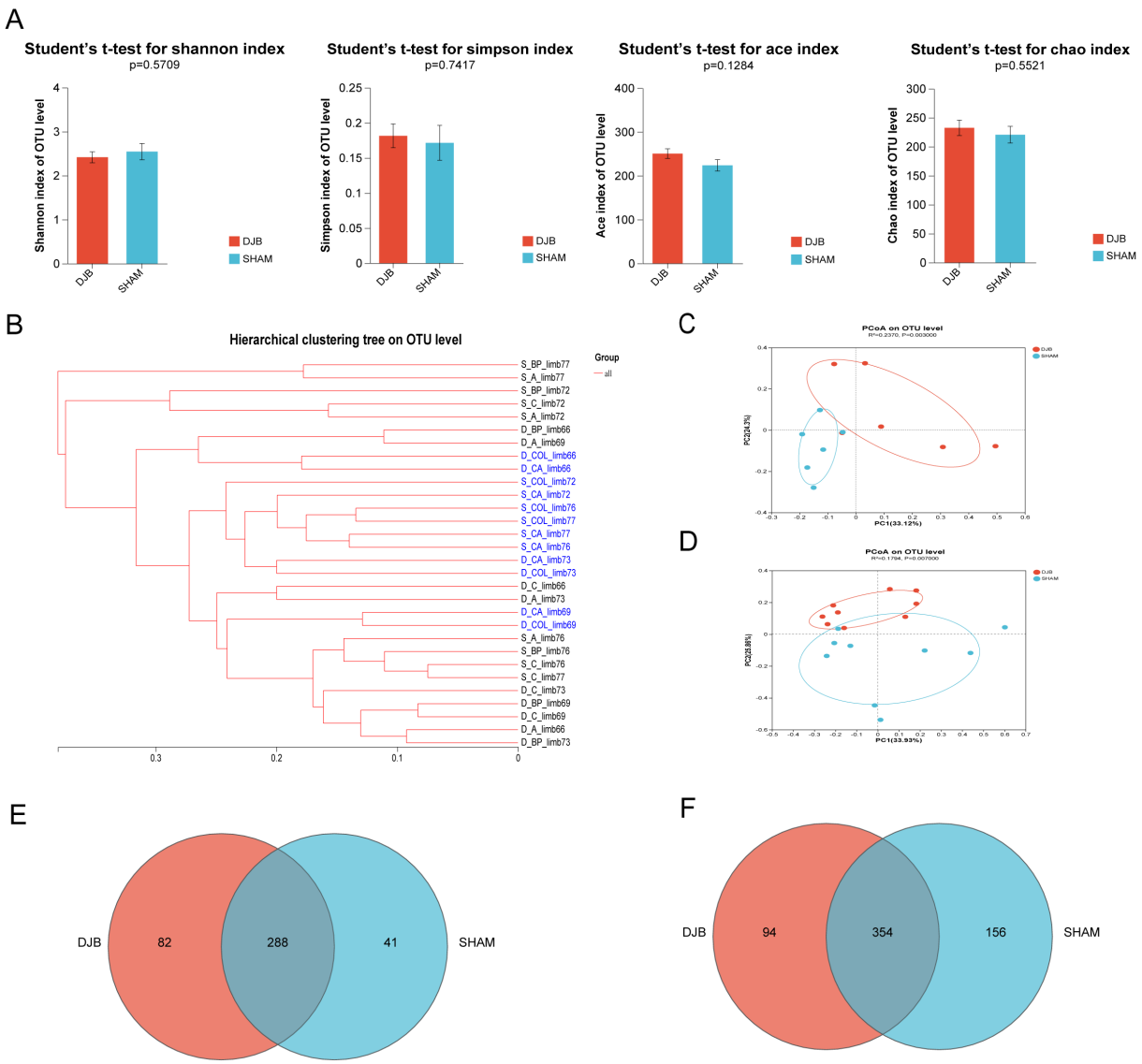

FIGURE 3
Overall effects of DJB on gut microbiota. **(A)** Alpha-diversity indexes including Shannon, Simpson, Ace, and Chao. **(B-D)** Beta-diversity was presented as a hierarchical clustering tree and PCoA at the OTU level. **(C)** PCoA shows the Bray-Curtis distance in the CA and COL limbs between DJB and SHAM groups, n=6. **(D)** PCoA shows the Bray-Curtis distance in the BP, A, and C limbs between DJB and SHAM groups. Each point represents each sample, n=9. **(E)** Venn diagram of common OTUs in the CA and COL limbs, n=6. **(F)** Venn diagram of common OTUs in the BP, A, and C limbs, n=9. The data are shown as mean ± SD. Statistical analyses were performed by a two-tailed, unpaired Student's *t*-test. BP limb, biliopancreatic limb; A limb, alimentary limb; C limb, common limb; CA limb, caecum limb; COL limb, colon limb.

3.3 DJB caused different segmental changes in the distal and proximal gut microbiota

Next, we investigated the effects of DJB surgery on the gut microbiota in the distal and proximal gut. Analysis of the gut microbial composition at the phylum level revealed no differences between the distal and proximal limbs (Figures 4A, B). However, the dominant microorganisms in the groups were explored using the linear discriminant analysis effect size (LEfSe) analysis (Linear discriminant analysis, LDA > 4, $P < 0.05$). In the CA and COL limbs, LEfSe analysis confirmed the enrichment of Proteobacteria, Gammaproteobacteria, Enterobacterales, and Enterobacteriaceae (Figure 4C). These changes are similar to those observed in RYGB animals (17). Conversely, the Faecalibaculum and Enterobacterales were enriched in DJB in the BP, A, and C limbs (Figure 4D). At the genus level, the relative abundance of norank_f_Desulfovibrionaceae in the CA limbs ($P < 0.05$, Figure 4E) and Colidextribacter, Blautia, and Lachnospiraceae_NK4A136_group in the COL limbs ($P < 0.05$, Figure 4F) significantly decreased after DJB (Supplementary Table 2). In addition, DJB mice exhibited a higher abundance of Faecalibaculum in the BP limbs ($P < 0.05$, Figure 4G) and Bifidobacterium in limb A ($P < 0.05$, Figure 4H). DJB surgery significantly decreased the abundance of Lactobacillus in the C limbs ($P < 0.05$; Figure 4I and Supplementary Table 3).

According to our findings, the changes in distal gut microbes were consistent with previous studies on bariatric surgery (17).

10.3389/fendo.2024.1456885

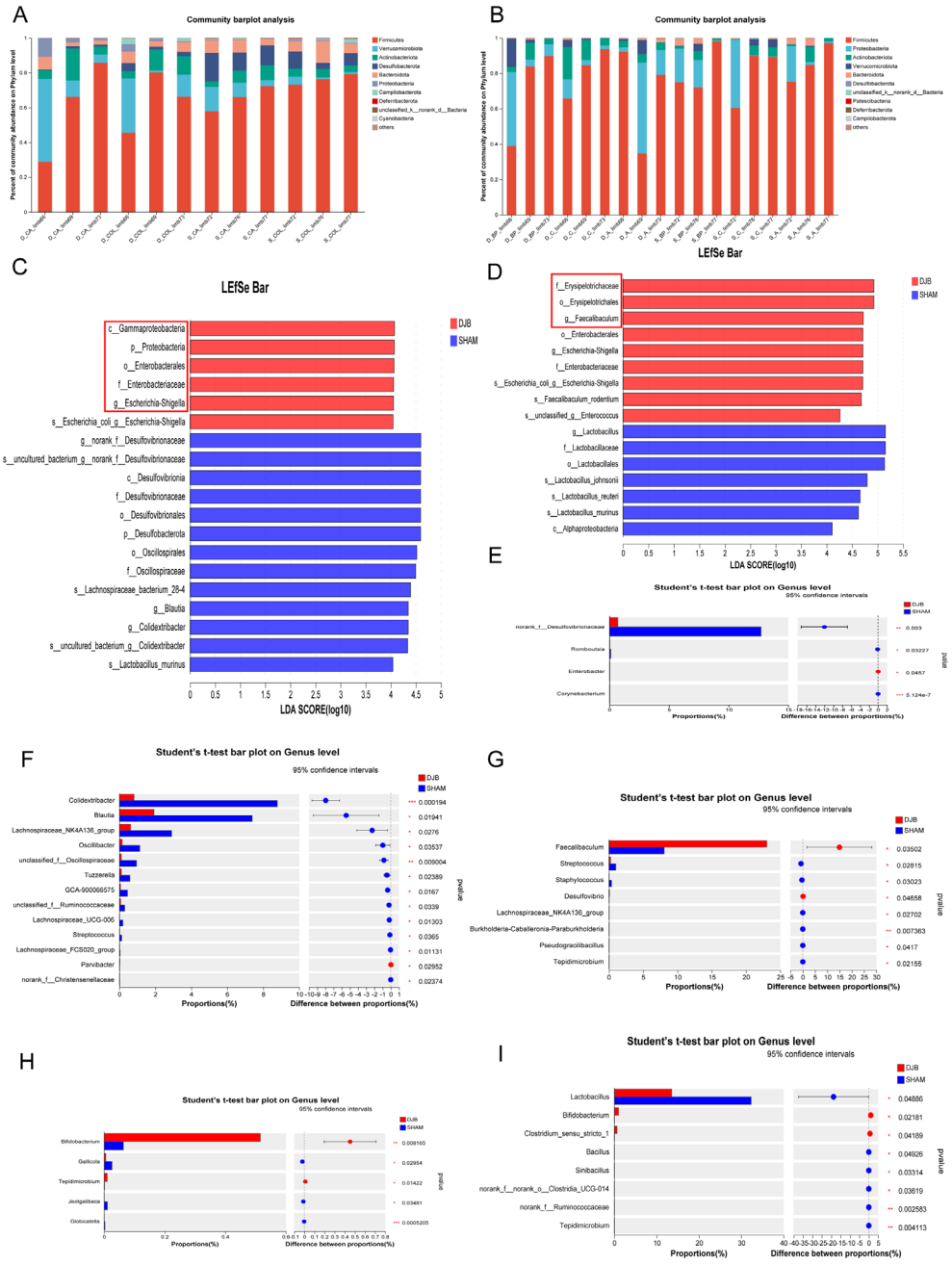

FIGURE 4
DJB caused different segmental changes in the distal and proximal intestinal limbs. **(A)** The relative abundance of gut microbiota between the CA and COL limbs at the phylum level. **(B)** The relative abundance of gut microbiota between the BP, A, and C limbs at the phylum level. **(C)** Linear discriminant analysis (LDA) effect size (LEfSe) analysis of microbiota composition in the CA and COL limbs between DJB and SHAM groups (LDA > 4, n=6). **(D)** Linear discriminant analysis (LDA) effect size (LEfSe) analysis of microbiota composition in the BP, A, and C limbs between DJB and SHAM groups (LDA > 4, n=9). **(E)** Bacteria with significant changes in the relative abundance in limb CA at the genus level, n=3. **(F)** Bacteria with significant changes in the relative abundance in limb COL at the genus level, n=3. **(G)** Bacteria with significant changes in the relative abundance in limb BP at the genus level, n=3. **(H)** Bacteria with significant changes in the relative abundance in limb A at the genus level, n=3. **(I)** Bacteria with significant changes in the relative abundance in limb C at the genus level, n=3. The data are shown as mean ± SD. Statistical analyses were performed by a two-tailed, unpaired Student's *t*-test. $^{*}P < 0.05$, $^{**}P < 0.01$, $^{***}P < 0.001$. LDA, Linear discriminant analysis; BP limb, biliopancreatic limb; A limb, alimentary limb; C limb, common limb; CA limb, caecum limb; COL limb, colon limb.

However, most studies have focused on distal gut microbiota, such as fecal microbiota, neglecting the equally important proximal intestinal gut microbiota. In the analysis of bacterial differences, we found that DJB surgery increased the abundance of beneficial bacteria in the BP, A, and C limbs compared to the distal gut. Therefore, we believe that intestinal rearrangement after DJB surgery leads to the dominance of the proximal small intestine in improving glucose metabolism.

3.4 DJB improved the gut barrier of biliopancreatic limbs, alimentary limbs, and common limbs

To determine whether the proximal gut microbiota affects the gut barrier, we examined inflammation and permeability in different segments of the proximal jejunum after DJB. The IHC results showed that the expression of IL-1β ($P < 0.05$, Figures 5A, D) and IL-6 ($P < 0.05$; Figures 5B, E) in BP, A, and C limbs were significantly decreased after DJB, as well as the expression of TNF-α in the three intestinal segments ($P > 0.05$, Figures 5C, F) compared to the SHAM group. In addition, we detected a decreased serum level of IL-1β, IL-6, and TNF-α in DJB groups (Figure 5G). Thus, DJB surgery can be inferred to have reduced inflammation in obese T2D mice. Meanwhile, DJB surgery decreased the villus height/crypt depth (V/C) of the BP limbs (Figure 5H). Compared with the SHAM group, the (V/C) of the A limbs increased significantly in the DJB group, and there was no significant change in the C limbs. After DJB, mice exhibit significant adaptive intestinal changes (18).

To further elucidate the effect of DJB on the mucosal barrier of the proximal small intestine, immunofluorescence and qRT-PCR were used to detect the expression of zonula occludens 1 (ZO-1) and claudin-5, respectively. Immunofluorescence analysis showed that ZO-1 and claudin-5 were strongly expressed in the intestinal surface epithelial cells of A (Figure 5J) and C limbs (Figure 5K) after DJB surgery, showing characteristic lateral membrane staining. After DJB, staining was concentrated at the tips of the villi and cells in the crypt. However, there were no significant changes in the BP limbs (Figure 5I). Similar changes were also found by qRT-PCR, with increased expression levels of ZO-1 and claudin-5 mRNA in the A and C limbs, and decreased expression levels in the BP limbs (Figure 5L). These findings suggest that DJB maintains intestinal epithelial homeostasis by regulating TJ protein distribution and expression.

3.5 Changes in the overall status of the metabolome after DJB surgery

To identify the potential metabolic signals that could lead to the loss of blood glucose levels, we examined the effects of DJB surgery on the serum metabolism profile of mice. A total of 378 metabolites were identified. In total, 107 differential metabolites were detected (Supplementary Table 4), of which 75 were upregulated and 32 were downregulated (Figure 6A). Orthogonal partial least squares discriminant analysis (OPLS-DA) showed (Figures 6B, C) that DJB surgery significantly altered the metabolic profile of diabetic mice.

In addition, the Kyoto Encyclopedia of Genes and Genomes (KEGG) analysis of the 107 differential metabolites showed significant enrichment of pathways related to membrane transport, amino acid metabolism, and the digestive system (Figure 6D). To further identify the pathways affected by DJB, we performed an enrichment analysis of the KEGG pathway for important metabolites with known KEGG IDs among which the top 20 pathways are shown in Figure 6E ($P < 0.05$). Changes in metabolic pathways were mainly related to ABC transporters, purine metabolism, and protein digestion and absorption pathways. Interestingly, L-Glutamine is involved in these metabolic pathways (Figure 6F and Supplementary Table 5). In addition, we found that bile acids (deoxycholic acid, tauroursodeoxycholic acid, taurocholate, apolicholic acid, and tauro-alpha-muricholic acid), branched-chain amino acids (Leucine and Valine) (Figure 6F), and three short-chain fatty acids (SCFAs) (Supplementary Table 6) were elevated after DJB.

3.6 Correlation analysis between metabolism and gut microbiota

To further understand the correlation between differential metabolites and microbiota at the genus level, Spearman's correlation analysis was performed (Figure 7). The results showed that the differential metabolites correlated with changes in the microbiota. We found that L-Glutamine is positively correlated with Escherichia-Shigella and Bifidobacterium and negatively correlated with Colidextribacter and Alistipes. Branched-chain amino acids (Leucine and Valine) were positively correlated with Alistipes, Desulfovibrionaceae, Staphylococcus, Blautia, and Muribaculaceae and negatively correlated with Faecalibaculum.

4 Discussion

It is increasingly evident that bariatric/metabolic surgery involves multiple weight-independent mechanisms to improve glucose homeostasis and enhance insulin sensitivity and secretion, particularly during specific surgeries (19). In this study, despite observing no significant disparities in body weight between the DJB and SHAM groups, the mice had a relatively lower weight post-DJB surgery. The results of random blood glucose and OGTT showed that DJB significantly improved glucose metabolism and tolerance in obese T2D mice, coupled with a noteworthy increase in serum GLP-1 expression. In addition to stimulating insulin secretion, GLP-1 also promotes insulin biosynthesis as well as β-cell proliferation and survival (20). These findings are consistent with those of previous studies (21, 22) that DJB surgery could be used as a treatment for T2D.

Our study was designed to assess changes in the gut microbial ecology before and after surgery. Marked changes were evident in the microbial composition of CA limbs and COL limbs, with a pronounced increase in the abundance of the Proteobacteria (class: Gammaproteobacteria, order: Enterobacteriales, family: Enterobacteriaceae, genus: Escherichia-Shigella). Similar results were observed in the fecal microbiota of human patients and rats after bariatric surgery (1, 4, 23). At the genus level, we observed a significant decline in Colidextribacter, Blautia, Lachnospiraceae_NK4A136_group, and norank _f_Desulfovibrionaceae. One study reported (24) that Colidextribacter, Blautia, and the Lachnospiraceae _NK4A136_group are closely related to branched-chain amino acids (BCAAs). As important metabolites of the diet or gut microbiome, BCAAs are prevalent and significantly elevated in obese and/or T2D

10.3389/fendo.2024.1456885

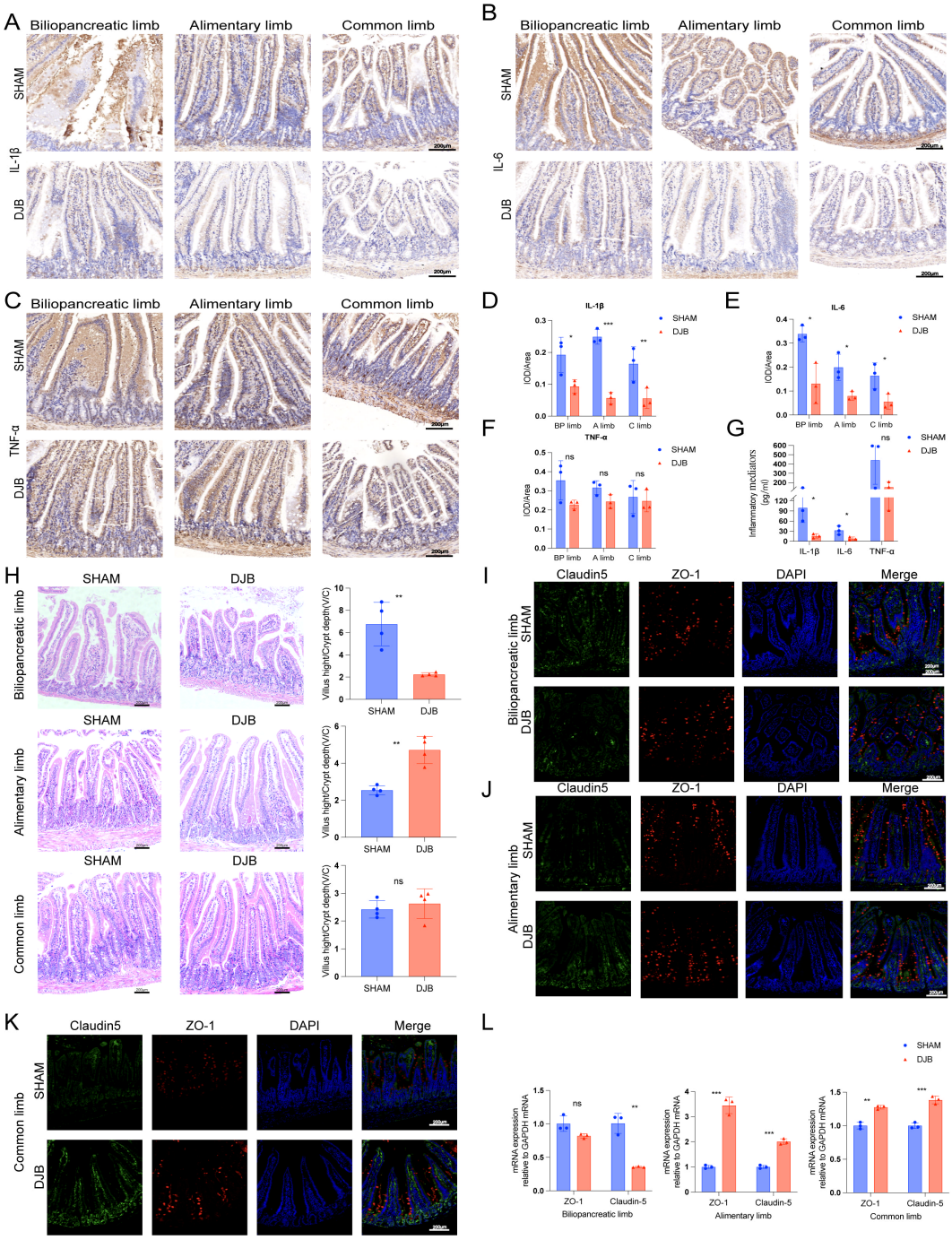

FIGURE 5
DJB improved the gut barrier in BP limbs, A limbs, and C limbs. Representative micrographs of Immunohistochemical staining **(A)** and quantitative data **(D)** of IL-1β in intestinal tissue sections of each group of mice, n=3. Representative micrographs of Immunohistochemical staining **(B)** and quantitative data **(E)** of IL-6 in intestinal tissue sections of each group of mice, n=3. Representative micrographs of Immunohistochemical staining **(C)** and quantitative data **(F)** of TNF-α in intestinal tissue sections of each group of mice, n=3. **(G)** The quantitative levels of IL-1β, IL-6, and TNF-α in the serum of each group of mice detected by ELISA, n=3. **(H)** Representative micrographs of HE staining and quantitative analysis of V/C in the BP, A, and C limbs, n=4. **(I)** Double-immunofluorescence staining analysis of Claudin-5 and ZO-1 in the biliopancreatic limbs. **(J)** Double-immunofluorescence staining analysis of Claudin-5 and ZO-1 in the alimentary limbs. **(K)** Double-immunofluorescence staining analysis of Claudin-5 and ZO-1 in the common limbs. **(L)** The mRNA levels of ZO-1 and Claudin-5 were detected by qRT-PCR in intestinal tissue sections of each group of mice, n=3. The data are shown as mean ± SD. Statistical analyses were performed by two-tailed, unpaired Student's *t*-test. $^{*}P < 0.05$, $^{**}P < 0.01$, $^{***}P < 0.001$. Scales bars = 200 μm. ZO-1, zonula occludens 1; IL-1β, interleukin-1β; TNF-α, tumor necrosis factor-α; IL-6, interleukin-6; BP limb, biliopancreatic limb; A limb, alimentary limb; C limb, common limb; ns, no significance.

10.3389/fendo.2024.1456885

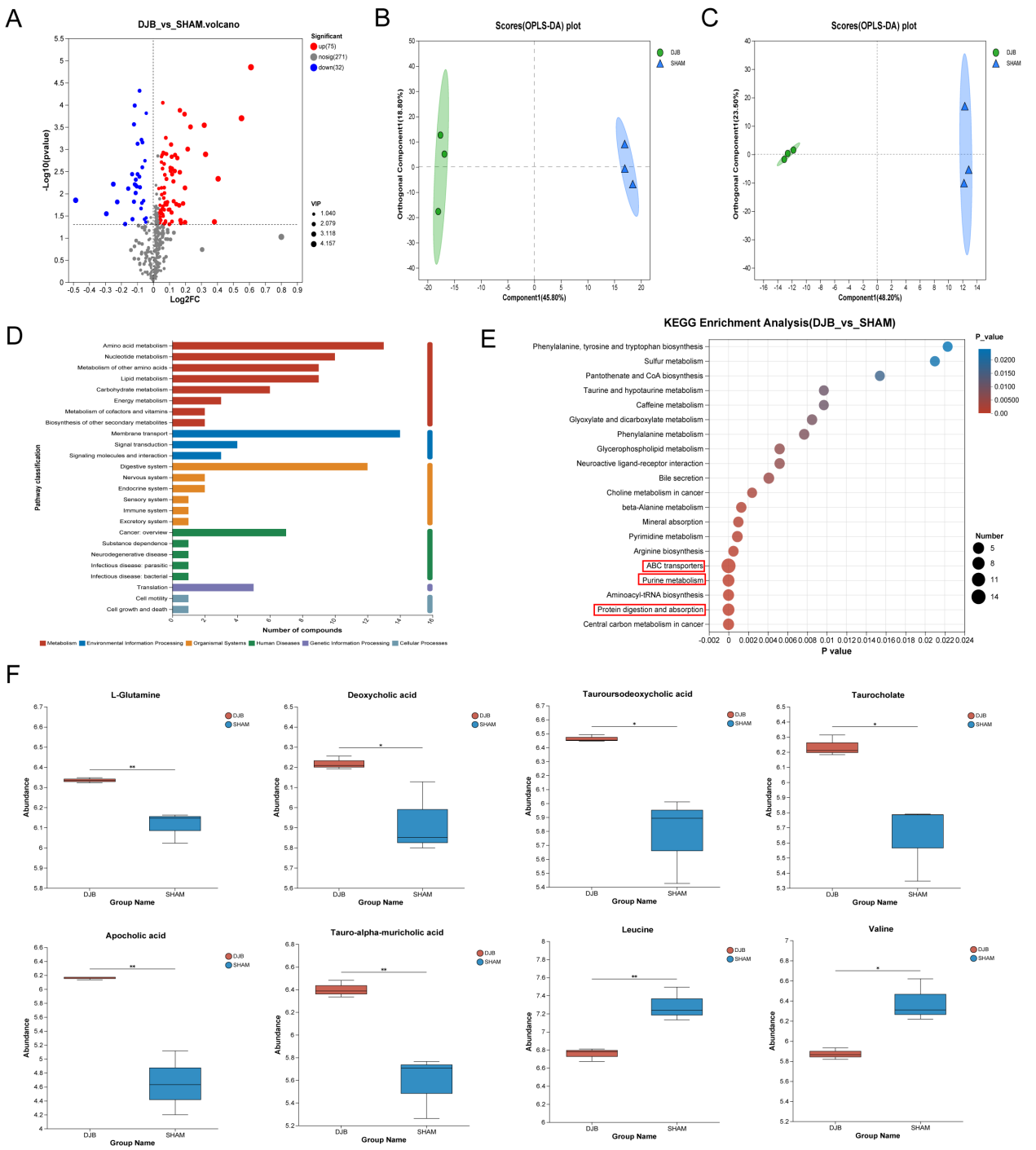

FIGURE 6
LC–MS-based metabolomics analysis of the serum samples from DJB and SHAM groups. **(A)** Volcano map of metabolites between DJB and SHAM groups. Red dots represent significantly upregulated metabolites, and blue dots represent significantly downregulated metabolites, and gray dots represent non-significant differential metabolites. The differential metabolites were identified as VIP > 1 and P < 0.05. **(B)** Orthogonal partial least squares discriminant analysis (OPLS-DA) map of a positive ion. **(C)** OPLS-DA map of negative ion. **(D)** KEGG pathways on level 1 and level 2 are related to differential metabolites. The ordinate is the name of pathway level 2, and the abscissa is the number of metabolites related to the pathway. Different colors represent different pathways on level 1. **(E)** Bubble diagram showing the enriched KEGG pathways. The ordinate is the name of Pathway 3. The size of the bubbles in the figure represents how much of the pathway is enriched into the metabolic compound. Generally, a p value less than 0.05 is considered a significant enrichment item. **(F)** Comparison of the relative abundance of L-Glutamine, Deoxycholic acid, Tauroursodeoxycholic acid, Taurocholate, Apocholic acid, Tauro-alpha-muricholic acid, Leucine, and Valine between DJB and SHAM groups, n=3. The data are shown as mean ± SD. *$P < 0.05$, **$P < 0.01$.

10.3389/fendo.2024.1456885

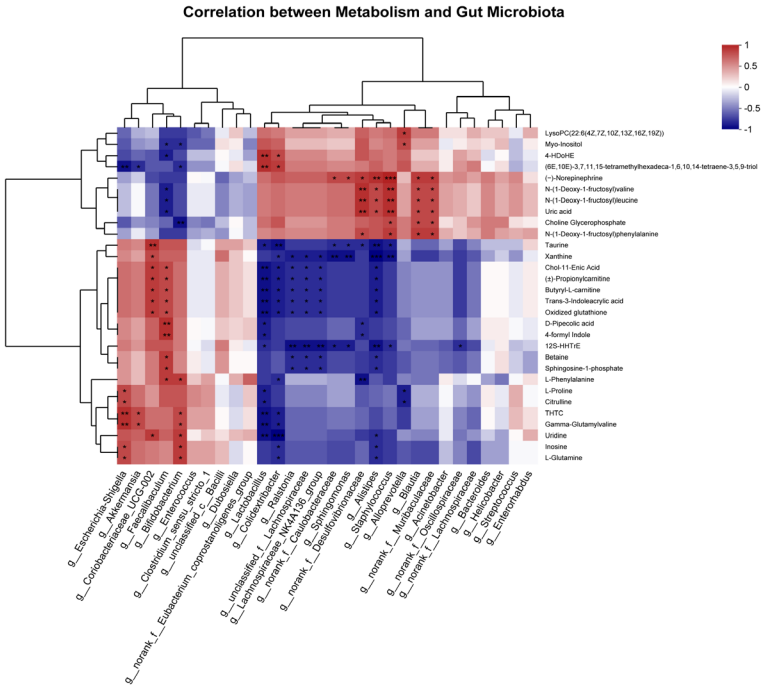

FIGURE 7
Spearman correlation analysis of the top 30 between differential metabolites and gut microbiota at the genus level. *$P < 0.05$, **$P < 0.01$, ***$P < 0.001$.

hosts, suggesting that BCAAs can inhibit the function of beta cells in regulating insulin secretion, and are strongly associated with insulin resistance and the risk of developing T2DM (25, 26). Similar results were observed in our study, where BCAA levels decreased significantly in the serum and were associated with Blautia after DJB surgery. This suggests that Alistipes, Desulfovisbrionaceae, Staphylococcus, and Muribaculaceae are closely related to the occurrence and development of T2DM.

Additionally, in BP limbs, A limbs, and C limbs, significant enrichment of Erysipelotrichales (family: Erysipelotrichaceae, genus: Faecalibaculum) after DJB surgery was observed. DJB surgery also resulted in a significant increase in Faecalibaculum and Bifidobacterium and a decrease in Lactobacillus. Increased levels of Bifidobacterium are associated with improved glucose tolerance, glucose-induced insulin secretion, decreased body weight, and decreased levels of inflammatory mediators (27, 28). As previously reported, Faecalibaculum has anti-inflammatory properties and significantly reduces the percentage of intestinal microbiota in patients with T2D (29, 30). Furthermore, SCFAs can inhibit bacterial invasion, maintain intestinal barrier integrity, and regulate inflammatory responses (31). Bifidobacterium and Faecalibaculum are important commensal bacteria that produce SCFAs (22). Lactobacillus, classified as a probiotic, exerts beneficial effects on human health. However, our study revealed a reduction in the abundance of Lactobacilli following DJB surgery. Despite their known benefits, the results of meta-analyses indicate that Lactobacillus may also affect weight gain (32). The number of lactobacilli in obese and obese patients with type 2 diabetes is higher than that in healthy individuals (33, 34), which can be considered in the context of the results of this study. This suggests that the different effects of Lactobacillus on weight may be species- and strain-specific. These studies suggest that DJB surgery not only reduces weight gain but also decreases the number of proximal gut Lactobacillus species present.

Given the proximal intestinal rearrangement after DJB surgery, we cannot overlook the potential impact of microbial changes on the gut barrier and insulin resistance. The results indicated a significant decrease in the expression of the three inflammatory factors in A and BP limbs with a similar trend observed in the C limb. As documented in previous studies, chronic inflammation facilitates the development of T2DM by promoting insulin resistance and β-cell failure while decreasing insulin sensitivity (35–37). Targeted regulation of the inflammatory system can significantly improve hyperglycemia and may gradually become a therapeutic strategy for T2DM (38). Chronic inflammatory diseases of the intestine may lead to the dysregulation of TJ proteins (39). Based on these findings, we investigated the distribution and expression of ZO-1 and claudin-5 in three intestinal segments. DJB altered the distribution and expression of ZO-1 and claudin-5 in the A and C limbs. Notably, both TJ proteins exhibited similar patterns of redistribution after surgery. These results are consistent with those of previous studies, showing that TJ proteins are redistributed under various pathological conditions (40). Our data showed that intestinal permeability decreased in limbs A and C after DJB, whereas there was no significant improvement in the limbs with BP. This is consistent with the results of a study by Yang et al. in rats (41). Additionally, DJB surgery promoted epithelial cell proliferation and adaptive changes in the gut, as evidenced by increased V/C ratios in limbs A and C. These results are consistent with those reported by Li et al. (42). In accordance with previous

reports (18), macronutrients, including carbohydrates, proteins, and fats, stimulate intestinal adaptation, which supports the finding that the intestinal permeability of BP limbs does not improve after DJB. In conclusion, strengthening epithelial barrier function and tight junctions may be an adaptive mechanism after DJB.

KEGG analysis revealed that differential metabolites further revealed changes in several pathways. These include membrane transport, amino acid metabolism, and digestive systems, as well as pathways associated with ABC transporters and purine metabolism. Studies have found that ABC transporters (43) play an important physiological role in higher plants and animals and use the energy generated by the hydrolysis of adenosine triphosphate (ATP) to transport various molecules bound to it across the membrane, thereby promoting intestinal cell development. Our KEGG pathway analysis showed that purine metabolism was enriched, suggesting an active microbial reproduction at this stage. Furthermore, the surgery may facilitate transport across the membrane and amino acid digestion and absorption to protect the gut by preventing intestinal atrophy and other metabolic complications. Therefore, we speculate that the surgery may ameliorate diabetes through these pathways. Simultaneously, some metabolites associated with improved glucose metabolism increased after the DJB surgery. Glutamine levels are significantly elevated after DJB surgery and are involved in multiple metabolic pathways. Glutamine is the main energy source for intestinal cells and can regulate the phosphorylation of tight junction proteins, thereby improving the intestinal barrier function (44). Glutamine supplementation may maintain intestinal homeostasis through intestinal microbial metabolites, improve intestinal immunity, and alleviate intestinal inflammation (45). Moreover, studies have shown that bile acids play important roles in glucose homeostasis (46). Changes in gastrointestinal anatomy may also affect the enterohepatic recirculation of bile acids, possibly mediating an increase in GLP-1 through increased uptake of bile acids in the intestine, helping to improve blood glucose (47).

However, this study has some limitations. Firstly, in the analysis of gut microbial diversity, there was no statistically significant difference between the groups. Since we studied proximal gut microbes instead of fecal microbes, this may indicate a substantial similarity in the proximal gut microbiota. In addition, similar body weights may be a possible mechanism for the undifferentiated gut microbiome. Second, because the sample size was small and there was a lack of negative control groups for the gut microbiome analysis, the correlation was not verified. In future studies, it will be necessary to expand the sample size and conduct further validation. Finally, the current study mainly focused on the effect of intestinal rearrangement in the proximal small intestine on improving glucose metabolism after DJB surgery, and did not explore the specific effect on blood lipids. In addition, this study only explored the effects of proximal intestinal structural rearrangements on gut microbiota and metabolism, and further studies are needed to explore the underlying mechanisms.

In summary, we provide a valuable mouse model for investigating the mechanism by which T2D improves without weight loss and provide new insights into the BP, A, and C limbs after DJB surgery. Our results reveal that the post-DJB changes in the gut microbiota and metabolites were sufficiently robust to attenuate inflammatory responses and intestinal permeability, consequently bolstering the stability of glycemic metabolism. These findings suggest that proximal intestinal rearrangements play an important role in surgery-related improvements in patients with T2DM.

Data availability statement

The datasets presented in this study can be found in online repositories. The names of the repository/repositories and accession number(s) can be found below: https://www.ncbi.nlm.nih.gov/, PRJNA1087303.

Ethics statement

The animal study was approved by Animal Care and Use Committee of the General Hospital of the Southern Theater Command. The study was conducted in accordance with the local legislation and institutional requirements.

Author contributions

LW: Conceptualization, Writing – review & editing. HL: Conceptualization, Methodology, Software, Writing – original draft. JPH: Conceptualization, Data curation, Software, Writing – original draft. JH: Investigation, Visualization, Writing – review & editing. CH: Investigation, Visualization, Writing – review & editing. XD: Investigation, Visualization, Writing – review & editing. ZS: Software, Supervision, Validation, Writing – review & editing. QL: Software, Supervision, Validation, Writing – review & editing. ZW: Software, Supervision, Validation, Writing – review & editing. HH: Project administration, Resources, Writing – review & editing. YD: Project administration, Resources, Writing – review & editing. TQ: Project administration, Resources, Writing – review & editing. HZ: Conceptualization, Writing – review & editing.

Funding

The author(s) declare financial support was received for the research, authorship, and/or publication of this article. This research was supported by a grant from the Science and Technology Planning Project of Guangdong Province of China (No. 202002020069) and the National Natural Science Foundation of P. R. China (NSFC 82300470).

Conflict of interest

Author LW was employed by Guangzhou Hualiang Qingying Biotechnology Co. Ltd.

The remaining authors declare that the research was conducted in the absence of any commercial or financial relationships that could be construed as a potential conflict of interest.

Publisher's note

All claims expressed in this article are solely those of the authors and do not necessarily represent those of their affiliated organizations, or those of the publisher, the editors and the reviewers. Any product that may be evaluated in this article, or claim that may be made by its manufacturer, is not guaranteed or endorsed by the publisher.

Supplementary material

The Supplementary Material for this article can be found online at: https://www.frontiersin.org/articles/10.3389/fendo.2024.1456885/full#supplementary-material

References

1. Li JV, Ashrafian H, Bueter M, Kinross J, Sands C, le Roux CW, et al. Metabolic surgery profoundly influences gut microbial-host metabolic cross-talk. *Gut*. (2011) 60:1214–23. doi: 10.1136/gut.2010.234708

2. Eizirik DL, Pasquali L, Cnop M. Pancreatic β-cells in type 1 and type 2 diabetes mellitus: different pathways to failure. *Nat Rev Endocrinol*. (2020) 16:349–62. doi: 10.1038/s41574-020-0355-7

3. Thaker VV, Kwee LC, Chen H, Bahnson J, Ilkayeva O, Muehlbauer MJ, et al. Metabolite signature of diabetes remission in individuals with obesity undergoing weight loss interventions. *Obes (Silver Spring)*. (2023) 32,2(2024):304–14. doi: 10.1002/oby.23943

4. Furet JP, Kong LC, Tap J, Poitou C, Basdevant A, Bouillot JL, et al. Differential adaptation of human gut microbiota to bariatric surgery-induced weight loss: links with metabolic and low-grade inflammation markers. *Diabetes*. (2010) 59:3049–57. doi: 10.2337/db10-0253

5. Monte SV, Caruana JA, Ghanim H, Sia CL, Korzeniewski K, Schentag JJ, et al. Reduction in endotoxemia, oxidative and inflammatory stress, and insulin resistance after Roux-en-Y gastric bypass surgery in patients with morbid obesity and type 2 diabetes mellitus. *Surgery*. (2012) 151:587–93. doi: 10.1016/j.surg.2011.09.038

6. Muñoz R, Dominguez A, Muñoz F, Muñoz C, Slako M, Turiel D, et al. Baseline glycated hemoglobin levels are associated with duodenal-jejunal bypass liner-induced weight loss in obese patients. *Surg Endosc*. (2014) 28:1056–62. doi: 10.1007/s00464-013-3283-y

7. Breen DM, Rasmussen BA, Côté CD, Jackson VM, Lam TK. Nutrient-sensing mechanisms in the gut as therapeutic targets for diabetes. *Diabetes*. (2013) 62:3005–13. doi: 10.2337/db13-0523

8. Rubino F, Forgione A, Cummings DE, Vix M, Gnuli D, Mingrone G, et al. The mechanism of diabetes control after gastrointestinal bypass surgery reveals a role of the proximal small intestine in the pathophysiology of type 2 diabetes. *Ann Surg*. (2006) 244:741–9. doi: 10.1097/01.sla.0000224726.61448.1b

9. Jiang B, Wang H, Li N, Yan Q, Wang W, Wang Y, et al. Role of proximal intestinal glucose sensing and metabolism in the blood glucose control in type 2 diabetic rats after duodenal jejunal bypass surgery. *Obes Surg*. (2022) 32:1119–29. doi: 10.1007/s11695-021-05871-3

10. Yang G, Wei J, Liu P, Zhang Q, Tian Y, Hou G, et al. Role of the gut microbiota in type 2 diabetes and related diseases. *Metabolism*. (2021) 117:154712. doi: 10.1016/j.metabol.2021.154712

11. Liu R, Zou Y, Wang WQ, Chen JH, Zhang L, Feng J, et al. Gut microbial structural variation associates with immune checkpoint inhibitor response. *Nat Commun*. (2023) 14:7421. doi: 10.1038/s41467-023-42997-7

12. Bäckhed F, Ley RE, Sonnenburg JL, Peterson DA, Gordon JI. Host-bacterial mutualism in the human intestine. *Science*. (2005) 307:1915–20. doi: 10.1126/science.1104816

13. Schneeberger EE, Lynch RD. The tight junction: a multifunctional complex. *Am J Physiol Cell Physiol*. (2004) 286:C1213–28. doi: 10.1152/ajpcell.00558.2003

14. Thingholm LB, Rühlemann MC, Koch M, Fuqua B, Laucke G, Boehm R, et al. Obese individuals with and without type 2 diabetes show different gut microbial functional capacity and composition. *Cell Host Microbe*. (2019) 26:252–64.e10. doi: 10.1016/j.chom.2019.07.004

15. Lian B, Li Z, Wu N, Li M, Chen X, Zheng H, et al. Phase II clinical trial of neoadjuvant anti-PD-1 (Toripalimab) combined with axitinib in resectable mucosal melanoma. *Ann Oncol*. (2023) 35,2 (2024):211–20. doi: 10.1016/j.annonc.2023.10.793

16. Zhou X, Zhang B, Zhao X, Zhang P, Guo J, Zhuang Y, et al. Coffee leaf tea extracts improve hyperuricemia nephropathy and its associated negative effect in gut microbiota and amino acid metabolism in rats. *J Agric Food Chem*. (2023) 71:17775–87. doi: 10.1021/acs.jafc.3c02797

17. Liou AP, Paziuk M, Luevano JM Jr., Machineni S, Turnbaugh PJ, Kaplan LM. Conserved shifts in the gut microbiota due to gastric bypass reduce host weight and adiposity. *Sci Transl Med*. (2013) 5:178ra41. doi: 10.1126/scitranslmed.3005687

18. Tappenden KA. Mechanisms of enteral nutrient-enhanced intestinal adaptation. *Gastroenterology*. (2006) 130:S93–9. doi: 10.1053/j.gastro.2005.11.051

19. Mingrone G, Cummings DE. Changes of insulin sensitivity and secretion after bariatric/metabolic surgery. *Surg Obes Relat Dis*. (2016) 12:1199–205. doi: 10.1016/j.soard.2016.05.013

20. Kim W, Egan JM. The role of incretins in glucose homeostasis and diabetes treatment. *Pharmacol Rev*. (2008) 60:470–512. doi: 10.1124/pr.108.000604

21. Ueno T, Tanaka N, Imoto H, Maekawa M, Kohyama A, Watanabe K, et al. Mechanism of bile acid reabsorption in the biliopancreatic limb after duodenal-jejunal bypass in rats. *Obes Surg*. (2020) 30:2528–37. doi: 10.1007/s11695-020-04506-3

22. Yu X, Wu Z, Song Z, Zhang H, Zhan J, Yu H, et al. Single-anastomosis duodenal jejunal bypass improve glucose metabolism by regulating gut microbiota and short-chain fatty acids in goto-kakisaki rats. *Front Microbiol*. (2020) 11:273. doi: 10.3389/fmicb.2020.00273

23. Zhang H, DiBaise JK, Zuccolo A, Kudrna D, Braidotti M, Yu Y, et al. Human gut microbiota in obesity and after gastric bypass. *Proc Natl Acad Sci U S A*. (2009) 106:2365–70. doi: 10.1073/pnas.0812600106

24. Zheng XX, Li DX, Li YT, Chen YL, Zhao YL, Ji S, et al. Mulberry leaf water extract alleviates type 2 diabetes in mice via modulating gut microbiota-host co-metabolism of branched-chain amino acid. *Phytother Res*. (2023) 37:3195–210. doi: 10.1002/ptr.7822

25. Newgard CB, An J, Bain JR, Muehlbauer MJ, Stevens RD, Lien LF, et al. A branched-chain amino acid-related metabolic signature that differentiates obese and lean humans and contributes to insulin resistance. *Cell Metab*. (2009) 9:311–26. doi: 10.1016/j.cmet.2009.02.002

26. Gojda J, Cahova M. Gut microbiota as the link between elevated BCAA serum levels and insulin resistance. *Biomolecules*. (2021) 11:1414. doi: 10.3390/biom11101414

27. Cani PD, Neyrinck AM, Fava F, Knauf C, Burcelin RG, Tuohy KM, et al. Selective increases of bifidobacteria in gut microflora improve high-fat-diet-induced diabetes in mice through a mechanism associated with endotoxaemia. *Diabetologia*. (2007) 50:2374–83. doi: 10.1007/s00125-007-0791-0

28. Amar J, Chabo C, Waget A, Klopp P, Vachoux C, Bermúdez-Humarán LG, et al. Intestinal mucosal adherence and translocation of commensal bacteria at the early onset of type 2 diabetes: molecular mechanisms and probiotic treatment. *EMBO Mol Med*. (2011) 3:559–72. doi: 10.1002/emmm.201100159

29. Vrieze A, Van Nood E, Holleman F, Salojärvi J, Kootte RS, Bartelsman JF, et al. Transfer of intestinal microbiota from lean donors increases insulin sensitivity in individuals with metabolic syndrome. *Gastroenterology*. (2012) 143:913–6.e7. doi: 10.1053/j.gastro.2012.06.031

30. Faucher Q, Jardou M, Brossier C, Picard N, Marquet P, Lawson R. Is intestinal dysbiosis-associated with immunosuppressive therapy a key factor in the pathophysiology of post-transplant diabetes mellitus? *Front Endocrinol (Lausanne)*. (2022) 13:898878. doi: 10.3389/fendo.2022.898878

31. Kim M, Qie Y, Park J, Kim CH. Gut microbial metabolites fuel host antibody responses. *Cell Host Microbe*. (2016) 20:202–14. doi: 10.1016/j.chom.2016.07.001

32. Angelakis E, Merhej V, Raoult D. Related actions of probiotics and antibiotics on gut microbiota and weight modification. *Lancet Infect Dis*. (2013) 13:889–99. doi: 10.1016/s1473-3099(13)70179-8

33. Jin J, Cheng R, Ren Y, Shen X, Wang J, Xue Y, et al. Distinctive gut microbiota in patients with overweight and obesity with dyslipidemia and its responses to long-term orlistat and ezetimibe intervention: A randomized controlled open-label trial. *Front Pharmacol*. (2021) 12:732541. doi: 10.3389/fphar.2021.732541

34. Bervoets L, Van Hoorenbeeck K, Kortleven I, Van Noten C, Hens N, Vael C, et al. Differences in gut microbiota composition between obese and lean children: a cross-sectional study. *Gut Pathog*. (2013) 5:10. doi: 10.1186/1757-4749-5-10

35. Reinehr T, Roth CL. Inflammation markers in type 2 diabetes and the metabolic syndrome in the pediatric population. *Curr Diabetes Rep*. (2018) 18:131. doi: 10.1007/s11892-018-1110-5

36. Larsen CM, Faulenbach M, Vaag A, Vølund A, Ehses JA, Seifert B, et al. Interleukin-1-receptor antagonist in type 2 diabetes mellitus. *N Engl J Med*. (2007) 356:1517–26. doi: 10.1056/NEJMoa065213

37. Donath MY, Shoelson SE. Type 2 diabetes as an inflammatory disease. *Nat Rev Immunol*. (2011) 11:98–107. doi: 10.1038/nri2925

38. Reinehr T. Inflammatory markers in children and adolescents with type 2 diabetes mellitus. *Clin Chim Acta*. (2019) 496:100–7. doi: 10.1016/j.cca.2019.07.006

39. Sandle GI. Pathogenesis of diarrhea in ulcerative colitis: new views on an old problem. *J Clin Gastroenterol*. (2005) 39:S49–52. doi: 10.1097/01.mcg.0000155520.04253.37

40. Zeissig S, Bürgel N, Günzel D, Richter J, Mankertz J, Wahnschaffe U, et al. Changes in expression and distribution of claudin 2, 5 and 8 lead to discontinuous tight junctions and barrier dysfunction in active Crohn's disease. *Gut*. (2007) 56:61–72. doi: 10.1136/gut.2006.094375

41. Yang PJ, Yang WS, Nien HC, Chen CN, Lee PH, Yu LC, et al. Duodenojejunal bypass leads to altered gut microbiota and strengthened epithelial barriers in rats. *Obes Surg*. (2016) 26:1576–83. doi: 10.1007/s11695-015-1968-0

42. Li B, Lu Y, Srikant CB, Gao ZH, Liu JL. Intestinal adaptation and Reg gene expression induced by antidiabetic duodenal-jejunal bypass surgery in Zucker fatty rats. *Am J Physiol Gastrointest Liver Physiol*. (2013) 304:G635–45. doi: 10.1152/ajpgi.00275.2012

43. Ponte-Sucre A. Availability and applications of ATP-binding cassette (ABC) transporter blockers. *Appl Microbiol Biotechnol*. (2007) 76:279–86. doi: 10.1007/s00253-007-1017-6

44. Parry-Billings M, Evans J, Calder PC, Newsholme EA. Does glutamine contribute to immunosuppression after major burns? *Lancet*. (1990) 336:523–5. doi: 10.1016/0140-6736(90)92083-t

45. Li S, Wen X, Yang X, Wang L, Gao K, Liang X, et al. Glutamine protects intestinal immunity through microbial metabolites rather than microbiota. *Int Immunopharmacol*. (2023) 124:110832. doi: 10.1016/j.intimp.2023.110832

46. Lefebvre P, Cariou B, Lien F, Kuipers F, Staels B. Role of bile acids and bile acid receptors in metabolic regulation. *Physiol Rev*. (2009) 89:147–91. doi: 10.1152/physrev.00010.2008

47. Patti ME, Houten SM, Bianco AC, Bernier R, Larsen PR, Holst JJ, et al. Serum bile acids are higher in humans with prior gastric bypass: potential contribution to improved glucose and lipid metabolism. *Obes (Silver Spring)*. (2009) 17:1671–7. doi: 10.1038/oby.2009.102

Frontiers in Endocrinology

Explores the endocrine system to find new therapies for key health issues

The second most-cited endocrinology and metabolism journal, which advances our understanding of the endocrine system. It uncovers new therapies for prevalent health issues such as obesity, diabetes, reproduction, and aging.

Discover the latest Research Topics

See more →

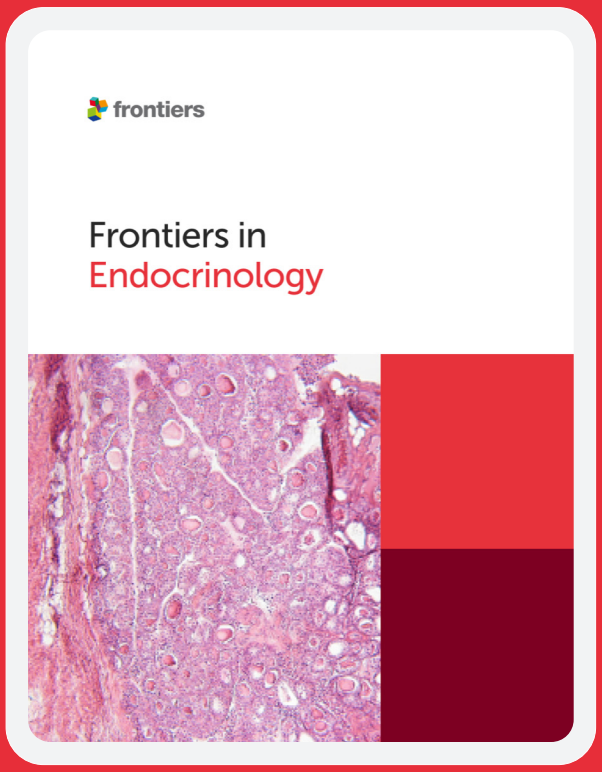

Frontiers

Avenue du Tribunal-Fédéral 34
1005 Lausanne, Switzerland
frontiersin.org

Contact us

+41 (0)21 510 17 00
frontiersin.org/about/contact